Helmholz-Zentrum Potsdam Deutsches GeoForschungsZentrum,
Sektion 5.2: Klimadynamik und Landschaftsentwicklung

An appraisal of a new method for the full-vector reconstruction of the Earth's magnetic field - applied to volcanic rocks from Mexico

Dissertation
zur Erlangung des akademischen Grades
"doctor rerum naturalium"
(Dr. rer. nat.)
in der Wissenschaftsdisziplin Geophysik

eingereicht an der
Mathematisch-Naturwissenschaftlichen Fakultät
der Universität Potsdam

vorgelegt von

Daniel M. Michalk

Potsdam, Februar 2009

Doctoral thesis by Daniel M. Michalk

Supervised by Dr. habil. Norbert R. Nowaczyk and Professor Dr. Gerald Haug
Co-supervised by Dr. Harald Böhnel (Geociencias UNAM, Mexico)

Reviewers:

Professor Dr. Gerald Haug (Universität Potsdam)
Professor Dr. Heinrich Soffel (Ludwig-Maximilians-Universität München)
P.D. Dr. Michael Urbat (Universität zu Köln)

Date of oral defense: 20th of May, 2009

Published online at the
Institutional Repository of the University of Potsdam:
http://opus.kobv.de/ubp/volltexte/2009/3186/
urn:nbn:de:kobv:517-opus-31868
[http://nbn-resolving.de/urn:nbn:de:kobv:517-opus-31868]

Table of contents

Abstract

The Earth's magnetic field (EMF) is generated by convections in the electrically conducting liquid iron-rich outer core, modified by the Earth's rotation. A drastic manifestation of the dynamics of this fluid body is the occurrence of geomagnetic field reversals in the Earth's history but also geomagnetic excursions, which are more frequent features of otherwise stable polarity chrons, but often poorly constrained in the geological record. Even though numerical models of the highly complex dynamics in the liquid outer core exist, the computing power needed for these models is still insufficient. To better understand the origin of the field, we need to know how the field has varied on different geological timescales. This includes not only information about changes in the ancient field's direction but also about the absolute intensity (palaeointensity) and the age. This palaeointensity record is needed for compiling a full-vector description of the field. A palaeomagnetic and palaeointensity study on lava flows allows gaining insights about the evolution of the EMF through time and space. However, constraining the EMF evolution over different geological timescales remains a difficult objective due to the paucity of available palaeointensity data. This is because most current methods of palaeointensity determination are based on various modifications of the Thellier method, which only works on material of single-domain magnetic structure, and which suffers from often high failure rates and time consuming laboratory work. In consequence the global database of absolute palaeointensities still remains sparse through time and space. One new alternative approach in palaeointensity studies is the recently proposed multispecimen parallel differential pTRM (MS) method, which has potentially several advantages over the commonly used Thellier method, because it is in theory independent of magnetic domain state, less prone to biasing effects, such as thermal alteration and significantly faster to perform in the laboratory. Thus, in theory, it offers the possibility to acquire significantly larger data sets of palaeointensities.

A study of highly active volcanic regions, such as the Trans-Mexican Volcanic Belt, seems promising when attempting a full-vector reconstruction or when looking for field excursions. One aim of this thesis was to gain new information about the occurrence and global validity of geomagnetic excursions from the Brunhes- or Matuyama Chron. For this purpose some 75 lava flows from within the Trans-Mexican Volcanic Belt were sampled for palaeomagnetic analyses. Rock magnetic analyses revealed that in most cases the remanence was carried by Ti-poor titanomagnetites of pseudo-single domain magnetic grain size that underwent different degrees of high temperature deuteric oxidation on primary cooling. Occasionally titanomagnetites with higher Ti-contents and additional contributions of (titano-) haematite were also present. The scatter of virtual geomagnetic poles from lavas younger than 1.7 Ma was used for estimating palaeosecular variation and was found to be consistent with latitude dependent Model G and other high quality palaeomagnetic data from Mexico. The palaeomagnetic mean-vectors of 56 lavas were correlated to the Geomagnetic Polarity Timescale supplemented with information on geomagnetic excursions. On the grounds of their associated radioisotopic ages, four lavas were tentatively correlated with known excursions from marine records. Two lava flows dating of Brunhes Chron were associated with the Big Lost and Delts/Stage 17 excursions, respectively. From further two flows dating of Matuyama Chron, one flow was associated with either the Santa Rosa- or Kamikatsura excursions, while the other could have been emplaced during the Gilsa excursion. The most significant outcome was the finding that both Brunhes excursional flows display nearly fully reversed directions that deviate almost 180°C from the expected normal polarity direction. This observation could indicate that in particular the Big Lost and Delta/Stage17 excursions may represent other short periods during which the field completed a full reversal for a short time, such as was previously found for other older cryptochrons or tiny wiggles.

Another focus of this thesis was set on estimating the feasibility of the new MS method for routine palaeointensity determination. This was accomplished by applying the MS method to samples from 11 historical lava flows from Mexico and Iceland from which the actual field intensity was either known

from contemporary observatory data, or deduced from magnetic field models. Comparing observed with expected intensity values allowed to test the accuracy of the MS method. It a was found that the majority of palaeointensity estimates after the MS method yielded results that were very close or indistinguishable within the range of uncertainty from the expected values. However, a general trend towards an overestimate in the palaeointensity was also observed, which, on the grounds of corroborating rock magnetic analyses, was associated with multidomain material. This observation was taken as first evidence that the MS method is not entirely independent of magnetic domain state, as was originally claimed. However, a second experiment in which a modification of the most widely used Thellier method was applied to sister samples from 5 Icelandic flows revealed that, in comparison to the MS method, the latter produced more accurate and statistically better defined palaeointensities. Thus, from these first results, the MS method appeared as a viable alternative for future palaeointensity studies.

Subsequently it was attempted to corroborate the directional record from Mexican lavas with palaeointensity data. For this purpose the MS method was chosen and applied for the first time to rocks with ages of up to 3.5 Ma, although most being younger than 1 Ma. It was possible to acquire palaeointensity estimates for 32 out of 51 investigated lava flows. These results were compared to reconstructions of the dipole moment based on the current global database of absolute palaeointensity. It revealed that the new MS palaeointensities for Mexico are, with a high degree of statistical significance, around 30% higher than expected. Other PI data from Mexico from lava flows of comparable age (although rare), was also observed to be high, relative to global records. This observation could indicate a persistent influence of the non-dipole field for Mexico, which similar to today's situation, would account for the high intensities. However, the paucity of available PI data from Mexico obscures the significance of this observation and the current quality of the global database of palaeointnsity does not allow for an evaluation of non-dipole effects through geological time. The balance of evidence therefore rather suggests an artificial biasing of most measurements towards high values. The generally high palaeointensities seem to corroborate the results obtained from historical lava flows in this study and other previous studies on synthetic samples where domain state effects were found to cause overestimates in the palaeointensity of up to 30 per cent in the MS method. The primary process that leads to this overestimate is assigned to an asymmetry in the demagnetisation and remagnetisation process, i.e. to effective demagnetisation during thermal cycling in an applied laboratory field, which seems to be more important for grains of pseudo-single domain magnetic structure. Yet, this overestimate is expected to be no larger than what might be expected from Thellier experiments performed on samples with a given degree of multidomain behaviour. Future studies should therefore investigate this asymmetry effect in detail and find ways to possibly correct for it.

Zusammenfassung

Das Magnetfeld der Erde wird durch Konvektionsströmungen im elektrisch leitfähigen, flüssigen eisenreichen äußeren Erdkern erzeugt. Eine drastische Ausprägung der dynamischen Prozesse im äußeren Erdkern sind sowohl Polaritätswechsel über geologische Zeiträume, als auch geomagnetische Feldexkursionen (kurze Umpolungen). Letztere sind ein charakteristisches Merkmal von sonst überwiegend stabilen Polaritäts Chron, aber in geologischen Archiven, sedimentären oder vulkanischen, häufig unzureichend dokumentiert. Zwar liegen numerische Modelle der hochkomplexen Prozesse im äußeren Erdkern vor, jedoch ist die benötigte Rechenkapazität hierfür bei weitem noch nicht ausreichend. Für ein verbessertes Verständnis über die Entwicklung des Erdmagnetfeldes in geologischer Vergangenheit benötigen wir Informationen über die Geometrie des gesamten Vektorfeldes, wofür neben der Bestimmung der Feldrichtungen auch die Bestimmung der absoluten Paläointensität und des Alters notwendig ist. Insbesondere Vulkanite bieten die Möglichkeit, Daten über die Richtung und vor allem auch die Intensität des Erdmagnetfeldes zur Zeit ihrer Platznahme zu gewinnen. Bisweilen ist eine genaue Charakterisierung der Entwicklung des Erdmagnetfeldes in Zeit und Raum schwer möglich, was sich in erster Linie auf den generellen Mangel an Paläointensitätsdaten zurückführen lässt. Ein Grund hierfür ist, dass die meisten Methoden zur absoluten Paläointensitätsbestimmung, auf verschiedenen Modifikationen der so genannten Thellier Methode basieren, welche nur auf magnetische Minerale im Einbereichs-Domänenzustand anwendbar ist und zudem neben zeitintensiven Laborexperimenten, hohe Ausschussraten liefert. Hieraus resultiert, dass die gegenwärtige globale Datenbasis absoluter Paläointensitäten als spärlich zu bezeichnen ist. Eine alternative Methode zur Bestimmung der absoluten Paläointensität ist die kürzlich entwickelte „multispecimen parallel differential pTRM“ (MS) Methode. Diese hat im Vergleich zur Thellier Methode den Vorteil, dass sie theoretisch unabhängig ist vom Domänenzustand der magnetischen Minerale, weniger anfällig für thermische Alterationen und außerdem wesentlich schneller im Laborexperiment durchzuführen ist. Sie ermöglicht daher theoretisch die Möglichkeit, bedeutend größere Datensätze von Paläointensitäten zu schaffen.

Ein Schwerpunkt dieser Arbeit lag darauf, neue Informationen über das Auftreten und gegebenfalls die globale Gültigkeit von geomagnetischen Feldexkursionen während des Brunhes- oder Matuyama Polaritäts Chron zu gewinnen. Hierfür wurden etwa 75 Lavaflüsse des Transmexikanischen Vulkangürtels für paläomagnetische Studien beprobt. Die Trägerminerale der charakteristischen remanenten Magnetisierung sind stets titanarme Titanomagnetite im Pseudo-Einbereichs Domänenzustand, wobei höhere Titangehalte und zusätzlicher (Titano-) Hämatit in einigen Fällen auch vorkommen. Diese Partikel weisen meist Entmischungslamellen auf, ein deutliches Anzeichen einer syngenetischen, primären Oxidation bei hohen Temperaturen. Es kann daher gefolgert werden, dass die magnetischen Informationen über Richtung und Intensität des Paläofeldes kurz nach der Extrusion der einzelnen Lavaflüsse erworben wurde. Die Streuung der virtuellen geomagnetischen Pole von Laven jünger als 1,7 Millionen Jahre, diente zur Bestimmung der Paläosekularvariation. Diese ergab einen Wert, der sowohl in Übereinstimmung mit dem breitenabhängigen Sekularvariationsmodel „Model G“ als auch mit anderen publizierten paläomagnetischen Daten für Mexiko ist. Eine Korrelation der mittleren Paläorichtungen von 56 mexikanischen Laven mit einer um Feldexkursionen ergänzten geomagnetischen Polaritätszeitskala, lieferte Hinweise auf 4 Exkursionen. Zwei Laven mir annährend komplett inverser Polarität geben neue Hinweise auf die Big Lost und Delta/Stage 17 Exkursionen während des Brunhes Chron. Von zwei Laven mit normaler Polarität könnte eine entweder während der Santa Rosa oder Kamikatsura Exkursion extruiert worden sein, und die andere während der Gilsa Exkursion ihre Platznahme gefunden haben. Ein bedeutendes Ergebnis sind die annährend komplett inversen Richtungen beider Exkursionslaven der Brunhes Chron. Dies gibt einen Hinweis darauf, dass im Speziellen die Big Lost und die Delta/Stage17 Exkursionen Zeitintervalle inverser Polarität mit globaler Gültigkeit

repräsentieren könnten, in der das Ermagnetfeld seine Polarität für kurze Zeit wechselte, so wie es bereits für andere ältere, Cryptochrons oder Ozeanboden Anomalien festgestellt wurde.

Ein weiterer Schwerpunkt der vorliegenden Arbeit war, die neue MS Methode auf ihre Anwendbarkeit und Genauigkeit hin zu testen. Hierfür wurden zunächst Paläointensitätsexperimente nach der MS Methode an 11 historischen Laven aus Mexiko und Island durchgeführt, wobei Daten von magnetischen Observatorien oder von magnetischen Feldmodellen zum direkten Vergleich herangezogen werden konnten. Die MS Paläontensitätsdaten waren zu gut der Hälfte, im Rahmen ihrer Fehlergrenzen, nicht von den erwarteten Intensität zu unterscheiden. Es wurde aber auch ein genereller Trend zur Überschätzung der Paläointensität beobachtet, welcher anhand von komplementierenden gesteinsmagnetischen Daten mit magnetischen Mineralen im Mehrbereichsteilchen-Zustand in Verbindung gebracht werden konnte. Diese Beobachtung ergab demnach einen ersten Beweis dafür, dass die MS Methode möglicherweise nicht wie ursprünglich angenommen in vollem Umfang unabhängig vom Domänenzustand der Trägerminerale ist. Ein zweites Experiment, in dem eine Abwandlung der Thellier Methode auf 5 Isländische Laven angewendet wurde, zeigte jedoch, dass im Vergleich zur MS Methode, die Daten letzterer näher an den erwarteten Intensitätswerten lagen und zudem statistisch besser definiert waren. Auf Grund dieser ersten Ergebnisse erschien die MS Methode deshalb als eine viel versprechende Alternative für weitere Paläointensitätsstudien.

Im weiteren wurde eine Komplementierung der Richtungsdaten mexikanischer Laven durch absolute Paläointensitätsbestimmungen angestrebt. Hierfür wurde die MS Methode herangezogen und zum ersten Mal in großem Umfang auf Vulkanite mit Altern von bis zu 3,5 Millionen Jahre (jedoch überwiegend jünger als 1 Millionen Jahre) angewendet. Von insgesamt 51 untersuchten Laven wurden 32 neue Paläointensitäten nach der MS Methode geschaffen. Ein Vergleich mit Rekonstruktionen des Dipol-Momentes, welche auf den Daten der gegenwärtigen globalen Paläointensitätsdatanbasis basieren, ergaben, dass diese MS Daten mit hoher statistischer Wahrscheinlichkeit im Mittel etwa 30% höher sind. Andere publizierte Paläointensitätsdaten mexikanischer Laven weisen jedoch auch eine ähnliche Überschätzung auf, was auf einen beständigen Einfluss des nicht-Dipolfeldes schließen lassen könnte, ähnlich wie es beim rezenten Erdmagnetfeld für Mexiko der Fall ist. Hier ist allerdings hervorzuheben, dass Qualität und Umfang der globalen Paläointensitätsdatenbasis eine Evaluierung eines nicht-Dipolfeldes für Mexiko in der geologischen Vergangenheit nicht erlaubt. Die generell zu hohen Paläonintensitäten nach der MS Methode bekräftigen daher vielmehr die Ergebnisse von historischen Laven dieser Arbeit, sowie anderer experimenteller Studien an synthetischen Proben, bei denen Überschätzungen von MS Paläointensitäten von bis zu 30% festgestellt wurden. Der Process, aus dem diese Überschätzung der Paläointensität resultiert ist eine Asymetrie des Entmagnetisierungs- und Remagnetisierungsprozesses heisst, dass ein effektives Entmagnetisieren während der Remagnetisierung im angelegten Laborfeld erfolgt. Diese Asymetrie scheint besonders bei Pseudo-Einbereichsteilchen ausgeprägt zu sein. Es wird allerdings davon ausgegangen, dass diese Überschätzung nicht größer ist, als was man bei einem Thellier Experiment an Proben mit ähnlicher magnetischer Korngröße erwarten würde. Diesen Asymetrie Effekt gilt es in zukünftigen Studien detailiert zu evaluieren und Wege zu finden um gegebenfalls dafür zu korrigieren.

Acknowledgements

This project would have not been possible without the ever lasting support of many people.

First of all I would like to thank Norbert Nowaczyk, head of the palaeomagnetic laboratory at GFZ, for his constant support over the years of my PhD. I am grateful that you gave me the chance to join GFZ and so much freedom to conduct my research independently. I would like to thank Harald Böhnel for his guidance and support and especially his hospitality during my three visits to Mexico. Special thanks to Professor Gerald Haug, who was head of section 3.3 during my first two years at GFZ. He constantly motivated me and other PhD students to publish our results and I am particularly thankful for the financial support you provided during the last 6 Month of my PhD. I would like to thank Professor Jörg Negendank for his advice in ore-microscopy studies and some interesting discussions on Mexican geology during a field trip to Mexico in 2006. Much appreciated assistance in the collection of palaeomagnetic samples during three fieldwork seasons in Mexico came from Ivan Barajas, Gildardo Gonzalez and Jose Luise. Very special thanks to Adrian Muxworthy, with whom I shared an office for almost a year. You taught me a lot about the potential of the FORC-technique and took me on an unforgettable fieldtrip to Iceland. I would like to thank my German palaeomag colleagues, especially Roman Leonhardt for giving me a first crash-course in palaeointensity studies. Michael Winklhofer, Karl Fabian, David Krása and Dave Heslop are thanked for their interest in my work and many inspiring discussions. I would also like to thank Professor Rixiang Zhu and Yongxin Pan who were my hosts during a short-term fellowship stay at the palaeomagnetism and geochronology lab (PGL) in Beijing in 2007. I would like to thank all technical staff from GFZ, in particular Dieter Berger, Gabi Arnold and Michael Köhler for their help in the sample preparation, Juliane Herwig for her assistance during SEM studies, and Mr. Steiner and Reik Sünkel for their help in designing and building a custom-made sample holder for palaeointensity studies. I thank Michael Sczurlies and Martina Duwe for their advice and assistance on all kinds of technical questions. Daniel Melnick is thanked for many great discussions beyond palaeomagnetism. Monika Korte is thanked for providing me magnetic field model data and Jean-Pierre Valet for providing the SINT2000 data. I also would like to thank Mark Dekkers and Cor Langereis for some interesting discussions and for giving me the opportunity to present my work to the Utrecht palaeomagnetic group. Very special thanks to Andrew Biggin and Mads Knudsen, who were both equally supportive during the last couple of month of my PhD and always a source of inspiration and motivation to me. And of course I would like to thank my family for their never ending support over the years and their interest in my work. Finally I thank you Talia, mi amor, for your never ending patience and support especially during the writing up stage of my thesis.

This project was funded by the Deutsche Forschungsgemeinschaft (DFG) in the framework of the priority programme ”Geomagnetic variations” (grants Ne154/45-1, No334/1-2 and No334/5-1).

1. Introduction

The Earth's magnetic field (EMF) is generated by convection in the iron-rich liquid outer core of the Earth by magnetohydrodynamic processes, referred to as the geodynamo, and it is confined by the action of the solar wind into a volume called the magnetosphere (e.g. Merrill et al., 1996). The EMF is a complex function of space and time and subject to changes in its direction and intensity on various timescales ranging from seconds to millennia and even millions of years. Because it interacts with the atmosphere, the biosphere, the deep mantle and even the inner core, some knowledge on how the field behaves is useful to all Earth Sciences. At the Earth's surface the EMF is to the first order best approximated by a magnetic dipole located at the Earth's centre and inclined by 11° relative to the rotation axis. This tilted geocentric dipole model describes around 90% of the present field at the Earth's surface, with the remaining 10% categorized as non–dipolar. These non-dipole features may be described by the higher order components of a spherical harmonic representation (i.e. quadrupole, octupole etc.), which vary in strength and direction on a much shorter timescale, typically between one year and 10^5 years. Variations of such shorter periodicities are referred to as secular variation (SV). The non-dipole field is responsible for large areas of magnetic flux patches, with anomalous directions and intensities. These may be attributed to eddy currents and other inhomogeneities at the core-mantle boundary (Merrill et al., 1996). When averaged over several thousands of years, the geomagnetic field is best approximated by a field generated by a centred axial dipole aligned along the rotation axis. This observation led to the two fundamental palaeomagnetic standard characteristics of the field, the virtual palaeomagnetic pole (VGP) and the virtual dipole moment (VDM). Magnetic field data has been systematically recorded since the 16th century. These early records consist mainly of marine observations obtained by sailors (Jackson et al., 2000). The first continuous magnetic observatory measurements of magnetic parameters, such as inclination, declination and intensity started around the same time in London. Today, satellites (e.g. Magsat, Ørsted, CHAMP, SAC-C, SWARM) not only monitor the magnetic field of the Earth, but also the magnetic fields of other planets and their moons. For investigating the EMF field further back, through geological time, one must rely on information contained in rocks.

The directional characteristics of the EMF are recorded by sediments and volcanics, but both have their advantages and limitations as recording media. Marine and lacustrine sediments record geomagnetic field variations in their detrital magnetisations (e.g. Opdyke et al., 1974), which means that already magnetised particles align in the direction of the ambient field while settling through the water column before they finally become fixed in that orientation within the sediment matrix. Hence, sediments provide continuous records of the ancient geomagnetic field behaviour, which depends on the sedimentation rate in the area of deposition. However, when sediments are used as a recording unit, the field record may be subject to several remanence acquisition processes, e.g. to post-depositional modifications through organisms (bioturbation), to compaction, to diagenesis, to the acquisition of viscous remanences, or to a delayed lock-in of magnetic remanence, which may falsify the recording of the geomagnetic field (e.g. Kok and Tauxe, 1996; Roberts and Winklhofer, 2004). Furthermore, sedimentary records sometimes suffer from the problem of precise age-dating and allow only the determination of the relative palaeointensity (PI), which is estimated by normalising the natural remanent magnetisation (NRM) by a concentration proxy parameter such as magnetic susceptibility, anhysteretic remanent magnetisation or saturation magnetisation (Tauxe, 1993).

Volcanic rocks (i.e. lava flows) on the other hand acquire a thermo remanent magnetisation (TRM) when the elementary magnetic domains of magnetic minerals align with the direction of the ambient field, as they cool below the Curie temperature (T_C) and their net moment will be proportional to the field intensity at that time. Due to this different remanence acquisition process, volcanics have the advantage to provide information about the absolute field intensity at the time the lava was emplaced, which can be retrieved by laboratory experiments in which the TRM intensity of the rock is compared with an

artificially imprinted magnetisation. This absolute PI record is needed for compiling the full-vector description of the geomagnetic field through time, which includes the declination D, the inclination I, and the intensity B. Volcanics can also be dated by radioisotopic methods (e.g. $^{40}Ar/^{39}Ar$) thus allowing for the determination of the absolute PI at various times in the geological past. However, since volcanic eruptions are sporadic events, volcanics have the disadvantage of just providing an instantaneous spot reading of the field at the time when the lava flow was emplaced. Yet, if they are sampled in sufficient detail and their ages are well constrained, they can provide semi continuous records of the full-vector field behaviour and may additionally be used for calibrating relative PI records from sediments to absolute values (e.g. Valet et al., 2005).

The most characteristic feature of the EMF is that over geological timescales the main dipolar field has frequently reversed between the two stable modes of a normal and a reversed state, though at different rates. For example during the Cretaceous the geomagnetic field remained in a state of normal polarity for about 35 Ma (Cretaceous Normal Superchron) while during the Neogene (the last 23 Ma) the field changed its polarity approximately every 0.4 Ma. The last full polarity reversal (Matuyama/Brunhes reversal) occurred around 780 ka ago. Since that time the field has dominantly remained in its present state of a normal polarity. Polarity chrons are further interrupted by geomagnetic excursions. These are characterised by pronounced lows in field intensity that result in large-scale fluctuations of the field direction, similar in magnitude to those observed during reversals, but without entailing a polarity flip. Depending on the location on the globe, geomagnetic excursions may last for ~2 ka up to ~ 10 ka, making their recognition difficult in marine and lacustrine sediments with low deposition rates, but also in volcanic rocks that are extruded only sporadically.

Bonhommet and Babkine (1967) were the first to discover intermediate to almost fully reversed magnetisation directions recorded in 41 ka old lava flows close to the village of Lachamp in the French Massive Central. For a long time, these anomalous directions were interpreted as rockmagnetic artefacts, primarily because some samples from the same locality were found to display a self-reversal of the TRM (Heller, 1980). Several subsequent studies on lava flows at the type locality and other locations within the Massive Central later documented intermediate to almost fully reversed directions. Thus the initial study of Bonhommet and Babkine (1967) is now accepted as the first evidence that the Brunhes Chron was not always a phase of stable normal polarity. Today the Lachamp excursion is the most thoroughly studied and best documented geomagnetic excursion and has been confirmed to have occurred globally (e.g. Kristjansson and Gudmundson, 1980; Levi et al, 1990; Nowaczyk and Antonow, 1997; Nowaczyk and Knies, 2000; Oda et al, 2002; Nowaczyk et al., 2003; Lund et al, 2005; Channell, 2006; Laj et al, 2006) at about 41 ka (Guillou et al, 2004). When high-resolution sedimentary records from the deep sea became available, it became apparent that excursions are frequent features of the geodynamo. However, only some excursions appear to be globally recorded, while others are still interpreted as local anomalies of the geomagnetic field (see Lund et al., 2006 and references therein). The chronology of geomagnetic excursions has clearly evolved rapidly in recent years (Fig. 1.1). While one of the earliest reviews based on literature available at the time, Champion et al. (1988) proposed the existence of eight excursions within the Brunhes Chron, a later review by Langereis et al. (1997) already proposed evidence for 12 excursions (seven well-dated global excursions and five restricted less certain excursions). In more recent papers (e.g. Lund et al., 2001a, 2001b, 2006) up to 17 excursions are proposed for the Brunhes Chron alone. Singer et al. (2002) developed the geomagnetic instability timescale (GITS), a concept for registration of the distortion of geomagnetic field geometry in the magnetic polarity record. The most recent version of the GITS includes radioisotopic ages for 11 excursions within the Brunhes- and 4 excursions within the reversed Matuyama Chron (Fig. 1.1 E).

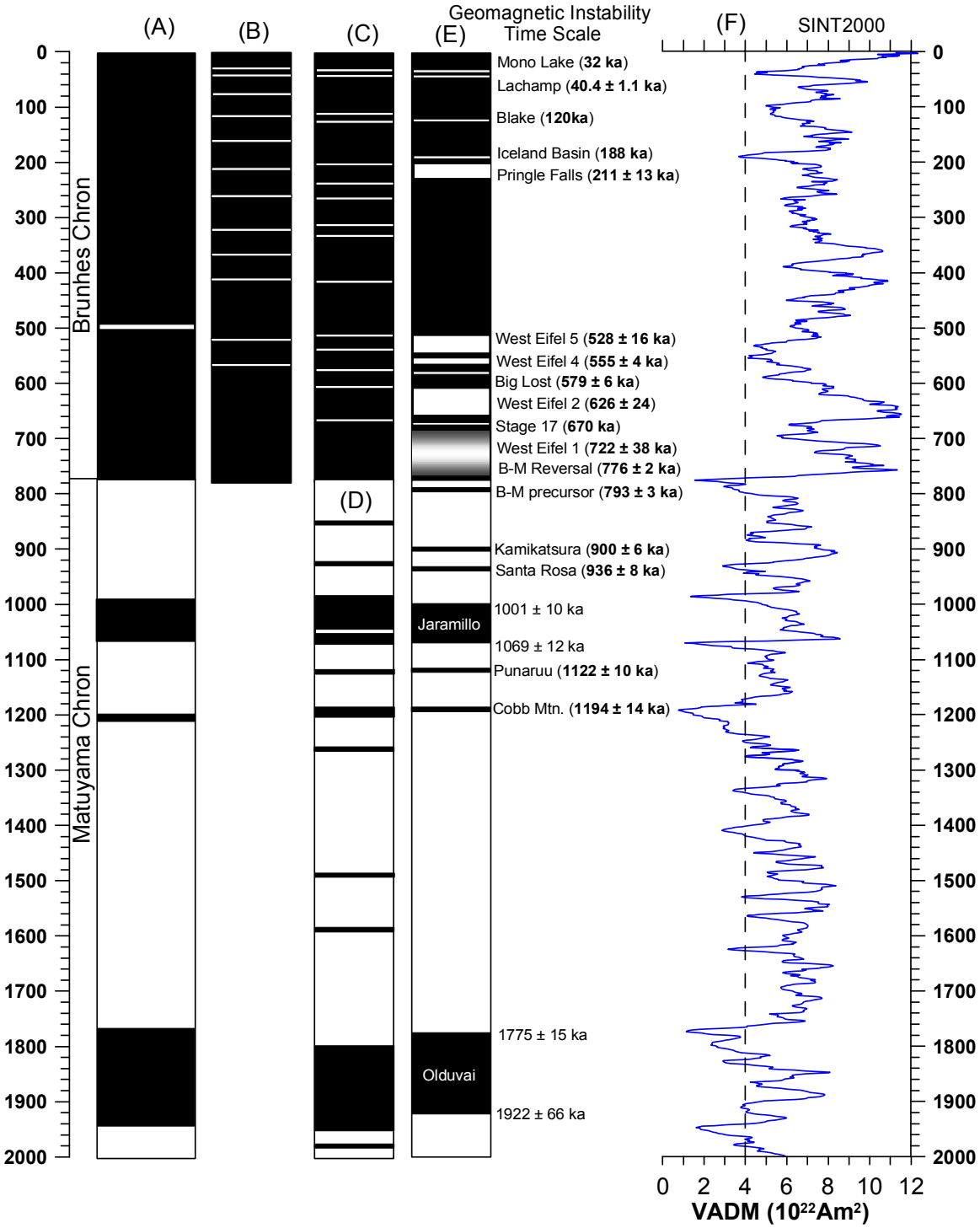

Figure 1.1. (A) Geomagnetic polarity timescale of Cande and Kent (1995); (B) to (E) chronology of geomagnetic excursions after several authors: (B) Langereis et al (1997); (C) Lund et al. (2001, 2006); (D) Channell et al. (2006); (E) Geomagnetic Instability Timescale (Singer et al., 2002, 2007, 2008a,b); (F) SINT2000 global stack of relative palaeointensity records calibrated to absolute values (Valet et al., 2005). The stippled line indicates the critical intensity threshold which is assumed for geomagnetic excursions (Langereis et al., 1997).

Even after more than 40 years of palaeomagnetic research, there is still little knowledge about the timing and duration and global validity of many of the excursions found in the Brunhes- and Matuyama Chron. However, knowing the precise number of excursions, their timing/duration, and recognizing them in different parts of the globe is essential for a more complete understanding of the complex dynamo processes. Up to the present, volcanic evidence exists for nine excursions within the Brunhes, and six within the Matuyama Chron, but for an unambiguous confirmation of excursional records from sediments and their global validity, more evidence from radioisotopically dated volcanic rocks sampled at different geographical locations is highly desired.

Furthermore, the primary process that leads to a geomagnetic excursion remains unclear and has been debated ever since its discovery. These interpretations range from aborted reversals (e.g. Doell and Cox, 1972; Opdyke, 1972) to anomalous or enhanced PSV (Cox et al., 1975; Hoffmann, 1981; Merrill and McFadden, 1994), or models in which the reversing field in the liquid outer core is held back by the influence of the solid inner core (Hollerbach and Jones, 1993; Galtzmeier and Roberts, 1995; Gubbins, 1999). Numerical dynamo simulations (Wicht, 2005) further suggest a strong site dependence on the occurrence and duration of excursions, which means that some excursions might not be global features of the geomagnetic field. One reason for these different views is the general lack of absolute PI data because obtaining reliable PI estimates still remains a difficult objective. This is because most common techniques in PI studies are based on various modifications of the Thellier method (Thellier, 1959), which suffers from high failure rates, often large uncertainties and time consuming laboratory work. As a consequence, the global data base of absolute PIs still gives a rather scattered image and remains sparse both temporally and spatially.

1.2 The importance of a full-vector geomagnetic field description

During the last 20 years scientists from different fields of research have started to recognize the importance of a complete full-vector description of the field. A better understanding of the full-vector evolution of the geomagnetic field would shed light on geophysical phenomena, such as the evolution of the Earth's core (Elsasser, 1956), variations in heat flow across the core-mantle-boundary (Galtzmaier et al., 1999), or the effect of the nucleation and growth of the solid inner core on the EMF (Smirnov et al., 2003). Full-vector records of the geomagnetic field are necessary to improve spherical harmonic models of the geomagnetic field (e.g. Hongre et al., 1998; Korte and Constable, 2005; Korte et al., submitted), or dynamo models (e.g. Wicht, 2005). One of the first attempts to include full-vector palaeomagnetic data into dynamo related analysis by Love (1999) showed that just six datasets from volcanic fields in different parts of the world, spanning the last 10 ka, were already sufficient to invalidate some of the simplifications often used in dynamo models. More high quality palaeointensity data could also resolve long standing issues in palaeomagnetism such as the Pacific-Non dipole low (e.g. Johnson and Constable, 1998), or heterogenous models of palaeosecular variation (e.g. Constable and Johnson, 1999). One feature of the historical Earth magnetic field is that its dipole moment has decayed by around 10% over the last 170 years. Thus, a better understanding about the changes in field intensity and their periodicities would help to understand this historical decay of the field in a geological context and answer the question if the present day field is approaching a reversal (Hulot et al., 2002). Another recently debated topic is that of possible connections between changes in the geomagnetic field intensity and climate variability (e.g. Gallet et al., 2005; Courtillot et al., 2007; Thouveny et al., 2008), which is extremely difficult to assess due to the paucity of available data. Finally, a better knowledge of changes in the absolute PI is of crucial importance for studies where the shielding effect plays a role, e.g. in determining production rates of cosmogenic nuclides (Frank, 2000; Christl et al., 2003; Muscheler et al., 2005; Christl et al., 2007).

1.3 Objectives of this study:

A systematic study of volcanically highly active regions appears promising when looking for geomagnetic excursions and when attempting a full vector reconstruction of the geomagnetic field. In this respect, the Trans-Mexican volcanic belt (TMVB; Figures 1.2 and 1.3) offers a superb archive because it consists of approximately 8000 volcanic structures, with probably several hundred of them dating from the last 2 Ma. Thus, the TMVB was chosen as the main study area for this PhD project.

This PhD project had two principal objectives: (1) to identify, if possible, some of the geomagnetic excursions that occurred during the last 2 Ma in order to gain further information about their global validity, and (2) to increase the number of absolute palaeointensities for Mexico.

With this intention in mind, a large number of independent lava flows, previously dated by radioisotopic methods, were sampled and subjected to palaeomagnetic and palaeointensity studies.

1.4 Thesis structure

This thesis is composed of four manuscripts, published or submitted for publication in peer-reviewed ISI journals:

Paper 1, *"The use of mini-samples in palaeomagnetism"*, is a technical letter in which the site-mean directions and statistical parameters of 12 lava flows, sampled with two different palaeomagnetic sample sizes, i.e. 1 inch standard core samples and 12 mm mini-core samples, are compared. This study was carried out to determine the overall obtainable uncertainty of site mean directions for mini-samples, which where the preferred palaeomagnetic samples throughout this study.

Paper 2, *"Evaluation of the multispecimen parallel differential pTRM method: A test on historical lavas from Iceland and Mexico"*, presents a study in which the feasibility of the new multispecimen parallel differential pTRM (MS) method for palaeointensity, developed by Dekkers and Böhnel (2006), was estimated for routine palaeointensity studies. This was achieved by comparing PI results after the MS method and additionally after a modification of the Thellier method, with contemporary intensity data from magnetic observatories or with intensity data deduced from magnetic field models.

Paper 3, *"Evidence for geomagnetic excursions recorded in Brunhes- and Matuyama-Chron lavas from the Trans-Mexican Volcanic Belt"*, presents a correlation of palaeomagnetic mean-vectors from 56 lava flows from the Trans-Mexican Volcanic Belt to the geomagnetic polarity timescale, supplemented with information on geomagnetic excursions.

Paper 4, *"Application of the multispecimen palaeointensity method to Pleistocene lava flows from the Trans-Mexican Volcanic Belt"*, presents the application of the multispecimen parallel differential pTRM method to the oldest rock studied hitherto with this method and compares the PI results to reconstructions of the global dipole moment.

1.5 Study area:

The Trans-Mexican Volcanic Belt (TMVB; Figures 1.2 and 1.3), is one of the largest continental volcanic arcs on the North American plate and extends over about 1000 km from the Mexican Pacific coast to the coast of the Gulf of Mexico, over an irregular width between 80 and 230 km, where it follows an E-W orientation in its central and eastern sectors and a WNW-ESE orientation in its western sector (Gómez-Tuena et al., 2007). Its name relates to the most pronounced morphological feature because the TMVB is not oriented parallel to the Middle American Trench, but it is inclined by an angle of ~ 16° with respect to the trench (e.g. Gómez-Tuena et al., 2007). The TMVB relates to the subduction of the Cocos and Riviera plates under North American plate margin (Middle America Trench). The 9 Ma old Riviera microplate subducts at a fairly steep angle of around 50°, whereas the 12-18 Ma old Cocos plate subducts at around 30° along its border with the Riviera plate (Klitgord and Mammerickx, 1982). Seismic data indicates that the latter decreases in dip and becomes nearly sub-horizontal to the southeast beneath Mexico City (Pardo and Suarez, 1995). Mexican volcanoes have been studied for more than a century and comprehensive reviews about the tectonic- and stratigraphic framework of the TMVB, the petrology and geochemistry of its igneous constituents and its geologic and geophysical parameters are given in e.g. Demant et al. (1978), Nixon et al. (1987), Ferrari et al. (1999), Ferrari (2005) and Gomez-Tuena et al. (2007).

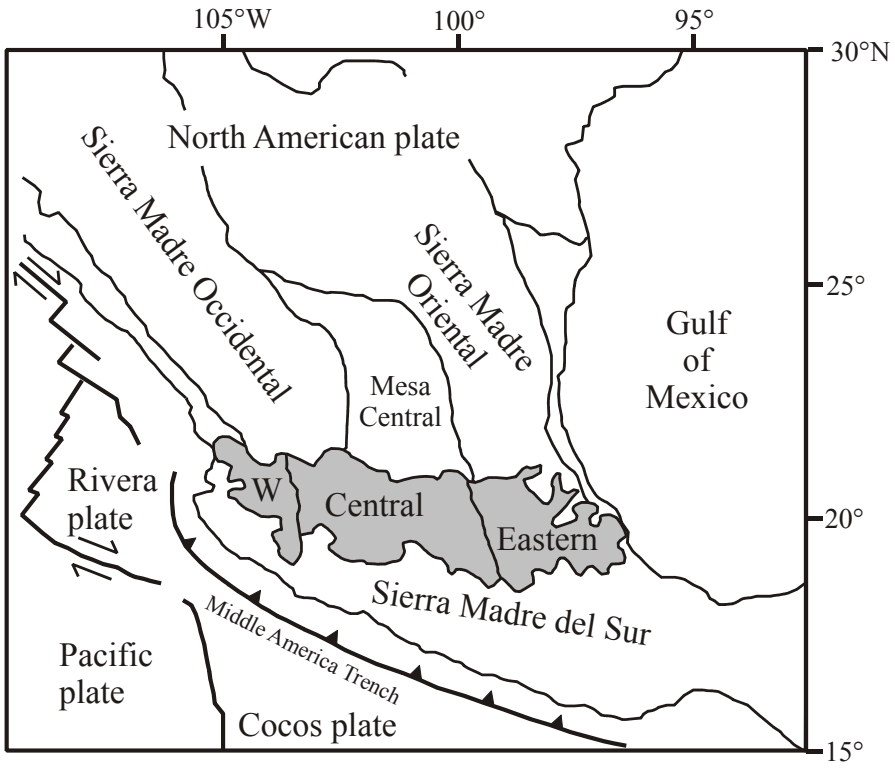

Figure 1.2. Location of the Trans-Mexican Volcanic Belt (grey) divided into three sectors. Also shown are the main geologic provinces of Mexico and the current tectonic configuration (modified from Gomez-Tuena et al., 2007).

The geological evolution of the TMVB has been a subject of debate for almost 40 years. The onset of TMVB activity was previously assigned to the late Olicocene (Mooser, 1972), early Pliocene (Nixon et al., 1987), late Pliocene (Cantagrel and Robin, 1979) or to the Quaternary (Demant, 1978). With the establishment of the first digital geological map of the TMVB (Fig. 1.3;

http://santori.geociencias.unam.mx/Centario/Gomez-Tuens.xls), which incorporates the information of 1300 ages, as well as more than 2000 geo-chemical analyses (Ferrari et al., 2005), it is now well established that the TMVB dates back to the middle to late Miocene period, as a result from a progressive counter clockwise rotation of the magmatic arc of the Sierra Madre Occidental. Compositional changes from silicic to intermediate-mafic at around 15 Ma ages suggest that the volcanic arc had almost the orientation of the modern TMVB since middle Miocene times (Ferrari et al., 1999).

1.6 Sampling:

Palaeomagnetic sampling was carried out during three fieldtrips between March 2005 and April 2007. In total 63 dated lava flows of Pleistocene age, although most being younger than 1 Ma, were sampled for palaeomagnetic and palaeointensity studies within five different field-areas that are:

(1) the Ceboruco San-Pedro Volcanic Field;
(2) the Tequila Volcanic Field;
(3) the Michoacan-Guanajuato Volcanic Field;
(4) the Valle de Bravo Volcanic Field, and
(5) the eastern part of the TMVB, within the N-S trending Pico de Orizaba – Cofre de Perote volcanic chain.

The majority of age chronological data was available from several previous studies that were primarily concerned with constraining volumetric estimates of magma eruption rates in different monogenetic volcanic fields. The petrography and element geochemistry of lava flows is discussed in these publications in detail (see appendix Table A1). The majority of lavas were dated using the $^{40}Ar/^{39}Ar$ method, with 5 further lavas using the ^{14}C method on charcoal found below the front of the lavas, and three lavas using the thermoluminescence (TL) method on quartz separates. Eleven new $^{40}Ar/^{39}Ar$ ages were additionally determined in the course of this study at CICESE in Ensenada, Mexico, by Margarita Lopez.

The preferred size of palaeomagnetic samples in this study were so called “mini-samples” with a diameter of 12 mm and a length of 10 mm. The mini-sample technique offered several advantages during fieldwork, as sampling localities were often located in difficult accessible terrains. Furthermore, due to the 90% smaller volume of the mini-samples compared to standard palaeomagnetic samples, it was later possible to measure them on the 2G cryogenic magnetometer with long-core setup, which allowed for a full automatic alternating field (AF) demagnetisation of suites of 8 mini-samples.

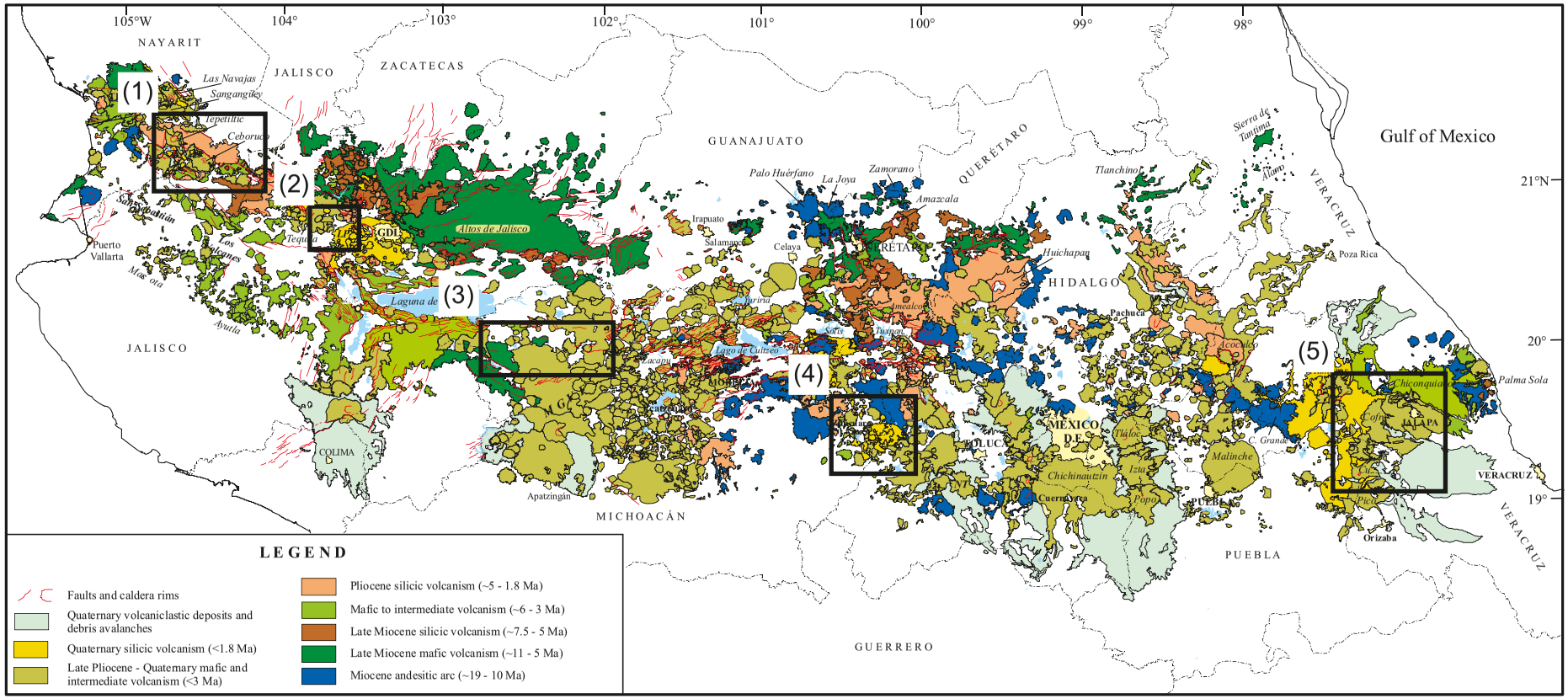

Figure 1.3. Simplified geological map of the Trans-Mexican Volcanic Belt (taken from Gomez-Tuena et al., 2007).
The fieldareas subjected to palaeomagnetic samling are indicated by rectangles:
(1) Ceboruco-San Pedro Volcanic Field, (2) Tequila Volcanic Field,
(3) Michoacan-Guanajuato Volcanic Field,
(4) Valle de Bravo Volcanic Field, and (5) Eastern Trans-Mexican Volcanic Belt.

1.7 Methods:

Several rock magnetic measurements were routinely performed on a number of samples from all investigated sites in order to build up a comprehensive profile of their magnetic mineral assemblages, to gain additional information about the nature of magnetisation recorded in the rocks, and the conditions under which this magnetisation was acquired. All laboratory experiments were carried out at the GFZ German Research Centre for Geosciences in Potsdam, Germany.

Hysteresis measurements were used as a diagnostic tool to analyse the magnetic mineral population of a rock sample, as they vary with domain state and mineral type. For this, an Alternating Gradient Field Magnetometer (AGFM) was used to determine hysteresis loops, on small chips of rock samples (20-70 mg) at room temperature. Hysteresis data allowed determining the bulk magnetic granulometry of a sample, which was deduced from a Day diagram (Day et al., 1977) by plotting the ratios M_{RS}/M_S versus B_{CR}/B_C for titanomagnetites. The AGFM was also used for measuring first order reversal curves (FORC) (Roberts at al., 2000). Using the FORC technique, the degree of magnetostatic interactions within a sample can be estimated. Thermomagnetic measurements were carried out to determine the Curie Temperature (T_C) of a particular magnetic mineral or phase. For this purpose, a Variable Field Translation Balance (VFTB) was preferably employed, which measures the saturation magnetisation (M_S) as a function of the temperature. From this data, Curie temperatures were determined after the method of Moskowitz (1981), using the software RockMag Analyser (Leonhardt, 2006). Furthermore, ore-microscopy studies under reflected light were carried out on thin sections. This non-magnetic technique provided additional information on the oxidation stages of magnetic minerals, i.e. if magnetic minerals underwent a high temperature deuteric oxidation on primary cooling, or if they were affected by a later low temperature oxidation (maghaemitisation). This information aided for a pre-selection of samples for PI experiments.

For measurements of the magnetisation, either a 2G Enterprises 755 superconducting 3-axis DC-SQUID magnetometer with long core setup or an AGICO spinner magnetometer (JR-6A) were used. The latter was employed in the case of strongly magnetic rocks. Whenever possible, the SQUID magnetometer was used because, with its in-line built AF demagnetiser, it allowed for full automatic measurements of suites of eight mini-samples at a time, with peak fields of up to 150 mT. The majority of samples were subjected to AF demagnetization, while the thermal demagnetisation technique was generally applied to smaller sets of samples. The directional analysis of the vector remanence datasets after demagnetisation treatment was done by using the palaeomagnetic software PMX written by N. R. Nowaczyk and M. Güntzel. This software uses the principle component analysis technique of Kirschwink (1980) with associated uncertainties.

Palaeointensity studies were carried out after the new multispecimen parallel differential pTRM method of Dekkers and Böhnel (2006). Additional PI experiments after the Thellier method on historical lava flows from Iceland were carried out using the IZZI protocol (Yu et al., 2004).

1.8 Determination of the absolute palaeointensity: The most widely used methods, their advantages and limitations

The Thellier method and its modifications

The Thellier-technique (Thellier and Thellier, 1959) is the most widely used method for the determination of the absolute PI. It relies on the comparison between thermal demagnetisation of the NRM and acquisition of a laboratory partial thermoremanent magnetization (pTRM) in the presence of a known laboratory field. The assumption that underlies the Thellier method is that the primary mechanism of a thermo remanent magnetization (TRM) by which volcanic rocks or fired archaeological materials become magnetised, can be approximately linearly related to low fields such as the Earth's. This assumption was found to be valid by Néel (1949; 1955) for uniaxial single domain grains, which will retain the same proportionality in the applied field over the entire temperature spectrum.

Thellier and Thellier (1959) showed that the acquisition of TRM in non-interacting single domain grains obeys three different laws:

(1) The law of reciprocity, which states that the blocking- (T_B) and unblocking (T_{UB}) temperatures (defined as the temperatures at which a material becomes magnetised and demagnetised, respectively) of the magnetic grains are equal, and thus a pTRM that is acquired between two temperatures T1 and T2 will be demagnetised completely by a zero-field heating in the same interval;
(2) The law of independence, which assumes that a pTRM is completely independent of another pTRM produced in a non-overlapping temperature interval in both intensity and direction; and
(3) The law of additivity, which assumes that the total TRM is finally achieved by adding the pTRMs together.

In practice this is done by separating the NRM and TRM components by vector addition at the same temperature steps and this operation is repeated at incremental temperature steps up to the highest Curie temperature. The PI is then determined by the slope of an Arai-plot (Nagata, 1963), which depicts the amount of NRM lost as a function of the pTRM gained for each successive temperature interval. In an ideal experiment, the ratio NRM over TRM should keep the same proportion for every temperature interval. Modifications of the original Thellier technique have been proposed by other researchers. Coe (1967a) described the most widely used variant of the Thellier technique, often referred to as the zero-field / in-field method (ZI) method. It requires a sample to be heated first in zero-field for determining the pNRM and then reheating it at the same temperature in a known laboratory field (H_{lab}) to determine the pTRM. A different approach was put forward by Aitken et al. (1988), who suggested heating the sample first in H_{lab} to determine the pTRM, and then successively demagnetizing the sample in zero-field to determine the pNRM (IZ- technique). Another important modification of the Thellier method is the IZZI-method (Yu et al., 2004), which by its name is a combination of the Coe and the Aitkin methods. It was also the preferred Thellier-type method used in this study (Chapter 2). This technique has the power to easily detect so called pTRM tails (as will be discussed later).

However, the biggest drawback in any Thellier-type study is the risk that chemical and mineralogical transformations will affect the magnetic grains during the multiple heating steps, and thus the laboratory induced TRM might not necessarily involve the same grains as the NRM (McClelland, 1996). In order to detect these problems, the pTRM check was introduced by Thellier and Thellier (1959). The pTRM check tests for duplication of a TRM at one or several previous temperatures by reheating the specimen at a lower temperature under H_{lab}. If the new value is significantly different from the previous one, it is likely that the magnetic grains were affected by alteration during the previous heating steps at higher temperatures, hence the measurement is not regarded as reliable. Another disadvantage lies in the fact that pTRM checks increase the number of heating steps, making a full Thellier experiment very time

consuming. In general the success rate of Thellier-type PI experiments does not exceed 20 % (Valet et al., 2003), which reinforces the importance of performing detailed preliminary rock magnetic analyses, which can help to discard unsuitable samples for PI experiments, i.e. samples that are most prone to alteration or most characterised by MD remanences.

Another limiting factor of the Thellier-type methods are MD remanences, which are quite common in lavas. Unlike SD grains, MD grains have diverging T_{UB} and T_B, thus violating the law of reciprocity. A direct consequence is the existence of two different slopes on the Arai plot. To detect for MD remanences during a PI experiment, the pTRM-tail check was introduced (e.g. Shcherbakova and Shcherbakov, 2000). The test consists of imparting a second pTRM at the same temperature Ti, after the sample had received a pTRM at Ti. If both pTRM at Ti are equal, then the ferromagnetic grains have the same blocking and unblocking temperature and the measurement is reliable. More recently, Krása et al. (2003) introduced a test for checking the additivity law. For the additivity check, a sample is demagnetised at a lower temperature after it has been heated in-field at two consecutive steps. In the case of MD grains with, the magnetisation will correspond to the actual difference of the pTRM between the two steps.

The Shaw method

An alternative approach for determining the absolute PI is the Shaw method (Shaw, 1974). It requires a single TRM acquisition above the highest Curie temperature and employs the laboratory proxy anhysteretic remanent magnetization (ARM). First the NRM of a sample is measured before it undergoes alternating field demagnetization in order to define its coercivity spectrum prior to heating. Then, the sample is given a first anhysteretic remanence (ARM_1) by subjecting the sample to progressively higher peak AF which decay in the presence of a small bias field. ARM_1 is then also AF demagnetized to establish the relationship between the coercivity spectrum of the NRM and the ARM. Then a total TRM is imparted above the highest T_C, which will again be demagnetised using AF. Finally, the sample is given a second ARM (ARM_2) and is AF demagnetised for the last time. The basis for determining the PI is the comparison of the demagnetization curves of NRM and TRM using the same coecivity spectra. If the first and second ARMs have the same coercivity spectrum, meaning that no alteration has occurred and this non-altered interval of AFs is then used to determine the PI as the slope NRM/TRM. If the coercivity spectrum has changed, the NRM/TRM ratio is suspect, and the sample probably underwent thermal alteration. Although this technique is significantly faster to perform compared to any Thellier approach, it suffers from the advanced risk of thermo-chemical alteration, which is significantly enhanced when heating a sample above its highest Curie temperature.

The microwave method

The same experimental protocols as in Thellier-type experiments can be carried out with specifically tuned microwave ovens instead of thermal ovens. Here, microwaves affect the magnetic grains in a similar fashion than standard thermal heating does, however, only the magnetic grains are affected directly by the microwaves while the bulk matrix is left untouched. Hence the possibility of alteration is significantly reduced. Compared to Thellier-type experiments, the measurement time using the microwave method is also significantly reduced. Concerns have been raised by Valet (2003) or LeGoff and Gallet (2004) that the theoretical equivalence between thermal- and microwave unblocking has not yet been explained. However, several recent studies using the microwave method have yielded promising results and comparison studies with Thellier-type studies as well as comparison with direct observatory data often showed excellent agreement (e.g. Casas et al., 2005). Up to date this technique is only employed by the Liverpool palaeomagnetic group, which operates the only microwave system available.

Alternative materials:

Rather than focusing on optimising the laboratory PI determination procedure, several other researchers have attempted to use materials that are less prone to biasing factors such as alteration and MD remanences. Pick and Tauxe (1993) were the first to propose that basaltic glass would be an ideal material for PI studies because its magnetic population is consistent with very fine titanomagnetite grains of single domain magnetic structure. Besides the difficulty in collecting submarine samples, the reason that prevents it from several palaeomagnetic applications is that basaltic glass samples do not allow to recover the direction of the field, thus making it impossible to deal with the full-vector. The use of single plagioclase crystals as a viable source for PI data has been advocated by Cottrell and Tarduno (1999). The reason is, similar to basaltic glass, that these crystals are less affected by alteration during laboratory heating. Furthermore the direction can be obtained from sister specimens, while plagioclase crystals are picked after crushing sub-samples from the same core. The main difficulty that limits a wider use of this technique is the sometimes extremely low intensity of the plagioclase crystals, which can be beyond the noise level of modern SQUID magnetometers.

The multispecimen parallel differential pTRM method

Unlike the Thellier method, the MS method of Dekkers and Böhnel (2006) is, according to the first-order symmetry theory of Biggin & Poidras (2006), independent of magnetic domain state, thus in theory allowing for all magnetic grain sizes to be processed. The sample processing time is also considerably shorter (25-50%) compared to a Thellier-type experiment because multiple samples are used, which are at best subjected to only one heating step each. The first-order symmetry property of pTRM in MD grains (Biggin and Poidras, 2006) states that partial demagnetisation and remagnetisation treatments performed on samples containing MD grains cause changes in magnetisation that differ only in their relative magnitudes (a property otherwise thought only to exist for non-interacting SD grains). Both Biggin and Poidras (2006) and Dekkers and Böhnel (2006) have shown experimentally that if a MD sample has a full TRM and a pTRM is induced parallel to the TRM, the intensity of the resultant remanence (pTRM + original TRM) will approximately equal the original TRM, if the laboratory field is equal to the inducing field of the TRM. If the laboratory field is less than the inducing field, the overall remanence will decrease, if greater, the remanence will increase. The laboratory field is applied during both the heating and the cooling cycle, which is necessary to avoid potentially significant demagnetisation of the sample. Applying this concept to a multispecimen PI experiment means that the palaeointensity is determined as the field strength at which the composite remanence after pTRM acquisition (the difference between pTRM and TRM) and the original TRM is zero. Therefore, simply plotting a linear regression through the composite remanences for a range of field values yields the PI. The MS method requires the use of multiple samples. Each sample is subjected to only one in-field heating step at a moderate temperature, which significantly reduces the effect of heating-induced alteration. The field values are progressively increased for different sub-samples. In an ideal MS experiment, the pTRMs are induced parallel to the original NRM.

1.9 Databases of absolute palaeointensities

Since the 1990's enormous effort has been devoted towards assembling absolute PI data in databases (e.g. Tanaka and Kono, 1994; Perrin and Shcherbakov, 1998; Perrin and Schnepp, 2004). Most currently available absolute PI data is now compiled in two databases, the GEOMAGIA50 database (Donadini et al., 2007; Korhonen et al., 2008 and the PINT08 database (Biggin,submitted). The GEOMAGIA50 includes only PI data from the last 50 ka that was acquired from natural rocks (i.e. lavas, intrusive bodies, baked contacts), as well as PI data obtained from fired archaeological artefacts (i.e. potteries, ceramics, bricks, kilns, etc.). Palaeointensity data from GEOMAGIA50 has recently been used for constructing new regularized spherical harmonic field models for the last 3 (Korte et al., submitted), or for a reconstruction

of the variation in dipole moment for the last 50 ka (Knudsen et al., 2008). The PINT08 database (Biggin, 2008) includes all other PI data obtained from lava flows, for the time period 0.05 to 3500 Ma. Figure 1.4 shows that the spatial and temporal distribution of PI data is, by far, not homogenous, with the main concentration of PI data being located in central Europe. The amount of PI data from GEOMAGIA50 decreases exponentially with increasing age. The majority of the 0.05-5 Ma PI data from the PINT08 data stem from the last 1 Ma. In both databases the Trans-Mexican Volcanic Belt is particularly underrepresented, which highlights the importance for acquiring more PI data from this region.

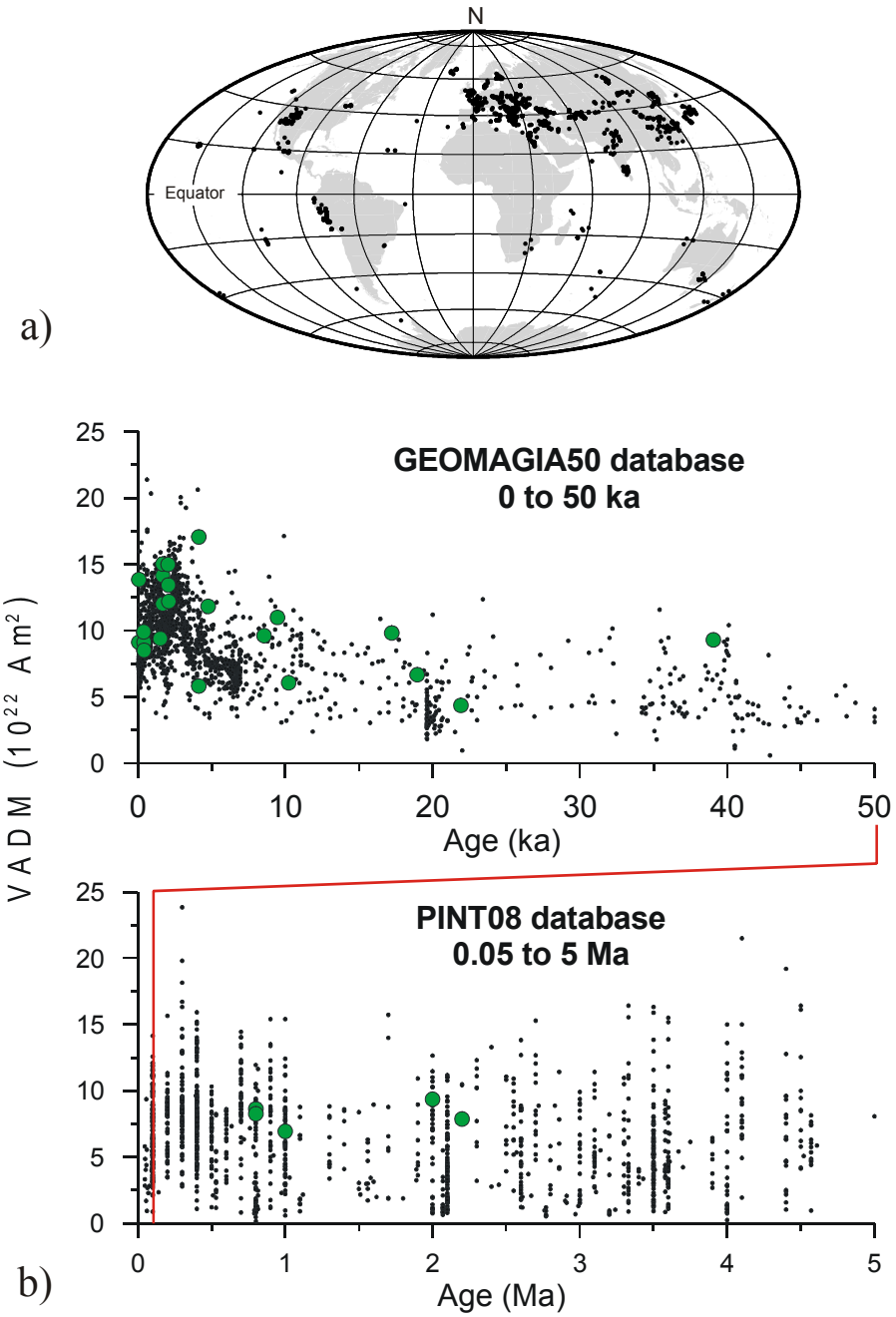

Figure 1.4. a) Global distribution of absolute palaeointensity data, b) Palaeointensity data from GEOMAGIA50 and PINT08 (0.05 to 5 Ma). Data from Mexico is indicated by green circles.

1.10 Review of manuscripts:

Manuscript 1

The use of mini-samples in palaeomagnetism

(H. Böhnel, **D.M. Michalk**, N.R. Nowaczyk and G.N. Gonzalez)

In this study the site-mean directions and statistical parameters of 12 lava flows are compared. The lava flows were sampled with commonly used one-inch standard palaeomagnetic samples (~25 mm diameter) and with mini-samples (~12 mm diameter). This data revealed that magnetic particle distribution is similar for both sample sizes and that site mean directions obtained for both sample sizes were indistinguishable in most cases. Dispersion parameters k were slightly lower for mini-samples than for standard-samples, which reflects that orienting and measurement errors are in generally larger for mini-samples. However, this was overcompensated by the generally larger number of mini-cores recovered in the field. Furthermore, for both k and α_{95} the data from mini-samples showed less variability than from standard-samples. This is interpreted also to result from the larger number of mini-samples per site, which better averages out the detrimental effect of undetected abnormal remanence directions. Results from this study indicate that for volcanic rocks, the mini-sampling technique does not present a disadvantage in terms of the overall obtainable precision. Moreover, mini-samples do represent advantages during the field work because they are more easily recovered and they can be processed faster in the laboratory, which is of particular advantage when carrying out paleointensity experiments.

Manuscript 2

Evaluation of the multispecimen parallel differential pTRM method: A test on historic lavas from Iceland and Mexico

(**D.M. Michalk**, A.R. Muxworthy, H. Böhnel, J. Mclennan and N.R. Nowaczyk)

In the view of the first encouraging experimental tests by Dekkers and Böhnel (2006) in which the MS method returned the correct PI in three simulated experiments performed on non-ideal material (natural and synthetic MD grain assemblages) and on one historic lava flow (the 1943-1952 Paricutin lava flow), the MS method was undergone a rigorous evaluation by applying the MS method to samples from 11 historical lava flows. For this, samples from historical lava flows from Iceland and Mexico were considered from which the actual field intensity was known, either from contemporary magnetic observatory data, or from magnetic field models. In addition, a set of sister samples sister from five Icelandic flows were used for a Thellier-type study (after the IZZI protocol) which also allowed for comparing the PI results from both methods. The aim of this study was to estimate the feasibility of using the MS method for routine PI determinations.

Results from the MS experiments revealed that 6 PI estimates from 11 historical lava flows are very close or indistinguishable within the range of error from the expected intensity. This observation largely confirmed the findings from the initial study of Dekkers and Böhnel (2006). However, a bias towards overestimation was observed because from in total 12 PI estimates, 10 gave results too high. A comparison between the intensity error fractions (IEF) with the bulk magnetic domain state parameter M_{RS}/M_S indicates that this overestimate increases as the material becomes more MD like (Fig. 1.5). This apparent bias implies that the MS method might not be entirely independent of magnetic domain state as previously proposed by Dekkers and Böhnel (2006). The main reason for this bias towards overestimates

in the palaeointensities is assigned to an effective demagnetisation of the samples during progressive re-magnetisation in the laboratory experiment. Yet, in comparison to Thellier data acquired on sister samples from 5 flows, the corresponding MS palaeointensities still returned estimates closer to the expected field values. Furthermore, Thellier data showed inaccuracies of up to around 20 % on individual high quality samples and a much lower success rate whereas the MS method returned PI estimates for all investigated flows. This included samples characterised by low Curie Temperatures which failed the Thellier experiment they suffered from thermal alteration on heating above 400°C. This observation is also taken as an indication that the MS method has a higher potential to retain PI estimates from such critical material. Thus, from the majority of results in this study, the MS method appeared as a viable alternative to the Thellier method for future PI studies.

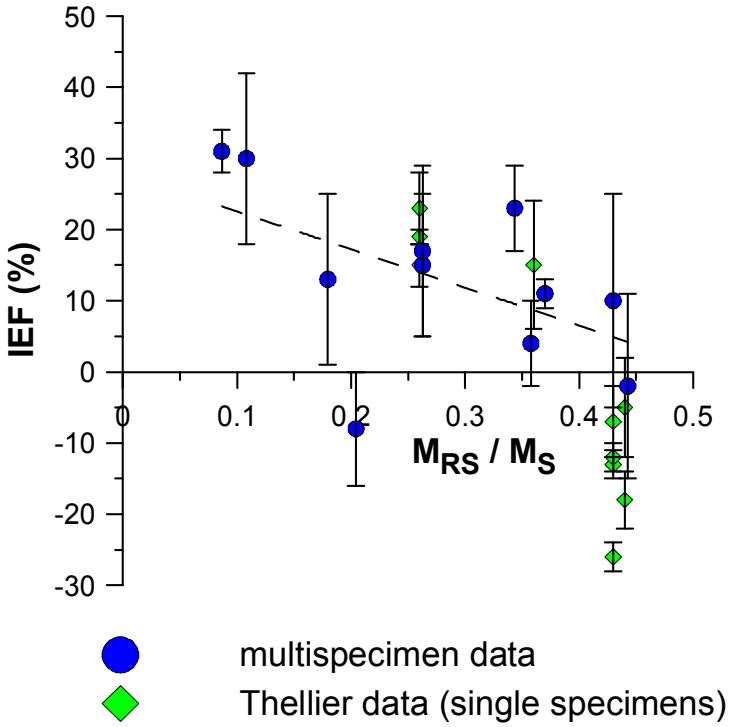

Figure 1.5. Intensity error fraction of the multispecimen (blue circles) and Thellier (green diamonds) palaeointensity experiments versus M_{RS}/M_S (treated as an estimate of multidomain contribution to the bulk magnetic remanence) for samples from historic lava flows from Iceland and Mexico. A linear regression (dashed line, $R^2 = 0.3$) is indicated by a dashed line for the multispecimen data.

Manuscript 3

Evidence for geomagnetic excursions recorded in Brunhes- and Matuyama-Chron lavas from the Trans-Mexican Volcanic Belt

(**D.M. Michalk**, N.R. Nowaczyk, H. Böhnel, G.J. Aguirre-Diaz, S. Ownby, M. Lopez-Martinez and J.F.W. Negendank)

This paper reports the results from an integrated palaeo- and rockmagnetic study on 63 radioisotopically dated lava flows from within the Trans-Mexican volcanic belt, with ages from 6.4 Ma to recent (but most being younger than 1 Ma), and new age data after the $^{40}Ar/^{39}Ar$, which were acquired for 11 lava flows. The main objective of this study was to find some of the geomagnetic excursions within the Brunhes- and Matuyama Chron in order to possibly constrain some of the geomagnetic excursions included in the geomagnetic instability timescale of Singer et al. (2002, 2007, 2008a,b).

Rock magnetic measurements revealed that, in general, the remanence was carried by titanomagnetites of pseudosingle-domain magnetic structure, although titanomagnetites with higher Ti-contents and (titano-) haematite was also occasionally present. The scatter of virtual geomagnetic poles was calculated from lava flows younger than 1.7 Ma and used to estimate palaeosecular variation. This data indicates normal values of palaeosecular variation for Mexico that are consistent with latitude dependent Model G of McFadden et al., (1988, 1991). A correlation of 56 palaeomagnetic mean-vectors to the Geomagnetic Polarity Timescale, supplemented with data on geomagnetic excursions, revealed that four, possibly five geomagnetic excursions were recorded by lava flows. Two lavas with nearly fully reversed directions (dated at 592 ± 20 and 671 ± 13 ka, respectively), were correlated to the Big Lost (579 ± 6 ka) and the Delta/Stage 17 (~ 670ka) excursions, respectively. Furthermore, seven lava flows dating of Matuyama Chron were found to have recorded normal polarity magnetizations. From these, one flow dated at 933 ± 40 ka could have been emplaced, either during the Kamikatsura- (900 ± 6 ka), or the Santa Rosa excursion (936 ± 8 ka), while another flow dated at 1600 ± 60 ka, could have possibly been emplaced during the Gilsa excursion (~ 1570 ka).

Figure 1.6. Palaeolatitude of the virtual geomagnetic poles of lavas investigated in this study with a tentative correlation to the geomagnetic polarity timescale modified for geomagnetic excursions of the last 2 Ma. Excursions highlighted in white are well documented excursions with acceptable age control. Excursions highlighted in grey indicate excursions with restricted age control, which require further ratification. Sites that are associated with Brunhes (Matuyama) Chron excursions are highlighted with green (yellow) rectangles and are indicated by red stars. The directional data of excursional flows is shown on stereoplots.

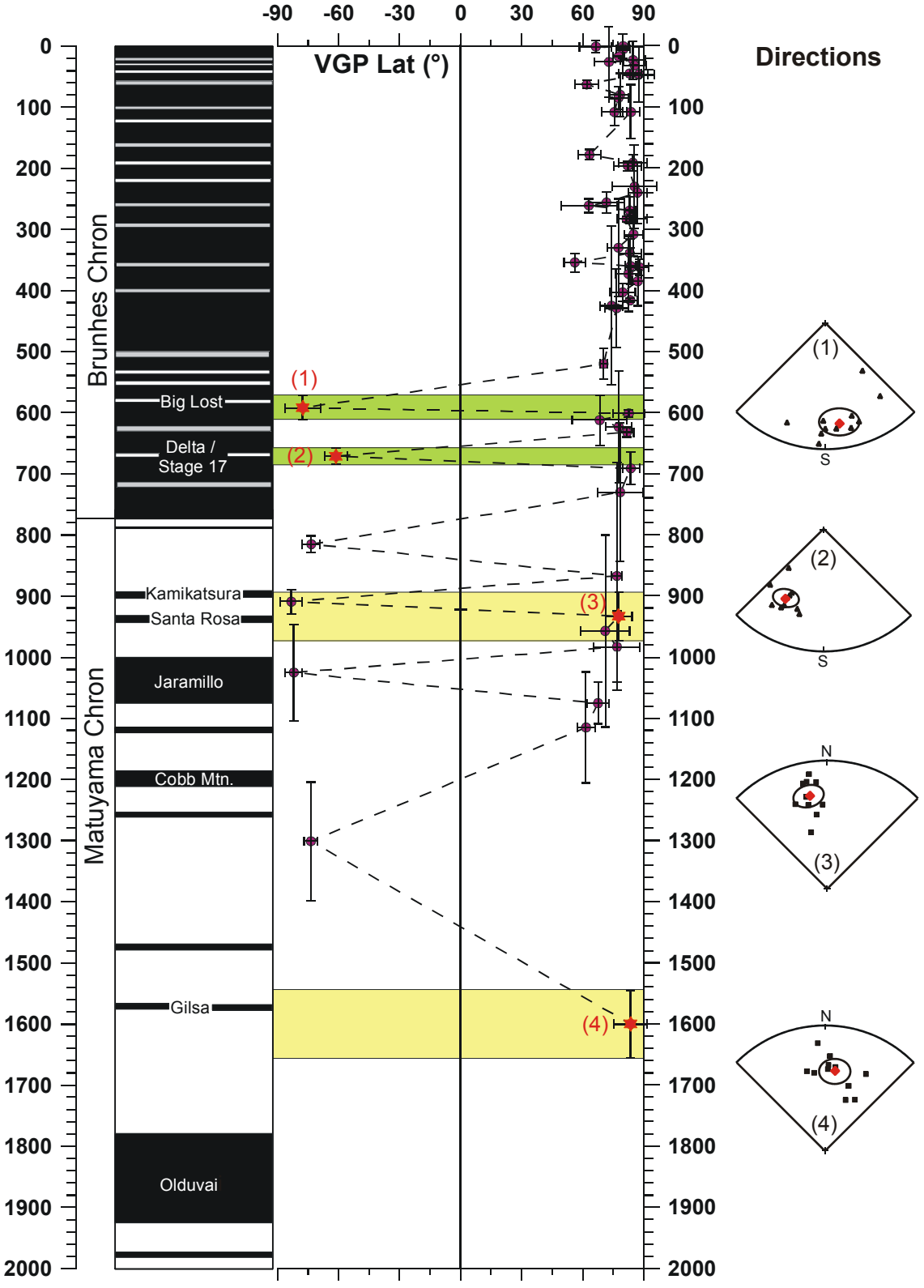
-90
-60
-30
0
30
60
90
VGP Lat (°)
Directions
Brunhes Chron
Matuyama Chron
Big Lost
Delta / Stage 17
Kamikatsura
Santa Rosa
Jaramillo
Cobb Mtn.
Gilsa
Olduvai
(1)
(2)
(3)
(4)
N
S
0
100
200
300
400
500
600
700
800
900
1000
1100
1200
1300
1400
1500
1600
1700
1800
1900
2000

Manuscript 4

Application of the multispecimen palaeointensity method to Pleistocene lava flows from the Trans-Mexican Volcanic Belt

(**D.M. Michalk**, A.J. Biggin, M.F. Knudsen, H.N. Böhnel, N.R. Nowaczyk and S. Ownby)

This paper reports 32 new PI estimates acquired on 51 lavas subjected to PI studies after the MS method from which palaeodirections are reported in Paper 3. This study reports the application of the MS method to the oldest rocks yet subjected to this method and had the aim to obtain further information about its applicability for future PI studies of older rocks.

The new PI estimates were compared to reconstructions of the global dipole moment based on PI data included in the GEOMAGIA50 and PINT08 databases of absolute paleointensity and to a global stack of relative PI curves calibrated to absolute values (Valet et al., 2005). It revealed that, with a high degree of statistical significance, the PI estimates were on average around 30 per cent higher than expected. However, other published PI data from Mexico, mainly after the Thellier method, were also observed to be high relative to global records. This could be taken to indicate that, similar to today's situation, persistent non-dipole geomagnetic features might be responsible for the higher than expected results in Mexico. While this possibility cannot be discounted completely, the balance of evidence rather suggests an artificial biasing of most measurements towards high values. The generally high PI estimates seem to corroborate the results from the study on historic lava flows (presented in Paper 2) and other studies on synthetic samples (e.g. Fabian and Leonhardt, 2007) in which domain state effects were found to cause overestimates of the PI by up to 30 per cent in the MS method. The cause of this overestimate is most likely related to an asymmetry in the pTRM demagnetisation and remagnetisation process, i.e. to effective demagnetisation during thermal cycling in an applied laboratory field. A previous study by Fabian and Leonhardt (2007) already suggested that this asymmetry is probably more important for grains of pseudo-single domain size. Since hysteresis data from this study suggests PSD grains to be present in most of the investigated rocks, their observation may explain at least some of the high PI values. However, the degree of the overestimate in the majority of these new PI estimates after the MS method is expected to be not larger than what might be expected from Thellier experiments performed on samples with a similar given degree of multidomain behaviour. In addition, seven lava flows, which were studied with a different experimental protocol that included a preceding demagnetisation step of 200°C in order to erase viscous remanences, produced results which may have been further biased towards higher intensities. This additional bias is expected from theoretical considerations and may represent a challenge to future application of the MS method to older rock units, but it could potentially be avoided in future studies by performing measurements of the sample moment at temperatures higher than the blocking temperature of any overprint, which would require the use of rather specialised equipment that allows the moment of a sample to be measured as it is heated.

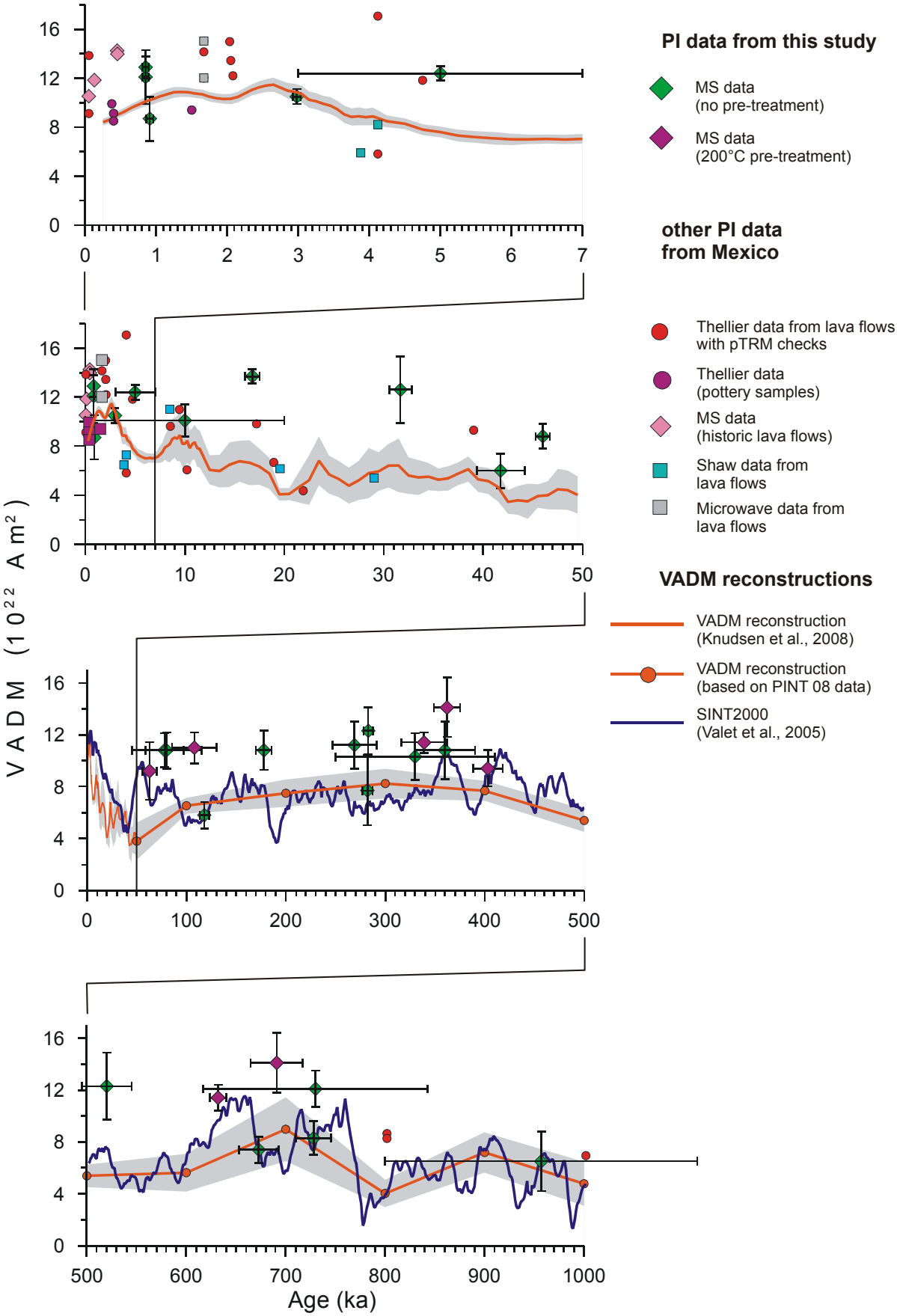

Figure 1.7. Multispecimen palaeointensity estimates from this study (diamonds) with associated uncertainties, depicted against reconstructions of the global dipole moment and existing palaeointensity data from Mexico.

1.11 Conclusions

This thesis work made new contributions to palaeointensity studies, geomagnetic excursions and palaeomagnetic sample methodology. A synthesis of the most significant findings is presented.

Palaeointensity studies

A study of 11 historical lava flows from Iceland and Mexico after the multispecimen parallel differential pTRM method allowed a thorough testing of the method. It revealed that the MS method may have the tendency towards overestimating the PI because from in total 12 PI estimates, 10 were higher than expected values. A loose inverse correlation between the intensity error fractions (IEF) versus the domain state parameter M_{RS}/M_S could be taken as an indication that domain state effects bias the MS method towards higher intensities, i.e. as the material becomes more MD like, the overestimate in PI increases. This implies that the MS method is most likely not entirely independent of domain-state as was originally proposed and corroborates the results from previous studies (McClelland et al., 1996; Fabian and Leonhardt, 2007) which have demonstrated that simply heating and cooling samples to temperatures below T_C while applying a magnetic field (the same process as is done in a MS experiment) can cause partial demagnetisation of a sample. If a sample demagnetises slightly during thermal cycling, then a higher field than that originally used to impart the full pTRM will be required to maintain the sample's magnetisation at its original level and as a consequence, this process will produce an overestimate in an MS experiment. However, in comparison to PI estimates after the most commonly used Thellier method on 5 flows, the corresponding MS PI estimates were found to be still closer to expected intensity values. In addition, the MS experiments were found to have a significantly higher experimental success rate than Thellier experiments and were successful in retrieving a reasonable PI estimate on critical material that failed the Thellier approach. Therefore, PI data on historical lava flows obtained in this study have not revealed any evidence that the most commonly used Thellier method has any particular advantages over the MS method, at least not on the material studied up to now.

This reasoning seemed probative to apply the MS method in the subsequent study to 51 lava flows dating from the last 3.5 Ma from the Trans-Mexican Volcanic belt and it revealed some further important constraints about the future applicability of the method in PI studies. A comparison of 32 new MS PI to reconstructions in the dipole moment based on PI data taken from the global PI databases revealed that these new MS results are, with a high degree of statistical significance, by about 30 per cent on average higher than expected. Interestingly, other published PI results from Mexico, although rare, mainly after the Thellier method, were also observed to be high relative to global records. In comparison to this published data, which was mainly acquired after the Thellier method, the MS PIs were found in most cases to be closer to global dipole records. The inferred high PIs with respect to global values on both, the published Mexican Thellier and MS data from this study, could be taken as an indication that, similar to today's situation, a persistent non-dipole field may be responsible for the higher than expected values. An evaluation of the effect of a non-dipole field for Mexico based on a comparison of regional and global dipole reconstructions for the last 3 ka revealed no apparent bias towards high filed intensities for Mexico, which obscures the significance of this observation and the current quality of the PI database does not yet allow assessing the role of non-dipole effects for earlier periods. Such persistent non-dipole effects can not be discounted altogether at this stage, but it would mean that the required non-dipole effect must have been present over a longer period than the timescales at which normal secular variation operates. It seems therefore more likely that the MS measurements are artificially biased towards higher values. As corresponding hysteresis data suggests that PSD grains are likely to be present in most of the investigated rocks it is assumed that the earlier mentioned asymmetry in the pTRM demagnetisation and remagnetisation process might be an explanation at least for some of the high PI values. This asymmetry, was demonstrated in a previous study by Fabian and Leohardt (2007), to be most important for grains of pseudo-single domain magnetic structure. The observation of PSD grains in most investigated lavas in

conjunction with the results obtained on historical lavas in this study strongly suggest that domain state effects can bias the MS method towards high intensities.

This study also revealed that an additional bias may be expected for lava flows that are processed with a different experimental protocol that includes a preceding demagnetisation treatment. Seven flows that were processed with an additional 200°C demagnetisation step in order step to erase viscous remanences before the MS experiment returned PI estimates which are likely to be additionally biased towards higher values. This additional bias, which is expected for samples with non-SD magnetic properties from theoretical considerations, is independent from the violation of pTRM symmetry constraints and represents a major challenge that must be carefully evaluated in the future if the MS method is to be successfully applied to older rocks. However, it could potentially be avoided by measuring the sample moment at a temperature higher than the blocking temperature of any overprint by using equipment that allows the moment of a sample to be measured as it is heated.

Geomagnetic excursions

A new record of 56 palaeomagnetic mean vectors obtained on Mexican lava flows revealed further volcanic evidence for at least 4 geomagnetic excursions, i.e. the Big Lost- and the Delta/Stage17 excursions during the normal Brunhes Chron, and either the Santa Rosa- or Kamaikatsura- and the Gilsa excursions during the reverse Matuyama Chron. The two lava flows, which are correlated with the Big Lost- and Delta/Stage17 excursions, respectively, were found to have recorded directions that deviate by almost 180° from the geographic North Pole. These reversed polarity magnetisations may give some new evidence that in particular the Big Lost- and the Delta/Stage17 excursions may represent short periods of reversed geomagnetic polarity of global validity, such as was previously found for older cryptochrons or tiny wiggles, during which the field completed a full reversal for a short time (e.g. Roberts and Lewin-Harris, 2000).

Palaeomagnetic sampling

For palaeomagnetic studies of volcanic rocks, the 12 mm mini-sample technique, which was applied throughout this study, seems to offer no disadvantage in terms of the overall obtainable uncertainty of site-mean directions over the still commonly used 25 mm standard-sample technique. Magnetic particle distribution was found similar on the scales of 1 cm^3 for mini- and 11 cm^3 for standard samples and potentially limiting factors such as orienting and measurement errors are easily compensated for by taking larger numbers of mini-drill cores in the field. The latter also helps for averaging out the detrimental effect of abnormal remanence directions. Because mini-samples are more easily recovered in the field and processed faster in the laboratory, this technique is of particular advantage when carrying out PI experiments. Results from this study have shown that for volcanic rocks, the mini-sample technique can be taken as a viable alternative to the commonly used standard-sample technique.

1.12 Future outlook

For a better understanding of the complex dynamo process and in order to improve a more detailed view on the Earth's magnetic field behaviour in the past, more high quality absolute PI data is still needed. The new multispecimen parallel differential pTRM method clearly offers the possibility to acquire significantly larger datasets than the Thellier method due to the reduction in laboratory processing time and because it is less prone to biasing effects such as thermal alteration. However, as this study has shown, it is not entirely domain size independent, which means that it should not be applied a priori to all lava samples of a study. Future studies should therefore investigate this domain state bias in detail and find ways to possibly correct for this bias. As a next step it is suggested to carefully investigate the effect

of the pTRM acquisition temperature in the MS experiment. This could be done by applying a MS experiment at different temperatures to several sets of samples either from one historical lava flow, or alternatively to synthetic samples that were imparted by a laboratory TRM of known strength.

More comparison studies of different PI methods are also needed, in particular on different historical lava flows with distinct magnetomineralogical characteristics. This could show if some of the PI methods in use are more suitable for certain types of samples than others. This study has already revealed some indication that the MS method has most likely a higher potential in acquiring PI estimates on lavas characterised by low Curie temperatures, which could mean that the MS method should preferably be used on such critical material.

Lastly, for studies on geomagnetic excursions recorded in lava flows, more high quality age data is indispensable. The majority of lava flows investigated in this study had unfortunately large dating errors. Considering the resolution of the Earth's magnetic field with the associated distortion of its geometry, age errors should be at least less than 10 ka. In this respect, the lava flows from this study, tentatively correlated with known geomagnetic excursions, should be precisely re-dated before including them in the Geomagnetic Instability Timescale.

2. The use of mini-samples in paleomagnetism

Harald N. Böhnel [a], Daniel M. Michalk [b], Norbert R. Nowaczyk [b], and Gildardo G. Naranjo [a]

[a] *Centro de Geociencias, UNAM-Campus Juriquilla, Queretaro, Mexico*
[b] *Helmholz-Zentrum Potsdam, Deutsches GeoForschungsZentrum, Germany*

Submitted to: Geophysical Journal International

Abstract Rock cores of ~25 mm diameter are widely used in paleomagnetism but smaller diameters are occasionally used as well. We sampled 12 lava flows with 25 mm standard-cores and additionally with 12 mm mini-cores, and compared the obtained site-mean directions and their statistical parameters. Site-mean directions obtained for both sample sizes are indistinguishable in most cases. Dispersion parameters k are on average slightly lower but confidence limits α_{95} are also slightly smaller for 12 mm mini-samples than for 25 mm standard-samples. This probably reflects that orienting and measurement errors are larger for mini-samples, but this is overcompensated by a generally larger number of cores that are recovered in the field. For both k and α_{95} the data from mini-samples show less variability than from standard-samples. This is also interpreted to result from the larger number of mini-samples per site, which better averages out the detrimental effect of undetected abnormal remanence directions. Sampling of volcanic rocks with mini-samples therefore does not present a disadvantage in terms of the overall obtainable uncertainty of site mean directions. Apart from that, mini-samples do present advantages during the field work and can be processed faster in the laboratory, which is of particular advantage when carrying out paleointensity experiments.

1. Introduction

The size of paleomagnetic samples has changed over time, according to the prevailing sampling and measurement methods (e.g, Collinson, 1983). In times of astatic magnetometers samples were large as they were collected as oriented blocks. With the use of rotating spinner magnetometers (with induction or fluxgate sensors), smaller samples were required, typically cylinders of 20-25 mm length and 25 mm diameter (hereafter referred to as standard-samples). Today, such standard-samples of about 11 cm^3 are still used in almost all paleomagnetic laboratories worldwide. Besides that, cubic or rectangular samples of similar volume are used for sampling unconsolidated sediments in small plastic containers. In consequence, most paleomagnetic laboratory instruments are designed for measuring such samples, so are rock drills and orienting devices to recover samples in the field.

Before the advent of the superconducting technology, sample size was indeed of major importance. Because of the higher signal to noise ratios in modern magnetometers today the accurate determination of the magnetization intensity and direction of standard samples is less of a problem. In fact, the sensitivity of modern magnetometers is more limited by effects such as holder contamination and electronic interferences than by its ultimate noise level. In this work we evaluate the effects of using 10 mm long cylindrical samples with a diameter of 12 mm (hereafter referred to as mini-samples), in terms of the total

dispersion obtained from sampling over laboratory measurements to data analysis. The present paper differs from Borradaile et al. (2006), who limited their analysis to the effect of using mini-samples with cubic adapters in a Molspin spinner magnetometer to increase the orienting precision when inserting the samples in three perpendicular positions, thus only considering the effect on the measurement precision. The present paper also pretends to demonstrate by direct comparison of data that previous work using mini-samples by Michalk et al. (2008, and submitted) on Mexican volcanic rocks, is of similar overall precision compared to standard-samples. At the time of publishing that, work this hypothesis could only be proposed on the basis of a general comparison of overall dispersion of paleomagnetic data recovered from different volcanic rocks of the Trans-Mexican Volcanic Belt.

2. Comparison between mini- and standard-size sample methods

2.1 Field Work

Standard-samples are recovered in the field mostly by using gasoline powered portable rock drills. Commercially available rock drills built for that purpose use small combustion engines as from chain-saws or portable drills. A water jacket is attached to the engine, which takes a diamond tipped drill bit. Water from a pressurized fumigation tank is used as a drilling fluid/coolant, and to remove the debris out of the drill hole. Such a rock drill typically weights between 5 and 8 kg plus the water tank.

For the recovery of 12 mm mini-cores similar but much smaller equipment can be used, because less cutting power is required due to the reduced torque and reduced amount of rock to be cut. Small electric drills with an attached water jacket are perfectly suitable for this application. There are many choices between commercially available drills, such as cordless drills or 110/220 Volt drills. The former are easily carried to the field and several charged battery packs give sufficient autonomy for the recovery of a reasonable number of 12 mm drill cores, in general 12 to 15 cores per charge, as practical experiences have shown. The latter drills may be connected to a small generator or via a dc to ac inverter connected to the car battery. An extension cable of suitable length then allows for a good working radius around the generator or the car. Depending on the model, the weight of such an electrical drill is about 20-50% of a combustion engine drill. Additionally the amount of the required cooling water is much reduced.

Today, geological field work is often carried out in remote and difficult accessible areas, which makes volume and weight of field equipment and number of recovered samples an important aspect. For such considerations, mini-samples offer clear advantages, especially when the rock units are not accessible by field trucks and when the drill, the water and the samples have to be carried to and back from sampling localities. Thus, lighter and more ergonomic rock drills will generally make it easier to carry out successful field campaigns.

2.2 Core orientation

Orientation of drill cores in the field is the main contribution to the experimental dispersion of paleomagnetic remanence directions (e.g., Böhnel & Schnepp, 1998). Such errors occur when marking a reference line with a brass rod onto the core, which later serves as a reference line for orienting the sample in any measurement instrument. As the accuracy of this marking also depends on the circumference of the core, a mini-core with a smaller diameter core will produce larger orientation dispersion than a standard-size core (ca. 2 to 1 circumference relation between 25 mm and 12 mm cores). This effect is difficult to determine experimentally, but a potentially higher dispersion produced by random orientation errors could be accounted for by collecting a higher number of drill cores. Sampling more drill cores would further reduce other random contributions to the site-mean dispersion, produced by features such as fractures, cooling joints, or paleofield inhomogeneities (e.g., Böhnel & Schnepp, 1998).

2.3 Laboratory instruments

Mini-samples can be studied with the same instruments as standard-samples and this was done for the data shown in Tables 2.1 and 2.2. For this purpose, non-magnetic adapters have to be used to insert the mini-sample into the instruments. In Figure 2.1 examples of cylindrical and cubic adapters made of Perspex are shown that can be used e.g. on rotation and long-core superconducting magnetometers. The use of such adapters of course requires that these are cleaned periodically. If future instruments would be designed with holders specifically for mini-samples, such adapters would become unnecessary and the potential contamination would be eliminated.

Figure 2.1. Two mini-samples of 12 mm diameter with four non-magnetic adapters. Cylindrical adapters allow for measuring mini-samples in equipment that is designed for standard-size samples such as the JR5/JR6 spinner magnetometers, cubic adapters e.g. for measurements on the long-core 2G system. A standard-size sample with 25 mm diameter is shown for comparison.

Coil systems or electromagnets such as in alternating field (AF) demagnetizers and pulsemagnetizers are used to generate high magnetic fields. Energy requirements to produce a magnetic field of certain intensity are proportional to the volume of the coil and therefore proportional to the size of the sample (e.g. Collinson, 1983), thus they could be reduced considerably for mini-samples. High-field instruments could therefore be of much smaller size, requiring less power-consuming components, and hence making them less expensive. The latter would be of particular importance if these systems use mumetal shieldings, like AF demagnetizers do. Smaller instruments would also reduce space requirements in laboratories. Finally, using similar design criteria as for instruments for standard-samples, higher fields could be achieved. A good example are some pulsemagnetizers, which produce peak fields of 3 Tesla for 25 mm samples but 9 Tesla for 12 mm samples (e.g. Magnetic Measurements Ltd model MMPM10).

Thermal demagnetizers could be designed and built considerably smaller, with important cost benefits due to the much smaller and more effective mumetal shields. Power requirements would be reduced as well. Again, using current designs a considerable larger amount of samples could be accommodated in the heating chamber of thermal demagnetizers, allowing for a significantly higher sample processing rate for each heating step. The higher sample throughput would be of particular advantage for paleointensity experiments, as these require multiple heating steps and thus are more time-consuming than

demagnetization experiments alone. Figure 2.2 shows a sample holder design used in a Magnetic Measurements Ltd model MTD18 with an interior sample space of 40 mm diameter. This holder allows for thermal treatment of 21 mini-specimens oriented with their remanence vectors parallel to the field in the furnace. Up to two similar holders could be used in the ASC Scientific instrument model TD48 and up to four holders in the Magnetic Measurements Ltd MTD80 model, which both have larger heating chambers. Combining this advantage with the already reduced time needed for the multi-specimen parallel differential pTRM paleointensity method (Dekkers and Böhnel, 2006; Böhnel et al., 2008; Michalk et al., 2008), a considerably higher sample processing rate is possible, allowing to extend considerably the paleointensity data base needed for global modeling of the geomagnetic field.

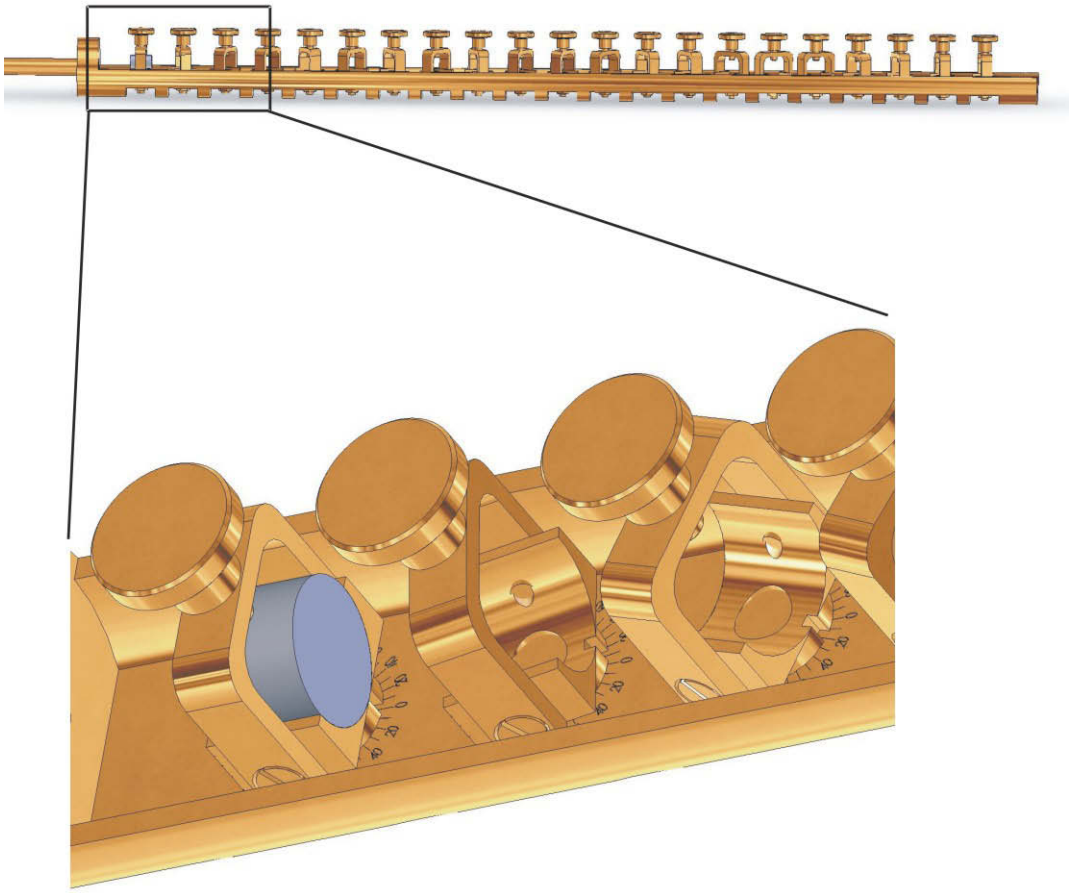

Figure 2.2 Sampleholder for paleointensity experiments made of non-magnetic brass. This prototype, designed and built at GFZ Potsdam, takes up to 21 mini-samples and allows for an orientation of their magnetization vectors parallel to an induced oven field, as it is done in the multispecimen parallel differential pTRM paleointensity method.

Spinner magnetometers would not benefit from mini-samples, as these are already compact. A re-design would only adapt the sensitivity to the smaller samples (smaller pick-up coils or fluxgate ring-cores) and allow a higher rotation speed. In the case of SQUID magnetometers, the access hole could be reduced to half of the diameter as in use today. This would reduce the surface area of the access hole in the dewar and that way reduce the heat loss from the SQUIDs to the environment. Consequently the dewar and the whole system could be reduced in size, and the required cryo-cooler capacity would be less. SQUID pick-up coils would shrink accordingly and positioned closer to the sample, which means that the loss of sample magnetic moment due to its reduced volume could be partly compensated.

Modern SQUID magnetometers are often combined with inline AF-demagnetizers. That way, automated demagnetization routines can be used, allowing for fully automatic measurements of samples and consequently a higher sample processing rate. 2G Enterprises commercializes such a system, where using their long-core setup, suites of up to 8 samples can be demagnetized in one run. AF-demagnetization in 10-12 steps (from 0-100 mT) of one sample set takes around 30 minutes, making it at least 5 times faster than processing the samples manually. This automatic setup can normally not be used for volcanic rocks of standard-sample size, because their high magnetization intensity would saturate the magnetometer. Mini-samples have a magnetic moment that is one order of magnitude smaller and generally within the dynamic range of those SQUID magnetometers, thus allowing for a fast and automatic measurement.

Automated magnetometer systems have not yet been developed for the thermal demagnetization method, except in form of non-commercial prototypes. Mini-samples have only around 11% of the volume of standard-samples, with a c.a. double surface to volume ratio, and may therefore be heated and cooled significantly faster. It seems possible to construct an automated system, in which a mini-sample is subjected to stepwise thermal demagnetization by using a fast, low thermal inertia heater design.

3. Field and laboratory work

In order to evaluate how mini-samples compare with standard size samples in terms of the statistical precision of their results, we sampled 12 sites with both standard- and mini-samples, and applied similar complete paleomagnetic AF demagnetization technique on both sets. As this was done in different field seasons and initially related to the work of Michalk et al. (2008), the number of drill cores and the used laboratory instruments were not identical for both sample sizes. Nevertheless, we consider this experiment useful, because it can be taken as a test for the reproducibility of paleomagnetic measurements performed at different laboratories and by different experimentalists. The reproducibility of results was tested in detail on one lava flow (site LQW), where the same number of drill cores were collected with both sample sizes in close proximity to each other. The remaining 11 sites were sampled with variable numbers of drill cores that were distributed more randomly with respect to each other.

Site LQW is a recent road cut of a massive Tertiary lava flow that was sampled by 13 standard-size drill cores as well as mini-sample cores. At each drill point, standard- and mini-samples were taken separated by less than 10 cm (Fig. 2.3). Six drill cores come from one massive block of about 2 m size, without any fractures or visible internal deformation, while the remnant cores were distributed along the outcrop over a distance of around 40 m. All samples were oriented with similar devices using magnetic and solar compasses. Re-checking orientation values with different devices (e.g., one built in our own workshop and a Pomeroy model OR-2 device, both for 25 mm cores) revealed average differences of azimuth and dip readings smaller than one degree that were random between different drill cores. The average length of drill cores was 58 (38) mm for standard (mini) samples. All cores were later cut into samples of the same length to a diameter ratio of ~0.86, providing 29 standard- and 40 mini-samples. In this study, the

innermost samples of each core were always used (with the exception of three 25 mm cores) to reduce possible alteration effects caused by weathering.

Eleven other sites of lava flows were sampled with both sample sizes. The typical number of drill cores used in paleomagnetic studies were recovered, i.e. ~8 for standard-samples, but ~14 cores for mini-samples. The higher number of mini-sample cores was chosen to compensate for potentially larger orienting errors due to their ~50% smaller circumference. As the recovery of a mini-sample core is so much faster, compared to a standard-sample core, a larger number of such cores can be recovered. In fact the number of cores is less restricted by the drilling itself, but rather by the time required for orienting these cores. In practical terms, almost twice the number of oriented mini-sample cores may be recovered per time unit than standard-sample cores. Results for these sites are shown in Table 2.2. We present the results in terms of Fisher's (1953) unit vector sum R and the precision and dispersion parameters k and α_{95} and the probability that two site mean directions are indistinguishable according to McFadden (1982).

Magnetic susceptibility was measured with an AGICO KLY3 instrument, remanent magnetization vectors determined using AGICO JR5 or JR6 induction magnetometers and all values were corrected for volume differences. Stepwise AF demagnetization was done with an AGICO LDA instrument using a tumbling mechanism. Four mini-sample sets were measured and demagnetized using a 2G Enterprises long-core magnetometer with attached AF demagnetizer. All demagnetization data were analyzed using orthogonal vector plots and principal component analysis (PCA) (Kirschvink, 1980).

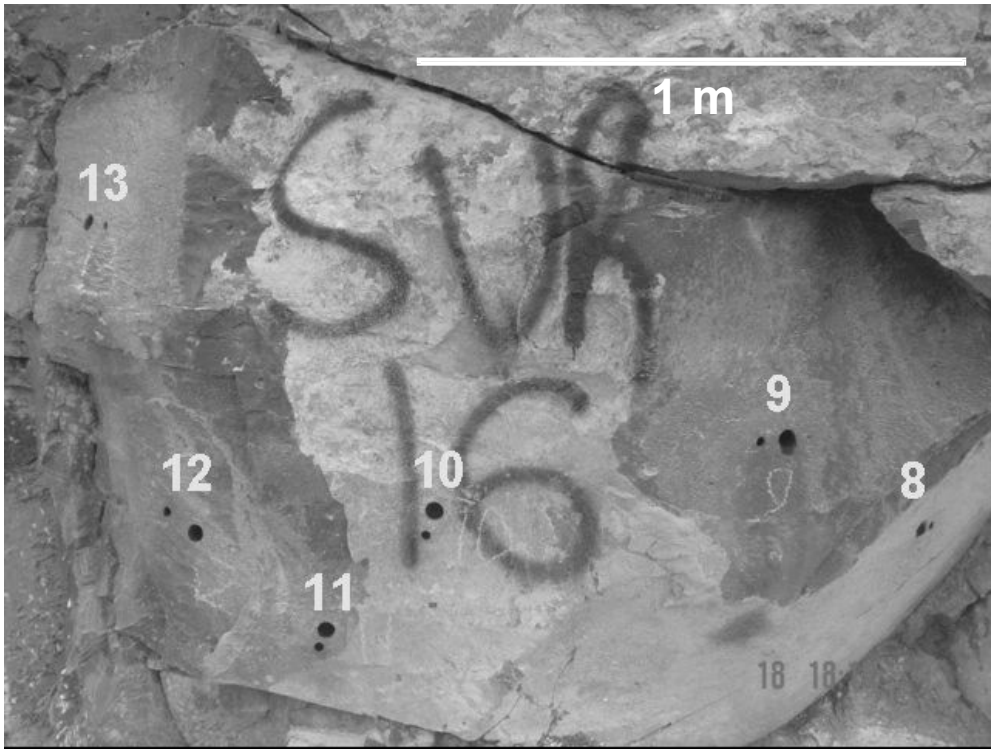

Figure 2.3. Detail of lava flow LQW, sampled in parallel by mini-samples and standard-samples. Numbers are used for sample codes in Table 2.1.

4. Results and Discussion

Table 2.1 lists the results obtained from site LQW for one sample from each core. The natural remanent magnetization (NRM) intensity and magnetic susceptibility were similar for neighboring drill cores, and their overall mean values are indistinguishable when considering their standard deviations, which are between 23% and 37%. Core 10 is characterized by larger NRM intensity and susceptibility than the rest. Here the differences are also larger comparing the two sample sizes, which probably indicates a stronger local inhomogeneity within the lava flow. Otherwise NRM as well as susceptibility show a linear relationship between both sample sizes (Fig. 2.4), with correlation factors close to 1. It shows that there is no significant difference in the distribution of magnetic particles on the scales of 1 cm^3 to 11 cm^3 volume and up to 10 cm distance between the drill cores.

To obtain characteristic remanence magnetization (ChRM) directions, all samples were demagnetized in 6-14 steps up to a maximum of 100 mT. Initially, four of the standard-samples were demagnetized in more detail than the rest, to test for their demagnetization behavior and to detect secondary magnetization components. PCA analysis was generally based on 5 or more data points and resulted in maximum angular deviation (MAD) values between 0.4° and 3.1°, on average 1.5° for both standard- and mini-samples (see Table 2.1). Secondary components were small and easily removed by AF fields of 15 to 30 mT. Only core 5 showed a more persistent secondary overprint, which could not be completely removed even by AF fields of up to 60 mT. Its ChRM direction is based on 3 demagnetization steps only and is therefore regarded as less reliable than the others. Median destructive fields (MDF) were in the range of 50 to 90 mT, which characterizes the lava to be of relatively high coercivity and magnetic stability.

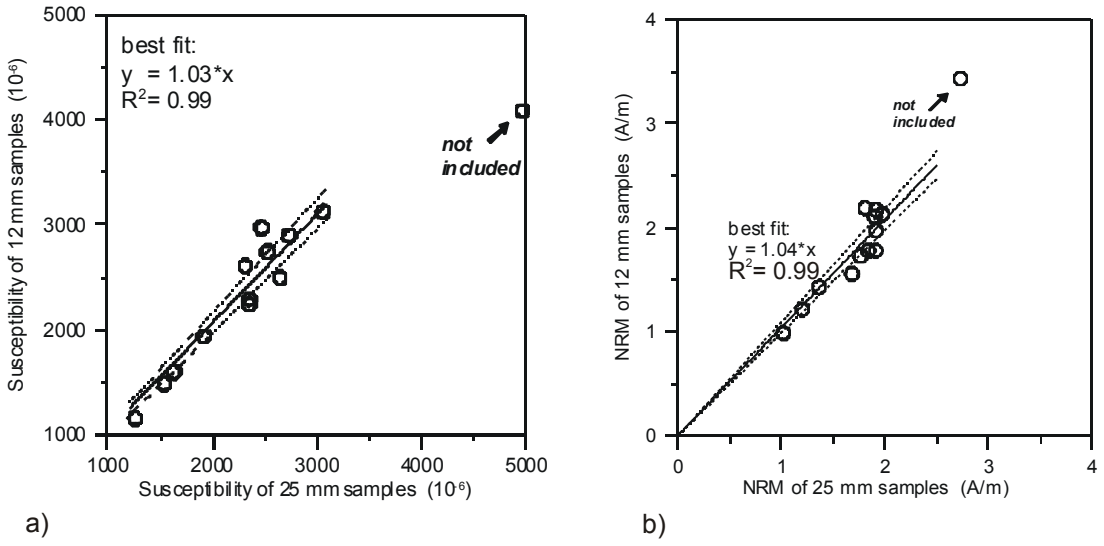

Figure 2.4. Comparison of magnetic susceptibility (left) and NRM intensity (right) as measured for standard- and mini-samples. Diagonal lines denote best fits through the origin, and interrupted lines the standard deviation of that fit.

Table 2.1. Comparison of bulk magnetic properties, demagnetization data, and ChRM directions for standard-size samples and mini-samples from massive lava flow LQW. NRM, natural remanent magnetization intensity; susc, magnetic susceptibility in SI-units; AF-range, range of field amplitudes used to calculate the ChRM direction; Steps, number of demagnetization steps used for PCA; MAD, maximum angular deviation for PCA fit; Dec/Inc, ChRM declination/inclination; a.d.., angular distance between ChRM direction of sample pairs; s.d., standard deviation of average value.

	Standard-size samples (25 mm diameter)								Mini-samples (12 mm diameter)							
Sample	NRM (A/m)	susc (10^{-6})	AF-range (mT)	Steps	MAD (°)	Dec (°E)	Inc (°)	Sample	NRM (A/m)	susc (10^{-6})	AF-range (mT)	Steps	MAD (°)	Dec (°E)	Inc (°)	a.d. (°)
1Z-STD	1.203	1632	23.0	15-100	3.1	345.0	35.3	1Z-MS	1.213	1594	10-100	7	1.5	353.1	48.2	14.2
2Z-STD	1.910	2525	23.6	15-100	1.5	352.4	52.3	2Z-MS	1.779	2744	15-100	6	1.8	359.7	40.6	12.7
3M-STD	1.974	3057	20.2	20-100	1.7	338.4	47.7	3Z-MS	2.129	3124	30-100	5	1.1	355.8	46.5	11.9
4A-STD	1.018	1263	25.2	25-100	2.0	358.8	46.0	4Z-MS	0.986	1153	30-100	5	1.6	357.2	44.7	1.8
5Z-STD	1.766	1540	35.8	80-100	1.8	3.3	47.7	5Z-MS	1.726	1483	60-100	3	2.6	3.7	44.5	3.2
6M-STD	1.913	2313	25.9	25-100	1.0	342.9	55.6	6Z-MS	2.169	2608	30-100	5	1.8	350.8	48.6	8.5
7Z-STD	1.913	2647	22.6	30-100	1.5	349.1	50.4	7R-MS	1.970	2495	15-100	6	1.5	359.1	41.4	11.4
8A-STD	1.839	2356	24.4	30-100	1.3	336.8	51.5	8Z-MS	1.779	2291	15-100	6	1.2	350.8	42.5	14.3
9Z-STD	1.808	2470	22.9	15-100	0.7	356.8	51.0	9Z-MS	2.189	2971	30-100	5	1.4	354.6	49.8	2.2
10M-STD	2.730	4965	17.2	30-100	1.4	359.2	51.8	10Z-MS	3.434	4084	30-100	5	1.6	349.1	52.0	6.2
11A-STD	1.900	2733	21.7	30-100	1.4	346.6	48.9	11Z-MS	2.107	2898	30-100	5	1.4	351.3	52.2	4.1
12M-STD	1.682	2351	22.4	30-100	1.2	1.5	50.7	12Z-MS	1.557	2243	45-100	4	0.7	354.4	45.4	7.1
13A-STD	1.494	2143	21.8	20-90	0.4	346.9	43.8	13Z-MS	1.430	1935	15-100	6	1.4	357.1	46.9	7.8
average	1.771	2444	23.6		1.5	350.6	48.7		1.882	2433		5.2	1.5	355.1	46.4	8.1
s.d.	0.419	915	4.3			8.8	5.0		0.599	785				4.2	3.7	4.5

Comparing individual sample pairs, the angular distance between their ChRM directions varies between 2.2° and 14.3°, which is similar to the angular distances between the site mean and individual directions of standard-samples. We would like to note here that in a previous data set sample 13Z-STD gave a clearly abnormal direction that could not be explained by orienting errors or deficient demagnetization behavior. This was later substituted by sample 13A-STD from the same drill core (Table 2.1), which did provide a ChRM direction very similar to the rest. The occurrence of one abnormal direction obviously increases the overall dispersion and thus the confidence circle α_{95} of a site mean direction. While its influence is amplified when the total number of samples decreases, this effect is less detrimental in the case of mini-samples, which in the proposed sampling strategy are recovered in a larger quantity than standard-samples.

Regarding average ChRM directions, we first consider the average for the massive block sampled by cores 8 to 13 (Table 2.1). Both sample sizes provide mean directions with only 2.0° angular distance between them, and they are indistinguishable at the 95% probability level. Mini-samples show a smaller scatter of ChRM directions, with an α_{95} of 3.6° compared to 5.6° for the standard-samples. For overall site means the result is similar: mean directions are indistinguishable and mini-samples again show a smaller dispersion of α_{95}=2.4° compared to α_{95}=3.9° for the standard-samples. Precision parameters *k* for the massive block and the whole site are always smaller for mini-samples than standard-samples. We must therefore conclude that for this particular site, mini-samples provide a better defined mean direction than standards-samples. This result is surprising as one would expect a larger orientation error for mini-cores than for standard-size cores, and this error would propagate through all magnetometer measurements. However, this observation seems to be just fortuitous, as will be shown in further comparisons as described below.

Table 2.2 lists the results of all 12 sites where both standard- and mini-sample data were collected, and Figure 2.5 compares precision parameters *k* and α_{95} for the data sets. Precision parameters *k* of standard-samples are larger for 7 out of 12 sites, in average by a factor of 1.39. While this could represent a higher orienting precision of standard-samples, we must note that this relation is much dependent on individual values (see above), producing a higher standard deviation of the average *k* for standard-samples of 137% compared to 64% for mini-samples. Eliminating one of the extreme *k* values (8 for BP, 1363 for Q14) therefore changes drastically this relation, which in consequence is not considered to be significant. Similarly, confidence limits α_{95} are larger for standard-samples in half of the cases, in total average by a factor of 2. While this could mean that the on average larger number of mini-samples (13.6 compared to 8.6 for standard size samples) overcompensates for a reduced orienting precision, this relation is again biased by two sites of standard-samples, i.e. site BP and BQ with an α_{95} of 19.6° and 12.9°, respectively. It is therefore impossible to decide on the basis of the present limited data set if there are significant differences in precision and confidence between sample sizes. On the other hand it is notable that precision and confidence data from sites with mini-samples are more homogeneous than for standard size samples. As mentioned above this may reflect the unrecognized presence of abnormal individual directions in some site mean directions of standard-samples, which is less effectively averaged out than in the case of the larger number of mini-samples.

Site-mean direction pairs are very similar, with angular distances between them of 2.0° to 8.8°, on average 4.5°. This value is comparable to the average angular distance of 3.7° observed for repeated measurements on 37 Eifel volcanic rocks (Böhnel and Schnepp, 1999), although these were all done on standard-samples. In order to test for a statistical difference between site means we used the test proposed by McFadden (1982) (equation 14) for the general case of two sites with different precision parameters *k* (Table 2.2). If the observed value (Obs.) is larger than the expected value (Exp.), the corresponding site means are considered different at the 95% probability level. This is the case for three rock units, where the difference between the test values is marginal for sites Q3M/Q3 and Q14M/Q14, and a larger difference is observed for site Q14M/Q14. All other sites are indistinguishable at the 95% probability

level. The case of Q14M/Q14 is characterized by the large number of outliers for standard-samples (two out of seven), which yields to a reduction of the number of samples used for calculation of the site-mean. This could have biased the site-mean direction and resulted in the significant difference. If this is true, it would suggest a basing of a site-mean on more than five samples. In general we conclude that mini-samples produce mostly indistinguishable site-mean directions of similar precisions than standard-samples.

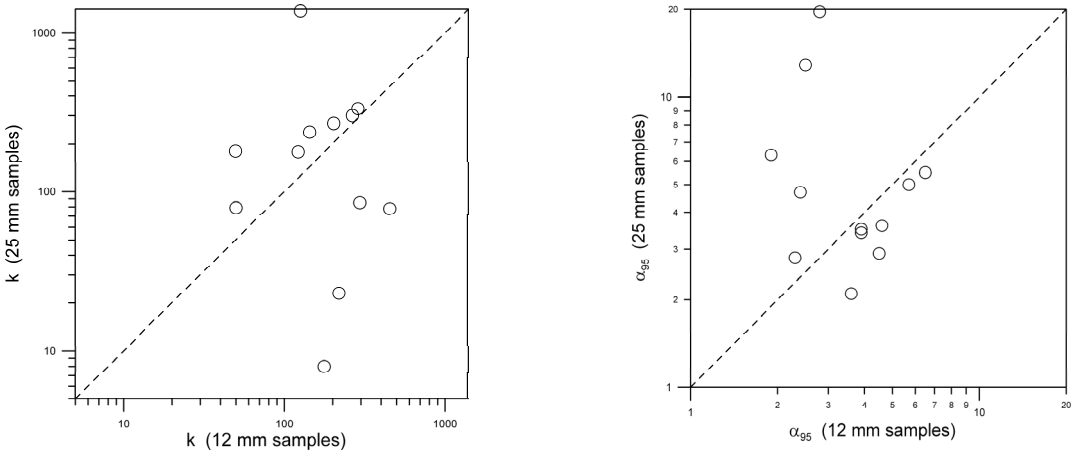

a) b)

Figure 2.4: Comparison of precision parameters k (a) and 95% confidence limits α_{95} (b) for site-mean directions obtained using 25 and 12 mm diameter samples.

For the moment our conclusion is restricted to samples from volcanic rocks. Future studies will have to show if this observation is also valid for sedimentary or intrusive rocks. For sediments the measurement precision could become an important factor as their magnetization intensity is often much lower, for exsample in limestones. In such rocks the potential sample contamination, e.g. from the drill bits or during handling the samples in the field or in the laboratory, becomes more of a problem because of their larger surface to volume ratio. In certain sediments the distribution of particles in separate layers could also result in a more inhomogeneous mini-sample that produces larger measurement errors, particularly in rotation magnetometers. Intrusive rocks are generally composed of larger minerals than volcanic rocks, due to their much slower cooling history. According to our experience, such large crystals may result in problems to recover samples in the field, as intrusive rocks can be more brittle and drill cores tend to break more easily for 12 mm cores due to their smaller diameter. Intrusive rocks may also be more inhomogeneous than volcanic rocks, even at the size of standard-samples, provoking larger measurements errors for mini-samples.

Table 2.2. Comparison of site-mean directions from sites where both mini-samples and standard-sized samples were collected. Instrument: 2G, 2G Enterprises long core magnetometer; JR5 and JR6A, induction magnetometers from AGICO; Digico, Digico fluxgate spinner magnetometer. n/rej., number of accepted/rejected samples for site-mean calculation. *k* and α_{95}, statistical parameters. Dec, Inc, site-mean declination and inclination. N_{total}, total number of combined remanence vectors. R, vector sum of unity-length remanence vectors. R_{total}, vector sum of unity-length remanence vectors combining both sample sets. a.d., angular distance between site mean directions. Obs., Exp., comparison values for hypothesis of indistinguishable site mean directions at 95% probability level according to McFadden and Lowes (1981).

Site	samples	instrument	n/rej.	k	α_{95} (°)	Dec (°)	Inc (°)	R	R_{total}	a.d. (°)	Obs.	Exp.
LQW(8-13)	Mini	JR5	6/0	348	3.6	352.9	48.2	5.98562				
	Standard	JR5	6/0	145	5.6	351.2	49.9	5.96531	11.94905	2.0	.038	.349
LQW(all)	Mini	JR5	13/0	295	2.4	355.3	46.5	12.95931				
	Standard	JR5	13/0	113	3.9	350.5	49.0	12.89380	25.83671	4.1	0.111	0.133
BM	Mini	JR6A	11/0	50	6.5	168.7	17.3	10.80040				
NL1	Standard	JR5	10/0	79	5.5	171.7	17.7	9.93173	20.73060	2.9	0.026	0.171
BN	Mini	2G	8/1	145	4.6	202.5	8.3	7.95166				
NL2	Standard	JR5	8/0	238	3.6	205.3	5.9	7.97053	15.91402	3.7	0.105	0.239
BO	Mini	2G	14/0	78	4.5	205.4	12.3	13.83226				
NL3	Standard	JR5	10/0	269	2.9	205.3	8.2	9.96655	23.78397	4.1	0.089	0.146
BP	Mini	2G	16/0	177	2.8	357.9	21.9	15.91525				
STR	Standard	JR5	9/0	8	19.6	6.1	26.6	7.97995	23.83261	8.8	0.032	0.139
BQ	Mini	2G	16/0	221	2.5	353.3	22.4	15.93197				
JQA	Standard	JR5	7/2	23	12.9	0.0	19.5	6.73671	22.63441	6.9	0.051	0.153
Q6M	Mini	JR5	17/0	268	2.2	206.8	-0.6	16.94018				
Q6	Standard	Digico	7/0	300	3.5	205.2	2.6	6.97997	23.91051	3.6	0.127	0.146
CIM	Mini	JR5	12/1	123	3.9	210.4	10.2	11.91061				
CI1	Standard	JR5	11/1	179	3.4	207.1	12.1	10.94425	22.84262	3.8	0.086	0.153
Q11M	Mini	JR5	14/1	50	5.7	180.3	-56.3	13.74048				
Q11	Standard	Digico	6/1	181	5.0	182.7	-63.5	5.97234	19.67906	7.3	0.189	0.181
Q14M	Mini	JR5	14/0	126	3.6	357.9	24.6	13.89620				
Q14	Standard	Digico	5/2	1363	2.1	351.4	22.5	4.99706	18.87093	3.8	0.450	0.193
ESM	Mini	JR5	14/0	453	1.9	354.8	46.3	13.97131				
ES3	Standard	JR5	8/0	78	6.3	351.0	48.3	7.91038	21.87351	3.3	0.046	0.162
Q3M	Mini	JR5	14/0	290	2.3	346.0	40.0	13.95515				
Q3	Standard	Digico	9/0	332	2.8	341.5	41.6	8.97591	22.91452	3.8	0.176	0.153

5. Conclusions

Mini-samples with 12 mm diameter from volcanic rocks are characterized by similar bulk magnetic properties such as magnetization intensity and magnetic susceptibility compared to standard-samples of 25 mm diameter. Magnetic particle distribution in lava thus seems to be similar at 1 cm^3 and 10 cm^3 volumes. Mini-samples provide directional data which are on average of slightly lower precision parameters k but also slightly smaller α_{95} confidence limits compared to standard-samples. This may indicate that the lower orienting precision for mini-samples is compensated easily by a larger number of drill cores. As these relations strongly depend on the inclusion or rejection of individual data, this is not considered to be significant. For only one site a significant difference was observed for site-mean directions, which was most likely influenced by rejecting two out of seven standard-samples. This suggests that mini-samples provide similar site-mean directions as standard-samples. Based on the data set available, we conclude the use of mini-samples as a valid methodological alternative to standard-samples in paleomagnetic studies on volcanic rocks. So far there are no direct comparison studies for sedimentary and intrusive rocks, where remanence intensity and inhomogeneous distribution of magnetic minerals could pose problems on using the mini-sample technique.

Acknowledgements

This work was supported from Conacyt (project 46213) and DFG (project NO 334/1-2).

3. Evaluation of the multispecimen parallel differential pTRM method: A test on historical lavas from Iceland and Mexico

Daniel M. Michalk [a], Adrian R. Muxworthy [b], Harald N. Böhnel [c], John Maclennan [d] and Norbert R. Nowaczyk [a]

[a] *Helmholz-Zentrum Potsdam, Deutsches GeoForschungsZentrum, Germany*
[b] *Department of Earth Science and Engineering, Imperial College London , U.K.*
[c] *Centro de Geociencias, UNAM-Campus Juriquilla, Queretaro, Mexico*
[d] *Department of Earth Science, University of Cambridge,UK*

Published in: Geophysical Journal International, 173 (2), 409-420, 2008

Abstract Obtaining reliable geomagnetic palaeointensity (PI) estimates is still a difficult objective. Most common techniques in PI studies are based on various modifications of the Thellier method, but high failure rates and large uncertainties are common. Furthermore, only rocks which obey stringent criteria are assumed to yield faithful palaeointensity estimates. In general, magnetic particles must be of single domain size, the magnetisation must be a thermoremanent magnetisation and chemical alteration of magnetic carriers must be avoided during the laboratory experiment. Recently, a new method for obtaining palaeointensities was proposed, which, on the grounds of results from two historic lavas and three simulated experiments, is assumed to be independent of magnetic domain state. This method uses multiple samples subjected to only one heating step at moderate temperatures. Here we present a test of the multispecimen parallel differential pTRM method on 11 historical lavas from Iceland and Mexico, from which the actual field intensity is known, either from magnetic observatory data, or from magnetic field models. Our results show, that the majority of PI estimates after the multispecimen parallel differential pTRM method yielded results that are very close or indistinguishable within the range of error from the expected intensity and thus largely confirm the findings from the initial study, however, there is in general a small overestimate, which we show is associated with multidomain material. When compared to a Thellier-type palaeointensity experiment, carried out on sister samples from five Icelandic lava flows, the average multispecimen PI is closer to the actual field intensity. Samples from one lava, characterized by low Curie temperatures, failed the Thellier approach due to laboratory induced alteration, but here the multispecimen method returned a reasonable PI. Even though there is evidence that the method is not entirely independent of magnetic domain state, as previously proposed, we regard this method as a valuable alternative in future PI studies.

1. Introduction

To understand the origin of the earth's magnetic field, we need to know how the field has varied on geological timescales; not just the direction but also the ancient field's absolute intensity (palaeointensity). This absolute palaeointensity (PI) record is particularly important, because when palaeomagnetic data are only directional this leads to non-linear calculations of the ancient geomagnetic field, whereas, if the absolute palaeointensity is known, the problem becomes linear and analytically solvable. Absolute PI data provide constraints for various numerical dynamo models, and information about the geodynamo processes and its evolution over geological timescales. Many workers have attempted to determine full vector records of the ancient geomagnetic field, however, current methods of PI determination have high failure rates and often the reliability of the PI estimate is unknown. As a result

the global data base of palaeointensities (Perrin & Schnepp, 2004) gives a rather scattered image and still remains sparse both temporally and spatially.

Generally, the high failure rates and accompanying large uncertainties of PI data are due to a number of effects, including (1) chemical alteration of magnetic minerals in situ, e.g., low temperature oxidation (maghemitization), (2) chemical alteration during repeated heating in the laboratory PI determination, (3) differences between natural and laboratory cooling rates, and (4) the presence of remanence carried by multidomain (MD) grains that violate Thelliers' law of independence of partial thermoremanence (pTRM) (Thellier & Thellier, 1959), an essential criterion in any Thellier-type PI study. Many scientists have attempted to account for, or minimize the effects of these factors by applying different sets of strict, often time consuming, reliability criteria and measurements (e.g. Perrin, 1998; Selkin & Tauxe, 2000; Riisager & Riisager, 2001). As a result the number of samples, which are considered to be suitable PI recorders, is limited to a small fraction of the original, as MD grains are commonly present and chemical alteration during the experimental procedure is also common.

Recently, Dekkers & Böhnel (2006) have presented a new method of determining palaeointensities; the multispecimen parallel differential pTRM method (hereafter referred to as multispecimen method). They claim that this method is independent of magnetic domain state, allowing for samples containing MD grains to be processed. The method requires heating to only low / moderate temperatures in the laboratory. Consequently, failure due to chemical alteration is greatly reduced.

The basic assumption that underlies the method proposed by Dekkers & Böhnel (2006) is the first-order symmetry properties of pTRM in MD ferromagnetic grains, experimentally observed by Biggin & Poidras (2006). They found that partial demagnetisation and remagnetisation of MD TRM, displays first-order mirror- reflected symmetry in the change in magnetisation, in a similar fashion to that displayed by and expected for non-interacting SD grains (Néel, 1949). One conclusion of their phenomenological model is that if a MD sample has a full TRM and a pTRM is induced parallel to the TRM, the intensity of the resultant remanence (pTRM and original TRM) will equal the original TRM, if the laboratory field is equal to the inducing field of the TRM. If the laboratory field is less than the inducing field, the overall remanence will decrease, if greater, the overall remanence will increase. Therefore, simply plotting the resultant remanence minus the original TRM, for a range of field values, say 10-100 μT, yields the original intensity.

Dekkers & Böhnel (2006) applied this concept to the development of their new multispecimen method. In contrast to the most common methods of PI determination, which are based on modifications on Thellier-type methods, this multispecimen approach requires the use of multiple samples. Each sample is subjected to only one in-field low/moderate-temperature heating step. That each sample is heated only once is thought to significantly reduce from the effects of laboratory alteration. In addition, according to the model of Biggin & Poidras (2006), during pTRM acquisition it is important to apply the magnetic field during both the warming and cooling.

Dekkers & Böhnel (2006) tested this new method on natural and synthetic MD grain assemblages induced with a laboratory TRM with a known field, and on only two historical lavas from the Trans Mexican Volcanic Belt (TMVB). The synthetic samples returned the correct result within error. The same samples failed to yield correct PI estimates using a double-heating Thellier method. One mean result, based on three PI experiments, obtained from the 1943-1952 Paricutin lava yielded a PI, which is statistically indistinguishable within the range of error of the expected intensity. Another result from samples belonging to the 1759-1774 Jorullo lava was of lower quality but still close to the expected intensity. In addition to these encouraging experimental tests, the laboratory processing time of the multispecimen approach is significantly faster (about 2-4 times) than Thellier-type determinations. According to Dekkers & Böhnel (2006) the multispecimen method has the potential to supersede standard

Thellier-type techniques, however, the method has produced only one accurate determination from two historical lavas.

In this paper we present a test of the multispecimen method on 11 recent historical lavas of known ages from Iceland and Mexico, with a range of different well-defined rock-magnetic characteristics. We compare the palaeointensity results from our experiments with the expected intensity, known from magnetic observatory data or magnetic field models (Jackson et al., 2000). This study allows us to estimate the feasibility of using this method for routine palaeointensity determinations. We directly compare the multispecimen estimates with Thellier-type PI determinations performed on sister samples from five lavas flows.

2. Sample description

We considered historical samples from both Iceland and Mexico (Table 3.1). Icelandic samples are associated with eruptions from two Icelandic volcanoes; five lava flows (1878, 1913, 1980, 1991 and 2000 A.D.) from Mount Hekla in southwest Iceland, and two lava flows (1729 and 1981 A.D.) from Mount Krafla in the northeast of Iceland. The Krafla samples were taken from the two most recent basaltic fissure eruptions in the Krafla volcanic system. This system is dominated by the eruption of tholeiitic basalts which form by adiabatic decompression melting of unusually hot mantle under a spreading center. In contrast, the transitional basalts that are parental to the Hekla system are generated by mantle melting under a southwards-propagating rift segment. The north Atlantic has been the site of frequent volcanic activity through much of the Cenozoic, and on-land exposures in Iceland preserve a superb archive of the last 16 Myr of geomagnetic history (Wilson et al., 1972).

The volcanism of the TMVB is related to the Neogene subduction of the Cocos and Rivera Plates under the south-western margin of the North American Plate. It comprises at least 8000 volcanic structures and crosses Mexico at latitudes from ~19 to 21°N and extends approximately over 1000 km from the Pacific Ocean to the Gulf of Mexico with a width of 20-150 km. For this study, we sampled four historic lavas; one from the 1943 lava flow of Paricutin (active period: 1943-1952), two eruptions from Ceboruco volcano (1870 and 1550 respectively) and Pico de Orizaba (1545) (also known as Citlaltépetl), which is at 5610 m the highest volcano in Mexico. Our Paricutin site (BK) is a direct re-sampling of the locality "Paricutin site 2" from the initial study of Dekkers & Böhnel (2006). Paricutin is the youngest cinder cone of the TMVB and belongs to the Michoacan-Guanajuato Volcanic Field. Ceboruco lies in the Ceboruco-San Pedro Volcanic Field while Pico de Orizaba is part of the TMVB.

Table 3.1. Sample codes, origin, associated volcano, site coordinates and associated ages (A.D.).

Site	Origin	volcano	age (A.D.)	Lat. (°N)	Long. (°W)
H00	Iceland	Hekla	2000	63.9405	19.6490
H91	Iceland	Hekla	1991	63.9599	19.5952
HB	Iceland	Hekla	1980	64.0209	19.7441
HG	Iceland	Hekla	1913	63.9993	19.5109
HE	Iceland	Hekla	1878	64.0077	19.5055
KA	Iceland	Krafla	1981	65.4373	16.5127
KB	Iceland	Krafla	1729	65.4373	16.5127
BK	Mexico	Paricutin	1943	19.3163	102.1390
EH	Mexico	Ceboruco	1870	21.0967	104.5853
EE	Mexico	Ceboruco	1550	21.1755	104.5292
DY	Mexico	Pico de Orizaba	1545	19.0101	97.2910

A set of 10 to 15 oriented mini-core samples with a diameter of 11 mm for the Icelandic samples and 12 mm for the Mexican samples were taken from each cooling unit with a battery powered electric drill. Due to the very fresh nature of the Icelandic lavas, penetration into the lava field was typically less than 300 m. Effort was made to sample original, un-rotated cooling structures, such as lava tubes. Where possible, multiple structures were sampled within a radius of < 50 m. This was also the case for the Mexican samples, except for site DY. Here, the lava flow had an *in situ* exposure of ~ 15 m over which the samples were dispersed vertically and horizontally.

3. Experimental techniques

In the laboratory, samples were cut into specimens of 10 mm length, after scraping the outermost 1-1.5 cm, which then yielded two to five specimens for each drill core. To minimize the risk of using samples that might have been affected by surface weathering, we preferably used the specimens closer to the bottom of the core in the laboratory experiments. To test for their demagnetisation behaviour, e.g. uni-vectorial remanences or possible viscous overprinting, we subjected sets of five specimens from each flow unit to progressive alternating field (AF) demagnetisation with maximum fields of 150 mT. Additionally two samples were subjected to thermal demagnetisation to obtain the blocking temperature spectrum of the NRM. Low-field susceptibility (χ) was measured on a Bartington susceptibility meter to detect chemical alteration during heating. Remanence measurements were made either on a 2G cryogenic magnetometer with long core setup or on an Agico JR6 spinner magnetometer. For thermal demagnetisation and PI experiments, we used a temperature and field calibrated Magnetic measurements Ltd. MMTD oven. The field was calibrated to an accuracy of ± 0.1 μT along the length of the heating chamber.

A set of rock magnetic measurements was performed on selected samples from each flow to ascertain the magneto-mineralogy and to assess for possible thermal alteration. Thermomagnetic curves were measured on five samples per flow with a Petersen Instruments Variable Field Translation Balance (VFTB) from room temperature to 600° C with Argon flushing, using a field of 500 mT. Curie temperatures were calculated after the method of Moskowitz (1981). For detailed monitoring of possible alteration effects, two samples per flow were additionally subjected to thermal cycling with 100°C steps, starting at room temperature up to the highest temperature of 600°C. For each flow a set of three to six hysteresis measurements and back field curves were made on small chips of 30-50 mg using a Princeton measurements alternating gradient magnetometer (AGM), with a peak field of 1 Tesla. From these data sets, we determined the standard hysteresis parameters, i.e., saturation magnetisation, M_S, saturation remanence, M_{RS}, coercive force, B_C, and coercivity of remanence, B_{CR}. Using the ratios M_{RS}/M_S and B_{CR}/B_C a Day-plot was created (Day et al. 1977; Fig 3.2). We also calculated the shape parameter δ_{Hys} (Fabian, 2003). Additionally first-order reversal curves (FORCs) (Roberts et al., 2000) were measured on a selection of samples to identify the degree of magnetostatic interactions.

Two different techniques were used to determine the palaeointensity. Firstly, PI measurements by the multispecimen method following the protocol of Dekkers & Böhnel (2006). A basic requirement of the multispecimen method is that after each in-field pTRM acquisition treatment, the pTRM is scaled to the original NRM to determine the fraction of pTRM lost / gained (%). If scaled to the NRM, the remanence must be uni-vectorial, or, in the case of viscous overprints, the characteristic remanent magnetisation (ChRM) must be isolated before the PI experiment by a preceding demagnetisation treatment. Previous AF-demagnetisation experiments on sister samples indicated for three lavas (sites H00, H91 and HG) that a field of 5 mT was required to erase a small viscous overprint, while for one set of samples (site DY) it was necessary to apply a slightly higher field of 10 mT. Dekkers & Böhnel (2006) used a thermal pre-treatment of a 200°C demagnetisation step on one set of samples from Jorullo. We used an AFD pre-treatment as we suggest that AF-demagnetisation at such low fields is a sufficient tool for erasing small fractions of viscous magnetisations and that each additional thermal treatment would rather increase the

risk of inducing laboratory alteration effects. In the multispecimen PI determination, these four samples were AF-demagnetised after each remagnetisation step for normalisation purposes. For all the other samples the magnetisation was found to be uni-vectorial and free of viscous components and consequently pTRMs were scaled to the NRM.

During the experiments, pTRMs were induced parallel to the original NRM to avoid effects of high temperature tails of multidomain pTRMs (Yu & Dunlop, 2003; Xu & Dunlop, 2004). As it was possible to orient ChRM of the samples parallel to the induced field in a special designed sample holder with a precision of less than <10°, no later mathematical correction, to account for inaccuracies in orientation, was required on the final data. Ideally, in a multispecimen experiment, the unblocking temperature spectrum (T_{UB}) of all specimens used in one experiment should be the same. We included one more demagnetisation step in zero-field at the same temperature at which the pTRM was acquired after the pTRM acquisition, i.e. similar to a pTRM tail check (e.g. Walton, 1984; McClelland & Briden, 1996). We used this as a criterion to further characterize the T_{UB} spectrum of each sample. We discarded measurements with anomalous values of NRM remaining after demagnetisation. For the multispecimen experiment it is necessary to select a temperature for the pTRM acquisition, which is below the point where chemical alteration is significant and above where viscous components persist. The temperature was chosen high enough that the fraction of TRM lost after heating in zero-field was in the order of 30-60% and increases in magnetic susceptibility were less than 5%. We applied successively increasing fields in 10 μT steps from 10 μT to 80 μT, sometimes 90 μT. After each remagnetisation experiment, the bulk susceptibility was measured.

In conjunction and for comparison with the multispecimen PI experiments, we subjected a set of sister samples from five Icelandic flows to a Thellier-type palaeointensity experiment. We used the IZZI protocol described by Tauxe & Staudigel (2004) and Yu et al. (2004). We included both pTRM checks and pTRM tail checks as described by Yu et al. (2004). No pTRM additivity checks (Krása et al., 2003) where measured.

4. Rock magnetic analysis

4.1 Thermomagnetic properties

Thermomagnetic results from the VFTB are categorized into four groups (Fig. 3.1, Table 3. 2.)

Group 1 samples (Fig. 3.1a) show a single ferromagnetic phase with a broad Curie temperature (T_C) between 390 and 460°C, which is likely to be due to titanomagnetite that has undergone some degree of high temperature (deuteric) oxidation. Heating and cooling branches show excellent reversibility, indicating that no thermal alteration occurs. This behaviour was observed in samples from sites DY and BK.

Group 2 samples (Figs 3.1b and c) are characterized by two ferromagnetic phases. Phase one has a low T_C in the range of 180 to 220°C, which is indicative of high-Ti titanomagnetite, the second phase has a higher T_C between 510 and 560°C, indicative of low-Ti titanomagnetite. Both Curie temperatures are seen in the heating and cooling curve, which again show reversible behaviour. Such thermomagnetic curves were observed in the majority of samples (Table 3.2).

Group 3 samples (sites HG and KB, Figs 3.1d and e) show a range of different Curie temperatures rather than a single pronounced Curie temperature, and again the behaviour is reversible.

Samples from site KA are categorized as Group 4 samples (Fig. 3.1f) and show a dominant ferromagnetic phase with a T_C between 105 and 140°C, which indicates the presence of high-Ti titano-magnetite phase

close to TM60 in composition, suggesting fast cooling of the lava before high-temperature oxidation could occur (Mankinen et al., 1985). In these samples, thermal cycling above 400°C shows progressive irreversibility in the cooling curve, which is likely to be due to progressive inversion of titanomaghemite during laboratory heating (i.e., Krasa & Matzka, 2007). The final product is a magnetic phase with a T_C ~580°C close to that of pure magnetite.

4.2 Hysteresis properties

The bulk magnetic hysteresis properties for the Icelandic and Mexican samples is shown in Figure 3.2 and tabulated in Table 3.2. The majority of Icelandic samples (indicated by dots) have average values of M_{RS}/M_S of 0.45-0.26 and B_{CR}/B_C values of 1.49-1.37 and plot in the upper left corner of the pseudo-single domain (PSD) range in the Day diagram. Two lavas (H00 and H91) have slightly lower values of M_{RS}/M_S and higher values of B_{CR}/B_C. FORC diagrams show closed contours about a central peak, which are typical for SD particle assemblages (Figs 3.3a and b). The presence of a negative region or a low in the FORC distribution near the bottom left-hand region in these FORC diagrams is highly indicative of non-interacting SD material with a dominant uniaxial anisotropy (Muxworthy et al., 2004; Newell, 2005), i.e., ideal material for recording the PI.

Hysteresis properties of the Mexican samples (indicated as squares) show a broader range of magnetic domain states. While samples from BK show a similar behaviour like the majority of the Icelandic samples (Fig. 3.3c), and site EH samples still plot well in the PSD region, samples from DY and EE are characterized by rather lower values of M_{RS}/M_S (0.09 and 0.11) and higher values of B_{CR}/B_C (4.68 and 5.05), which indicates some contribution of multidomain (MD) grains. This can be more clearly seen in the FORC diagrams (Figs 3.5d-f), which plot closer to the vertical axis and display a greater vertical spread in the distribution along the B_i -axis. This is similar to published FORC diagrams for PSD powdered magnetite (Muxworthy & Roberts, 2007).

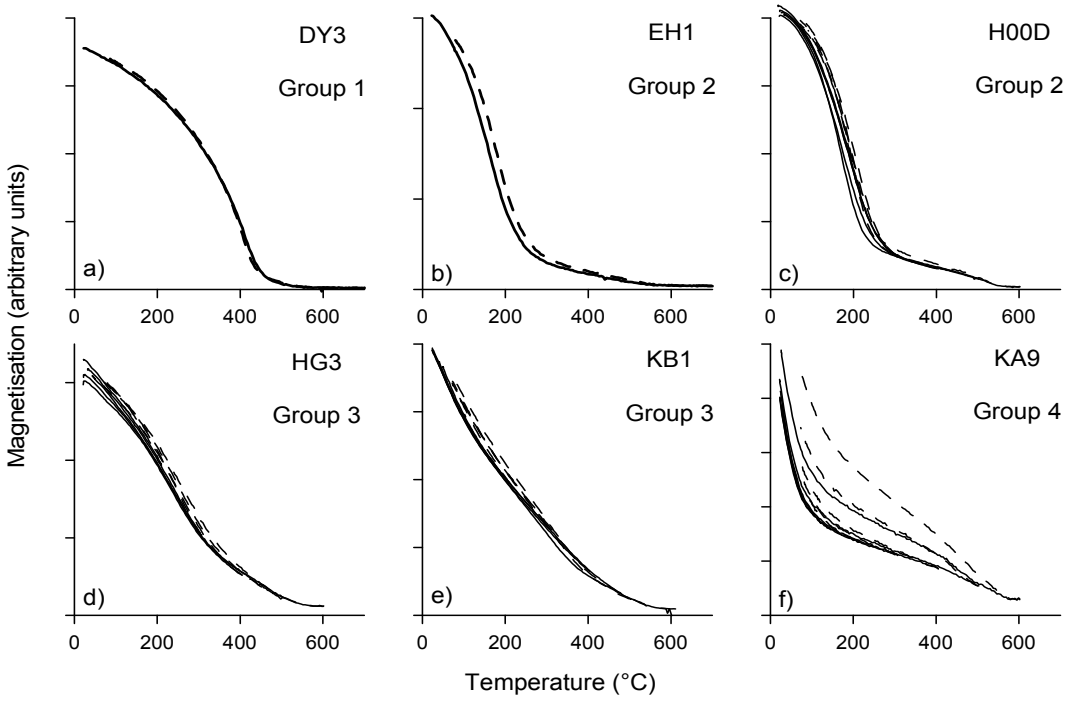

Figure 3.1. Representative examples of thermomagnetic curve types, measured with an applied field of 500 mT from room temperature to 200°, 300°, 400°, 500°, 600° and 700° C. Heating (solid line) and cooling (dashed line) was conducted in Argon.

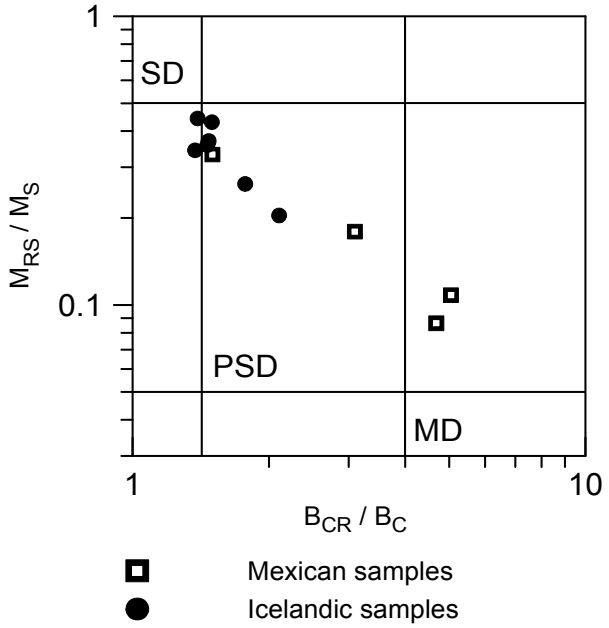

Figure 3.2. Bulk magnetic hysteresis properties for Icelandic samples (indicated as dots) and Mexican samples (indicated as open squares), plotted on a Day diagram, using the data tabulated in Table 3.2.

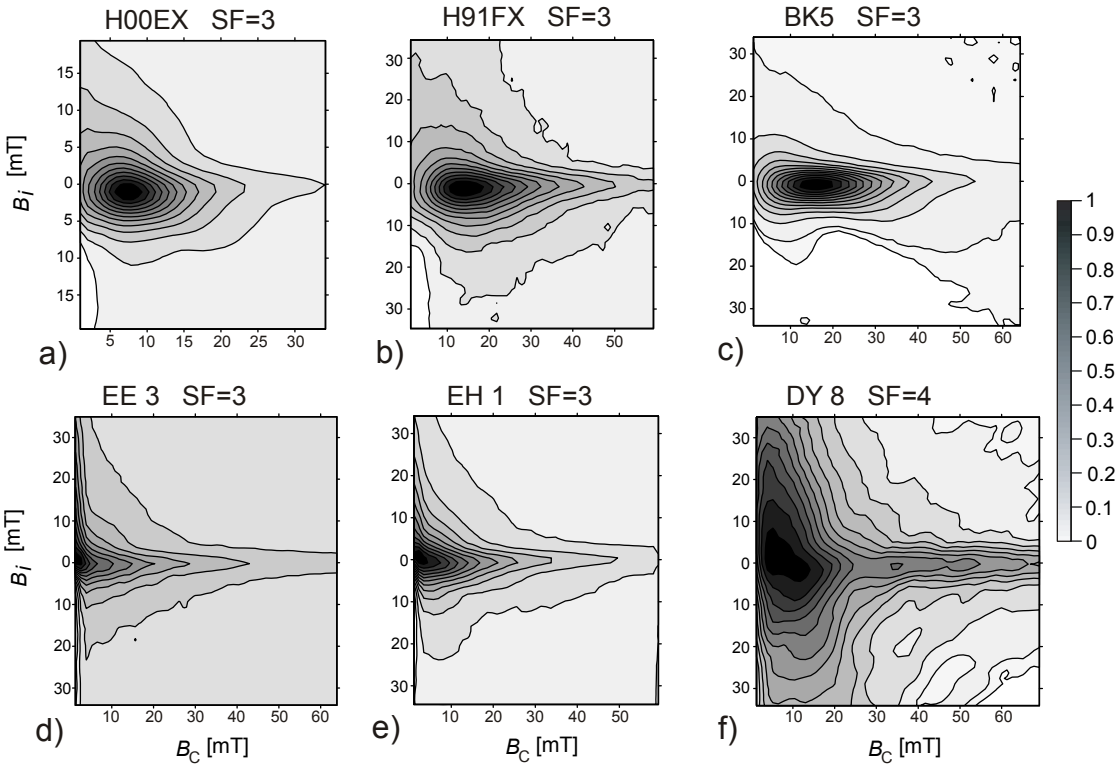

Figure 3.3. Representative first order reversal curve (FORC) diagrams (normalized to peak values). a) and b) Icelandic samples and c) to f) Mexican samples. B_C corresponds roughly to the coercivity distribution in the sample, and B_i is an indicator of interaction field strength. The smoothing factors (SF) are indicated on the diagram. The measuring time for all the samples was 100 ms. Each FORC diagram was constructed from 120 FORCs.

Table 3.2. Average site hysteresis values for the parameters B_C, B_{CR} and M_{RS}/M_S; δ*Hys* is the shape parameter (Fabian 2003); also shown is the thermomagnetic classification as described in 4.1 and shown in Figure 1.

site	B_C	B_{CR}	M_{RS}/M_S	δHys	Ms(T) curve type
H00	8.0 ± 1.2	14.2 ± 2.5	0.26 ± 0.04	0.12 ± 0.10	2
H91	9.9 ± 3.8	19.7 ± 4.3	0.20 ± 0.06	0.32 ± 0.21	2
HB	15.1 ± 9.4	21.5 ± 12.2	0.36 ± 0.07	0.43 ± 0.11	2
HG	26.5 ± 7.7	38.3 ± 7.0	0.43 ± 0.07	0.11 ± 0.05	3
HE	34.4 ± 2.9	48.0 ± 5.4	0.44 ± 0.02	0.24 ± 0.08	2
KA	15.2 ± 4.0	21.0 ± 6.4	0.34 ± 0.08	0.46 ± 0.17	4
KB	14.1 ± 2.3	20.7 ± 3.2	0.37 ± 0.06	0.22 ± 0.13	3
BK	14.7 ± 6.3	21.4 ± 7.8	0.33 ± 0.09	0.17 ± 0.13	1
EH	8.3 ± 1.6	25.2 ± 2.5	0.18 ± 0.04	0.02 ± 0.16	2
EE	6.3 ± 1.4	31.0 ± 7.6	0.11 ± 0.02	0.14 ± 0.15	2
DY	8.1 ± 2.7	35.4 ± 4.2	0.09 ± 0.03	0.30 ± 0.12	1

5. Palaeointensity experiments

5.1 Multispecimen PI

Figure 3.4 shows the results of the multispecimen PI experiments per site. At eight sites we used nine samples, i.e., nine applied fields, and for four sites, eight samples for each experiment. As stated in 3, the multispecimen method relies on the temperature selected for pTRM acquisition at which the field is applied during heating and cooling. Because of the large variations in unblocking spectra determined from sister samples and thermomagnetic curve analyses (Figure 3.1, Table 3.2), we used five different temperatures for the pTRM acquisition step: 130°C (sites KA and KB), 200°C (sites H00, HB, EH), 280°C (sites H00, HG and BK), 300°C (sites HE and EE) and 400°C (site DY).
For comparison of the measured palaeointensity (I_{meas}) with the expected palaeointensity (I_{exp}), we use the intensity error fraction (IEF) equation,

(1) $$IEF = (I_{meas} - I_{exp}) / I_{exp}$$

For the post 1900 flows, expected intensity values were deduced from the International Geomagnetic Reference Field (IGRF), and for the pre-1900 flows, they were calculated using the GUFM1 model (Jackson et al., 2000). The GUFM model assumes a 15 nT/yr decrease in dipole moment in its pre-1840 intensity estimates. As this model only extends back to 1590, intensity values for the two flows pre-dating 1590 (sites EE and DY), were calculated by extrapolating back using secular variation rates provided from the GUFM model for 1590 (Table 3.3).

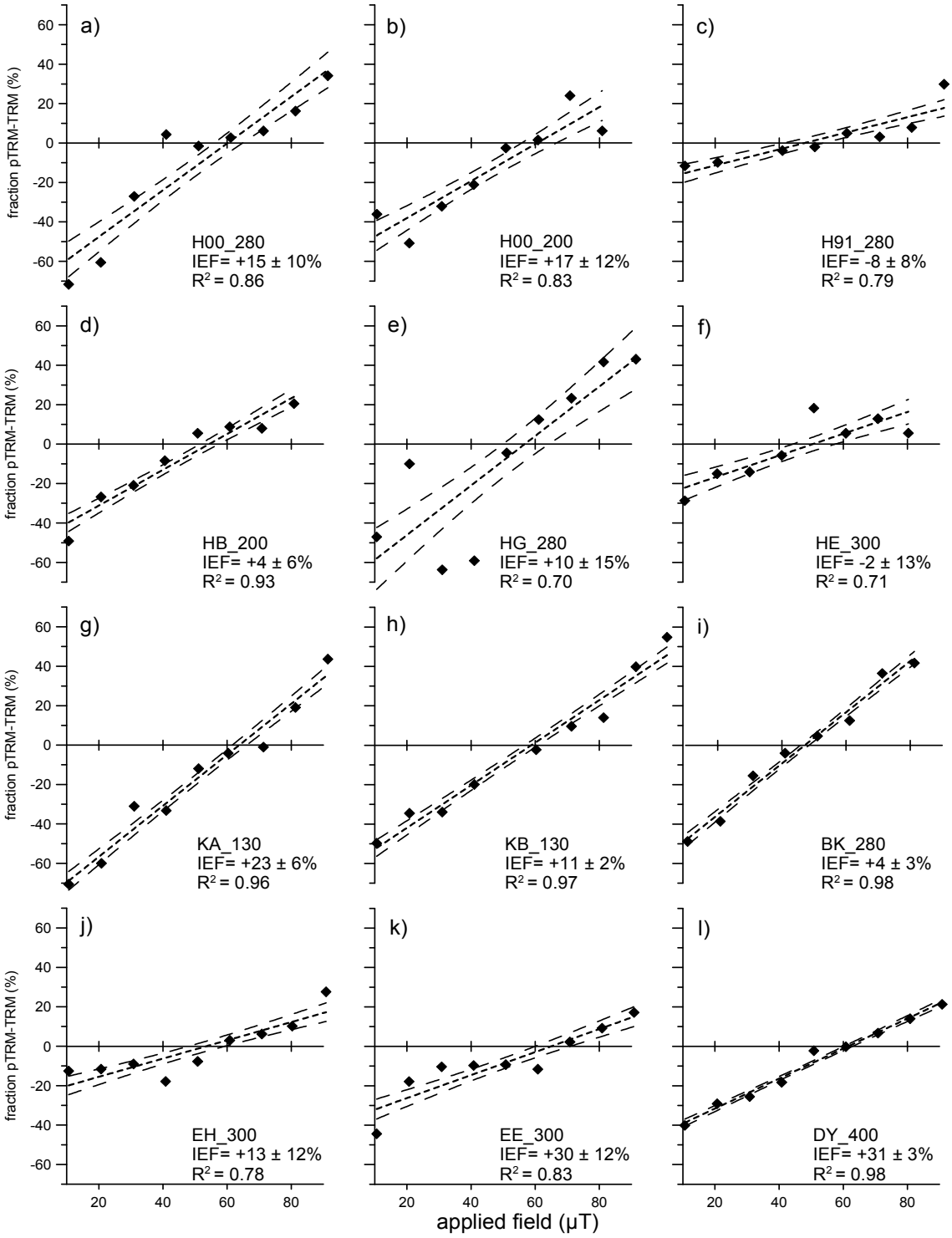

Figure 3.4. Application of the multispecimen protocol to 11 historic lavas, with two estimates for the Icelandic site H00 (a and b). A linear regression is shown (dashed line) with the 68% confidence zone (one standard deviation), indicated by the longer dashed lines. The abbreviation indicates the temperature for the pTRM acquisition (e.g. H00_280, pTRM acquisition at 280°C). IEF is the intensity error fraction (%) and R^2 is the correlation coefficient of the linear regression.

5.1.1 Icelandic samples

For site H00, we had sufficient material to conduct two PI measurements (Fig. 3.4a and b) at two different temperatures (280° and 200°C respectively). For the experiment at 280°C we used an AF-demagnetisation pre-treatment as described in 3, while for the experiment at 200°C remanences were scaled to the NRM. The pTRM induced at 280°C gave a PI estimate of 60 ± 5 μT (R^2= 0.86, IEF= +15 ± 10%), whilst the pTRM induced at the lower temperature of 200°C and gave a PI of 61 ± 6 μT (R^2= 0.83, IEF= +17 ± 12%). As expected, the curve for the 200°C experiment has a slightly flatter slope than for the 280°C experiment because a smaller fraction of NRM is removed at 200° than at 280°C. Both the correlation coefficients R^2 have similar values and based on statistical results, palaeointensities are indistinguishable from one another. A minor improvement of clustering is observed in the samples subjected to the 5 mT AF pre-treatment, which could be due to randomizing small grains that might have formed during the experiment, as discussed in Böhnel & Dekkers (2006) but overall it had a negligible effect on the final result.

Site H91 (Fig. 3.4c) yielded a PI estimate of 48 ± 4 (R^2= 0.79, IEF= -8 ± 8%). This result is within the range of error indistinguishable from the expected PI of 52 μT. The data is rather noisy, as indicated by the rather low R^2 value. Samples from site HB (Fig. 3.4d) yielded an estimate of 54 ± 3 μT, (R^2= 0.93, IEF= +4 ± 6%), which is also indistinguishable from the expected value of 52 μT within the range of error. Larger scatter was observed in the data of site HG (Fig. 3.4e). Here, the lower part of the diagram shows fairly noisy data. Due to the remagnetisation nature of the experiment, it would be expected that measurements where the pTRM field intensity is greater than the original inducing field to display less scatter, i.e., the scatter in the data will decrease as the field increases. Calculating a PI estimate from all measurements gave a PI of 57 ± 8 μT (R^2= 0.70, IEF= +10 ± 15%). Samples from site HE produced rather noisy data (Fig. 3.4f), but again gave a PI which is close to the expected value (51± 7 μT, R^2= 0.72, IEF= -2 ± 13%).

Both sites from Krafla (sites KA and KB) are characterized by low Curie temperatures and unblocking spectra; 80 % of the NRM thermally demagnetised at 150°C. A pTRM temperature of 130°C was chosen. Both experiments (Figs 3.4g and h) display linear behaviour with high R^2 values of 0.96 and 0.97 respectively. However, the PI estimates are rather high, at 64 ± 3 μT and 58.8 ± 1.2 μT respectively, with corresponding IEFs of +23 ± 6% and +11 ± 2%.

5.1.2 Mexican samples

Our experiment on the samples from Paricutin (BK) (Fig. 3.4i), produced a PI of 47.1 ± 1.4 μT (R^2= 0.98, IEF= +4 ± 3%), which is very close to the expected intensity of 45 μT. Dekkers & Böhnel (2006) sampled exactly the same locality (Paricutin site 2 in their publication) and obtained a result of 47.2 ± 1.6 μT. Our estimate is in excellent agreement with their data.

Site EH gave a PI estimate of 54 ± 6 μT (R^2= 0.777, IEF= +13 ± 12%, Fig. 3.4j). Although this is a relatively poorly defined result, it is, within the range of error indistinguishable from the expected intensity of 48 μT. Results from sites EE and DY (Figs. 4k and l), on the other hand, showed the largest overestimates from all historical lava flows investigated in this study (65 ± 6 μT, R^2= 0.83, IEF= 30 ± 12% and 61.6 ± 1.3 μT, R^2= 0.98, IEF= 31 ± 3%). Due to a sharp T_{UB} spectrum between 350 and 450°C the temperature for the pTRM acquisition for the samples from site DY was chosen with 400°C the highest from all in this study.

As stated in section 3, we subjected four lavas to an AF demagnetisation pre-treatment before the pTRM acquisition step, to erase small amounts of viscous magnetisation, and after the pTRM acquisition, for normalization purposes. No adverse effects were found on the final outcome of the multispecimen

experiment. However, we want to emphasize that the effects of an AF pre-treatment still have to be experimentally evaluated before this approach should be considered in a multispecimen experiment on older samples of geological ages.

Table 3.3. Average PI results from the Thellier-type experiment and PI results from the multispecimen PI experiments; R^2 is the correlation coefficient of the linear regression; IEF is the intensity error fraction (%).

Site	Actual Field (IGRF) (μT)	**Multi-specimen PI (μT)**	pTRM acquisition at T (°C)	R^2	IEF (%)	**Thellier estimate (μT)**	success rate	IEF (%)
H00	52	60 ± 5	280	0.86	+15 ± 10	62 ± 2	3/4	+19 ± 4
		61 ± 6	200	0.83	+17 ± 12			
H91	52	48 ± 4	280	0.79	-8 ± 8	na	na	
HB	52	54 ± 3	200	0.93	+4 ± 6	60 ± 4	1/5	+15 ± 7
HG	52	57 ± 8	280	0.70	+10 ± 15	43 ± 7	4/5	-17 ± 13
HE	*52	51 ± 7	300	0.71	-2 ± 13	46 ± 7	2/5	-11 ± 13
KA	52	64 ± 3	130	0.96	+23 ± 6	na	na	
KB	*53	58.8 ± 1.2	130	0.97	+11 ± 2	FAIL	0/4	
BK	45	47.1 ± 1.4	280	0.98	+4 ± 3	na	na	
EH	*48	54 ± 6	300	0.78	+13 ± 12	na	na	
EE	**50	65 ± 6	300	0.83	+30 ± 12	na	na	
DY	**47	61.6 ± 1.3	400	0.98	+31 ± 3	na	na	

* field estimates for the pre-1900 flows were calculated after the model of Jackson et al., (2000).
** field estimates were extrapolated from 1590 values using secular variation rates (Jackson et al., 2000) of 0.112 μT /year (EE) and 0.118 μT /year (DY).

5.2 Thellier data

For comparison to the multispecimen PI experiments, we subjected sister samples from five Icelandic lavas (sites H00, HB, HE, HG and KB) to a Thellier-type palaeointensity experiment. We used the IZZI protocol (Tauxe and Staudigel, 2004) including pTRM checks (Coe et al., 1978) after each in-field temperature step to monitor changes in the capacity of the specimen to acquire a pTRM and alteration during laboratory treatment. Furthermore, pTRM-tail checks (e.g. Walton, 1984; McClelland & Briden, 1996) were used to test if the pTRM gained is completely removed by reheating to the same temperature step in zero-field and to estimate the importance of MD remanence. A laboratory field of 51.1 μT was used for all measurements and was applied during heating and cooling. All determinations were analyzed using the Thellier Tool 4.1 software (Leonhardt et al., 2004) applying the rigorous default quality criteria. Results from four specimens are shown in Figure 3.5.

Successful measurements were analyzed between room temperature or 100° and 300°/340°C over five to seven successive data points, comprising a NRM fraction f between 55 and 97%, with the exception of one sample (HE2Y, f= 0.34), before pTRM checks started to fail. The low-temperatures are due to the high Ti content, and resulting low Curie temperatures and low-unblocking-temperature spectra. In general a good linearity is observed on the NRM/pTRM diagrams with no zig-zagging behaviour (Tauxe & Staudigel, 2004) between alternating infield-zerofield (IZ) and zerofield-infield (ZI) steps. This behaviour is often interpreted as being indicative of SD remanences. In contrast, the phenomenological model of Biggin (2006) predicts that the similar behaviour would be expected from samples containing large MD grains, if the inducing laboratory field is not aligned between perpendicular and anti-parallel to a sample's NRM direction.

From the five specimens measured from each flow, site HG yielded four estimates that passed the Thellier Tool software's reliability standards (Leonhardt et al., 2004), site H00 three, site HE two and site HB one successful determination. Experiments on samples from site KB, however, were unsuccessful due to heating induced alteration at very low temperatures, as indicated by the drift in the pTRM checks (Fig. 3.5d). This behaviour follows the observations made during preliminary thermal cycling as discussed in 4.1. Palaeointensity results after the IZZI method are shown in Table 3.4.

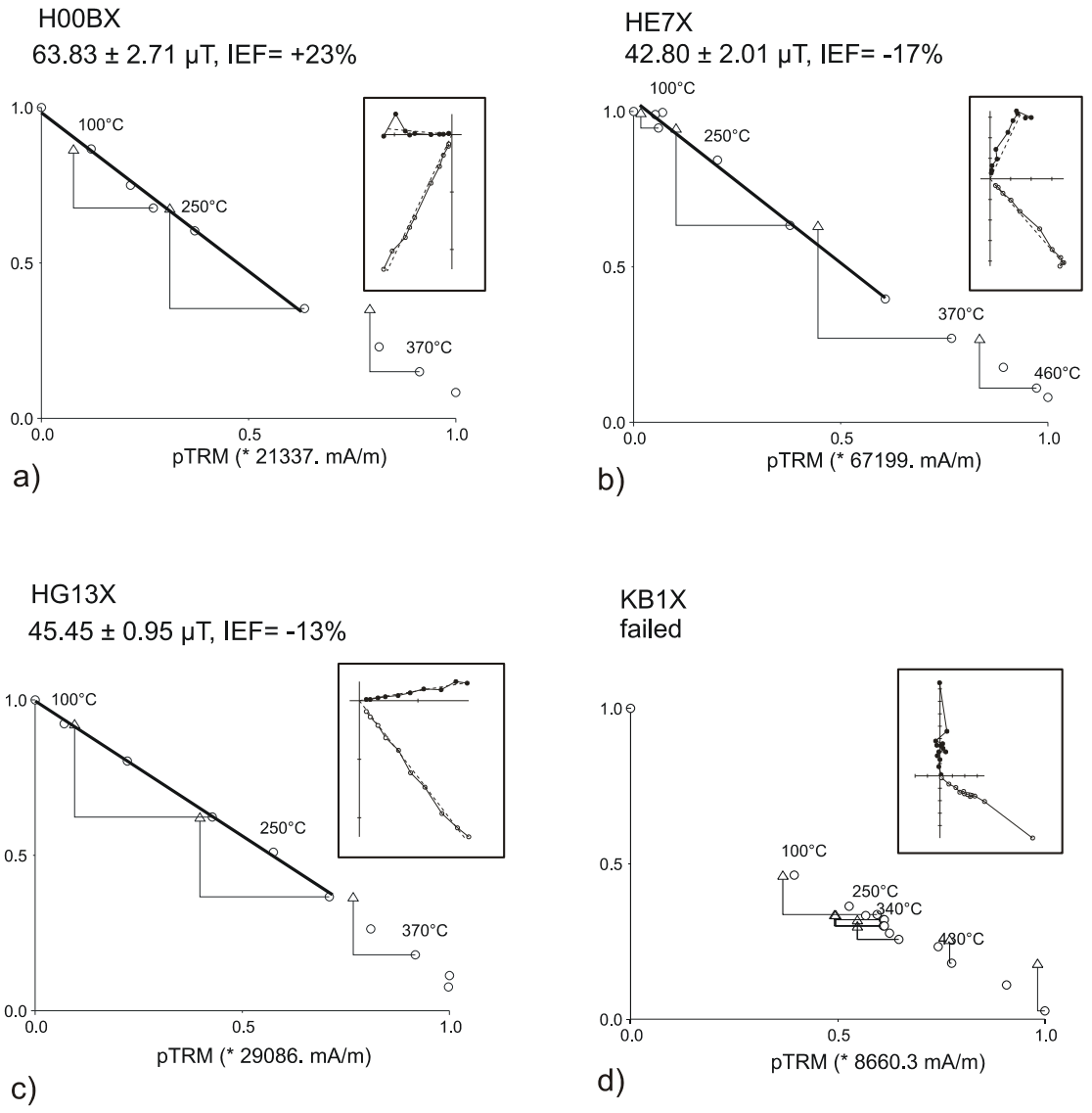

Figure 3.5. Four examples of NRM/pTRM diagrams from Thellier-type palaeointensity experiments after the IZZI protocol on the Icelandic lavas. In a), b), and c) the straight line segment covers more than 50% of the NRM, while d) shows an unsuccessful experiment. The pTRM checks are indicated by the triangles. The inset figure to the upper right of each diagram shows the demagnetisation behaviour of the specimen on a vector component plot.

Table 3.4. Results of the Thellier-type palaeointensity experiment after the IZZI protocol

site	n/N	Specimen	H ± S.D. (μT)	H exp.	IEF (%)	Tmin	Tmax	N	f	g	q	w	Class	δ (CK)	CK-diff	Drat	δ(t*)	δ (TR)
H00	3/4	AZ	61.23 ± 0.81	52	19	100	300	5	0.62	0.69	32.3	18.7	B	4.3	3.6	4.5	3.8	2.6
		BX	63.83 ± 2.71	52	23	0	300	6	0.65	0.74	11.4	5.7	A	4.4	4.9	4.2	0	2.4
		BY	59.97 ± 1.38	52	15	100	300	5	0.55	0.62	15.0	8.6	B	4.8	7.8	5.7	0	2.4
HB	1/5	4X	60.44 ± 3.84	52	15	0	300	6	0.97	0.48	7.4	3.7	B	6.9	7.7	4.6	2.0	0.8
HE	2/5	2Y	49.46 ± 3.46	52	-5	0	300	6	0.34	0.59	2.8	1.4	B	5.2	3.8	11.0	0	1.4
		7X	42.80 ± 2.01	52	-18	0	340	7	0.60	0.71	9.0	4.0	B	7.0	9.6	8.9	1.1	1.0
HG	4/5	12X	33.38 ± 1.36	52	-26	100	340	6	0.62	0.72	11.0	5.5	A	4.1	0.1	5.6	0	4.3
		12Y	48.53 ± 2.58	52	-7	0	300	6	0.60	0.78	8.8	4.4	A	2.1	3.4	2.5	0.7	1.4
		13X	45.45 ± 0.95	52	-13	0	300	6	0.63	0.78	23.6	11.8	A	2.5	0.1	3.0	0.2	0.7
		14Y	45.90 ± 1.08	52	-12	0	340	7	0.86	0.78	28.5	12.7	A	3.8	4.7	3.2	0	2.6

Notes: n/N shows successful versus attempted determinations; H is the palaeointensity value with associated standard deviation (S.D.); H_{exp} is the expected field intensity; IEF is the intensity error fraction; T_{min} and T_{max} denote the temperature range of the straight line segment calculated over N successive points; the fraction of NRM (f), the gap factor (g), the quality factor (q), calculated after Coe et al. (1978); w denotes the weighting factor (Prévot et al., 1985); the class is assigned by the determination criteria of Leonhardt et al., 2004; δ (CK) is the difference between pTRM*- check and repeated pTRM acquisition normalized to the TRM; Drat, like δ (CK) but normalized to the length of the selected segment (Selklin & Tauxe, 2000); δ(t*) is the relative extend of the true tail according to Leonhardt et al., 2004 and δ (TR) is the intensity difference of first and repeated demagnetization step normalized to NRMt.

6. Discussion

As can been seen from Table 3.3, many of the actual known field values fall within the error ranges of the multispecimen PI estimates, though there is clearly a tendency towards over-estimation; 10 out of the 12 estimations are too high. Interestingly the samples from the same locality as considered by Dekkers & Böhnel (2006) yielded one of the lowest IEF percentages. There are several possible mechanisms for this overestimation. The choice of pTRM acquisition temperature might have some effect on accuracy of the multispecimen experiment; however, for the one site (H00) where we repeated the experiment at a different acquisition temperature, both PI estimates were almost identical. Possible factors that govern overestimations of PI measurements are discussed in the following.

6.1 MD remanences as the possible cause of PI-overestimates

One possible reason for these overestimates is the presence of MD material. As stated in the introduction the multispecimen approach is based on the first-order symmetry findings of Biggen & Poidras (2006). However, the phenomenological model of Biggen & Poidras (2006) is not supported by the study of McClelland et al. (1996) who conducted a number of progressive re-magnetisation experiments for synthetic powders of sized MD magnetite, i.e., over-printing of TRM with successive pTRMs (field always on). In contrast to Biggen & Poidras (2006), they found that incrementally replacing a laboratory TRM, with parallel pTRMs induced at increasing temperatures, resulted in a systematic reduction of the total intensity (Fig. 3.7). The original TRM was repeatable. However, it is not known how reliable the samples (provided by Dankers (1978)) used in the McClelland et al. (1996) study are, as some of the larger samples display self-reversing behaviour (McClelland & Shcherbakov, 1995).

As a rough estimate of MD content, the ratio M_{RS}/M_S provides a crude estimate, i.e., as M_{RS}/M_S increases the material becomes more SD like. We plot IEF (%) versus M_{RS}/M_S (Fig. 3.6). With the exception of sample H91, it shows that there is a loose inverse correlation ($R^2 = 0.30$) between IEF (%) versus M_{RS}/M_S, i.e., as the material becomes more MD-like the overestimation in PI increases. This is particularly apparent for the two sites EE and DY, which yielded the highest overestimates (30% and 31%) and have the lowest M_{RS}/M_S ratios of ~ 0.1. However, it is intriguing that these sites are of similar age and show similar overestimates. It has to be noted, that the high IEFs observed here may partly be due to inaccuracies in the GUFM1 model and that the resolution of the field model is too low for such a detailed comparison study. Furthermore, uncertainties due to extrapolating back from the 1590 PI + secular variation estimates (see Table 3.3) to obtain I_{exp} values for these sites might introduce a further bias here. The only site, which does not follow the observed trend towards overestimation of the PI, is site H91. A FORC diagram from site H91 (Fig. 3.3b), is characteristic of SD material, yet its M_{RS}/M_S ratio is quite low. It is likely that the dominant carrier is SD, yet there is sufficient non-SD behaving material in the sample to reduce M_{RS}/M_S.

In general, the trend observed in Figure 3.7 stands in contrast to the results of Dekkers & Böhnel (2006), who obtained reasonable PI estimates for a laboratory induced TRM imparted in three MD magnetite-powder samples.

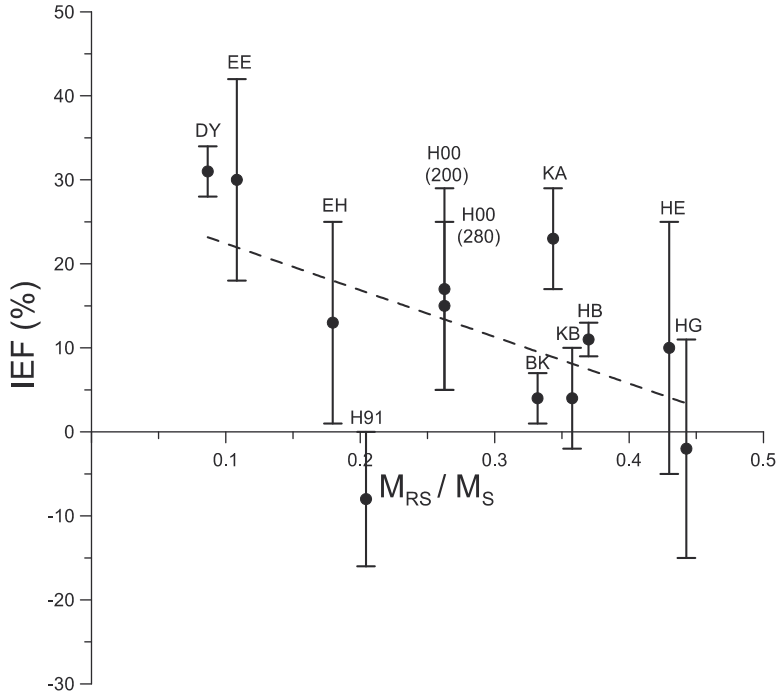

Figure 3.6. Intensity error fraction (IEF%) of the multispecimen PI experiments versus M_{RS}/M_S for samples considered in this study. M_{RS}/M_S is treated as an estimate of MD contribution to the bulk remanence. A linear regression (R^2= 0.30) is indicated by the dashed line.

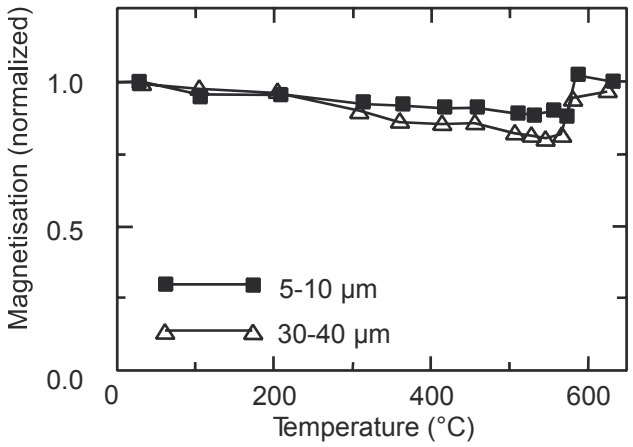

Figure 3.7. Progressive remagnetisation of a TRM by partial replacement with a pTRM on crushed and sieved stoichiometric magnetite samples with size fractions of 5-10 µm and 30-40 µm. Redrawn from McClelland et al. (1996).

6.2 Possible influences of cooling rate effects

Several studies have previously documented, that differences in cooling rates between the original remanence acquisition of a rock unit and that acquired in the laboratory, will yield erroneous PI results. In general, the TRM intensity in an assemblage of SD is positively correlated with cooling time (e.g. Fox & Aitken, 1980, McClelland-Brown, 1984, Selkin & Tauxe, 2000) and would produce rather higher palaeointensities because the cooling time in the laboratory is much faster (often not more than 30 minutes) than compared to the cooling of a lava flow in nature (up to several months). The effect of differences in the cooling rate on TRM intensity in MD and PSD assemblages is presently still a matter of

debate. McClelland-Brown (1984) argued that faster cooling rates will give rise to weaker TRMs. This would cause underestimations of the PI for samples characterized by a high amount of MD particles, which is in contrast to the trend observed in Figure 3.6. In their comparison study of several different palaeointensity techniques, performed on samples from Mt. Etna, Biggin et al. (2007) observed rather lower PIs from samples taken from the interior of the lavas flows, when compared to the samples from the upper flow units, which supports the argument of McClelland-Brown (1984). However, the samples used in this study, all came either from flow tops or the outer margins and fronts of lava flows. Thus they are assumed to have cooled rapidly. We therefore regard the effects of cooling rate difference as negligible for the outcome of our study.

6.3 Comparison with the IZZI protocol results

In Table 3.3, we compare the multispecimen results with the data derived from the Thellier-type IZZI protocol. Site KB failed to pass the quality checks, and hence failed to return an IZZI PI estimate. Four sites returned a PI estimate after both methods. It is apparent, that the multispecimen method produced PI estimates closer to the actual field than the IZZI estimates and additionally returned a reasonable PI estimate for the site KB, which failed the IZZI protocol. That is, on the five lavas subjected to both methods measured in this study, the multispecimen method produced more accurate PI estimates.
There are some important points and differences between the two approaches, which require a further discussion. The Thellier-type methods have been developed, refined and tested many times, resulting in much stricter analysis and selection criteria. For the multispecimen analysis the only assessment of quality is the quality of fit of the linear regression applied to the data.

In this study, the average of the IZZI IEFs is close to zero (-0.9%). In contrast, the average IEF for the multispecimen samples (+12%) shows positive values. Yet, the average multispecimen PI is closer to the actual field intensity. A possible reason for the increase in accuracy is the number of samples, or the total amount of material used to provide the PI estimates. In the IZZI approach, many samples fail the selection criteria for reliable palaeointensity determination (i.e. at site HB, only one specimen out of five produced a reliable PI estimate). Further we observe inaccuracies of up to ~20 % on an individual sample level, even for high quality samples displaying class A behaviour. It is assumed that this would be the case for any common Thellier-type method. It further highlights the importance, that a PI estimate should be based on the results from multiple samples, when adopting the Thellier method, i.e. $n \geq 5$, as previously proposed by Biggen et al., (2003). This is the case in the multispecimen approach because, by its very nature, it requires between eight and ten samples. Therefore, whilst the multispecimen approach provides only a single answer, the answer is based on average on more samples than used in a typical Thellier-type PI estimate from a single flow unit.

7. Conclusions

Results from this study place some important new constraints on the applicability of the multispecimen parallel differential pTRM method in future palaeointensity studies.

Results of six multispecimen PI experiments from 11 historic lava flows investigated in this study, yielded results that are very close, or indistinguishable within error from the expected intensity. This observation largely confirms the findings that were presented in the initial study of Dekkers & Böhnel (2006).

However, we observed a bias towards over-estimation because from in total 12 estimations, 10 gave values too high. The observed inverse correlation between IEF (%) versus M_{RS}/M_S, indicates that, as the material becomes more MD-like, the overestimation in PI increases. We interpret this being due to effective demagnetisation during progressive re-magnetisation, leading to an overestimate of the palaeointensity. This apparent bias in the final outcome of a multispecimen experiment implies that the method might not be entirely independent of magnetic domain state as previously proposed by Dekkers & Böhnel (2006).

On sister samples from five lavas, additional Thellier-type experiments were carried out. When compared to the corresponding multispecimen PI experiments, we found that the latter gave palaeointensity estimates that were closer to the expected intensity values. Besides showing inaccuracies of > 20 % on individual high quality samples, the Thellier-type approach had a much lower success rate in obtaining a PI estimate. Furthermore, it was not possible to process samples from one lava flow with very low Curie temperatures (Tc= 105°- 140°C) with a Thellier-type approach, due to experimentally induced alteration. Here, the multispecimen experiment was still successful in producing one PI estimate for this site, suggesting that the multispecimen method has a higher potential in obtaining PI estimates from such critical material.

We suggest that by performing sets of different experiments at different pTRM acquisition temperatures with smaller field steps will increase statistical precision and minimize other biasing effects i.e. thermal alteration during the laboratory experiment. The issue of MD contribution to multispecimen PI estimates needs to be fully quantified, and other potential factors that might govern incomplete remagnetisation, e.g., increased internal stress, need to be experimentally evaluated.

From the majority of results obtained in this study, the multispecimen method appears to be a viable alternative for future palaeointensity studies. The significantly faster sample processing rate will open up the possibility for acquiring larger datasets of palaeointensity data. Future studies need to develop reliability tests and assess the quality of PI estimates for the multispecimen parallel differential pTRM method.

Acknowledgements

We thank Michael Winklhofer for providing the FORCobello computer program and David Gubbins for providing the GUFM1 program. Andrew Biggin and David Krása are thanked for giving some valuable comments to improve the manuscript. Much appreciated assistance during the collection of the Mexican samples came from Ivan Barajas and Gildardo Gonzalez. Collection of the Mexican samples was funded by DFG grant 334/1-2 and Conacyt grant 46213. Collection of the Icelandic samples was funded through NERC grant NE/D000351/1. ARM is funded by the Royal Society.

4. Evidence for geomagnetic excursions recorded in Brunhes- and Matuyama – Chron lavas from the Trans-Mexican Volcanic Belt

Daniel M. Michalk [a], Norbert R. Nowaczyk [a], Harald N. Böhnel [b], Gerardo J. Aguírre-Diaz [b], Steven Ownby [c], Margarita López-Martínez [d] and Jörg F.W. Negendank [a]

[a] *Helmholz-Zentrum Potsdam, Deutsches GeoForschungsZentrum, Germany*
[b] *Centro de Geociencias, UNAM-Campus Juriquilla, Queretaro, Mexico*
[c] *Department of Geological Sciences, University of Michigan, USA*
[d] *Departamento de Geología, Centro de Investigación Científica y Educación Superior de Ensenada, Ensenada, México.*

Submitted to: Journal of Geophysical Research

Abstract This study presents palaeomagnetic data from 56 independent lava flows from the Trans- Mexican Volcanic Belt (TMVB) with ages from 6.4 Ma to recent, but most being younger than 1 Ma, and 11 new age determinations after the $^{40}Ar/^{39}Ar$ method. Generally, the remanence was found to be carried by Ti-poor titanomagnetites of pseudosingle-domain magnetic structure, except for nine lavas that contain small amounts of titanomaghemite, and four lavas, which contain additional (titano-) hematite. Palaeosecular variation, estimated from the scatter of virtual geomagnetic poles of lava flows younger than 1.7 Ma, is consistent with latitude dependent Model G and is also in agreement with other high quality palaeomagnetic data based on Pleistocene lava flows from the TMVB. The directional record of lavas that erupted during the Brunhes- and Matuyama Chrons was correlated to the geomagnetic polarity timescale extended with geomagnetic excursions and there is evidence for at least 4 geomagnetic excursions. One lava flow with a fully reversed palaeodirection, dated at 592 ± 20 ka, most likely erupted during the Big Lost excursion (579 ± 6 ka). Another fully reversed flow, dated at 671 ± 13 ka, gives new volcanic evidence for the Delta / Stage 17 excursion (~670 ka). From the Matuyama age lavas, one flow with normal polarity magnetization, dated at 933 ± 40 ka, could either be related to the Kamikatsura excursion (900 ± 6) or the Santa Rosa excursion (936 ± 8 ka) and a normal polarity flow, dated at 1600 ± 60 ka, could have been emplaced during the Gilsa excursion (~ 1570 ka).

1. Introduction

It is known since Brunhes (1906) that the Earth's magnetic field switches polarity, and from the geological record it is known that complete polarity field reversals have occurred intermittently through geological time (Cande and Kent, 1992, 1995). The last geomagnetic reversal occurred 776±2 ka ago (Coe et al., 2004; Singer et al., 2005) when it changed from a reversed polarity regime (Matuyama Chron, 0.78-2.56 Ma) to its present normal polarity regime (Brunhes Chron). However, numerous palaeomagnetic studies indicate that the magnetic field was not entirely in its dominantly dipolar configuration neither throughout the Brunhes Chron, nor the Matuyama Chron. Instead, the magnetic field departed several times from its predominant axial dipole configuration, as indicated by numerous geomagnetic excursions and events reported in the literature (e.g. Champion et al., 1988; Langereis et al., 1997; Lund et al., 1998, 2006; Singer et al., 1999, 2002, 2008a,b). Geomagnetic excursions can be defined as relatively short periods within an otherwise stable polarity chron, during which the field directions lie outside the range of expected secular variation of the geocentric axial dipole (GAD) field

configuration. In the case of a geomagnetic excursion the field returns after a few thousand years to the same polarity, whereas in the case of a geomagnetic event, the field reverses completely for a short time. Depending on the location on the globe, geomagnetic excursions / events may last for ~2 ka up to ~10 ka, making their recognition difficult in marine and lacustrine sediments with low deposition rates, but also in volcanic rocks that are only extruded sporadically. There is still a considerable debate about the number of true excursions there being arguably as many as 17 excursions within the Brunhes Chron alone (Lund et al., 2006) and up to 9 within the reverse Matuyama Chron (Channell et al., 2002).

Excursions are generally accompanied with intensity lows as documented in relative palaeointensity records from marine sediment cores (see Lund et al., 2006 and references therein) but little is known about the primary geodynamic processes that lead to a geomagnetic excursion as well as the total duration of an excursion. Doell and Cox (1972) and Opdyke (1972) suggested that a geomagnetic excursion represents an incomplete polarity transition (aborted reversal) before the field returns back to a stable polarity state. More recently, Gubbins (1999) proposed that excursions reflect shorter and more frequent weakenings of the main dipole field where the field only reverses in the liquid outer core, on short timescales of around 500 years, but not in the solid inner core, where diffusion time of magnetic flux must exceed about 3 ka in order to maintain a full reversal for a longer time. This hypothesis has been challenged by Knudsen et al. (2007), who present evidence that the field spent around 7 to 8 ka in a transitional state (including virtual geomagnetic poles reaching high southerly latitudes), which is a similar time span to the estimated duration of a polarity reversal (Clement, 2004). Numerical dynamo simulations by Wicht (2005) suggest a strong site dependence on the occurrence and duration of excursions, which means that many excursions might not be a global feature of the geomagnetic field. There is little knowledge about the timing, duration and global validity of excursions but it is now assumed by many workers that during the Brunhes Chron and perhaps the Matuyama Chron, the geodynamo was characterized by up to 20% of the time by a weak non dipole state (e.g. Merrill & McFadden, 1994; Guyodo and Valet, 1999), and it is likely that this was true for other polarity chrons as well. Therefore, knowing the precise number of geomagnetic excursions, their timing / duration, and recognizing them in different parts of the globe is essential for a more complete understanding of the complex dynamo processes. Up to the present, volcanic evidence exists for nine excursions within the Brunhes chron (Lachamp, possibly Nowegian-Greenland Sea, Blake, Pringle Falls, Calabrian Ridge 2 / West Eifel 5, West Eifel 4, Big Lost / West Eifel 3, West Eifel 2 and 1) and six within the Matuyama (Kamikatsura, Santa Rosa, Punaruu, Cobb Mountain, Gilsa and Réunion; see Singer et al., 2002, 2004, 2007, and 2008a,b). Yet, for an unambiguous confirmation of excursional records from sediments and their global validity, more evidence from radioisotopically dated volcanic rocks is highly desired. If ages are well constraied, they provide geochronologic tie points for calibrating the global record of relative palaeointensity and associated distortions of its geometry.

We report a detailed integrated rock-and palaeomagnetic study of 63 independent lava flows with radioisotopically constrained ages from Recent back to 6.4 Ma from within the Trans-Mexican Volcanic Belt (TMVB). New age data were determined for 11 lavas in this study using the $^{40}Ar/^{39}Ar$ method. The main objective was to identify if possible, some of the geomagnetic excursions within the Brunhes- and Matuyama Chrons in order to better constrain the geomagnetic instability timescale (Singer et al., 2002, 2008a,b).

2. Geological setting and geochronology

The target of the present study was the E-W trending TMVB, which crosses central Mexico from coast to coast at latitudes from 19 to 21°N with a width between 20 and 150 km (Fig. 4.1). Nearly 1000 km long, it is one of the largest continental volcanic arcs on the North American Plate. Its western part is associated with the subduction of the Rivera Plate (commencing at ~ 9 Ma), whereas the eastern part relates to the subduction of the Cocos Plate (commencing at 12-18 Ma) under the North American Plate (middle

American Trench) (Klitgord and Mammerickx, 1982). The TMVB comprises roughly 8000 volcanic structures, mainly stratovolcanoes, cinder cones and caldera complexes, with probably several hundreds of them being younger than 2 million years (Demant, 1978; Aguirre-Díaz et al., 1998).

Four monogenic volcanic fields have been reported in the TMVB (Aguirre-Díaz et al., 2006); these are: Michoacán-Guanajuato, Jilotepec, Chichinautzin and Valle de Bravo. Palaeomagnetic sampling was carried out in two of them, Michoacán-Guanajuato and Valle de Bravo, and in other localities relevant for this study. In summary, samples were collected at (1) Ceboruco-San Pedro- (CEB), (2) Tequila- (TEQ), (3) Michoacan Guanajuato- (MG) and (4) Valle de Bravo (VdB) Volcanic Field and (5) Cofre de Perote-Pico de Orizaba at the eastern part of the TMVB (hereafter referred to as E-TMVB). Our criteria in the selection of the sampling sites were 1) the availability of reliable radioisotopic age determinations from previous geochronological studies and, 2) a representative coverage of the TMVB from west to east. Detailed landsat-photos of the field areas are included in the appendix.

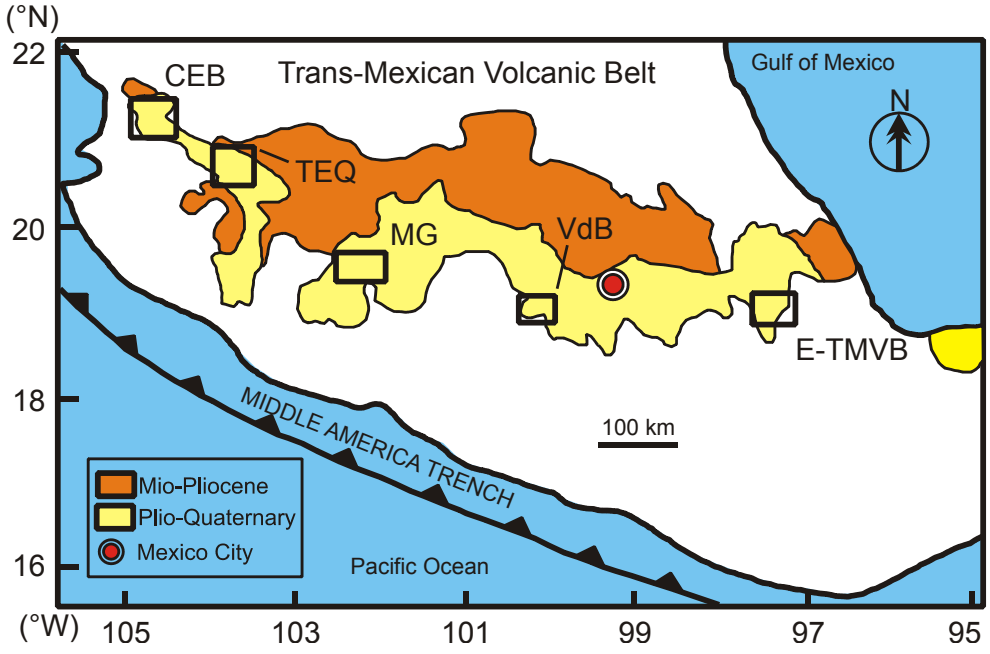

Figure 4.1. Schematic map of the Trans-Mexican Volcanic Belt showing the sampling areas indicated by solid rectangles. CEB = Ceboruco San-Pedro Volcanic Field, TEQ = Tequila Volcanic Field, MG = Michoacan Guanajuato Volcanic Field, VdB = Valle de Bravo Volcanic Field, E-TMVB = Eastern Trans-Mexican Volcanic Belt (Modified after Aguirre-Díaz, 1996).

3. Geochronology

The majority of lavas were previously dated by the ^{40}Ar-^{39}Ar method, with three further lavas using thermoluminescence (TL) methods on quartz separates (Schaaf and Ramírez-Luna, 2008). In the course of the present study, 11 new $^{40}Ar/^{39}Ar$ ages of lava flows from the VdB were determined at CICESE, Ensenada, Mexico. All the samples were irradiated in position 5c of the uranium enriched, nuclear reactor of McMaster University in Canada. The samples were irradiated in three different groups: CIC-45 (samples DG, AN, DH); CIC-46 (samples DF, AF, DE, AO) and CIC-56 (samples AL2, BV, BZ, BW). Capsules CIC-45 and CIC-46 received a dose of 10 MWH and included as irradiation monitors biotite CATAV 7-4 (88.53 ± 0.39 Ma: internal standard calibrated with hornblende hb 3gr at the University of Toronto and with hornblende MMhb 1 at the University of Nice) and biotite HD-B1 (23.61 ± 0.22 Ma; Furhmann et al., 1978). Capsule CIC-56 received a dose of 30 MWH using Cd liner and included as irradiation monitor sanidine TCR-2 (28.34 ± 0.16 Ma for TCR / 28.02 ± 0.16 Ma for FCT sanidine, Renne et al., 1998). The aliquots of the monitors were distributed evenly between the samples. The age of the samples was calculated with the J value obtained from the average of the monitors closest to them. The first step heating experiments were conducted with a Modification Ltd Ta furnace (samples DE and DH, Table 1), on line with an MS-10 mass spectrometer, for these experiments aliquots of 1 to 2 g were analyzed. The rest of the experiments were performed with the VG5400 mass spectrometer using less than 0.001 g of sample. A Coherent Innova 70c argon laser was used to step heat the samples. To verify the reproducibility of the experiments, two samples (codes DF and AN) were analyzed on both mass spectrometers. The first step of the data reduction was the blank correction, to do this, blanks were routinely measured before each experiment with all the argon masses measured, the blank correction was performed on a mass to mass basis because the blank composition is not atmospheric. The blanks for the MS-10 runs, consisted of a one-step measurement at 1350°C, a temperature dependent factor was applied for the blank correction (F = 0.3 for T< 800°C; F = 0.4 for 800 < T < 1100°C; F = 0.6 T > 1100°C). Typical blanks for mass 40 were ~2.6 E-8 cc STP and ~0.9 E-10 cc STP for mass 36. For the laser step-heating experiments conducted on the VG5400 mass spectrometer, every sample measurement was preceded by a blank run, the blank runs were performed following the same procedure for the sample with the exception of turning on the laser. Blanks for the VG5400 have a typical composition of 1.3 E-12 cc STP for mass 40 and ~6.7 E-14 CC STP for mass 36. Upon blank subtraction the argon isotopes were corrected for mass discrimination, calcium, potassium and chlorine neutron induced interference reactions: $(^{39}Ar/^{37}Ar)_{Ca} = (6.51 \pm 0.31) \times 10^{-4}$; $(^{36}Ar/^{37}Ar)_{Ca} = (2.54 \pm 0.09) \times 10^{-4}$; $(^{40}Ar/^{39}Ar)_{K} = (1.560 \pm 0.040) \times 10^{-2}$ for CIC-45 and CIC-46 and $(^{39}Ar/^{37}Ar)_{Ca} = (6.50 \pm 0.47) \times 10^{-4}$; $(^{36}Ar/^{37}Ar)_{Ca} = (2.55 \pm 0.28) \times 10^{-4}$; $(^{40}Ar/^{39}Ar)_{K} = 0$ for CIC-56 in which a Cd liner was used). Mass 36 was also corrected for chlorine derived ^{36}Ar (^{35}Cl (n, γ) $^{36}Cl \rightarrow {}^{36}Ar + \beta$ with $t_{½} = 3.1\times10^{5}$ a). Isotopes ^{37}Ar and ^{39}Ar were corrected for radioactive decay. The constants recommended by Steiger and Jäger 1977 were used in all the calculations while all the straight line calculations were performed with the equations presented in York et al., 2004. All errors are reported at 1σ level. The errors in the integrated, plateau and isochron age include the uncertainty in the J parameter. Additionally for the plateau and isochron ages, the goodness of fit was included in the age uncertainty whenever the MSWD exceeded 1. The integrated ages were calculated adding the fractions of the step-heating experiments. Plateau ages were calculated with the weighted mean of three or more consecutive fractions which were in agreement within 1 σ errors excluding the uncertainty in J. All the data were plotted in the $^{36}Ar/^{40}Ar$ versus $^{39}Ar/^{40}Ar$ diagram to determine the composition of the $(^{40}Ar/^{36}Ar)_{i}$ of the samples, however some samples were characterized by poor ^{40}Ar radiogenic content, therefore the data distribution in the correlation diagram did not yield well defined straight lines, this behaviour did not permit the calculation of reliable isochron ages, in these cases the plateau ages were taken as the best estimate for the cooling age of the lavas.

The TMVB has been the target of numerous paleomagnetic studies since the 1970's. The earliest studies (e.g. Mooser et al., 1974) were primarily carried out for magnetostratigraphic purposes, while several subsequent studies were concerned with studying the palaeosecular variation (PSV) (e.g. Herrero-Bervera & Pal, 1977; Böhnel & Negendank, 1981; Steele, 1985; Herrero-Bervera et al., 1986). Later studies focused on studying the PSV and absolute palaeointensity (PI) on lava flows younger than 40 ka (Gonzales et al, 1997; Morales et al., 2001; Böhnel & Molina-Garza, 2002). Böhnel and Molina-Garza (2002) presented a compilation of PSV and PI data from Mexico covering the last 40 ka. Another comprehensive compilation of PSV data ranging from Pleistocene to recent age is presented by Mejia et al. (2005), who applied a strict quality index to previously published palaeomagnetic data. This data indicates values of PSV for Mexico that are consistent with latitude dependent Model G of McFadden et al. (1988, 1991) and a time averaged field, which is best described by an axial geocentric dipole plus a 5% quadrupole. More recently, two studies from Mexico were published with evidence that some Brunhes Chron lava flows recorded geomagnetic excursions. Petronille et al. (2005) report results from three lavas with intermediate to fully reversed directions being contemporary with the Big Lost excursion (Champion et al., 1988) and the Brunhes / Matuyama precursor (Singer et al., 2005). In another study Ceja et al. (2006) link three lavas with intermediate to reversed magnetizations to the Levantine excursion (Ryan, 1972; Biswas et al., 1999) and the Delta excursion (Creer et al., 1980), respectively.

3. Palaeomagnetic sampling and experimental techniques

Volcanic rocks were sampled using drill bits of 12 mm diameter, which yielded so called "mini-core" samples. Palaeomagnetic samples were dispersed both vertically and horizontally across an outcrop interval as large as possible, in general more than 15 m and were then oriented with both, magnetic and sun compasses. We sampled only fresh outcrops that showed no apparent signs of alteration due to weathering. Later, samples were cut into successive specimens of 10 mm length from which the outer 15 to 20 mm were discarded in order to further minimize effects of surface weathering.

The natural remanent magnetization (NRM) of 5 to 21 specimens from each flow was measured using a cryogenic magnetometer (2G Enterprises 755 SRM) with long core setup at the Deutsches GeoForschungsZentrum. The only exception was site DH, from which only three oriented cores were recovered. Stepwise alternating field (AF) demagnetization was carried out fully automatically with the in-line 3-axis alternating field demagnetizer over 10/11 demagnetization steps with peak fields up to 100/125 mT, while thermal demagnetization was applied to a smaller subset of samples (2 - 4 samples per flow) over 11 to 13 demagnetization steps with a Magnetic Measurements Ltd. MMTD oven. After each thermal demagnetization step, low field susceptibility (χ) was measured with a Bartington MS2B susceptibility sensor to monitor possible chemical alterations during heating. A combination of sets of different rock magnetic measurements was performed on selected samples to confidently ascertain the magnetic mineralogy and grainsize, as well as the mechanisms by which this remanence was acquired.
Thermomagnetic curves (M_S-T curves) were measured on 2 samples per flow, with a Variable Field Translation Balance (VFTB) from room temperature to 600 / 700°C in an Argon environment, applying a field of 500 mT. Curie temperatures (T_C) were then determined after the method of Moskowitz (1981). Sets of 2-3 hysteresis measurements, backfield- and isothermal remanent magnetization (IRM) acquisition curves were measured on 30-50 mg chips with a Princeton Measurements Alternating Field Gradient Magnetometer (AGFM). From that data (after the removal of the paramagnetic contribution), the standard hysteresis parameters were determined: the saturation magnetization (M_S), the saturation remanence (M_{RS}), the coercivity force (B_C) and the coercivity of remanence (B_{CR}). Using the ratios M_{RS} / M_S and B_{CR} / B_C, a Day-plot was created (Day et al., 1977, Dunlop, 2002) to deduce the bulk magnetic domain state. The S-ratio (Bloemendal et al., 1992) and the shape-parameter (Fabian, 2003), were also determined. Polished thin sections were prepared for ore microscopy studies.

4. Results

4.1 Rock magnetic properties

4.1.1 Thermomagnetic behaviour

According to the obtained results, in the M_S(T) curves 8 different types of thermomagnetic behaviour (A-G) can be distinguished (Fig. 4.2).

Type A curves show good reversibility and a single magnetic phase with a high Curie Temperature between 510-575° C, which is indicative of Ti-poor titanomagnetites (Fig. 4.2a). Type A' curves (Fig. 4.2b) show similar behaviour as type A curves but with a slight decrease in magnetization on the cooling branch probably due to the production of a magnetic mineral with a smaller magnetic moment on heating (probably hematite), at the expense of one with a larger moment (probably magnetite), either by inversion or oxidation during laboratory heating. Such curves still show good reversibility, suggesting that the former process is dominant. Type A or A' behaviour was observed in 44 out of a total of 63 samples.

Type B curves (sites DF and CF) show excellent reversibility and a T_C between 320 and 420°C (Fig. 4.2c), indicative of titanomagnetites with compositional parameter between $x \approx 0.25$-0.4 (O'Reilly, 1984).

Type C behaviour (Fig. 4.2d) was found in samples from three sites (DX, DH and CN). Two Curie Temperatures were observed on the heating curve, the low temperature phase ($T_C \sim$ 220-370°C) being probably due to cation-deficient titanomagnetite, as this phase is not seen in the cooling curve, while the high temperature phase again indicates Ti-poor titanomagnetite. Reversibility is still good, although a slight increase of M_S is observed in the cooling curve.

Samples displaying two different T_C's at ~ 310-350° C and ~ 520-560° C (Fig. 4.2e) are classified as Type D samples (site CK and CI). Curves are fairly reversible and both T_C's are seen on the heating and cooling branches, again with a small increase of M_S in the cooling curve. This behaviour is interpreted as being indicative of two different titanomagnetites with differing Ti content.

Type E behaviour (Fig. 4.2f), is characterized by a single phase of titanomagnetite with a T_C between 190 and 290°C, which indicates a fairly high Ti content ($x \approx 0.6$-0.4). Such curves (sites AY, AV and CP) are typical for titanomagnetites where no deuteric oxidation occurred on primary cooling, but since then have undergone some low-temperature oxidation (maghemitization), as indicated by the irreversibility and higher M_S values seen in the cooling curve.

Samples showing a titanomaghemite inversion peak at around 350 to 430° C (Fig. 4.2g) are classified as Type F samples (sites CT, CV, CY and AN). On continued heating above the inversion peak, titanomaghemite is transformed to a magnetic phase with a T_C of around 580°C, close to that of pure magnetite.

In samples showing Type G behaviour (Fig. 4.2h) a pronounced Curie temperature is masked by the paramagnetic contribution. Samples showing this rather noisy behaviour (sites AL2, EK, EI and CM) generally displayed the weakest magnetizations.

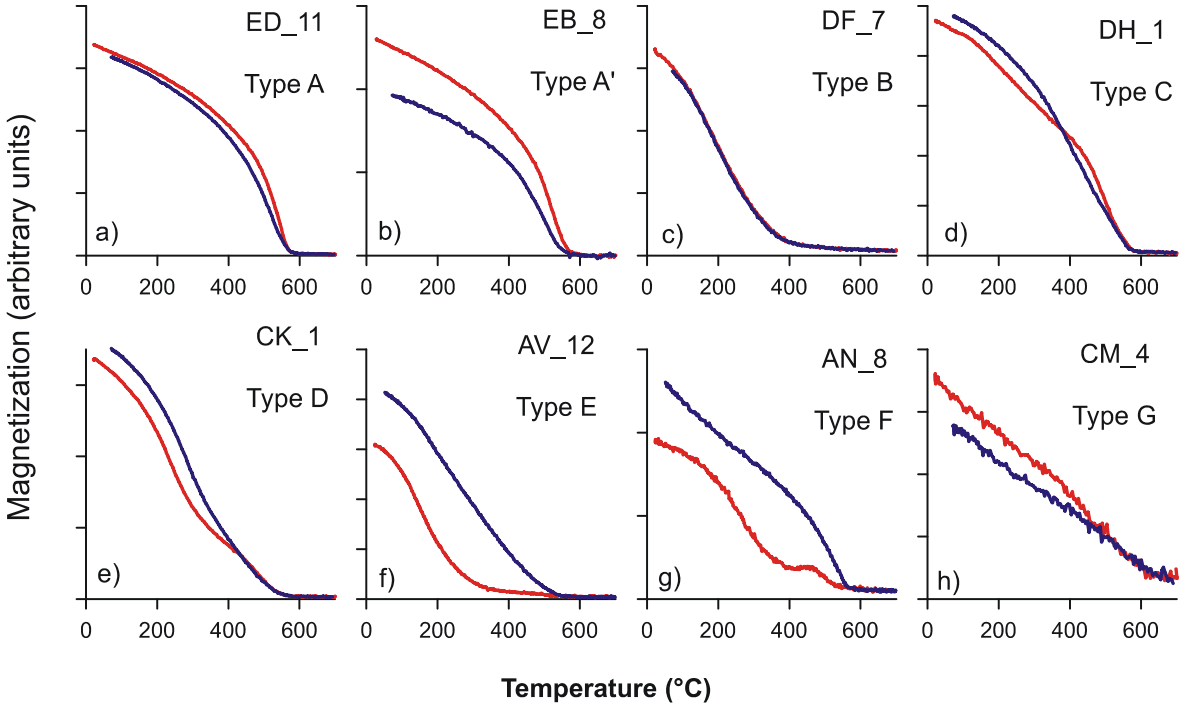

Figure 4.2. Different types of thermomagnetic curves obtained with a Variable Field Translation Balance (VFTB) in a field of 500 mT from room temperature to 700°C. Heating (red line) and cooling (blue line) was conducted under Argon flushing. A correction for paramagnetic content was not necessary as magnetizations above the highest Curie temperature were small (generally between 6 and less than 2 per cent).

4.1.2 Microscopy studies

Reflected light microscopy studies revealed that samples with high Curie Temperatures between 510 and 575 °C and thermomagnetic behaviour of type A or A' often contain intermediately exsolved titanomagnetites (oxidation stages C3-C4, after Haggerty, 1991) with some ilmenite lamellae (Fig. 4.3a).

Skeletal or needle-like titanomagnetites were found in lavas showing thermomagnetic Type E behaviour (sites AY and AV). Here, titanomagnetites appear unblemished, indicating a fast cooling of the lava before deuteric oxidation could occur (Fig. 4.3b). This habitus is similar to the ones reported by Urrutia-Fucugauchi et al. (1984) from a columnar basalt from Central Mexico, or from mid ocean ridge basalt samples reported by Krása and Matzka (2007). Visual signs of maghemitization were found in samples from sites AR, BH and CQ. Here, titanomagnetites display the typical surface cracks on the crystals, as a result from the change in volume due to diffusion of Fe^{2+} from the crystal lattice structure to the surface, where it is converted to Fe^{3+} (Fig. 4.3c). However, thermal stability does not seem to be greatly affected, as samples from these lavas still displayed reversible behaviour during the thermomagnetic experiment. Samples from two sites showing thermomagnetic Type G behaviour (AL2 and AF) are clearly characterized by contributions of (titano-) hematite, which likely causes the noisy behaviour during the thermomagnetic experiments. These samples appeared red in colour, and ore microscopy studies revealed that almost all the primary spinel minerals were altered/limonitised to rutile with goethite and lepidocrocite by low temperature oxidation (or perhaps hydrothermal alteration, Fig. 4.4a and b). However, as seen in the backscattered electron micrograph in Figure 4c, very small titanomagnetites, often of sub-micron size are observed along needles of pyroxene. These titanomagnetites appear unblemished and probably remained unaffected by the oxygen fugacity. In samples from site AQ, characterized by (titano-) hematite, large titanomagnetite grains showed signs of replacement stage oxidation (C6) as indicated by the graphical / myrmecitic intergrowth of pseudobrookite (Fig. 4.4d and e).

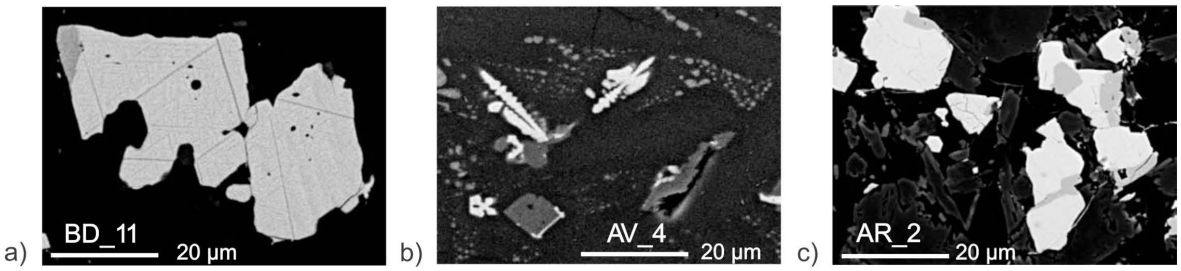

Figure 4.3. Zeiss DSM962 backscattered electron microscope micrographs of a) Ti-poor titanomagnetite with exsolved ilmenite lamellae (sample BD_11 from the Michoacan-Guanajuato volcanic field; oxidation stage C3- C4), b) Skeletal titanomagnetite grains classified as the cruciform type (sample AV_4 from the Ceboruco San-Pedro volcanic field; oxidation stage C1), c) large unexsolved titanomagnetite grains with shrinking cracks due to low temperature oxidation / maghemitization (sample AR_2 from the Ceboruco San-Pedro volcanic field). Classifications follow Haggerty (1991).

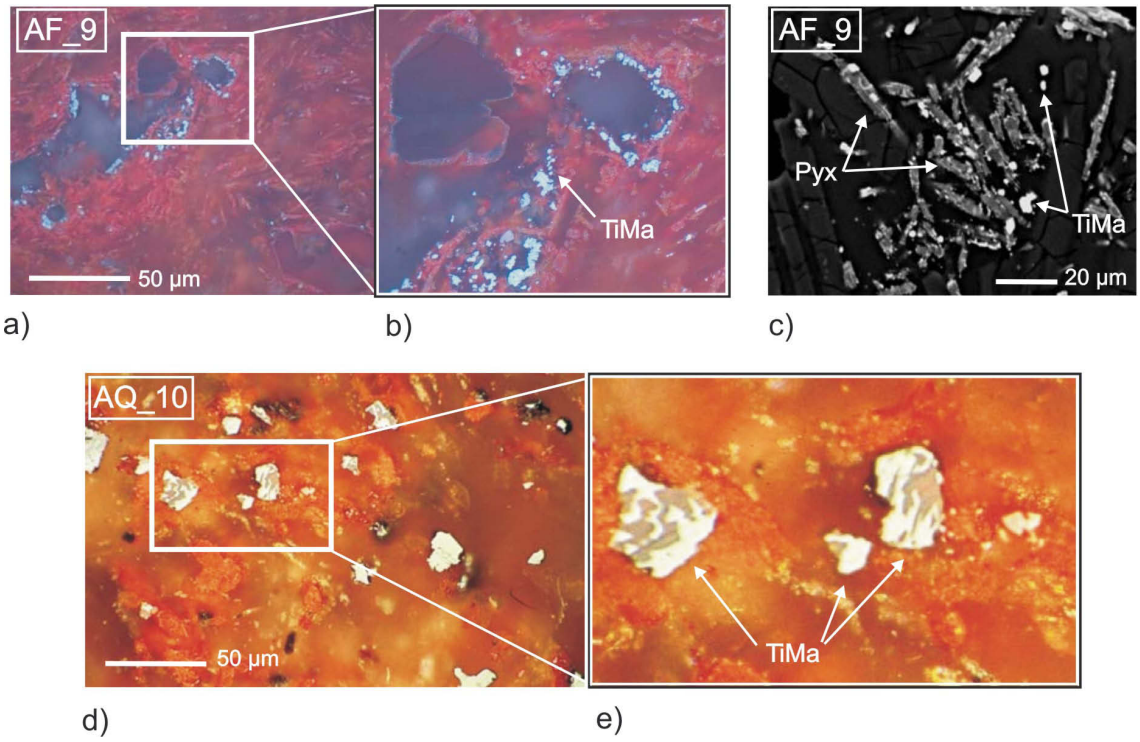

Figure 4.4. Examples of reflected-light microscopy; 4a-c: highly oxidized lava (sample AF_9 from the Valle de Bravo volcanic field), dominated by (titano-) hematite, which appears red in colour; inset (4b): small titanomagnetites (TiMa) unaffected by alteration, which appear grey in colour; 4c: backscattered electron microscope micrograph from the same sample, showing small unblemished titanomagnetites (in bright colour) along needles of pyroxene (Pyx, grey in colour); 4d and e: sample AQ_10 from the Ceboruco San-Pedro vocanic field, dominated by (titano-) hematite with large titanomagnetite grains showing signs of replacement stage oxidation (oxidation stage C7).

4.1.3 Hysteresis properties

Figure 4.5 shows six examples of hysteresis data with corresponding IRM acquisition curves and Figure 6 shows the Day-plot, generated from the hysteresis parameters tabulated in table 4.1. In Fig. 4.5, the left column (a-c), three examples of hysteresis loops are shown that are characteristic for the majority of samples investigated in this study. No waspwaisted behaviour is observed near the origin of these loops, which indicates restricted coercivities (Tauxe, 1996) and IRM curves are fully saturated at fields of 100-300 mT. Samples from site CV (Fig. 4.5d) are characterized by a bimodal distribution of coercivities (as seen in the IRM acquisition rate) and the hysteresis loop is waspwaisted. As these samples are characterized by low Curie temperatures, it is likely that besides a titanomagnetite with high Ti content, some additional magnetite is present. Thus, this behaviour probably relates to two fractions of titanomagnetite and magnetite. Samples, characterized by contributions of (titano-) hematite had clearly waspwaisted loops and IRM acquisition curves are not saturated at IRM peak fields of 2T (Fig. 4.5 e and f). As hysteresis measurements were carried out to a maximum field of 1T, M_S is underestimated and consequently these samples plot away from the mixing lines, more towards the right side of the Day-plot (Fig. 4.6), particularly obvious for samples from site CM). The majority of samples plot within the pseudo single domain (PSD) range along the theoretical linear mixing curves of Dunlop (2002).

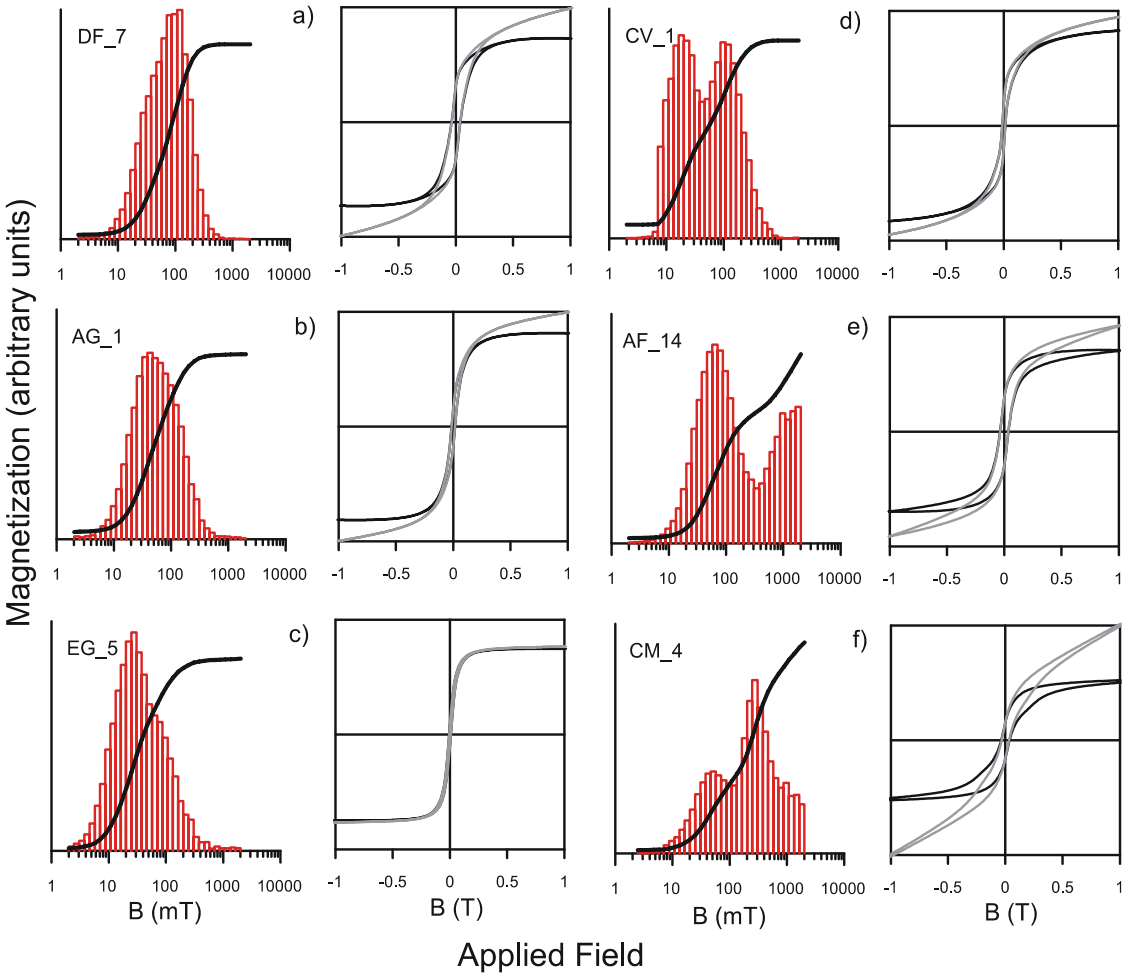

Figure 4.5. Examples of hysteresis loops, black line (grey line) corrected (uncorrected) for paramagnetic content and corresponding acquisition curves (solid line) and acquisition rates per field step (red bars) of the isothermal remanent magnetization (IRM).

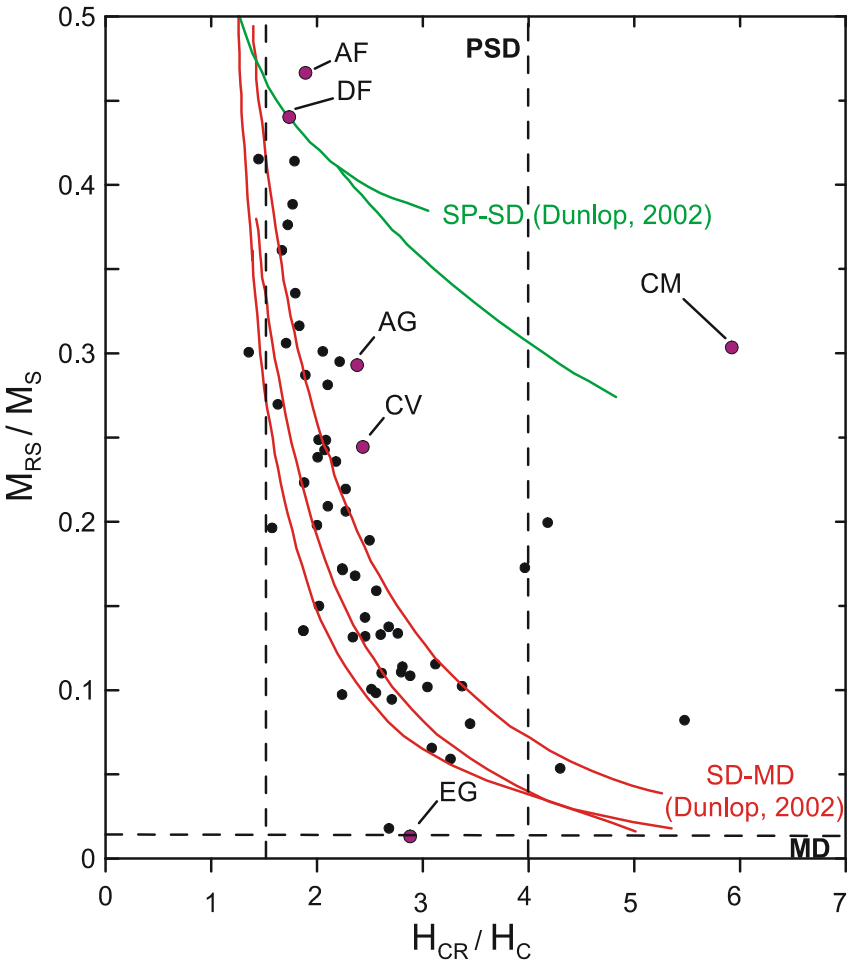

Figure 4.6. Plot of bulk magnetic domain states (Day et al., 1977) for site-averaged hysteresis parameters of the 63 lavas investigated in this study. Theoretical mixing curves of Dunlop (2002) are shown for reference; red lines (single domain-multi domain) and green lines (super paramagnetic-single domain); in magenta: data from samples shown in Figure 4.5.

Due to the information gained from rock-magnetic analyses, we interpret low Ti titanomagnetites as the remanence carrier in the majority of samples from this study. Samples are considered to be mixtures of single domain (and/or pseudo single domain) and multi domain particles. Small contributions of (titano-) maghemite are probably present in samples from 9 sites (AY, AV, CP, CT, CV, CY and AN) as indicated by thermomagnetic behaviour (Type E and F behaviour, Fig. 4.2) and ore microscopy (AR, BH and CQ), while samples from 4 sites (AL2, AF, AQ and CM) additionally contain (titano-) hematite.

Table 4.1. Site averaged hysteresis values for the parameters B_C (coercivity) / B_{CR} (remanent coercivity) and M_{RS} (remanent saturation magnetization) / M_S (saturation magnetization); S-300 is the s-ratio (Bloemendal et al., 1992); δ_{HYS} is the shape parameter (Fabian, 2003); also shown is the thermomagnetic classification as described in 4.1 (see also Fig. 4.2); Curie temperatures, determined after the method of Moskowitz (1981).

Site	B_C (mT)	B_{CR} (mT)	M_{RS} / M_S	S-300	δ_{HYS}	M_S(T) behaviour	T_C (°C)
DR	22.6	38.9	0.38	0.83	0.5734	A	518
AX	13.0	34.8	0.02	0.99	-0.2671	A	516
AG2	18.8	44.8	0.29	0.99	-0.0843	A'	521
DV	18.6	31.8	0.31	0.98	0.2164	A'	537
AY	9.6	15.1	0.20	1.00	-0.1357	E	210
BC	13.7	29.9	0.24	0.99	0.0266	A	574
EA	12.7	32.6	0.16	0.98	-0.0697	A	521
DX	17.2	68.1	0.17	0.95	0.0690	C	369, 503
BB	14.9	31.2	0.28	0.97	0.0784	A	511
EG	7.7	22.2	0.01	0.99	0.0605	A'	527
DG	16.2	32.3	0.20	1.00	-0.2112	A	535
DF	38.3	66.4	0.44	0.99	-0.0079	B	396
EJ	28.0	58.4	0.25	0.98	-0.2472	A	551
AV	5.8	13.0	0.10	1.00	n.a.	E	291
AL2	19.5	35.8	0.32	0.86	0.5053	G	592
CP	13.2	21.4	0.27	0.99	0.0436	F	250, 499
CT	15.2	63.5	0.20	0.94	0.3942	F	370, 580
CV	13.1	32.0	0.24	0.97	0.3859	F	256
BH	11.2	27.5	0.14	0.98	-0.3636	A	575
DQ	7.9	22.7	0.11	1.00	-0.3005	A	529
BI	8.0	24.5	0.10	0.99	-0.3915	A	512
CU	13.3	26.9	0.15	1.00	-0.4192	A'	502
CD	14.0	37.6	0.14	0.98	-0.2755	A	562
AH	14.7	36.8	0.19	0.95	n.a.	A'	526
AT	14.8	36.3	0.13	0.99	-0.4581	A'	548
AM	13.6	28.6	0.21	0.98	-0.2697	A'	562
AF	33.6	63.4	0.47	0.76	0.4337	E, G	?
DT	28.4	51.0	0.34	0.99	0.1922	A	546
CF	6.5	35.8	0.08	0.97	-0.3268	B	420
CY	26.4	54.2	0.30	0.97	-0.0171	F	369, 580
BJ	21.6	44.7	0.24	0.99	-0.2047	A'	532
EL	7.8	14.5	0.14	1.00	-0.2288	A'	568
CJ	20.5	41.2	0.25	1.00	-0.3816	A	528
CO	17.9	40.0	0.17	0.99	-0.0193	A	485
EK	16.6	36.6	0.30	0.98	0.2622	G	348, 534
CR	14.2	39.2	0.13	0.96	-0.0600	A	515
AR	6.2	19.3	0.07	1.01	-0.5064	A	580
BD	14.9	33.7	0.21	0.99	-0.1264	A'	573
AS	10.9	28.6	0.11	0.99	-0.4371	A	555
AQ	13.5	24.2	0.41	0.82	0.3378	A'	538
EI	19.7	26.7	0.30	0.97	0.1949	G	301, 568
EO	6.6	16.7	0.10	1.01	-0.1951	A	490
EB	12.0	40.6	0.10	0.98	-0.3189	A'	525
CK	24.0	48.1	0.24	0.99	-0.2291	D	314, 524
EF	12.0	28.1	0.13	1.00	-0.3259	A	517
ED	15.7	40.9	0.13	0.98	-0.4014	A	556
CW	6.0	20.8	0.08	0.99	-0.4998	A'	533
EN	7.8	14.5	0.14	0.99	-0.3864	A'	507
CQ	10.1	28.2	0.11	1.00	-0.5940	A	536
AZ	18.4	30.7	0.36	0.95	-0.0738	A'	547
AW	9.9	25.3	0.10	1.00	-0.7842	A'	555
BV	10.4	32.3	0.12	0.93	0.3241	A'	543
CE	16.6	39.2	0.17	0.99	-0.2142	A'	561
AN	19.9	28.8	0.42	0.99	0.3240	F	368, 545
CI	18.4	34.6	0.22	1.00	-0.1970	D	367, 543
DE	17.6	39.9	0.22	0.99	-0.1454	C	377, 520
DH	11.9	26.7	0.17	1.00	-0.1784	C	314, 518
CN	6.9	18.8	0.09	1.00	-0.5395	A	513
AO	9.7	27.1	0.11	0.93	-0.0450	A	545
BZ	33.0	58.4	0.39	0.87	0.6239	A'	578
BW	4.8	15.6	0.06	1.00	-1.9954	A	534
BL	22.0	41.7	0.29	0.96	-0.1171	A'	577
CM	36.3	215.1	0.30	0.65	0.9217	G	507

4.2 Paleomagnetic directions

A characteristic remanent magnetization (ChRM) was successfully isolated either by AF or thermal demagnetization for most samples and determined using principal component analysis (PCA, Kirschwink, 1980), following the quality criteria of Tauxe et al. (2000), by using at least 5 vector endpoints and a maximum angular deviation (MAD) of less than 5°. Secondary viscous remanent magnetizations (VRM) that were easily removed by AF fields of 10-15 mT or thermal demagnetization to 200°C (Fig. 4.7a), were common. Occasionally, the vector sum of the VRM component was larger than from the ChRM (Fig. 4.7b). In some cases we observed that small quantities of NRM (5-15 %) persisted after peak AF demagnetization fields of 100 / 125 mT. However, as these samples generally displayed a linear decay of remanence towards the origin of the vector endpoint diagrams, and sister samples subjected to thermal demagnetization displayed similar directional behaviour, we are confident that the ChRM was correctly identified. In some samples subjected to thermal demagnetization most of the NRM was removed between 450° and 550°C (Fig. 4.7c). For samples containing (titano-) hematite, AF peak fields of 100 / 125 mT were not sufficient to fully demagnetize the NRM, leaving as much as 30-50 % of the NRM intact (Fig. 4.7d). This demagnetization behaviour correlates with samples showing non-saturated hysteresis loops. In such cases a combined demagnetization approach of AF- and thermal demagnetization was used (Fig. 4.7e). Samples with reversed magnetizations often showed a normal polarity viscous overprint, oriented antiparallel to the ChRM of reversed polarity, resulting from the post-reversal field (Fig. 4.7f). Occasionally significant secondary components were observed, which are likely due to a lightning stroke induced IRM (Fig. 4.7g). This was supported by anomalously high NRM intensities, which were sometimes several magnitudes higher than from unaffected samples of the same flow. Such samples were rejected from further analysis.

Mean palaeomagnetic directions (Table 4.2, Fig. 4.8) were calculated from at least 3, on average 10 samples applying Fisher statistics (Fisher, 1953). Fifty-one mean vectors have α_{95} values between 2° and 9° with an average of 6.1°, while seven sites (BH, CU, EO, CK, AZ, CI and DE) have α_{95} values >10°. Flow AM was affected by lightning to such a degree that it was not possible to determine reliable ChRM directions. For four sites (DG, AS, EI and EF) we found palaeomagnetic directions that were not well grouped, thus this data were rejected.

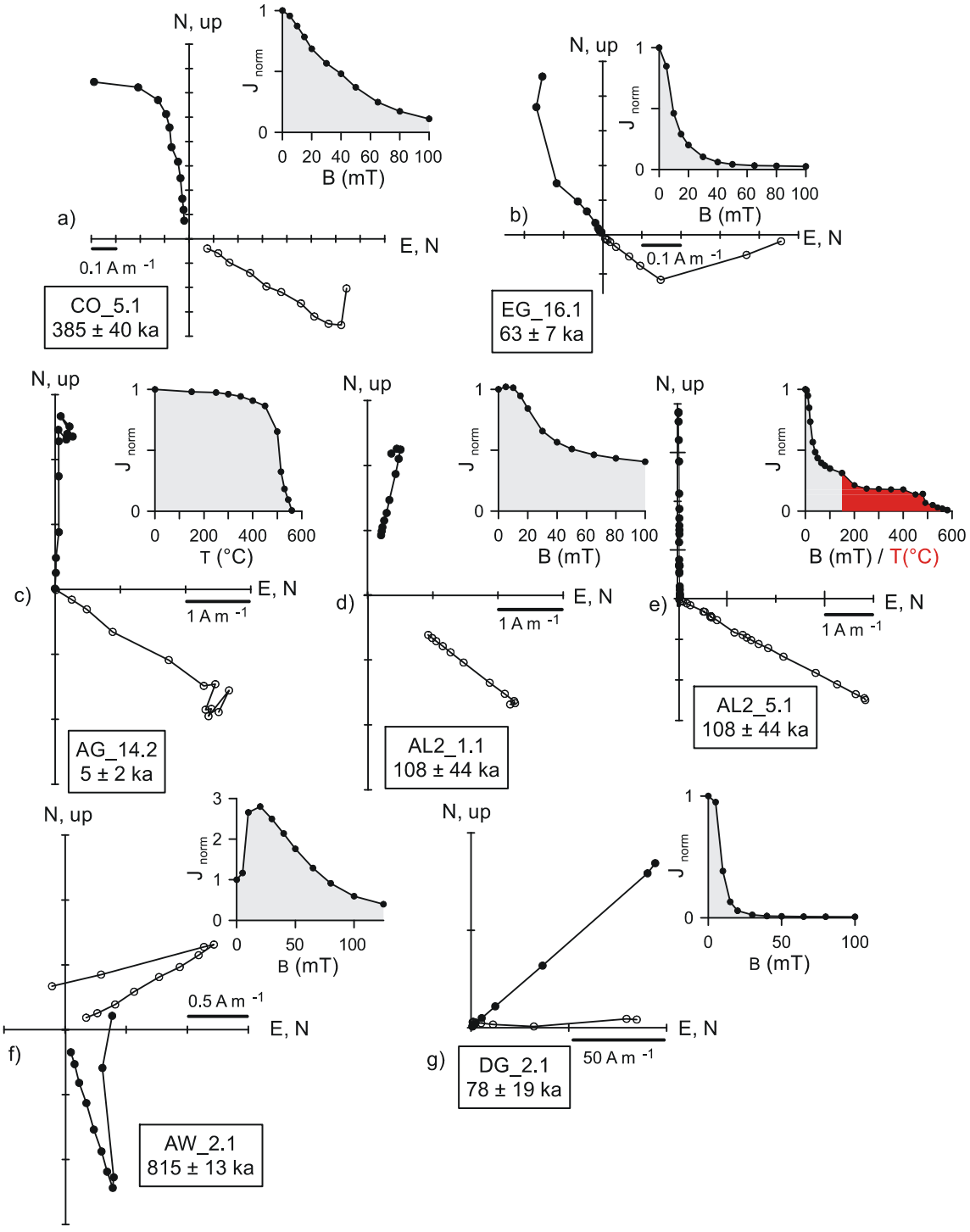

Figure 4.7. Orthogonal vector endpoint diagrams of representative demagnetization data, solid circles (open circles) projections into the horizontal (vertical) plane, and normalized intensity decay curves.

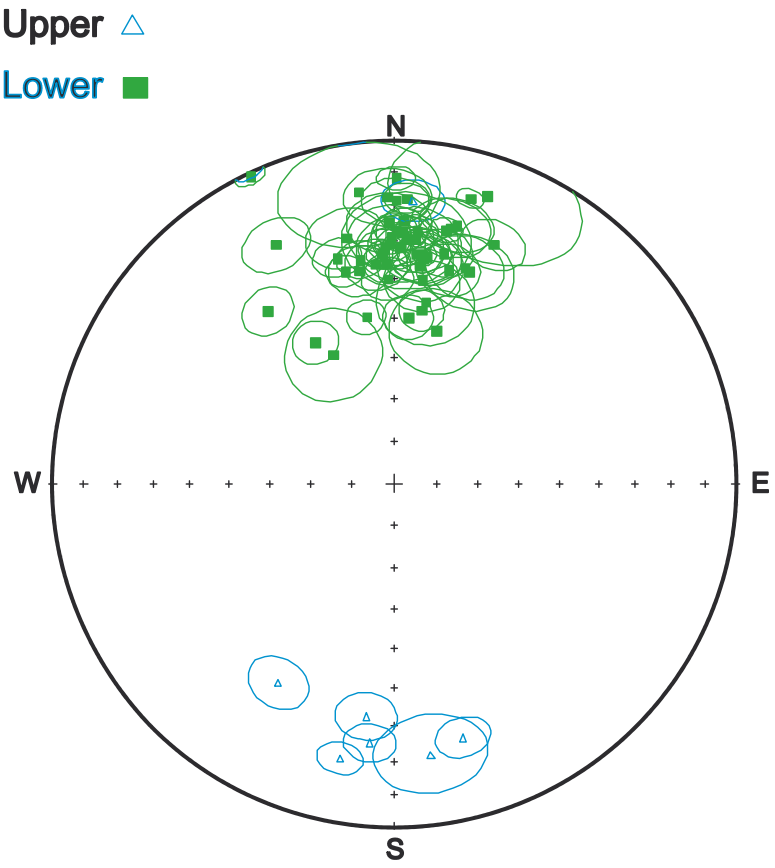

Figure 4.8. Stereographic projection of all mean characteristic remanent magnetization directions with 95 per cent confidence ellipses. Green squares (blue triangles) are projections on the lower (upper) hemisphere.

Table 4.2. Flow-mean palaeodirections of cleaned remanences for the sites investigated in this study. n, number of specimens used for the calculation of the mean direction; N, number of treated samples; k and α_{95}, precision parameter and radius of 95% confidence cone of Fisher statistics (Fisher, 1953), respectively; Dec, Declination; Inc, Inclination; *P*lat / *P*long, latitude / longitude of the corresponding virtual geomagnetic pole; A_{95}, 95% confidence limit of the virtual geomagnetic poles; dp and dm, uncertainty in the palaeo- latitude and longitude, respectively; Pol, magnetic polarity (N - normal polarity, R - reversed polarity; I – intermediate direction); n.a., not available / discarded data.

Site	age (ka)	n / N	k	α95 (°)	Dec (°)	Inc (°)	*P* lat	*P* long	A95	dp	dm	Pol.
DR	0 ± 20	9 / 10	233.7	3.4	9.6	27.8	79.8	16.4	2.7	2	3.7	N
AX	2 ± 10	13 / 16	22.9	8.8	334.9	37.1	66.4	175.3	7.9	6.1	10.3	N
AG2	5 ± 2	5 / 5	302.4	4.4	2.4	17.7	79.9	66.5	3.3	2.4	4.6	N
DV	16.8 ± 0.75	8 / 9	230.8	3.4	11.5	25.5	77.6	18.1	2.7	2.0	3.7	N
AY	23 ± 31	10 / 16	43.2	7.4	5.4	33.2	84.7	2.1	6.3	4.8	8.4	N
BC	26 ± 58	16 / 16	20.1	8.4	18.2	33.9	72.8	347.7	7.2	5.5	9.6	N
EA	31.7 ± 1.1	9 / 10	60.2	6.7	355.2	36	85.4	186.3	5.9	4.5	7.8	N
DX	46 ± 0.07	15 / 15	55.2	5.2	1.5	31.4	87.6	46.3	4.4	3.3	5.8	N
BB	47 ± 45	12 / 14	23.6	9.1	1.5	31.8	87.4	44.8	7.7	5.7	10.2	N
EG	63 ± 7	16 / 16	52.2	5.3	330.7	51	61.9	193.5	5.9	4.8	7.2	N
DG	78 ± 19	0 / 10	n.a.	n.a.	n.a.	n.a.	n.a.	n.a.	n.a.	n.a.	n.a.	n.a.
DF	80 ± 35	9 / 10	67.6	6.3	12	31.8	78.4	357.5	5.3	4	7.1	N
EJ	85 ± 19	14 / 14	83.9	4.4	350.4	49.2	77.5	213.3	4.7	3.9	5.8	N
AV	108 ± 22	10 / 14	36	8.2	12.4	24.5	75.5	18.7	6.4	4.7	8.8	N
AL2	118 ± 5	9 / 10	109.2	4.9	6.6	33.2	83.7	358.2	4.2	3.2	5.6	N
CP	178 ± 8	7 / 13	71.8	7.2	333.6	23.2	63.3	151.2	5.6	4.1	7.7	N
CT	191 ± 13	7 / 8	48.5	8.8	359.2	28.8	84.6	78.2	7.2	5.3	9.7	N
CV	196 ± 8	8 / 10	42.1	8.6	358.8	24.8	82.1	84.7	6.8	5	9.2	N
BH	230 ± 68	14 / 14	10	13.3	2.8	29.3	85.4	42	10.9	8.1	14.7	N
DQ	240 ± 50	10 / 12	76.8	5.5	357.7	32	86.9	128.8	4.6	3.5	6.2	N
BI	256 ± 18	12 / 13	20.1	9.9	19.5	34.8	71.6	345.1	8.6	6.6	11.4	N
CU	261 ± 11	9 / 11	21.8	11.3	334.5	55.7	63	206.2	13.7	11.6	16.2	N
CD	269 ± 22	12 / 13	141.9	3.7	1.9	24.3	83.1	62	2.9	2.1	4	N
AH	282 ± 5	6 / 7	56.8	9	4.9	29.2	84.1	26	7.4	9.9	5.5	N
AT	283 ± 5	10 / 12	105.1	5	351.3	34.3	81.5	150.9	4.3	3.3	5.7	N
AM	290 ± 12	0 / 12	n.a.	n.a.	n.a.	n.a.	n.a.	n.a.	n.a.	n.a.	n.a.	n.a.
AF	308 ± 36	17 / 21	39.9	5.7	358	39.9	84.9	102.1	4.6	3.4	6.2	N
DT	330 ± 80	16 / 16	53.8	5.1	9	47.6	77.5	302	5.4	4.3	6.6	N
CF	339 ± 23	8 / 9	74	6.5	7.3	34.3	83.1	350.8	5.6	4.3	7.4	N
CY	354 ± 15	11 / 12	60.9	5.9	323.6	37.6	56.1	173.4	5.3	4.1	6.9	N/ I ?
BJ	360 ± 30	15 / 16	147.2	3.2	6.7	33	83.5	358	2.7	2.1	3.6	N
EL	362 ± 13	15 / 16	56.4	5.1	358	35.8	87.9	138.4	4.5	3.4	5.9	N
CJ	373 ± 61	11 / 12	37.1	7.6	8	33.6	82.4	353.2	6.5	4.9	8.7	N
CO	385 ± 40	12 / 12	166.1	3.4	357	33.3	87	144.4	2.9	2.2	3.9	N
EK	403 ± 15	7 / 8	115.4	5.6	4.7	49.7	79.6	278.7	6.1	5	7.5	N
CR	416 ± 3	14 / 16	78.4	4.5	0.3	26.7	83.3	73.7	3.6	2.7	4.9	N
AR	425 ± 130	12 / 15	34.4	7.5	13.7	23.5	74.1	17.4	5.8	4.3	8	N
BD	429 ± 64	14 / 15	32.2	6.9	14.2	35.9	76.6	343.3	5.7	4.3	7.4	N
AS	512 ± 34	0 / 16	n.a.	n.a.	n.a.	n.a.	n.a.	n.a.	n.a.	n.a.	n.a.	n.a.
AQ	520 ± 25	16 / 16	182.6	2.7	15	15	70.2	26.1	2	1.4	2.8	N
EI	521 ± 15	0 / 16	n.a.	n.a.	n.a.	n.a.	n.a.	n.a.	n.a.	n.a.	n.a.	n.a.
EO	592 ± 20	11 / 13	17.2	11.3	172.3	-21.1	-77.6	294	8.6	6.3	11.9	R
EB	601 ± 6	9 / 10	39	8.3	7.8	39.8	82.6	332.5	7.7	6	10	N
CK	612 ± 41	6 / 6	14	18.6	18	12.8	68.3	21.2	13.5	9.7	19	N
EF	614 ± 16	0 / 16	n.a.	n.a.	n.a.	n.a.	n.a.	n.a.	n.a.	n.a.	n.a.	n.a.
ED	623 ± 91	11 / 15	30	8.5	358.6	17.3	77.6	81.8	6.3	4.6	8.8	N
CW	632 ± 8	10 / 12	122.3	4.4	5.2	26.9	81.7	38.4	3.5	2.6	4.8	N
EN	671 ± 12	10 / 11	52.3	6.7	210.3	-33	-61.3	166.8	5.7	4.3	7.6	R
CQ	691 ± 26	10 / 10	87	5.2	1.7	27.5	83.6	61.4	4.2	3.1	5.7	N
AZ	730 ± 113	10 / 13	20.7	10.9	9.8	45.3	78.4	306.9	11	8.8	13.8	N
AW	815 ± 13	14 / 16	50.5	5.6	164.8	-24.1	-73.4	321.7	4.3	3.1	5.9	R
BV	867 ± 186	10 / 11	184.6	3.6	357.3	11.8	76.7	91.6	2.6	3.7	1.9	N
CE	909 ± 20	13 / 14	42.2	6.5	186.9	-32	-83.2	182.9	5.5	4.1	7.3	R
AN	933 ± 40	10 / 12	34.6	8.3	348.8	27.8	77.6	210.5	6.4	8.7	4.7	N
CI	957 ± 157	13 / 13	16.1	10.6	15.3	51.9	71	300.6	12	9.9	14.5	N
DE	983 ± 58	6 / 10	19.6	15.5	352.9	15.3	77	112.8	11.4	8.2	15.9	N
DH	1025 ± 79	3 / 3	540.6	5.3	185.4	-24.8	-81.8	220.1	4.2	3.1	5.7	R
CN	1075 ± 34	10 / 11	51.5	6.8	22.6	25.4	67.5	359.8	5.4	3.9	7.3	N
AO	1115 ± 91	8 / 8	82	6.2	3.8	-18.3	61.6	286.2	4.5	6.2	3.2	N / I
BZ	1301 ± 97	14 / 16	74.2	4.6	194.1	-19.3	-73.6	201.7	3.5	2.5	4.8	R
BW	1600 ± 55	11 / 12	25.5	9.2	6.8	36.2	83.5	339.3	8.2	10.7	6.2	N
BL	3528 ± 64	16 / 16	177.9	2.8	334.8	1	59	133.6	2	1.4	2.8	N / I
CM	6461 ± 33	9 / 10	45.2	7.7	0.4	46.2	81.9	259.9	7.9	6.3	9.9	N

5. Discussion

5.1 Palaeosecular variation

To avoid using tectonically affected sites in the calculation of PSV, we restricted the analysis to lavas of Pleistocene age (younger than 1.8 Ma) because tectonic rotations appear to be significant in the TMVB for rocks exceeding that time range (Ruiz-Martinez et al., 2000).

Figure 4.9 shows a polar plot of virtual geomagnetic pole positions for normal and reversed polarity sites with Brunhes aged lavas indicated by red circles and Matuyama aged lavas by green diamonds. This indicates that two Brunhes age lavas have reversed polarity and seven sites of Matuyama age have normal polarity magnetizations. A possible relationship of these lavas with regard to geomagnetic excursions is discussed in section 5.2.

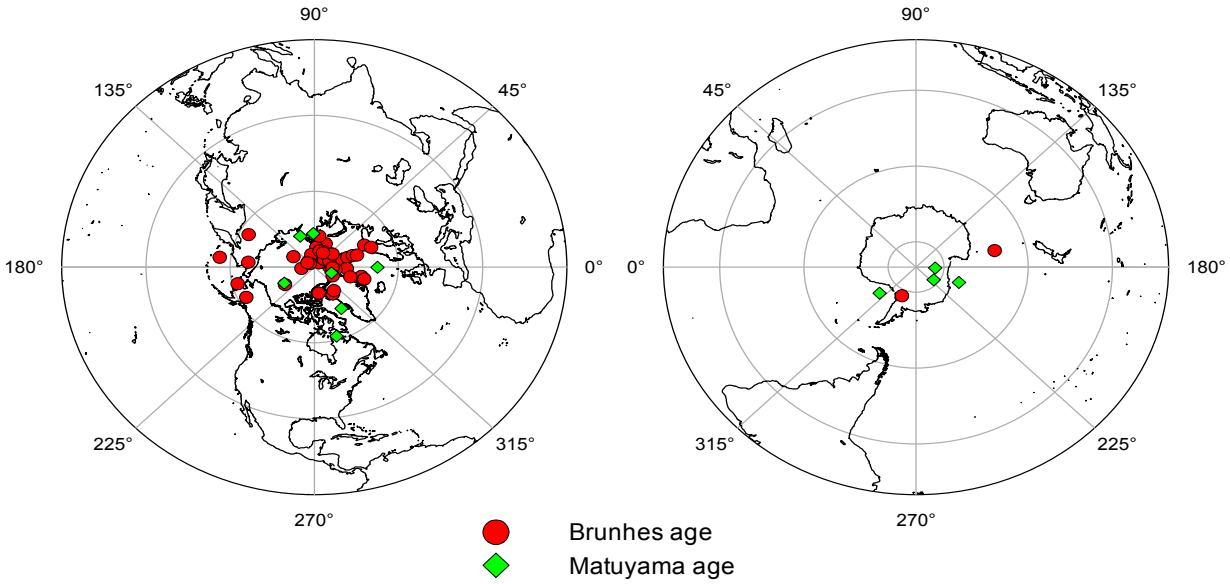

Figure 4.9. Polar projection of virtual geomagnetic poles from sites dating of Brunhes Chron (red circles) and Matuyama Chron (green diamonds). a) sites with normal polarity, b) sites with reversed polarity.

Palaosecular variation is estimated from the scatter of VGPs, determined by the root mean square angular deviation of VGPs by,

$$S = \sqrt{\frac{1}{N-1}\sum_{i=1}^{N}(\partial_i^2 - \frac{S_{wi}^2}{N_{si}})} \qquad (1)$$

where ∂_i is the angular standard deviation (ASD) of the VGP for the *i*th site from the mean VGP, N is the number of sites used in the calculation, and S is the geomagnetic signal remaining after correcting for within-site dispersion S_{wi} determined from N_{Si} samples (Johnson et al., 2008).

The global database of PSV, based on a compilation of 0-5 Ma lavas (Model G; McFadden et al., 1988, 1991), predicts an increase of S with latitude. For Model G, the average scatter for the latitude of Mexico (λ = 20°) is $S = 13.4^{14.0}_{12.9}$ (upper and lower confidence limits, respectively). A similar latitudinal trend is predicted by Model TK03 (Tauxe and Kent, 2004), which is based on a time averaged field specified by

GAD and 10,000 simulations at latitude increments of 5° using the McElhinny and McFadden (1997) high quality data compilation (DMAG 4 criteria). The TK03 Model predicts $S = 12.9^{13.0}_{12.7}$. Recently, Johnson et al. (2008) presented a new model for the 0-5 Ma time averaged field, to which we refer to as TAF-J. The TAF-J model is based on high quality palaeomagnetic directional data from over 2000 volcanic sites with sufficient spatial and temporal sampling, spanning latitudes from 78°S to 53° N. It indicates different latitudinal structure of PSV for the Brunhes- and Matuyama Chron, with less latitudinal variation of PSV for normal polarity Brunhes data (S = 16) and generally higher dispersion and some latitude dependence for reverse polarity Matuyama data ($S = 13.2^{15.8}_{10.7}$). The dispersion predicted by the TAF-J model based on normal polarity Brunhes data ($S = 11.2^{12.2}_{10.1}$, for λ = 20°) is lower than the one prediced by Model G but it has to be noted that this value is largely based on data from Hawaii (Lawrence et al., 2006), which was found to show large negative mean inclination anomalies. For the 0-5 Ma combined normal and reverse polarity data, Johnson et al. (2008) quote a dispersion of $S = 14.5^{15.2}_{13.8}$.

For estimating the PSV, reversed polarity mean directions were inverted to normal polarity, thus assuming symmetry in normal and reverse polarity fields. Choosing the correct cutoff angle (λ_{cut}) to separate normal PSV from an intermediate / transitional geomagnetic regime is still a matter of debate. Some previous palaeomagnetic studies from Mexico (Petronille et al., 2005, Ceja et al., 2006, Conte et al., 2006) combined two parameters: (1) a VGP latitude lower than 60° or (2) an angular distance from the mean direction exceeding 30°. We believe that these values can still be within the range of normal PSV. Instead, we chose a cutoff angle of 40° from the mean VGP latitude. Additionally, VGP cutoff values were calculated using the method of Vandamme (1994), in which the cutoff value is a function of the VGP scatter, calculated from Model G (McFadden et al., 1988, 1991) calculated with

$$\lambda_{cut} = (1.8S + 5)° \quad (2)$$

Both cutoff approaches (40° fixed cutoff and Vandamme cutoff) were applied and results are listed in Table 4.3.

Using a constant cutoff of 40°, we obtain dispersion values, which are consistent within the error range of Model G, TK03, and TAF-J. For combined Brunhes and Matuyama data we obtain $S = 14^{16.7}_{11.3}$ and slightly higher values $S = 15.3^{18.8}_{11.0}$ when restricting the analysis to high quality data (n > 4, k > 50) only. Treating Brunhes data separately gives a slightly lower dispersion of $S = 13.6^{16.7}_{10.3}$ for all data and $S = 13.9^{18.1}_{9.3}$ for high quality data. Matuyama data indicates some higher dispersion of $S = 16^{20.1}_{11.0}$, however here only 11 VGPs have been used in the calculation.

Significantly lower dispersion values are obtained when applying the cuttoff criteria of Vandamme (1994), which assumes that low latitude VGPs are outliers in the distribution. However, as the majority of data is rather tightly clustered, sites are already excluded with an angular standard deviation of > 22.2° (for all data) and > 19.7° (for Brunhes data only). We regard these to be unrepresentative of a transitional geomagnetic regime but to be still within the range of normal PSV and favour the fixed cutoff approach. In summary, PSV estimates from this study indicate “normal” values of PSV for Mexico, best described by latitude dependent models (Model G, TK03 and TAF-J). This is in agreement with previously published PSV estimates from the TMVB covering a similar time window, e.g. Mejia et al. (2005).

Table 4.3. Summary statistics of palaeosecular variation estimates obtained from data of lava flows younger than 1600 ka and for data from lava flows dating of Brunhes Chron and Matuyama Chron seperately. A fixed cutoff of 40° is applied and in a second calculation, cutoff values are calculated after the method of Vandamme (1994). No, number of sites; N, number of sites used in the calculation of the scatter of virtual geomagnetic poles (see Johnson et al., 2008); $\lambda_{cut,}$ cutoff angle used in the calculation; ASD max, maximum angular deviation from the mean virtual geomagnetic pole included in the calculation; S_no_ws, scatter of virtual geomagnetic poles uncorrected for within-site dispersion; S, scatter of virtual geomagnetic poles corrected for within-site dispersion; Su and Sl, upper and lower confidence limits of S, calculated after the method of Cox (1969).

all data		No	N	λ_{cut}	ASD max	S_no_ws	Sl	S	Su
	Fixed cutoff	56	56	40.0	36.6	14.5	11.3	14.0	16.7
	Vandamme	56	49	22.2	19.7	10.2	7.8	9.6	11.1
	N>4, k>50								
	Fixed cutoff	31	31	40.0	35.6	15.5	11.0	15.3	18.8
	Vandamme	31	26	22.1	18.7	10.0	7.5	9.7	11.7
Brunhes data									
	Fixed cutoff	45	45	40.0	36.3	14.1	10.3	13.6	16.7
	Vandamme	45	39	19.7	18.1	9.0	6.8	8.3	9.8
	N>4, k>50								
	Fixed cutoff	26	26	40.0	34.7	14.2	9.3	13.9	18.1
	Vandamme	26	23	19.2	16.4	8.3	5.5	7.9	9.7
Matuyama data									
	Fixed cutoff	11	11	40.0	28.6	16.5	11.0	16.0	20.1

5.2. Correlation to the geomagnetic instability timescale

Flow-mean VGP latitudes, declinations and inclinations are depicted in Fig. 4.11 against their age position in the geomagnetic polarity timescale supplemented with geomagnetic excursions reported in the literature. Most ages of geomagnetic excursions within the Brunhes Chron are adopted from the geomagnetic instability timescale of Singer et al. (2002, 2008a,b), which continues to develop, and from sedimentary data from numerous ODP (Ocean Drilling Project) palaeomagnetic studies summarized by Lund et al. (2006). Excursions within the Matuyama are mainly adopted from Singer and Brown (2004) and sedimentary data from ODP site 983 / 984, Iceland Basin (Channell et al., 2002). The latter is most likely the best dated (by a continuous stable oxygen isotope astrochronologic age model) and one of the most highly resolved marine sediment sequence covering the lower Brunhes- and most of the Matuyama Chron. In the following we discuss palaeomagnetic directions which according to our studies or those of Petronille et al. (2005) and Ceja et al. (2006) may be associated with geomagnetic excursions and events. Representative demagnetization data of sites that are discussed is shown in Figures 4.12 and 4.13.

- Site CY (354±15 ka) gave a mean direction of D=323.6°, I=37.6°, α_{95}=5.9°, n/N =11/13 (n = number of samples used in the calculation, N = number of treated samples), P_{lat}=56.1°. Ceja et al. (2006) obtained a rather poorly defined result based only on three samples (D=290.5°, I=14.5°, α_{95}=14.5°, n/N=3/7, P_{lat} = 24.9°, site TM10 in their publication). Using the quoted coordinates, which are identical to those given by Lewis-Kenedi et al. (2005) for their ^{40}Ar / ^{39}Ar dating sample, we were unable to locate their sampling locality. The lava exposure was rather poor, and it was only possible to sample a shallow interval of 4 m. The study of Ceja et al. (2006) yielded an intermediate direction and it was interpreted as new volcanic evidence for the Levantine event, first proposed by Ryan (1972), which is one of the rather poorly defined events in the Brunhes and which occurred at about 360 ka (Singer et al., 2002). Our result (Fig. 4.10a) is significantly different from the result published by Ceja et al. (2006), and, assuming a VGP cutoff angle of 40°, it lies also still within the range of usual PSV. Considering the rather poor outcrop exposure at this site, careful resampling is needed to confirm either result.

- Another result, site TM9 in the same study of Ceja et al. (2006), dated at 362±13 ka, was also linked to the Levantine event. Here, they obtained a direction of D=23.3°, I=5.8°, α95=6.2°, n/N=9/12, Plat= 61.3°, which was again interpreted as intermediate. Our site EL corresponds to that dated flow. Again, the blocky lava exposure was rather poor, with many moved blocks and no boreholes were spotted at the cited coordinates. We dispersed our samples over a large interval (> 30 m) and sampled several independent structures that were interpreted as original in situ cooling structures. A well defined normal polarity magnetization of D=358°, I=35.8°, α_{95}=5.1°, n=15/16, Plat = 87.9° was obtained, which again disagrees from the previously published result for presumably the same lava (Fig. 4.10b).

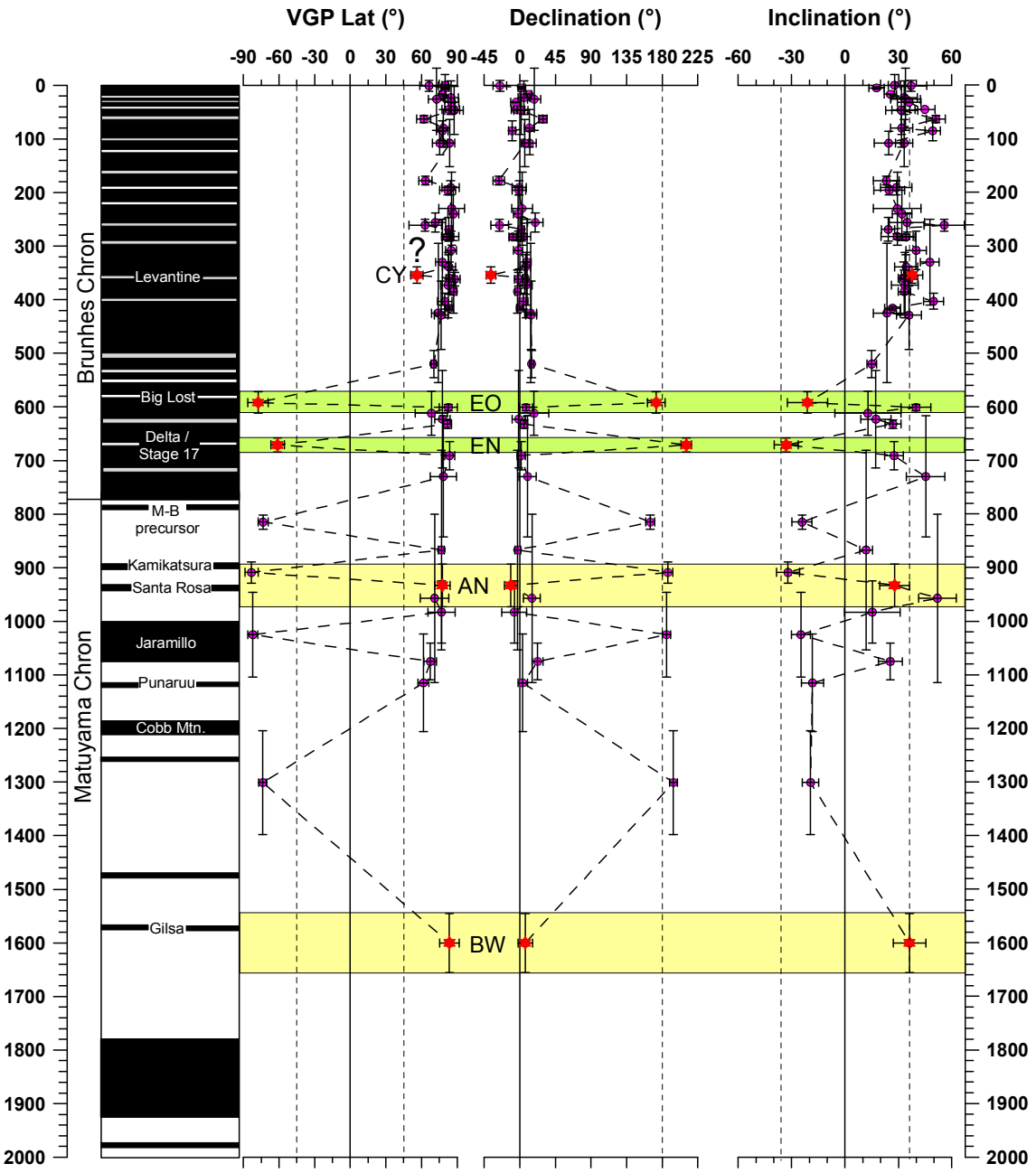

Figure 4.10. Palaeolatitude of the virtual geomagnetic poles (cutoff angle of 40° is indicated by the stippled line), flow-mean magnetic declinations and inclinations (geocentric axial dipole inclination in dicated by the stippled line) of lavas investigated in this study with a tentative correlation to the geomagnetic polarity timescale modified for geomagnetic excursions of the last 2 Ma compiled from Langereis et al. (1997), Nowaczyk & Frederichs (1999), Singer et al. (2002, 2007, 2008a,b), Nowaczyk & Knies (2000), Channell et al. (2002) and Lund et al. (2006). Excursions highlighted in white are well documented excursions with acceptable age control. Excursions highlighted in grey indicate excursions with restricted age control, which require further ratification. Sites that are associated with Brunhes (Matuyama) Chron excursions are highlighted with green (yellow) rectangles and are indicated by red stars.

- Flow EO (592±20 ka, Fig. 4.11a) has a reversed polarity magnetization of D = 173.3°, I = -21.1°, α_{95}=11.3°, n=11/14, Plat = -77.6°. According to its age, this flow could have erupted during the Big Lost excursion, initially constrained by K- Ar dating of a transitionally magnetized lava flow in Idaho to 565 ± 28 ka by Champion et al. (1988). The best estimated age for the Big Lost excursion is a weighted mean age of 579±6 ka (Singer, 2007), based on high quality ^{40}Ar-^{39}Ar age data obtained from transitionally magnetized lava sequences on La Palma (Canary Islands) dated by Singer et al. (2002) and on Tahiti (Hoffmann and Singer, 2004). Further volcanic evidence for this excursion comes from a group of three excursional flows (two of them with low palaeointensities) from the West Eifel, Germany, initially studied by Schnepp (1994) and Schnepp and Hradetzky (1994) and dated by Singer et al (2008b) at 578 ± 8 ka. Furthermore, relative palaeointensity minima of global extent have been found in numerous other studies with ages between 590 and 610 ka (e.g. Lund et al., 1998; Guyodo and Valet., 1999; Channell., 2004), which are most likely linked to the Big Lost excursion. We note that Ceja et al., (2006) also sampled this flow but were not successful in obtaining a mean direction (again no boreholes found at their site coordinates). They quote the direction of only one single sample with normal polarity (D=342.3°, I=9.2°, n=1/8). Interestingly, further evidence for the Big Lost excursion, recorded in lavas from Mexico, comes from the study of Petronille et al. (2005), who found two lava flows with fully reversed polarity magnetizations (site CB-04 and CB-13 in their publication) dating of 614±16 ka and 623±91 ka, respectively. Unaware of this study, we also sampled both of these flows. Our site EF corresponds to the exact sampling locality of site CB-04, and when revisiting the locality indeed boreholes were found. Unfortunately our ChRM directions were not well grouped at this site, which prevented us from calculating a mean direction. Yet, it has to be noted that from in total 15 directions, 6 were indeed reversed. Our site ED (Fig. 4.10c) corresponds to site CB13 but again no boreholes were found at the cited coordinates. Our site ED (Fig. 10c) has a normal polarity mean direction of D=358.6°, I=17.3°, α_{95}=8.5°, n/N=11/15, Plat = 77.6°. Thus, for an unambiguous confirmation of the excursional results of Petronille et al. (2005) again careful re-sampling of both flows is suggested.

- Site EN (671±13 ka, Fig. 11b) has a reversed polarity magnetization of D=210.3°, I=-33°, α95=6.7°, n/N=10/13, Plat = -61.3°. This flow could have been emplaced during the Delta / Stage17 excursion first indicated by inclination lows found in a sediment core from Calabria, Southern Italy, by Creer et al. (1980). Biswas et al. (1999) assigned intermediate to reversed directions to the Delta /Stage17 excursion occurring over about 7 ka at around 690 ka in a sediment core from the Osaka Basin, south-western Japan. However, as Singer et al. (2002) point out, the age of the Delta excursion requires further verification. There is evidence for the Delta / Stage17 excursion from sedimentary data obtained by Channell et al. (2004) who found inclination minima at around 665 ka in two astronomically dated cores (ODP sites 983 and 984) from the North Atlantic, Bjorn Drift / Iceland Basin. Carcaillet et al. (2004) report a VDM (virtual dipole moment) minimum at around 700 ka in a ^{10}Be derived VDM record from sedimentary records from the West Equatorial Pacific Ocean (North New Guinea). First evidence that lava flow EN recorded the Delta / Stage17 excursion came from the study of Ceja et al. (2006). They quote an intermediate direction of D=161.1°, I=21.4°, α_{95}=6.4°, n/N=8/8, P_{lat} = -54.7° (site TL-10 in their publication). We did not find their sampling locality at this site. Our result is different from the previously published one and now indicates a nearly fully reversed direction for this flow. However, there is a good chance that both results for the same lava flow might represent real features of the geomagnetic field and that this flow could have erupted and then cooled during a time of a short polarity event, when the field changed rather rapidly from a transitional regime to a fully reversed regime (or vice versa).

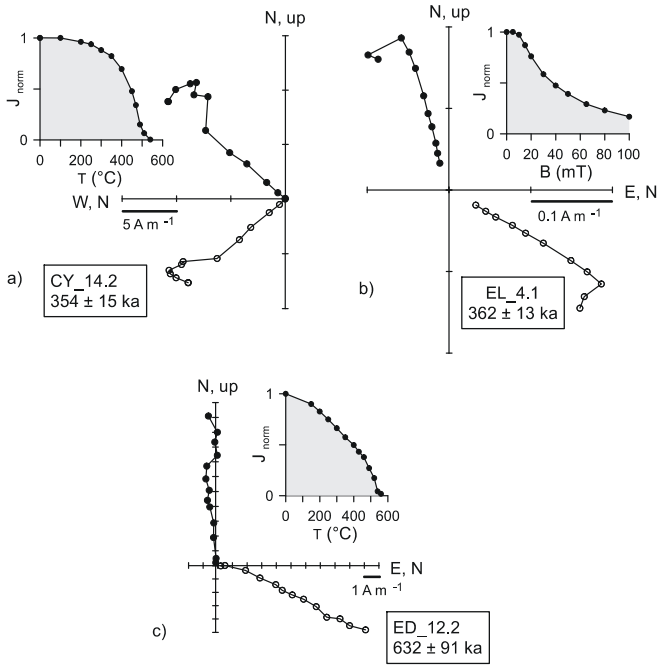

Figure 4.11. Orthogonal vector endpoint diagrams of demagnetization data from sites that yielded controversial results to previously published data.

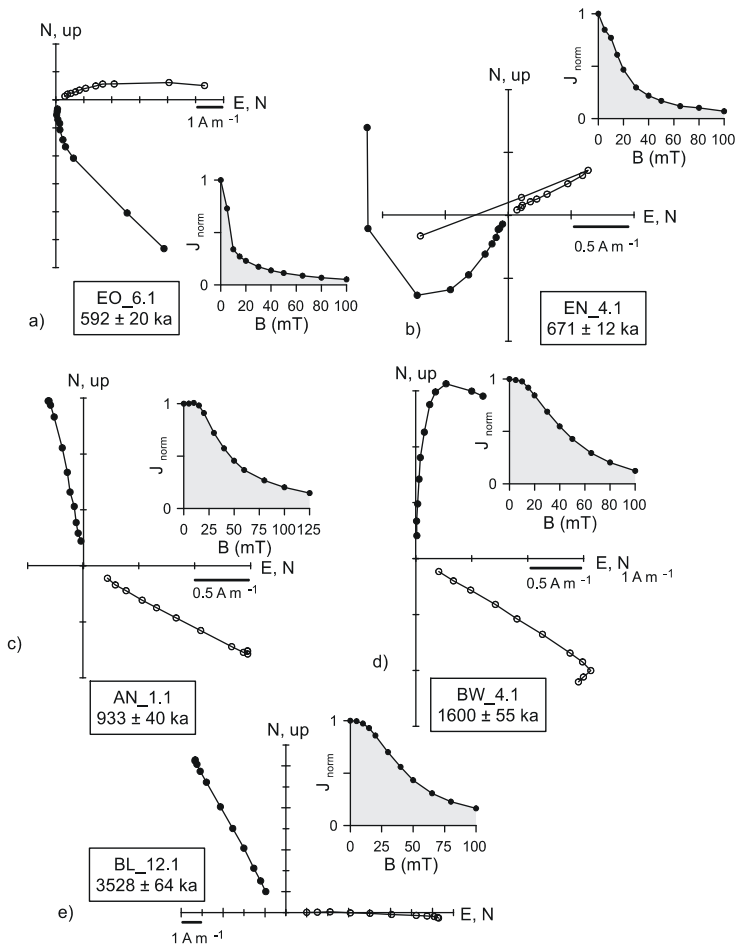

Figure 4.12. Orthogonal vector endpoint diagrams of demagnetization data from sites that are associated with geomagnetic excursions.

All remaining Brunhes Chron sites provided normal polarity magnetizations. Five lavas of normal polarity that are assigned to the Matuyama Chron are discussed below.

- Flow AN (933 ± 40 ka; Fig. 4.11c) has a normal polarity mean direction of D = 348.8°, I = 27.8°, α_{95}=8.3°, n/N=10/12, Plat = 77.6°. According to its age, it could have been emplaced either during the Kamikatsura- or the Santa Rosa excursion. The Kamikatsura excursion is constrained by Singer and Brown (2004) to 900 ± 6 ka, based on ^{40}Ar - ^{39}Ar ages from seven lavas with intermediate palaeodirections from the Punaruu Valley (Tahiti), initially studied by Chauvin et al. (1990), and in lava flows from Haleakala volcanoe (Hawaii), initially studied by Coe et al. (1985, 1995). The Santa Rosa excursion is constrained by Singer and Brown (2004) to 936 ± 8 ka, based on ^{40}Ar - ^{39}Ar ages obtained from the transitionally magnetised lavas from the Cerro San Rosa 1 rhyolite dome (New Mexico). Channell et al. (2002) identified a low in the relative palaeointensity and VGP latitudes crossing the equator at ODP sites 983 and suggest an age of 932 ka for the Santa Rosa excursion.

- Flows DE (983 ± 58) and CN (1075±34) have both normal magnetizations and were most likely emplaced during the worldwide recognized Jaramillo Normal Subchron, which had a duration of 68 ka, from 1001-1069 ka (Singer, 2007).

- Flow AO (1115±91 ka) has a rather unusual direction of D=3.8°, I=-18.3°, α_{95}=6.2°, n/N=8/10, Plat = 61.6°). However, assuming a cutoff angle of 40° this direction would be still within the range of normal PSV values. Due to the rather large age error, this flow could have been emplaced either during the younger part of the Jaramillo, or during one of the two preceding normal polarity intervals i.e. the Punaruu excursion or the Cobb Mountain Normal Subchron. Evidence for Punaruu excursion comes from normal to transitional magnetizations found in lavas from Punaruu Valley on the islands of Tahiti (Chauvin et al., 1990) and later dated by Singer (1999). Singer (2007) quote a recalibrated age of at 1122 ± 10 ka for the Punaruu excursion. This excursion also appears in several sedimentary records where normal polarity magnetizations associated with relative palaeointensity lows have been found around 1100 and 1115 ka (e.g. Guyodo et al., 1999; Channell et al., 2002). The worldwide observed Cobb Mountain Normal Subchron is estimated to span the time interval from 1190 to 1215 ka (Channell et al., 2002).

- Flow BW (1600±55 ka; Fig. 4.11d) has a normal polarity mean direction of D=6.8°, I=36.2°, α_{95}=9.2°, n/N=11/14, Plat = 83.5°. Its age suggests that is was most likely emplaced during the Gilsa excursion, first studied by McDougall and Wensink (1966) and later by Watkins et al. (1975) in a section of a normal polarity lavas with an K-Ar age of 1580 ka, overlying a normal polarity lava dated at 1670 ka in Iceland. Later, Clement & Kent (1987) presented new evidence for this excursion from sedimentary data from DSDP Site 609 / North Atlantic and suggested an interpolated age of 1550 ka and duration of 8.8 ka. A similar duration of 8 ka (1567 to 1575 ka) for the Gilsa excursion is suggested by Channel et al. (2002).

- Flow BL (3528 ± 64 ka; Fig. 4.11e) has an anomalously flat inclination. The obtained mean direction of D = 334.8°, I = 1°, α_{95}=2.8°, n/N=16/16, Plat = 59° could therefore be interpreted as intermediate to normal, although the VGP latitude suggests normal PSV. According to its age, flow BL could have been emplaced during the C2An.3n cryptochron, which is estimated to span the time interval from 3330 to 3580 ka and which is recognized in the marine magnetic anomaly record (Cande & Kent, 1995).

6. Conclusions

Palaeosecular variation as estimated from the scatter of virtual geomagnetic poles of Pleistocene age lava flows from Mexico analyzed in this study gave similar values to those predicted by latitude dependent Model G (McFadden et al., 1988, 1991) and is also in agreement with high quality Pleistocene palaeomagnetic data from Mexico compiled by Mejia et al. (2005). Palaeomagnetic mean vectors of 56 lava flows were correlated to the Geomagnetic Polarity Timescale of Cande and Kent (1992, 1995) supplemented with data on geomagnetic excursions. This record revealed some further evidence for at least four, possibly five geomagnetic excursions. We found that two lavas that erupted during the Brunhes chron (592 ± 20 ka and 671 ± 13 ka respectively) had nearly fully reversed magnetizations. According to their ages, the flow dated at 592 ± 20 ka most likely erupted during the Big Lost excursion (Champion et al., 1988; Singer et al., 2002, 2007) while the flow dated at 671 ± 13 gives new evidence for the Delta / Stage 17 excursion (Creer et al., 1980; Biswas et al., 1999). Furthermore, seven lava flows that erupted during the Matuyama chron were found to have recorded normal polarity magnetizations. From these, a flow dated at 933 ± 40 ka was correlated to the Santa Rosa excursion (Singer and Brown, 2002). Another flow dated at 1600 ± 60 ka most likely erupted during the Gilsa excursion (McDougal and Wensink, 1966). Furthermore, a lava flow of Pliocene age, dated at 3528 ± 54 ka, has a normal to intermediate direction and was most likely emplaced during cryptochron C2An.3n (Cande and Kent, 1995).

This study also revealed some findings in conflict with previously published data by Petronille et al. (2005) and Ceja et al. (2006). Two lava flows that were previously found by Ceja et al. (2006) to show intermediate directions, and on the grounds of their ages (354 ± 15 and 362 ± 13 ka, respectively), had been associated with the Levantine excursion (Ryan, 1972), were found to have normal polarity magnetizations within the range of usual PSV. Besides that, one result from a flow dated at 623 ± 91 ka with a reversed polarity magnetization that was correlated to the Big Lost excursion in a previous study by Petronille et al. (2005), was found to have a normal polarity magnetization. This highlights the importance for further verification of such results before adopting them in the Geomagnetic Instability Timescale of Singer et al. (2002, 2007, 2008a,b).

The most important outcome of our geomagnetic investigation is the finding of nearly fully reversed polarity magnetizations in two Brunhes Chron lavas, with directions deviating almost 180° from the geographic North Pole. The only cryptochron included in the geomagnetic polarity timescale of Cande and Kent (1992, 1995) in the Brunhes Chron is C1n-1, which spans the interval from 493 to 504 ka, but both flows with reversed polarity magnetizations found in this study do not fall into that time window. Most of the Brunhes Chron geomagnetic excursions are constrained by minima in the relative palaeointensity obtained from records from sediment cores, but often these records fail to record the brief directional changes associated with the relative palaeointensity minima. This could be due to a combination of factors, such as inadequacy of the recording medium due to low sedimentation rates, inadequate sampling methods, delay in the remanence acquisition due to bioturbation and a progressive magnetization lock-in that may lead to smearing of the NRM directions, thereby inhibiting the recording of a brief directional event (Roberts and Winkelhofer, 2006). In sedimentary records, palaeointensity minima seem to be captured more readily because they are presumably longer lasting features than the accompanying directional excursions, and possibly less affected by the filtering effect of a finite magnetization lock-in zone during a detrital remanent magnetization acquisition. Exceptions are the two best documented excursions, the Lachamp and the Iceland Basin excursion, which both represent paired reversals of the geomagnetic field as virtual geomagnetic poles reach high southerly latitudes (Channell, 1999; Laj et al., 2006). So far, the only evidence of a fully reversed geomagnetic event recorded in volcanic rocks within the Brunhes Chron comes from the study of Kundsen et al. (2003), who identified possibly the same excursion at two lava flow sequences on Santo Antào (Cape Verde Islands) occurring in eight and six lava flows, respectively. However, limited age control (the excursion could have occurred

at any time between 500-720 ka) prevented them from uniquely correlating it to the geomagnetic instability timescale.

The finding of fully reversed polarity magnetizations recorded in two lava flows at the low latitude geographical location of Mexico from the present study gives new evidence that in particular the Big Lost- and the Delta / Stage 17 excursions could represent other short periods of reversed geomagnetic polarity of global validity. It has been shown that other cryptochrons or tiny wiggles within Chron C5n.2n represent short polarity intervals during which the field completed a full reversal (Roberts and Lewin-Harris, 2000). Our data indicates that this could have also been the case for the Big Lost- and the Delta / Stage 17 excursions. Yet, this assumption needs further verification by volcanic data from other parts of the world.

Acknowledgements

We would like to thank D. Berger, G. Arnold and M. Köhler (GFZ) for their help in the sample preparation. J. Herwig (GFZ) is thanked for her assistance during backscattered electron microscope studies. Much appreciated assistance during fieldwork came from I. Barajas and G. Gonzalez (Centro de Geociencias, Queretaro). Peter Schaaf (UNAM) and Gerardo Carrasco Núñez (Centro de Geociencias, Queretaro) are thanked for providing us unpublished age data. This research was funded by DFG grants Ne154/45-1, No334/1-2 and No334/5-1, Conacyt grant 46213 and PAPIIT-UNAM grant IN114606.

5. Application of the multispecimen palaeointensity method to Pleistocene lava flows from the Trans-Mexican Volcanic Belt

Daniel M. Michalk [a], Andrew J. Biggin [b], Mads F. Knudsen [c], Harald N. Böhnel [d], Norbert R. Nowaczyk [a], and Steven Ownby [e]

[a] *Helmholz-Zentrum Potsdam Deutsches GeoForschungsZentrum, Germany*
[b] *Paleomagnetic Laboratory Fort Hoofddijk, University of Utrecht, Netherlands*
[c] *Department of Earth Sciences, University of Aarhus*
[d] *Centro de Geociencias, UNAM-Campus Juriquilla, Queretaro, Mexico*
[e] *Department of Geological Sciences, University of Michigan, USA*

Submitted to: Physics of the Earth and Planetary Interiors

Abstract Despite the many advances recently made in palaeointensity (PI) studies, more high quality PI data are required for a better understanding of the full-vector evolution of the ancient geomagnetic field. In this study, we applied the recently-proposed multispecimen parallel differential pTRM (MS) method for absolute PI determination to rocks older than those studied hitherto with this method. Fifty-one lava flows from within the Trans-Mexican volcanic belt, which are generally younger than 1 Ma, returned 32 new PI estimates. Rock magnetic investigations revealed that in most cases, the remanence was carried by Ti-poor titanomagnetites of pseudo-single domain magnetic structure although titanomagnetites with higher Ti-contents and additional contributions of (titano-) haematite were also occasionally present. Comparisons with reconstructions of the global dipole moment reveal that the PI estimates from this study were, on average, around 30 per cent higher than expected. Other, mainly Thellier-type, PI data from Mexico were also observed to be high relative to global records, which could indicate that persistent non-dipole features might be responsible for the higher than expected results. However, the paucity of available data obscures the significance of this observation and the balance of evidence rather suggests an artificial biasing of most measurements towards high values. Our results seem to corroborate results from previous studies on historical lava flows and synthetic samples in which domain state effects were found to cause overestimates of the PI by up to 30 per cent in the MS method. We expect that the degree of the overestimate in the majority of these new MS results is no larger than what might be expected from Thellier experiments performed on samples with a similar given degree of multidomain behaviour. However, seven of the lava flows which were studied here using the MS method were subjected to a preceding demagnetisation step of 200°C in order to erase viscous remanences and these may have produced results which were further biased towards higher intensities. This additional bias is expected from theoretical considerations and may represent a challenge to future application of the MS method to older rock units. It could, however, potentially be avoided in future studies by performing measurements of the sample moment at temperatures higher than the blocking temperature of any overprint.

1. Introduction

The geomagnetic field is generated by convection in the electrically conducting liquid outer core, modified by the Earth's rotation (Merrill et al., 1996). Its expression at the Earth's surface can be approximated by a time-varying dipole field and small non-dipole components. The virtual axial dipole moment (VADM) of today's field is 7.9×10^{22} Am^2 (Korte and Constable, 2005) but constraining its evolution over different geological timescales remains difficult due to the paucity of available

palaeointensity (PI) data. Detailed records of the ancient geomagnetic field are necessary to provide information about the underlying processes in the Earth's core, and to help understand the historically observed decay in dipole moment of ~ 10 % over the last 170 years in a geological context. They are also necessary to improve spherical harmonic models of the geomagnetic field (e.g. Hongre et al., 1998; Korte and Constable, 2005; Korte et al., 2008) and to resolve long standing issues in palaeomagnetism such as the Pacific-Non dipole low (e.g. Johnson and Constable, 1998) and heterogeneous models of palaeosecular variation (PSV) (e.g. Constable and Johnson, 1999). They are of importance for studies where the shielding effect of the geomagnetic field plays a role, e.g. in determining production rates of cosmogenic nuclides, and finally, they are necessary to gain new insights into the recently debated topic regarding possible connections between changes in the geomagnetic field intensity and climate variability (e.g. Gallet et al., 2005, Courtillot et al., 2007, Thouveny et al., 2008).

The absolute palaeointensity (PI) is perhaps the most difficult of geomagnetic observables to determine (Valet, 2003). Materials used in palaeointensity (PI) studies must satisfy rigorous criteria with respect to the nature of the magnetisation and how it was acquired, the magnetic mineralogy and its grain size, and magnetic interactions within the sample.
The most basic requirements that underlie any absolute PI study are:

(1) The material must have retained a primary magnetization of thermoremanent origin;
(2) Alteration of the magnetic carriers in nature and during the laboratory experiments must be avoided or corrected for.

The absolute PI is studied either on archaeomagnetic materials (e.g. pottery, bricks, ceramics) or lava flows, because these materials preserve a thermo-remanent magnetisation (TRM) from when they were heated or extruded and then cooled down through their blocking temperature (T_B) spectrum. Archaeomagnetic materials are often dated by the radiocarbon method or through their cultural context and are restricted to the late Holocene period. For information about earlier periods, one must rely on palaeointensities obtained from lava flows or other igneous materials. Although archaeomagnetic materials and lava flows provide only instantaneous spot readings of the geomagnetic field, they can (if their ages are well constrained) provide semi-continuous records of the full vector field behaviour if they are sampled in sufficient detail through time, and they may be used for calibrating relative PI records from sediment cores to absolute values (e.g. Valet et al., 2005).

The Thellier method (Thellier and Thellier, 1959) and its modifications (e.g. Coe, 1967, Tauxe & Staudigel, 2004) in combination with additional reliability checks for alteration (Coe, 1967) and multidomain (MD) remanences (Riisager and Riisager, 2001; Kràsa et al., 2003) are regarded by many palaeomagnetists as the most reliable absolute PI method (e.g. Selkin and Tauxe, 2000; Goguitchaichvili et al., 2004). In a Thellier-type experiment, the natural remanent magnetisation (NRM) of a sample is progressively replaced by a set of laboratory partial thermoremanent magnetisations (pTRMs) acquired over successively increased temperatures in a laboratory field of known strength. This carries the assumption that each pTRM segment is independent from the other, which is only valid for grains of single domain (SD) magnetic structure (Neel, 1949). However, suitable PI recorders are rare in nature, because MD grains and alteration of magnetic minerals *in situ* or during the laboratory experiment are common in rocks. Thus, failure rates in Thellier-type studies are large, typically on the order of 80 %.

The Thellier method has been tested extensively over the past years on historical lava flows, for which the actual intensity is known from contemporary magnetic observatory data. While these tests yielded the expected intensity in some cases (e.g. Pick and Tauxe, 1993; Chauvin et al., 2005), other studies have revealed more controversial results, indicating significant overestimates of the intensity or large within-flow inconsistencies (e.g. Calvo, et al., 2002; Biggin & Thomas, 2003; Yamamoto et al., 2003). Thus scepticism has risen regarding the Thellier method, and variants and alternatives have been sought.

Dekkers and Böhnel (2006) used their multispecimen parallel differential pTRM method (hereafter referred to as MS method) to obtain correct palaeointensities on the 1945 Paricutin lava flow from Mexico, and in three simulated experiments. Unlike the Thellier method, the MS method is, according to the first-order symmetry theory of Biggin & Poidras (2006), independent of magnetic domain state, allowing all magnetic grain sizes to be processed. The sample processing time is also considerably shorter (25-50%) compared to a Thellier-type experiment because multiple samples are used, which are at best subjected to only one heating step. In a recent study by Michalk et al. (2008), the MS method was further evaluated based on 11 historical lava flows from Iceland and Mexico where the actual field intensity was known from either magnetic observatory data or deduced from magnetic field models. In addition, Thellier data were obtained from sister samples from five lava flows. This study revealed that MS PI estimates from six of the eleven flows were close to or statistically indistinguishable from the expected intensity, although a small bias towards overestimation of the intensity was noticed which was interpreted as being MD in character. Relative to the Thellier PIs, the corresponding MS PIs were statistically better defined and found to give PI estimates closer to the expected intensity. The satisfactory statistical precision of the MS PI estimates, accompanied with the large overall success rate (all 11 lava flows returned PI estimates using the MS method, while more than half of the Thellier data did not pass the quality criteria and had to be discarded), led to the suggestion that the MS method appears to be a viable alternative for future PI studies and might open up the possibility for acquiring considerably larger PI data sets.

In this study we applied the MS method to the oldest volcanic rocks yet subjected to this method, i.e. lava flows with ages of up to 3.5 Ma (although mostly younger than 1 Ma). The target area was the Trans-Mexican Volcanic Belt (TMVB), which comprises roughly 8000 volcanic structures, of which several hundred are younger than 2 million years (e.g. Demant, 1978; Gómez-Tuena et al., 2007), thus offering a superb archive for studying the full vector evolution of the geomagnetic field. The aim of this study was to obtain further information about the applicability of the MS method for future PI studies of older rocks.

2. Geological setting and sampling

The volcanism of the E-W trending TMVB relates to the Neogene subduction of the Cocos and Riviera Plates beneath the southwestern margin of the North American plate and extends roughly from the Pacific Ocean to the Gulf of Mexico (e.g. Aguirre-Díaz et al., 1998) (Fig. 5.1). It has a width between 20 and 150 km and forms a 1000 to 2000 m high volcanic plateau. The main volcanic structures include stratovolcanoes (e.g. Popocatepetel, Cofre de Perrote, Pico de Orizaba), shield volcanoes, monogenetic cinder cones and silicic caldera complexes. A pronounced morphologic feature of the TMVB is that it is not oriented parallel to the Middle America Trench, but is inclined at an angle of around 20° with respect to the trench.

Palaeomagnetic samples from 51 independent cooling units were chosen for PI experiments using the MS method. Samples were collected in five different field areas:
(1) Ceboruco-San Pedro-, (2) Tequila-, (3) Michoacan-Guanajuato-, (4) Valle de Bravo volcanic fields and (5) the eastern part of the TMVB in the vicinities of volcanoes Cofre de Perote and Pico de Orizaba (Fig. 5.1). Palaeomagnetic directions from the lava flows investigated in this study were reported in previous studies (Böhnel and Molina-Garza, 2002; Michalk et al., submitted). The majority (48 from 51) of the studied lavas are younger than 1 Ma. The associated age constraints, which derive from Michalk et al. (2008b) and other geochronological studies (Table 5.1), are of mixed quality, and some are characterised by large age uncertainties. Most lavas (n = 44) were dated using the ^{40}Ar / ^{39}Ar method, while four flows were dated using the ^{14}C method on charcoal found below the lava flows, and three flows using the thermoluminiscence (TL) method. The majority of the youngest rocks sampled stem from

the eastern part of the TMVB, but overall there is no age trend from East to West between the different field areas.

Previous palaeomagnetic studies on lava flows from Mexico have primarily focused on studying the directional palaeosecular variation (PSV) (see Mejia et al., 2005, and references therein). Absolute PI data from Mexico that have appeared in peer reviewed journals were acquired either from historic lava flows or lava flows younger than 40 ka (e.g. Böhnel et al., 2003; Gonzales et al., 1997; Vlag et al., 2000; Böhnel and Molina-Garza, 2002). Alva-Valdivia et al. (2001) report the only three available PI estimates that are older than 40 ka and within the time range of interest for this study.

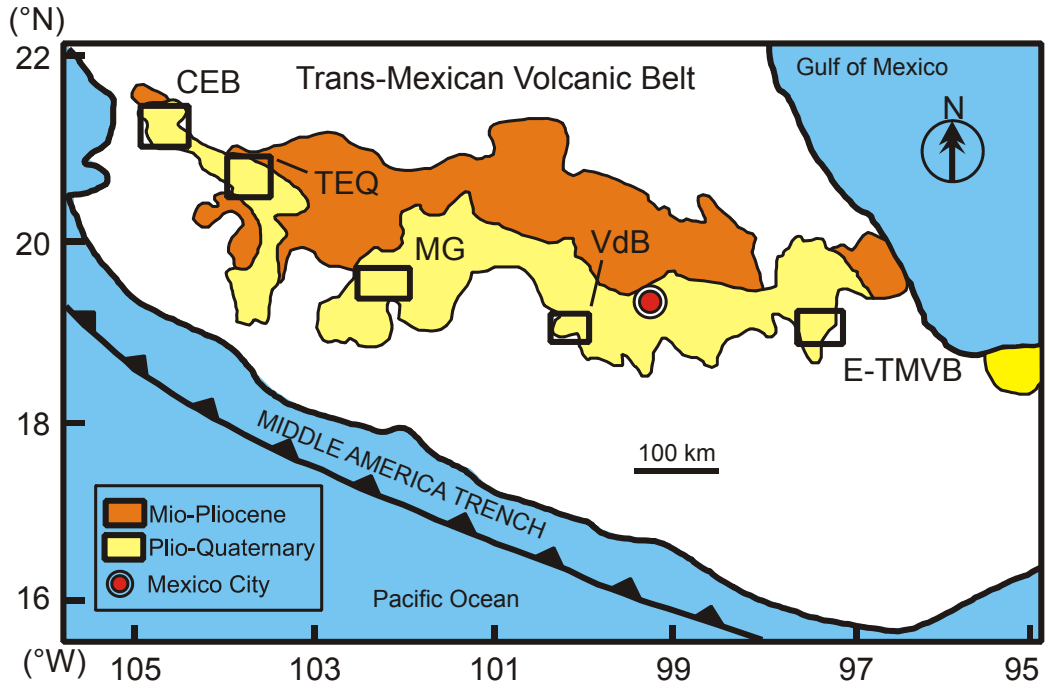

Figure 5.1. Schematic map of the Trans-Mexican Volcanic Belt showing the sampling areas indicated by solid rectangles. CEB = Ceboruco San-Pedro Volcanic Field, TEQ = Tequila Volcanic Field, MG = Michoacan Guanajuato Volcanic Field, VdB = Valle de Bravo Volcanic Field, E-TMVB = Eastern Trans-Mexican Volcanic Belt (Modified after Aguirre-Díaz, 1996).

Table 5.1. Lava flows investigated in this study with GPS site coordinates, volcanic origin (see Fig. 5.1), radiometric ages, dating methods applied and sources of age data : 1. this study, 2. Schaaf and Ramírez-Luna (2008), 3 Ownby et al. (2007), 4. Ownby et al. (submitted), 5. Blatter et al. (2001), 6. Lewis-Kenedi et al. (2005), 7. Frey et al. (2004), 8. Ort & Carrasco-Nunez (2009), 9. Carrasco-Nunez et al. (submitted), 10. Carrasco-Nunez et al. (2007), 11. Siebert and Carrasco-Nunez (2002).

code	Lat (°N)	Long (°W)	volcanic province	age (ka)	dating method	age ref.
DM	19.624	97.0317	E-TMVB	0.88 ± 0.04	^{14}C	11
DN	19.6223	97.0679	E-TMVB	0.88 ± 0.04	^{14}C	11
DL	19.624	96.9873	E-TMVB	0.91 ± 0.05	^{14}C	11
DR	19.1235	97.5377	E-TMVB	0 to 20	^{40}Ar / ^{39}Ar	8
DI	19.6447	96.9423	E-TMVB	2.98 ± 0.055	^{14}C	11
AG2	19.1770	100.251	VDB	5 ± 2	^{40}Ar / ^{39}Ar	5
DV	19.1230	97.6628	E-TMVB	16.8 ± 7.5	TL	2
EA	18.9257	97.4287	E-TMVB	31.7 ± 1.1	TL	2
DK	19.5896	96.9873	E-TMVB	41.76 ± 2.4	^{14}C	11
DX	18.9353	97.7250	E-TMVB	46 ± 0.68	TL	2
EG	21.1969	104.4720	CEB	63 ± 7	^{40}Ar / ^{39}Ar	7
DG	19.3845	100.3357	VDB	78 ± 19	^{40}Ar / ^{39}Ar	1
DF	19.1094	99.93160	VDB	80 ± 35	^{40}Ar / ^{39}Ar	1
EJ	21.0258	104.9390	CEB	85 ± 19	^{40}Ar / ^{39}Ar	7
AV	21.2177	104.9300	CEB	108 ± 22	^{40}Ar / ^{39}Ar	7
AL2	19.1664	100.2370	VDB	118 ± 44	^{40}Ar / ^{39}Ar	1
CP	20.866	103.8400	TEQ	178 ± 8	^{40}Ar / ^{39}Ar	6
CT	20.8100	103.4500	TEQ	191 ± 13	^{40}Ar / ^{39}Ar	6
CV	20.7902	103.5130	TEQ	196 ± 8	^{40}Ar / ^{39}Ar	6
BH	19.4281	102.5890	MG	230 ± 68	^{40}Ar / ^{39}Ar	4
DQ	19.4918	97.4980	E-TMVB	240 ± 50	^{40}Ar / ^{39}Ar	9
BI	19.4258	102.3500	MG	256 ± 18	^{40}Ar / ^{39}Ar	3
CU	20.8838	103.9930	TEQ	261 ± 11	^{40}Ar / ^{39}Ar	6
CD	19.3939	102.1110	MG	269 ± 22	^{40}Ar / ^{39}Ar	3
AH	19.1481	100.1470	VDB	282 ± 5	^{40}Ar / ^{39}Ar	5
AT	21.1631	104.0650	CEB	283 ± 5	^{40}Ar / ^{39}Ar	7
DT	19.3312	97.5350	E-TMVB	330 ± 80	^{40}Ar / ^{39}Ar	10
CF	19.3672	102.6580	MG	339 ± 23	^{40}Ar / ^{39}Ar	3
BJ	19.2811	102.8560	MG	360 ± 30	^{40}Ar / ^{39}Ar	4
EL	20.8269	103.9580	TEQ	362 ± 13	^{40}Ar / ^{39}Ar	6
CO	19.2575	102.6060	MG	385 ± 40	^{40}Ar / ^{39}Ar	3
EK	21.0356	104.5620	CEB	403 ± 15	^{40}Ar / ^{39}Ar	7
CR	20.8410	103.2770	TEQ	416 ± 3	^{40}Ar / ^{39}Ar	6
BD	19.3842	102.9310	MG	429 ± 64	^{40}Ar / ^{39}Ar	3
AQ	21.1975	104.7930	CEB	520 ± 25	^{40}Ar / ^{39}Ar	7
EI	21.0269	104.7920	CEB	521 ± 15	^{40}Ar / ^{39}Ar	7
EO	20.8998	103.2850	TEQ	592 ± 20	^{40}Ar / ^{39}Ar	6
EB	21.1569	104.0810	CEB	601 ± 6	^{40}Ar / ^{39}Ar	7
ED	21.1367	104.9690	CEB	623 ± 91	^{40}Ar / ^{39}Ar	7
CW	20.8635	103.7750	TEQ	632 ± 8	^{40}Ar / ^{39}Ar	6
EN	20.8992	103.3470	TEQ	671 ± 13	^{40}Ar / ^{39}Ar	6
CG	19.4161	102.4764	MG	673 ± 20	^{40}Ar / ^{39}Ar	3
CQ	20.7947	103.0720	TEQ	691 ± 26	^{40}Ar / ^{39}Ar	6
CH	19.4147	102.4803	MG	728 ± 18	^{40}Ar / ^{39}Ar	3
AZ	19.4353	102.2080	MG	730 ± 113	^{40}Ar / ^{39}Ar	4
CE	19.2589	102.4580	MG	909 ± 20	^{40}Ar / ^{39}Ar	4
CI	19.3753	102.9830	MG	957 ± 157	^{40}Ar / ^{39}Ar	4
DE	18.8188	100.1198	VDB	983 ± 58	^{40}Ar / ^{39}Ar	1
DH	19.3860	100.0142	VDB	1025 ± 79	^{40}Ar / ^{39}Ar	1
BW	19.0381	100.6860	VDB	1600 ± 55	^{40}Ar / ^{39}Ar	1
BL	19.2717	102.7280	MG	3528 ± 64	^{40}Ar / ^{39}Ar	4

3. Experimental techniques

Rock magnetic measurements included thermomagnetic (M_S-T) curves measured on at least two samples per flow using a Petersen Variable Field Translation Balance (VFTB). This involved heating the sample from room temperature to 600 / 700° C in an argon atmosphere whilst applying a field of 500 mT. Curie temperatures (T_C) were calculated using the method of Moskowitz (1981). In cases where M_S-T curves were found to show non-reversible behaviour, some samples were additionally subjected to thermal cycling with incremental heating steps of 100 °C until the highest Curie temperature was reached. Hysteresis measurements with a peak field of 1 T were made on small chips of 30-70 mg for a minimum of three samples per flow using a Princeton Measurements alternating gradient field magnetometer (AGFM). These allowed standard hysteresis parameters to be determined, namely, the saturation magnetisation, M_S, the saturation remanence, M_{RS}, the coercivity force, B_C and the coercivity of remanence, B_{CR}. A Day-plot (Day et al., 1977; Dunlop, 2002) was created using the ratios M_{RS} / M_S and B_{CR} / B_C to deduce the bulk magnetic domain size. In addition, first order reversal curves (FORCs) were measured (Roberts et al., 2000) on one sample per flow. Three FORC parameters were determined: (1) the main FORC peak (MFP), defined as the maximum of the FORC distribution along the B_C axis (Carvallo and Muxworthy, 2006); (2) the full width at half-maximum (FWHM) at B_C = MFP, defined as the full width at half maximum of the FORC distribution cut through MFP in the B_i direction indicative of the strength of magnetostatic interactions within a sample (Muxworthy and Williams, 2005); (3) the "width" parameter, defined as the interval in which the magnitude of the FORC distribution decreases to 10 per cent of its maximum, which reflects MD contribution to a sample (Carvallo et al., 2006).

Palaeointensity measurements were carried out following the multispecimen protocol described in Dekkers and Böhnel (2006). The basic assumption that underlies this PI method is the first-order symmetry property of pTRM in MD grains (Biggin and Poidras, 2006), which states that partial demagnetisation and remagnetisation treatments performed on samples containing MD grains cause changes in magnetisation that differ only in their relative magnitudes (a property otherwise thought only to exist for non-interacting SD grains). Both Biggin and Poidras (2006) and Dekkers and Böhnel (2006) have shown experimentally that if a MD sample has a full TRM and a pTRM is induced parallel to the TRM, the intensity of the resultant remanence (pTRM + original TRM) will approximately equal the original TRM, if the laboratory field is equal to the inducing field of the TRM. If the laboratory field is less than the inducing field, the overall remanence will decrease, if greater, the remanence will increase. Applying this concept to a multispecimen PI experiment means that the palaeointensity is determined as the field strength at which the composite remanence after pTRM acquisition (the difference between pTRM and TRM) and the original TRM is zero. Therefore, simply plotting a linear regression through the composite remanences for a range of field values yields the PI. The MS method requires the use of multiple samples. Each sample is subjected to only one in-field heating step at a moderate temperature, which significantly reduces the effect of heating-induced alteration. The field values are progressively increased for different sub-samples. In an ideal MS experiment, the pTRMs are induced parallel to the original NRM. To allow this, a specially designed sample holder was used which allowed orienting the ChRM of up to 15 samples parallel to the oven field with a precision of better than 10°. The laboratory field is applied during both the heating and the cooling cycle, which is necessary to avoid potentially significant demagnetisation of the sample. For the PI experiments, a temperature- and field-calibrated MMTD oven was used, for which the laboratory field was calibrated to an accuracy of 0.1 μT along the heating chamber. Remanence measurements were made either on a cryogenic magnetometer with long core setup (2G Enterprises 755 SRM) or on a spinner magnetometer (Agico JR6) at Deutsches GeoForschungsZentrum Potsdam.

Ideally, the multispecimen method only requires one heating step; after pTRM acquisition, the pTRM is scaled to the original NRM to determine the percentage value of pTRM lost / gained. This carries the assumption of a univectorial NRM that is free of secondary viscous components. Previous

demagnetisation experiments by Michalk et al., (submitted) revealed that secondary components of magnetisation are common in samples from some of the lava flows studied here. In such cases samples were subjected to an initial demagnetisation step to isolate the characteristic NRM. For the present study a thermal demagnetisation pre-treatment of 200°C was chosen, which was found to be sufficiently high to erase any viscous components. This differs from the approach of Michalk et al. (2008), who used small alternating fields (AF) of 5 mT to erase small fractions viscous overprints in samples from historic lava flows from Iceland and Mexico.

For samples that underwent a thermal pre-treatment it was required to include a second 200°C demagnetisation step after pTRM acquisition in zero field for normalisation purposes. In total 17 flows were processed using this routine. The thermal pre-treatment was chosen in favour of the AF alternative because in some cases the latter would have resulted in very severe overestimation of the palaeointensity. The reason for this is that the reapplication of this AF treatment (generally much higher than 5 mT) after the thermal remagnetisation step frequently removed most or all of the pTRM that had just been imparted. A temperature for the remagnetisation stage of the PI experiments was chosen so that the fraction of TRM removed was in the order of 20 to 70 per cent, and increases in magnetic susceptibility, measured at room temperature, were less than 10 %. The T_{UB} spectra were evaluated from at least two samples per flow by stepwise thermal demagnetisation, and the thermal stability of the samples was further evaluated from the M_S-T experiments.

The palaeomagnetic samples used in this study were so called ‘mini samples’ with a diameter of 12 mm and a length of 10 mm. For the PI experiments, samples that were closest to the bottom of the core were preferably chosen to minimise surface weathering effects. Ideally, in this PI experiment, all samples must have the same unblocking temperature characteristics and the same magnetic history. In order to use samples with similar magnetic properties, as many samples as possible were chosen from one drill core (each drill core yielded between 3 and 10 successive sample specimens), or samples were taken from cores located in close proximity to each other. For each drill core, one specimen was subjected to progressive AF- demagnetisation to check for secondary remanences, like viscous overprints or lightning-induced isothermal remanent magnetisations (IRMs).

4. Results

4.1 Thermomagnetic properties and ore-microscopy observations

The majority of samples (Table 5.2) showed reversible behaviour during the thermomagnetic experiments, suggesting a single magnetic phase with a high Curie temperature between 511 and 577° C, indicative of Ti-poor titanomagnetite (Fig. 5.2a-c). Ore-microscopy observations revealed that oxy-exsolved titanomagnetites with some ilmenite lamellae (oxidation stages C2-4 after Haggerty, 1991) are common in these samples (Fig. 5.3a).

Four sites (DK, DF, AV and CF) had lower T_Cs between 291 and 420°C, indicative of titanomagnetites with compositional parameters between x = 0.25 and 0.4, that must have undergone a smaller degree of deuteric oxidation (C1-2). Ore-microscopy observations of these four samples revealed the presence of unblemished skeletal titanomagnetites (Fig. 3b). Samples from sites DK (Fig. 5.2e), CF and DF displayed excellent reversibility, whereas the samples from site AV (Fig. 5.2h) displayed a moderate increase of M_S and the Curie temperature on the cooling branch. Thermal cycling indicated that this alteration began at approximately 400° C; it most likely reflects the continued oxy-exsolution of the titanomagnetite.

Samples from seven sites (DM, DL, DI, DX, CP, EK and CI) displayed two inflection points, the first between 250 and 370°C, and a second between 500 and 590°C. In the case of sites DX, DL (Fig, 5.2f and g) and CI, the curves were fully reversible indicating two stable phases of titanomagnetite. Irreversible

thermomagnetic behaviour was found in samples from sites DI (Fig. 5.2i), CP (Fig. 5.2j), DM (Fig. 5.2k), and EK, which displayed increases in M_S on cooling, starting from temperatures as low as 200°C or around 300° C.

Ore-microscopy observations on samples from sites BL (Fig. 5.3c), CW (Fig. 5.3d), AL2, BJ, and AQ revealed a red colour and iron oxides indicative of higher deuteric oxidation stages (C5-C7). Corresponding thermomagnetic curves showed Curie temperatures between 532 and 592°C, with M_S values generally slightly lower on cooling than on heating (e.g. BL_7; Fig. 5.2d). Alternating field demagnetisation experiments on samples from these sites revealed that peak fields of 100 / 125 mT were not sufficient to fully demagnetise the samples but left between 20 and 40% of the NRM intact (Michalk et al., submitted). This suggests the presence of (titano-) haematite which may not have been visible in the thermomagnetic curves on account of its small M_S.

The titanomagnetites in samples from sites CW (Fig, 5.3d), AQ and BJ appeared to be affected by maghaemitisation, although there was little evidence for maghaemite in the accompanying thermomagnetic curves. In the case where (titano-) maghaemite was detected in the thermomagnetic experiments (e.g. site CY; Fig 5.2l), the site was excluded from the PI experiments.

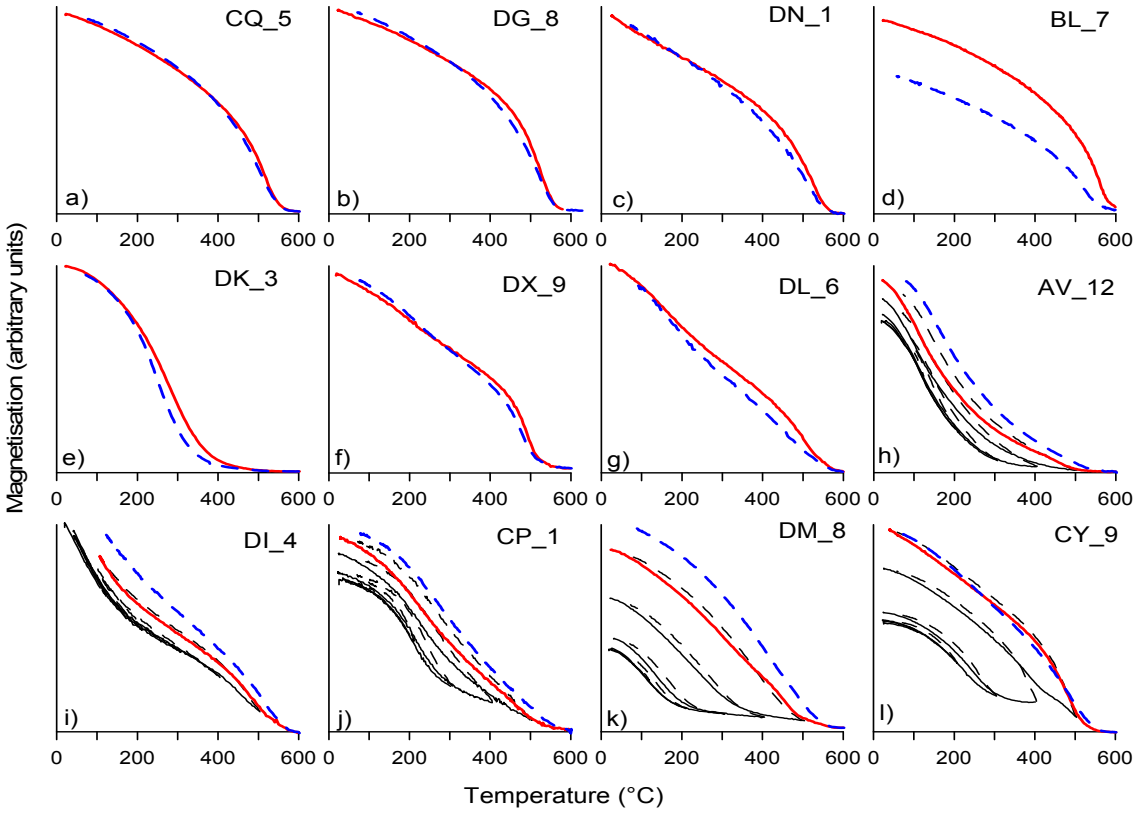

Figure 5.2. Examples of thermomagnetic curves obtained with a Variable Field Translation Balance (VFTB) in a field of 500 mT. Heating (red line) and cooling (blue line) were conducted under Argon flushing. a) to g) show single heating runs up to 600°C; h) to l) are samples subjected to an incremental thermal cycling with steps of 100°C from room temperature to 600°C; the final heating cycle is highlighted.

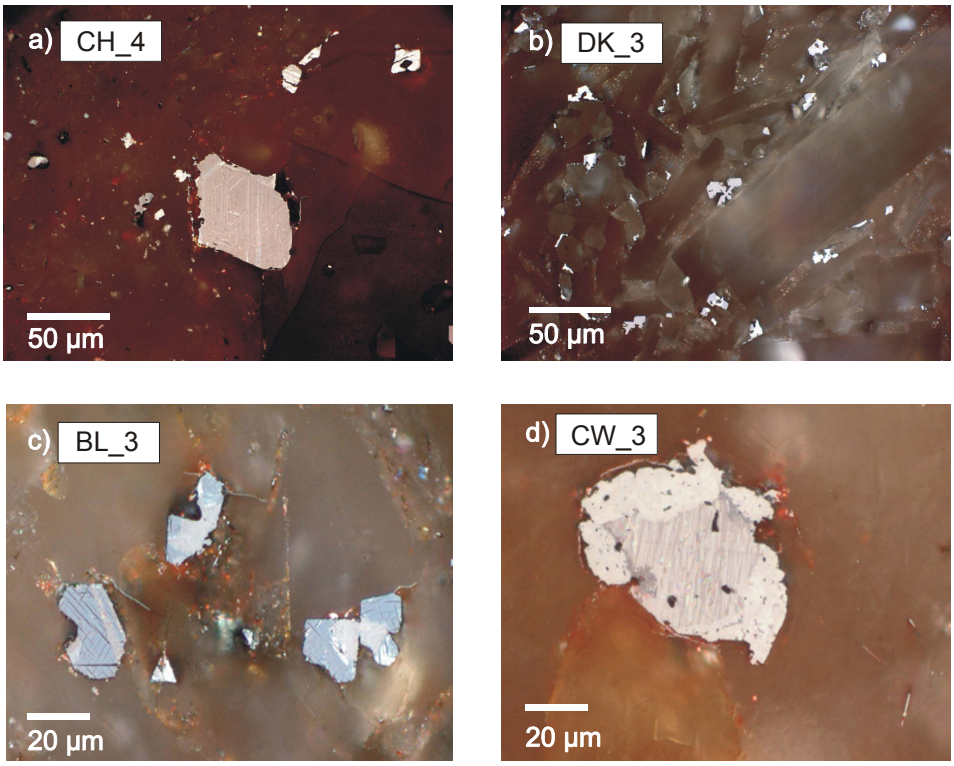

Figure 5.3. Examples of reflected-light microscopy: a) Exsolution of ilmenite lamellae in Ti-poor titanomagnetite (sample CH_4 from the Michoacan-Guanajuato volcanic field, 728 ± 18 ka); b) fresh, unblemished titanomagnetites with no visible signs of deuteric oxidation (sample DK_3 from the Eastern Trans-Mexican Volcanic Belt, 41.7 ± 2.4 ka); c) highly oxidised reddish lava with exsolved titanomagnetites (sample BL_3 from the Michoacan-Guanajuato volcanic field, 3528 ± 64 ka); d) highly oxidised reddish lava where titanomagnetites are severely affected by additional low temperature oxidation (sample CW_3 from the Tequila volcanic field, 632 ± 8 ka).

4.2 Hysteresis properties

The Day-plot (Fig. 5.4) shows that the majority of samples plot in the PSD range, slightly to the right of the theoretical mixing curves of Dunlop (2002). The FORC diagrams are broadly consistent with the results from the Day-plot and some representative examples are shown in Fig. 5.5.

Samples, which plot in the upper left region of the PSD range, with average M_{RS} / M_S values between 0.27 and 0.44 have dominantly closed contours with a well-defined central peak (Fig. 5.5a-d) and display a negative region in the FORC distribution, which is indicative of some contribution of non-interacting single domain material with dominant uniaxial anisotropy to the remanence (Muxworthy et al., 2004; Newell et al, 2005). These FORC diagrams are similar to published FORCs from PSD magnetites (Muxworthy, 2007). MFP values are between 8.6 and 16.4 mT and FWHM values between 6 and 15.4 mT. The negative region is not observed in samples with average M_{RS} / M_S values between 0.19 and 0.25 (Fig. 5.5 e and f), but contours are still dominantly closed. Sites with average M_{RS} / M_S values between 0.08 and 0.17 (Fig. 5.5g-k) show increasingly open contours reflecting an increasing contribution of MD material to the remanence. In the cases of CH_5 (Fig. 5.5i), the MFP is close to zero. Samples that plot away from the mixing curve more towards the right, e.g. DX_9 and CF_9, (Fig. 5.5g and k, respectively) had rather high FWHM values (19.5 and 28, respectively). The offset could be caused by increased magnetostatic interactions within these samples.

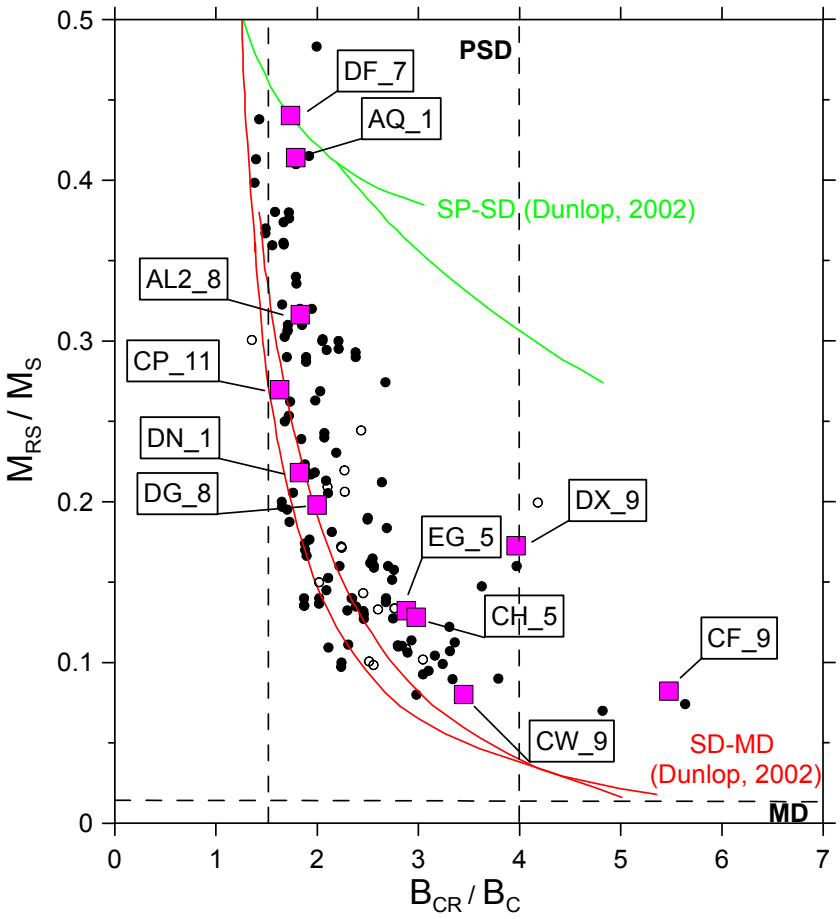

Figure 5.4. Plot of bulk magnetic domain states (Day et al., 1977) based on hysteresis parameters of the 51 lavas used for palaeointensity experiments. Filled circles: samples used in a successful palaeointensity experiment; open circles: samples that failed the palaeointensity experiments; theoretical mixing curves of Dunlop (2002) are shown for reference: red lines (single domain-multi domain) and green lines (super paramagnetic-single domain); The magenta coloured squares indicate samples for which FORC diagrams are shown in Figure 5.

In summary, rock magnetic investigations revealed that in most cases Ti-poor titanomagnetite dominated these lavas but that titanomagnetites with higher Ti contents were also occasionally present. These phases are produced by oxy-exsolution of the original titanomagnetite during initial flow cooling and thus the magnetisation of most of these flows is most likely of thermal origin. Samples from sites AL2, BJ, AQ, CW and BL are highly oxidised and, although it cannot be seen in the thermomagnetic curves, likely contain additional (titano-) haematite. According to ore-microscopy observations of samples from three of these sites, the presence of some additional (titano-) maghaemite cannot be ruled out completely and it is possible that their magnetisations could at least partly be carried by a later chemical remanent magnetisation (CRM). We shall therefore return to the PI results from these lavas later. Rock magnetic properties are summarised in Table 5.2.

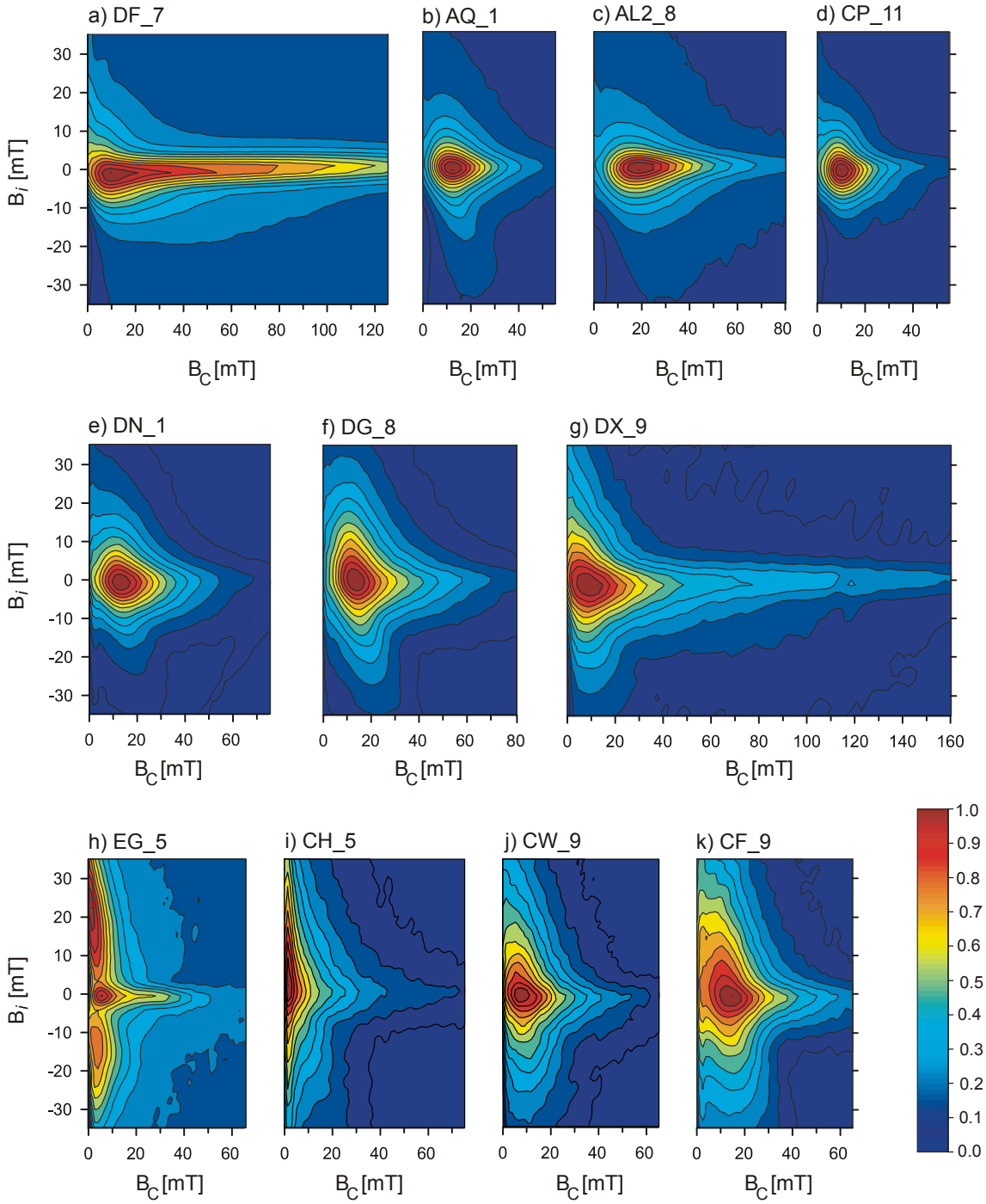

Figure 5.5. Representative examples of first order reversal curve (FORC) diagrams (normalised to peak values). B_C corresponds roughly to the coercivity distribution in the sample, and B_i is an indicator for the interaction field strength. The smoothing factor (SF) is 3 for all diagrams. The integration time for all samples was 100 ms and each diagram was constructed from 120 FORCs.

Table 5.2. Rock magnetic parameters for sites that returned PI estimates: Hysteresis values (site averages) for the parameters BC (coercivity) / BCR (remanent coercivity) and MRS (remanent saturation magnetisation) / MS (saturation magnetisation); Curie temperatures (TC) , determined after the method of Moskowitz (1981); first order reversal curve (FORC) parameters (single specimen data) that are: full width at half maximum (FWHM), the main FORC peak (MFP) and the "width" parameter determined at the point where the FORC distribution decreases to 10 per cent of its maximum.; and the dominant remanence carriers.

Site	B_C	B_{CR}	M_{RS} / M_S	T_C (°C)	FWHM	MFP	width	remanence carrier(s)
DM	20.8 ± 1.1	29.8 ± 2.6	0.40 ± 0.03	291, 590 #	6.0	11.7	7.3	Tima
DN	15.5 ± 1.6	28.2 ± 3.4	0.22 ± 0.02	543 *	13.5	10.8	18.8	Tima
DL	7.9 ± 0.3	15.0 ± 0.7	0.17 ± 0.01	420, 567 *	7.6	4.1	13.1	Tima
DR	15.8 ± 5.9	32.0 ± 6.1	0.22 ± 0.13	518 *	14.9	9.2	9.4	Tima
DI	6.1 ± 0.2	10.4 ± 0.5	0.19 ± 0.01	275, 504 #	4.6	3.2	4.7	Tima
AG2	13.9 ± 4.4	37.7 ± 6.5	0.20 ± 0.06	521 *	13.7	4.5	13.9	Tima
DV	16.8 ± 1.7	28.7 ± 2.7	0.29 ± 0.02	537 *	7.8	3.6	5.7	Tima
EA	11.6 ± 1.9	33.9 ± 3.1	0.16 ± 0.01	521 *	12.8	3.6	16.2	Tima
DK	5.0 ± 1.2	10.3 ± 2.4	0.13 ± 0.02	324 *	6.9	5.4	8.2	Tima
DX	15.9 ± 1.4	57.2 ± 15.3	0.17 ± 0.01	369, 503 *	19.5	7.6	24.2	Tima
EG	6.2 ± 1.6	22.8 ± 1.3	0.10 ± 0.03	527 *	42.5	4.6	41.9	Tima
DG	16.0 ± 0.7	32.5 ± 0.2	0.20 ± 0.02	535 *	19.4	10.6	23.7	Tima
DF	36.4 ± 2.3	68.3 ± 0.1	0.45 ± 0.03	396 *	8.8	8.9	7.5	Tima
AV	5.7 ± 0.1	13.1 ± 0.1	0.11 ± 0.02	291 #	7.5	3.3	8.0	Tima
AL2	20.6 ± 1.6	37.6 ± 5.5	0.34 ± 0.03	592 *	7.5	16.3	10.1	Tima + Tihae (Timagh)
CP	16.5 ± 6.3	30.8 ± 16.2	0.27 ± 0.02	250, 500 #	9.4	8.6	7.7	Tima
CD	13.1 ± 6.1	32.4 ± 10.7	0.15 ± 0.06	562 *	18.0	8.3	21.8	Tima
AH	13.0 ± 0.2	35.3 ± 2.5	0.16 ± 0.03	526 *	6.5	3.2	16.2	Tima
AT	13.2 ± 2.6	35.5 ± 4.9	0.13 ± 0.02	548 *	32.9	9.0	24.5	Tima
DT	20.8 ± 6.6	37.6 ± 11.7	0.29 ± 0.06	546 *	10.3	10.8	7.5	Tima
CF	7.6 ± 0.9	28.9 ± 6.0	0.08 ± 0.01	420 *	28.1	11.6	24.5	Tima
BJ	17.7 ± 5.5	39.8 ± 7.9	0.22 ± 0.03	532 *	14.1	13.1	24.4	Tima + Tihae (Timagh)
EL	16.2 ± 9.1	40.7 ± 27.4	0.19 ± 0.07	568 *	23.9	8.4	15.0	Tima
EK	19.6 ± 6.7	37.4 ± 12.9	0.29 ± 0.02	348, 534 #	9.1	13.4	11.0	Tima
AQ	14.6 ± 2.0	24.2 ± 2.1	0.36 ± 0.05	538 *	8.3	9.9	6.8	Tima+ Tihae (Timagh)
CW	7.3 ± 1.2	22.7 ± 1.7	0.10 ± 0.02	533 *	22.7	6.2	27.2	Tima + Tihae (Timagh)
CG	10.5 ± 1.9	27.2 ± 1.3	0.12 ± 0.02	562 *	14.8	11.6	20.1	Tima
CQ	10.7 ± 1.9	25.4 ± 3.5	0.16 ± 0.08	536 *	22.6	7.7	24.3	Tima
CH	10.7 ± 2.5	33.3± 3.5	0.11 ± 0.02	511 *	12.9	0.9	26.7	Tima
AZ	13.8 ± 5.3	27.0 ± 3.4	0.28 ± 0.15	547 *	7.7	12.5	4.9	Tima
CI	23.8 ± 12.4	39.6 ± 11.8	0.28 ± 0.11	367, 543 *	13.0	9.9	16.8	Tima
BL	21.6 ± 2.3	42.5 ± 5.2	0.27 ± 0.01	577 *	15.4	16.4	16.9	Tima + Tihae (Timagh)

4.3 Palaeointensity experiments:

Because of large deviations in the unblocking spectra and different thermomagnetic behaviour of samples from different flows, PI experiments were conducted at temperatures between 160°C (site DM) and a maximum of 480°C (sites AG2, DT, BJ and BL).
The following acceptance criteria were applied to the PI data:

(1) each PI estimate is based on at least six samples with no point being arbitrarily excluded from the analysis,

(2) the maximum angular deviation (MAD) of the full component of each associated sister sample used in the PI experiment is < 5°,

(3) lines with multiple zero crossings are not accepted,

(4) the correlation coefficient (R^2) of the linear regression is ≥ 0.75.

In total, 32 out of 51 PI experiments were successful which corresponds to an overall success rate of 63 %. Figure 5.6 shows seven examples of the MS PI experiments together with representative examples of demagnetisation data.

Samples from sites DM and DN derive from the same lava flow, with an estimated age of 0.88 ± 0.06 ka, but were processed at different temperatures (160° and 350°C, respectively) due to their different thermomagnetic behaviour (Fig. 5.2 k and c, respectively). Their PI estimates agree well (54 ± 5 and 57 ± 2 μT, respectively). All other results are based on single experiments and returned PI estimates between 26 μT (site Al2, Fig. 5.6c) and 64 μT that are based on 6 to 10 samples. Correlation coefficients of the linear regression were larger than 0.79 for all sites and in the case of sites DI, AG2, DV and CG, close to 1.0. From a total of 17 experiments that included a preceding 200°C demagnetisation step, only 7 sites (EG, AV, CF, EL, EK, CW, and CQ) returned PI estimates (e.g. site EK; Fig. 5.6d). In some cases, we found that the second demagnetisation at 200°C after pTRM acquisition removed most of the previously acquired magnetisation (e.g. site CE; Fig.5.6e).

Other experiments most likely failed because of differences in the T_{UB} spectra between the specimens used in the experiment, which resulted in a scattered behaviour with sometimes multiple zero crossings (e.g. site EB; Fig 5.6g). Sites DG, CG and CH returned PI estimates but lack directional information because palaeomagnetic directions were highly dispersed, either due to mis-orientation of the samples in the field or due to bad outcrop exposures, i.e. blocky lava flows (Michalk et al., submitted). Palaeointensity results are summarised in Table 5.3.

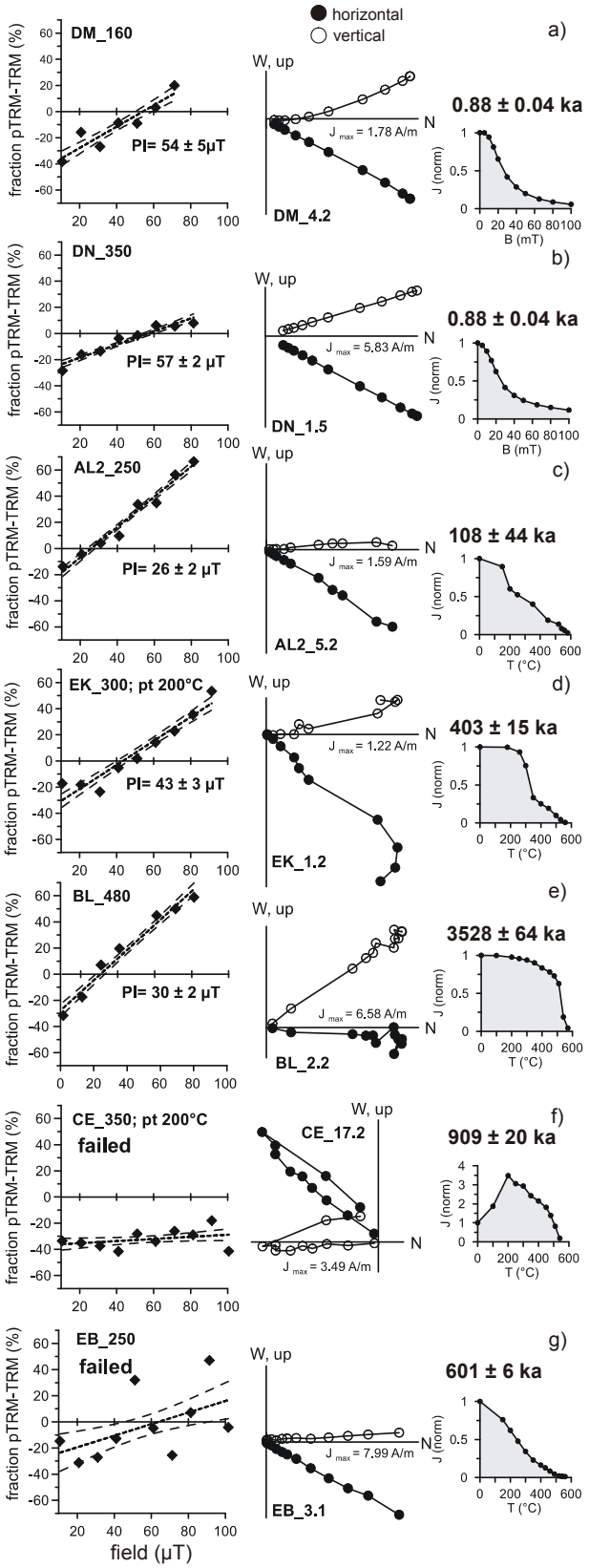

Figure 5.6. Examples of results from multispecimen PI experiments which succeeded (a-d) and failed (e-f). The linear regressions are indicated with a short-dashed line, the 68 per cent confidence zone (one standard error) are indicated by the longer-dashed lines. The abbreviation indicates the temperature for the pTRM acquisition (e.g. DM_160, pTRM acquisition at 160°C), pt 200°C indicates that samples were subjected to a thermal demagnetisation pre-treatment at 200°C. Middle and right columns: Associated representative Zijderveld diagrams with corresponding normalised intensity decay curves, respectively.

Table 5.3. Summary statistics of directional- and palaeointensity data. Left: Flow-mean palaeodirections of cleaned remanences for the sites that returned palaeointensity estimates. N, number of specimens used for the calculation of the mean direction; k and α95, precision parameter and radius of 95% confidence cone of Fisher statistics (Fisher, 1953), respectively; Dec, Declination; Inc, Inclination; Plat / Plong, latitude / longitude of the corresponding virtual geomagnetic pole; A95, 95% confidence limit of the virtual geomagnetic poles; Pol, magnetic polarity (N - normal polarity, R - reversed polarity; I intermediate direction); n.a., not available / discarded data; Right: NPI, number of specimens used for the calculation of the palaeointensity; T(°C) pTRM, temperature at which the pTRM was acquired, R2, correlation coefficient of the linear regression; VDM, virtual dipole moment; VADM, virtual axial dipole moment.

Directions											Intensities					
Site	age (ka)	N	k	α 95 (°)	Dec (°)	Inc (°)	*P* lat	*P* long	A95	Pol.	N	PI (μT)	pTRM acquisition at T (°C)	R^2	VDM ($10^{22}Am^2$)	VADM ($10^{22}Am^2$)
DM *	0.88 ± 0.04	26	248	1.8	345	34.4	75.8	172.5	1.6	N	7	54 ± 5	160	0.87	12.2 ± 2.2	12.1 ± 2.2
DN *	0.88 ± 0.04										8	57 ± 2	350	0.92	12.9 ± 0.9	12.9 ± 0.9
DL	0.91 ± 0.05	31	565.1	1.1	341.9	32.5	72.7	3.5	0.9	N	9	39 ± 4	250	0.89	8.9 ± 1.8	8.7 ± 1.8
DR	0 to 20	9	233.7	3.4	9.6	27.8	79.8	16.4	2.7	N	9	45 ± 3	300	0.94	10.1 ± 1.3	10.1 ± 1.3
DI *	2.98 ± 0.055	8	218	3.8	7.8	27.8	81.8	25	3.1	N	8	47 ± 1	200	0.98	11.1 ± 0.6	10.5 ± 0.6
AG2	5 ± 2	5	302.4	4.4	2.4	17.7	79.9	66.5	3.3	N	9	55 ± 1	480	0.99	13.7 ± 0.6	12.4 ± 0.6
DV	16.8 ± 7.5	8	230.8	3.4	11.5	25.5	77.6	18.1	2.7	N	9	61 ± 1	350	0.99	14.4 ± 0.6	13.7 ± 0.6
EA	31.7 ± 1.1	9	60.2	6.7	355.2	36	85.4	186.3	5.9	N	9	56 ± 3	250	0.94	12.5 ± 2.7	12.6 ± 2.7
DK *	41.76 ± 2.4	3	450	5.8	356.6	23.2	81.8	107.1	4.5	N	7	27 ± 3	200	0.93	6.6 ± 1.4	6.0 ± 1.4
DX	46 ± 0.68	15	55.2	5.2	1.5	31.4	87.6	46.3	4.4	N	9	39 ± 2	300	0.97	9.0 ± 1.0	8.8 ± 1.0
EG	63 ± 7	15	52.2	5.3	330.7	51	61.9	193.5	5.9	N	9	42 ± 5	280 **	0.94	8.0 ± 1.9	9.2 ± 2.2
DG	78 ± 19	n.a.	n.a.	n.a.	n.a.	n.a.	n.a.	n.a.	n.a.	n.a.	8	48 ± 3	300	0.90		10.8 ± 1.3
DF	80 ± 35	9	67.6	6.3	12	31.8	78.4	357.5	5.3	N	8	48 ± 3	200	0.79	11.0 ± 1.8	10.8 ± 1.4
AV	108 ± 22	10	36	8.2	12.4	24.5	75.5	18.7	6.4	N	8	50 ± 2	300 **	0.96	12.1 ± 1.1	11.0 ± 1.2
AL2	118 ± 5	9	109.2	4.9	6.6	33.2	83.7	358.2	4.2	N	8	26 ± 2	250	0.97	5.8 ± 1.0	5.8 ± 1.0
CP	178 ± 8	7	71.8	7.2	333.6	23.2	63.3	151.2	5.6	N	8	49 ± 3	250	0.91	11.9 ± 1.5	10.8 ± 1.5
CD	269 ± 22	12	141.9	3.7	1.9	24.3	83.1	62	2.9	N	9	50 ± 4	350	0.89	12.1 ± 2.0	11.2 ± 1.8
AH	282 ± 5	6	56.8	9	4.9	29.2	84.1	26	7.4	N	9	34 ± 6	250	0.79	7.0 ± 2.6	7.7 ± 2.7
AT	283 ± 5	10	105.1	5	351.3	34.3	81.5	150.9	4.3	N	9	56 ± 4	350	0.85	12.6 ± 1.8	12.3 ± 1.8
DT	330 ± 80	16	53.8	5.1	9	47.6	77.5	302	5.4	N	9	46 ± 4	480	0.88	9.3 ± 1.7	10.3 ± 1.8
CF	339 ± 23	8	74	6.5	7.3	34.3	83.1	350.8	5.6	N	9	51 ± 1	350 **	0.98	11.5 ± 0.7	11.4 ± 0.8
BJ	360 ± 30	15	147.2	3.2	6.7	33	83.5	358	2.7	N	10	48 ± 5	480	0.85	10.9 ± 2.3	10.8 ± 2.2
EL	362 ± 13	15	56.4	5.1	358	35.8	87.9	138.4	4.5	N	10	64 ± 5	300 **	0.86	14.3 ± 2.3	14.1 ± 2.3
EK	403 ± 15	7	115.4	5.6	4.7	49.7	79.6	278.7	6.1	N	9	43 ± 3	300 **	0.92	8.4 ± 1.3	9.4 ± 1.4
AQ	520 ± 25	16	182.6	2.7	15	15	70.2	26.1	2	N	6	56 ± 3	450	0.95	14.1 ± 1.5	12.3 ± 2.6
CW	632 ± 8	10	122.3	4.4	5.2	26.9	81.7	38.4	3.5	N	8	52 ± 2	300 **	0.97	12.4 ± 1.0	11.4 ± 1.0
CG	673 ± 20	n.a.	n.a.	n.a.	n.a.	n.a.	n.a.	n.a.	n.a.	n.a.	8	33 ± 1	250	0.98		7.4 ± 1.0
CQ	691 ± 26	10	87	5.2	1.7	27.5	83.6	61.4	4.2	N	9	64 ± 5	300 **	0.82	15.2 ± 2.4	14.1 ± 2.3
CH	728 ± 18	n.a.	n.a.	n.a.	n.a.	n.a.	n.a.	n.a.	n.a.	n.a.	9	37 ± 3	350	0.93		8.3 ± 1.3
AZ	730 ± 113	10	20.7	10.9	9.8	45.3	78.4	306.9	11	N	6	54 ± 2	450	0.98	11.0 ± 1.5	12.1 ± 1.4
CI	957 ± 157	13	16.1	10.6	15.3	51.9	71.0	300.6	12	N	8	29 ± 5	350	0.88	7.3 ± 2.5	6.5 ± 2.3
BL	3528 ± 64	16	177.9	2.8	334.8	1.0	59.0	133.6	2	N / I	7	30 ± 2	480	0.97	7.8 ± 1.0	6.7 ± 0.9

* directions by Böhnel & Molina-Garza (2002)
** samples subjected to an initial 200°C demagnetisation step

5. Discussion

In the following discussion, PI estimates are compared to reconstructions of the dipole moment and other PI data available from Mexico.

5.1 Palaeointensities from 0 to 7 ka

Knudsen et al. (2008) recently presented a reconstruction of variations in the geomagnetic dipole moment over the past 50 ka. Using a running window approach on the PI data included in the GEOMAGIA50 database (Donadini et al., 2007; Korhonen et al., 2008; http://data.geophysics.helsinki.fi) the axial dipole moment that provides the optimal least squares fit was determined. They grouped PI data in time windows of 500, 1000, 2000 and 4000 years (depending on the amount and age of data) to average out effects from the secular variation of the non-dipole (ND) field and calculated associated error estimates by using a bootstrap procedure. For realistic error propagation, a stochastic noise component was added to the data, thus the calculated error estimates reflect both the scatter and amount of data in each time interval. In Figure 5.7, the MS PI data (green diamonds) are plotted as VADMs against the VADM reconstruction of Knudsen et al. (2008) and other available absolute PI data from Mexico. It is noted however, that the PI of a single flow might not necessarily be expected to agree with global mean values because of possible local non-dipole contributions. The axial dipole moment is well-constrained back to around 7 ka, at which point there is a significant drop in the amount of latitudinal coverage of the PI data. In addition, we use two new regularized spherical harmonic field models from Korte et al., (2008, submitted), i.e. the ARCH3K.1 model (based exclusively on archaeomagnetic data from GEOMAGIA50) and CALS3K.3 model (based on all available GEOMAGIA50 data), to deduce the intensity for Mexico for the last 3 ka. The intensity data from the spherical harmonic field models were converted to VADMs and are shown in Figure 5.7 (stippled green and purple lines, respectively).

Results from sites DM and DN stem from the same lava flow, and both are slightly higher than the VADM curve. Yet, their PI estimates are similar and they agree well with the spherical harmonic field models of Korte et al. (submitted), which indicates that both PIs may well represent the field intensity at that time. The result from site DL plots slightly below the VADM curve but considering the PI uncertainties, it is indistinguishable from the VADM curve. The result from site DI is in very good agreement with the VADM curve. Besides two MS PI estimates from historical lavas (pink diamonds) from 450 and 455 years BP, which were found to overestimate the actual intensity by about 30 % (Michalk et al., submitted), the only MS PI estimate which is obviously higher than the VADM curve is that of site AG2. However, it is interesting to note that a Thellier PI estimate from Gonzalez et al. (1997), obtained on a flow of similar age (4.75 ± 0.2 ka), is close to the PI estimate for site AG2. In comparison to other PI data from Mexico, the MS PI estimates seem to agree better with the VADM curve, in particular in comparison with Thellier data from lava flows (red dots), from which at least 6 out of 9 PI estimates are too high.

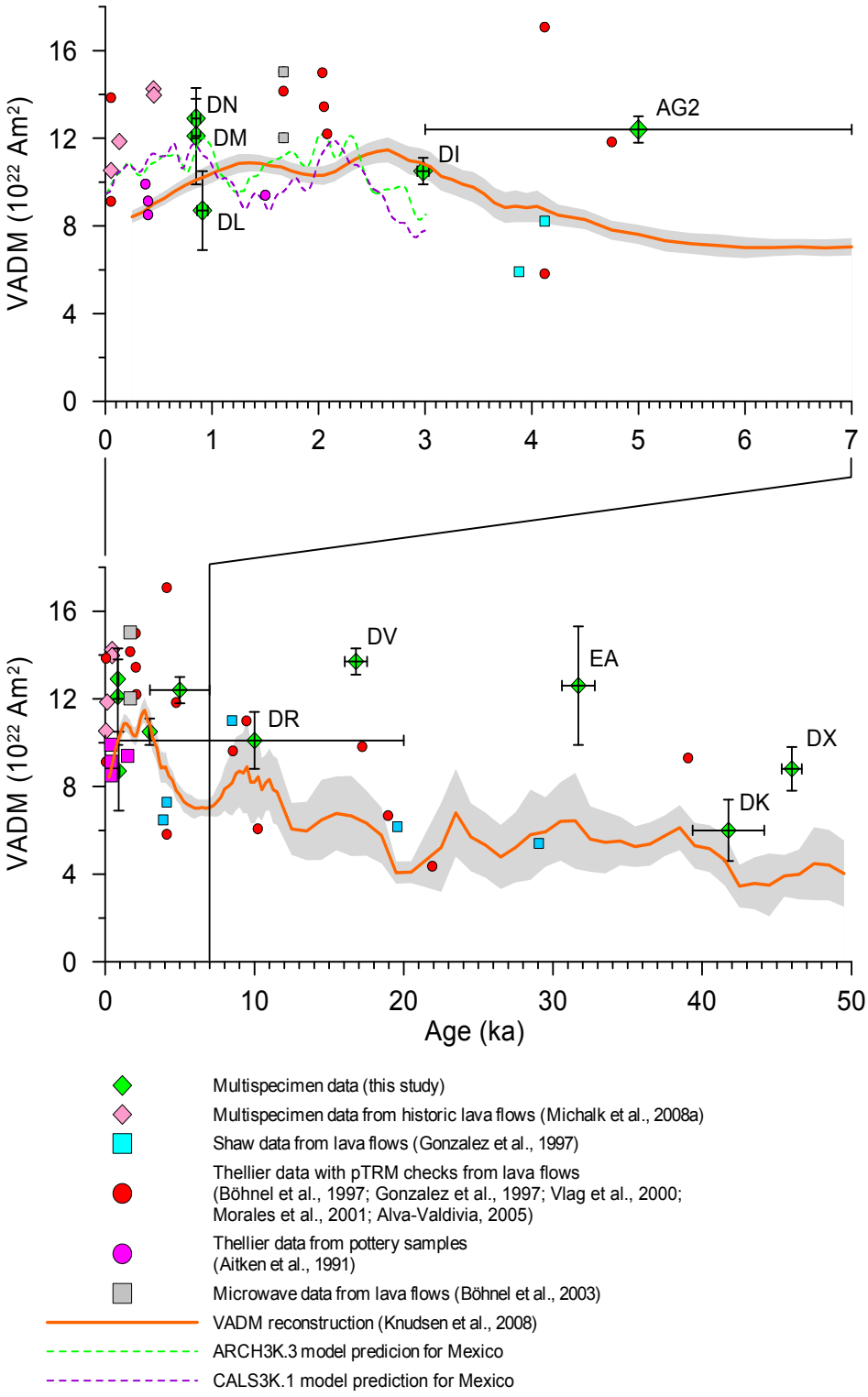

Figure 5.7. Comparison between multispecimen palaeointensity estimates from this study (green diamonds), the global dipole reconstruction of Knudsen et al. (2008) (orange line; uncertainties are shown in grey), two spherical harmonic field model predictions from Korte et al. (2008 submitted; dashed lines), and existing palaeointensity data from Mexico.

5.2 Palaeointensities from 7 to 50 ka

When extending the record further back in time to the last 50 ka, the VADM reconstruction of Knudsen et al. (2008) is less well constrained than for the Holocene. This is because the amount of available PI data is significantly reduced, while the geographical data distribution becomes increasingly biased and the associated age uncertainties increase. While these factors complicate a detailed analysis, some useful comparisons with our data can still be made. The most important trends that can be deduced from the VADM reconstruction is that the maximum Holocene dipole moment (~ 11.5 $\times 10^{22}$ Am^2) found around 2.5 ka was higher than at any point during the preceding ~ 38 ka where it fluctuated around 6×10^{22} Am^2. There are only four MS PI estimates (sites DV, EA, DK and DX) for this time period (site DR is poorly constrained to the period 0 to 20 ka, thus no meaningful comparison can be made) but this data does not follow the general trend towards lower field intensities. Figure 5.7 shows that three out of four MS PI estimates have significantly higher intensities than the VADM curve. Sites DV, EA, and DX yield estimates more than twice the mean values deduced from the VADM curve, while DK is only slightly higher. Concerning other PI data from Mexico from this time interval, six PI estimates are in good agreement, while four PI estimates are significantly higher than the VADM reconstruction.

Combining all the MS PI estimates from the period 0 to 50 ka (including the 4 PI estimates from historic lavas obtained by Michalk et al., 2008, but omitting the result from site DR due to its poorly defined age), we observe that 11 out of 13 (85%) are higher than the VADM curve of Knudsen et al. (2008). If there were to be equal probability of each estimate being higher or lower than this curve, the exact binomial probability of obtaining such a high ratio is ~ 1% (see e.g. http://faculty.vassar.edu/lowry/webtext.html). Consequently, we can say with high confidence that one or more external factors are causing the MS PI estimates to overestimate the intensities compared to the global VADM curve.

A similar offset is observed in the 0 to 50 ka lava Thellier data from lavas where 13 out of 16 measurements are higher than the VADM curve. The probability of obtaining this ratio or higher by chance is also ~1%.

5.3 Palaeointensities from 50 ka to 1 Ma

In order to compare MS PI estimates from the time interval 50 ka to 1 Ma with a global curve, VADMs and associated uncertainties were calculated for 100 ka time windows, using the approach of Knudsen et al. (2008) on the PI data from the PINT08 database (Fig. 5.8) (Biggin et al., 2008; http://www.geo.uu.nl/~forth/people/Andy/PINT08.htm). The calculation was restricted to Thellier data with pTRM checks (T+ data, n = 557), microwave data (n = 16), and LTD-DHT Shaw data (n = 25). For those estimates derived from more than one specimen, the quoted uncertainty was required to be less than 25% of the PI. Several problems were encountered in this reconstruction. First of all, age uncertainties are frequently large or absent altogether. Secondly, for some 100 ka bins, all available data stem from the same geographical location, which complicates the calculation of a reliable global VADM and also makes the uncertainties artificially small, i.e. it introduces a down bias in the uncertainties. Despite these problems, we believe that this reconstruction can be used for a rough comparison to the MS PI data. As a second guideline for comparison, we use the SINT 2000 global relative palaeointensity stack calibrated to absolute values (Valet et al., 2005). For calibration, Valet et al., (2005) used only PI data with reliability checks from the PINT03 database, which they grouped in time windows of 100 ka. The mean VADM from the period 0-800 ka ($7.46 \pm 1.16 \times 10^{22}$ Am^2) was used to calibrate the whole record to absolute values. We checked to see if new data added to the PINT database since the calibration of SINT2000 by Valet et al. (2005) made any difference to this calibration, but found it to be negligible.

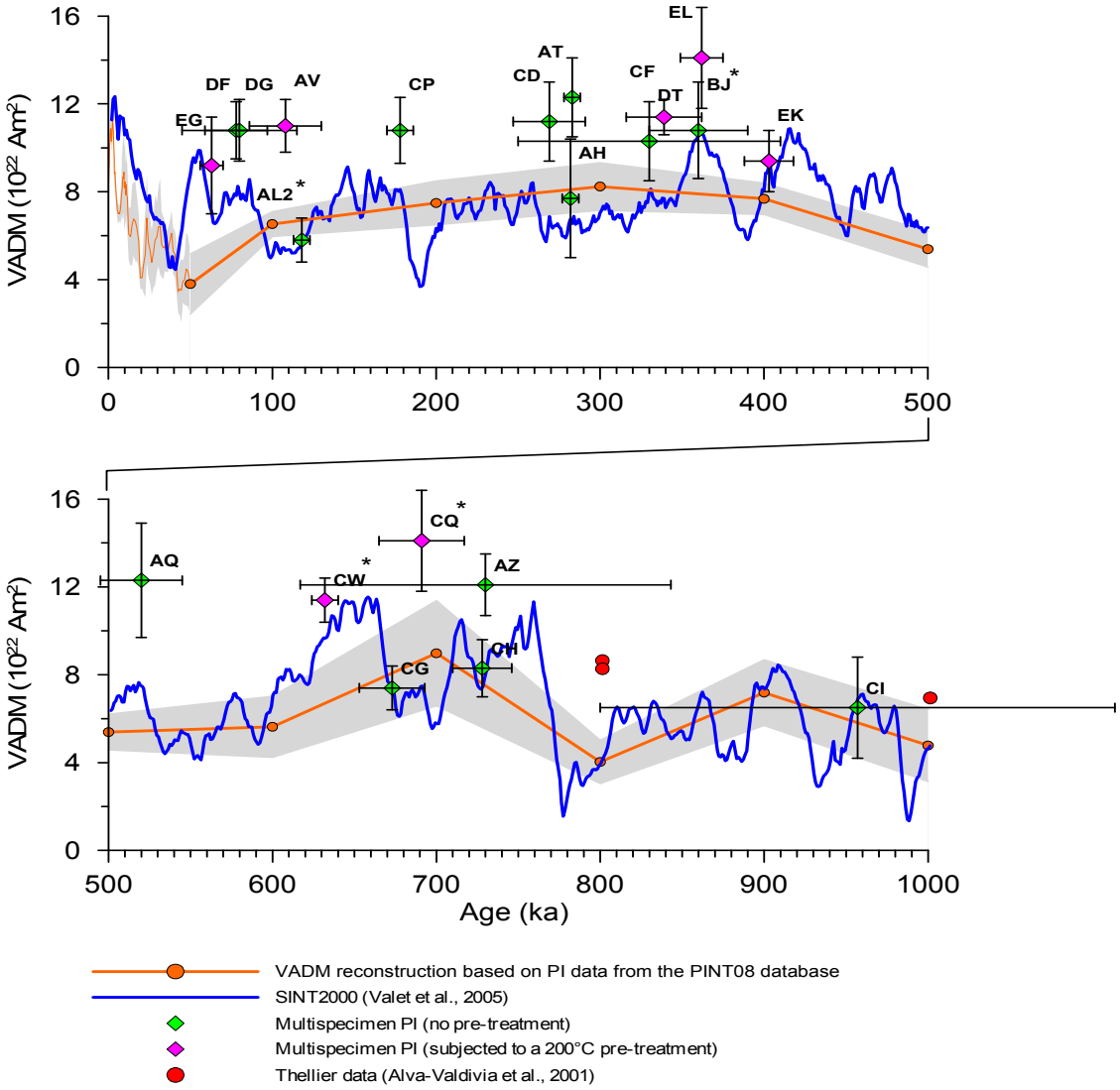

Figure 5.8. Multispecimen palaeointensity estimates from this study (diamonds) depicted against the SINT2000 record of Valet et al., (2005) calibrated to absolute values (blue curve), and to a reconstruction of the average global dipole moment (orange dots with grey error envelope) based on palaeointensity data from the PINT08 database. Green diamonds represent palaeointensity estimates based on samples that were subjected to one heating step and magenta diamonds represent palaeointensity estimates based on samples that were subjected to a thermal pre-treatment of 200°C. Sites which potentially contain (titano-) maghaemite (see text) are highlighted with asterisks. Red dots represent Thellier data from lava flows (Alva-Valdivia et al., 2001). Note that the result from site BL is not shown here as it has an associated age of ~3.5 Ma.

From the SINT2000 record (blue line), several long term features in the field behaviour can be recognised for the Brunhes Chron, such as prominent maxima in intensity at around 50, 350, 400, 650, 700 and 750 ka. Pronounced minima at around 40 and 190 ka can be ascribed to the Lachamp and Iceland Basin excursions, respectively.

In Figure 5.8 the PI estimates are depicted against both comparison records. Note that the average VADMs calculated using the approach of Knudsen et al. (2008) match the SINT2000 record reasonably well.

Of the 22 PI estimates with ages greater than 50 ka, only 4 (sites AH, CG, CH, and CI) fall within the error range of the global VADM reconstruction. Of the remaining sites, one PI estimate is lower than the global record and the other 17 are higher. Compared to the SINT2000 curve, 4 of those 17 PI estimates (sites EG, BJ, EK, and CW) show reasonable agreement. While in the case of sites DF, DG, DT, CF, and AZ the uncertainties in the ages and intensities might still allow them to be matched to SINT2000, this is not the case for seven other PI estimates (sites AV, CP, CD, AT, EL, AQ, and CQ), which display an obvious offset towards higher intensities. It is interesting to note that the PI estimates from sites DF and DG, statistically both of similar age (78 ± 19 and 80 ± 35 ka, respectively) returned the same PI (48 ± 3 μT). Site BL, dated at 3528 ± 64 ka, is the oldest lava flow studied and is not shown in Fig. 5.8. It returned a VADM estimate of 6.7 ± 0.9 × 10^{22} Am^2, which is also higher than the mean VADM of 4.9 ± 3.0 × 10^{22} Am^2 that was calculated from the 52 PIs with ages between 3400 and 3600 ka taken from the PINT08 database. Further PI data from Mexico include only three Thellier PI estimates (red dots) from two lava flows by Alva-Valdivia et al., (2001). Here, the two PIs obtained from one lava flow with an estimated age of 800 ± 100 ka, as well as the single estimate from a flow with an estimated age of 1000 ± 100 ka are slightly high relative to both of the global records. However, considering the large dating errors, this is not a very significant result.

In summary, MS PIs from the last 7 ka seem to be in reasonable agreement with the global VADM reconstruction of Knudsen et al. (2008) and field model calculations (ARCH3K.1 and CALS3K.3; Korte et al. submitted), and they are generally in better agreement with the global reconstructions than other PI data from Mexico. However, when extending the record further back to the last 50 ka and the last 1 Ma, most MS PI estimates appear too high. Unfortunately the paucity of available PI data, especially for Mexico, and the generally uneven geographical distribution of PI data complicate a more detailed comparison. A mean VADM of 10.6 ± 2.2 × $10^{22}Am^2$ calculated from all MS PIs with Brunhes Chron ages (n = 29) is in fact 30 % higher than the mean Brunhes VADM calculated from the global volcanic database, which is itself largely based on Thellier data. This value does not change when excluding the four sites, which could potentially contain additional (titano-) maghaemite (mean VADM = 10.6 ± 2.1 × $10^{22}Am^2$, n = 25). Since the majority of Thellier data from lavas in Mexico are also higher than global mean values, one could argue that the non-dipole (ND) field has a persistent influence on this region which is unaccounted for by the global field reconstructions. To test for possible ND effects that might bias our interpretation we compare the global dipole moment from Knudsen et al. (2008) with a similar reconstruction based on PI data from GEOMAGIA50 that derive from a region covering Mexico and a large part of the United States (λ = 0 to 50°N, ϕ = 210 to 300°E). In the regional VADM reconstruction (black diamonds), the interval covering the last 3 ka is the best defined (each bin contains between 5 and 46 PI data) and allows for a detailed comparison to the global VADM curve (Fig. 5.9). No systematic bias towards significantly higher or lower field intensities is observed and it consequently seems unlikely that ND effects are the cause of over-high PI values in the period 0-3 ka. It is of course impossible to assess the role of ND effects for earlier periods. However, we point out that in order to explain discrepancies going back to 1 Ma, the required ND effect must have been present over a period longer than the timescales at which normal secular variation operates. Such a persistent ND anomaly at this location cannot be discounted altogether at this stage but, before accepting it, we first turn to the alternative explanation: that the measurements of the PI are artificially biased towards higher values.

There is already considerable evidence suggesting that Thellier data from lavas overestimate the true PI (e.g. Calvo, et al., 2002; Biggin & Thomas, 2003; Yamamoto et al., 2003). The results from this study suggest that in some cases the MS method may introduce a similar kind of bias. A similar observation has recently been made by Böhnel et al. (submitted) who found that MS PI estimates on lava flows from the San Quintin volcanic field in Baja California (Mexico) were on average 28% higher than PI estimates obtained with the microwave method on sister samples from the same flows (although this value falls to 15% if three outlier results are excluded). Michalk et al. (2008) also found that multispecimen PI estimates were on average 12% higher than expected field values deduced from observatory data or field

models. In the following we discuss several factors that might control the tendency of both, the MS and the Thellier method, to overestimate the PI.

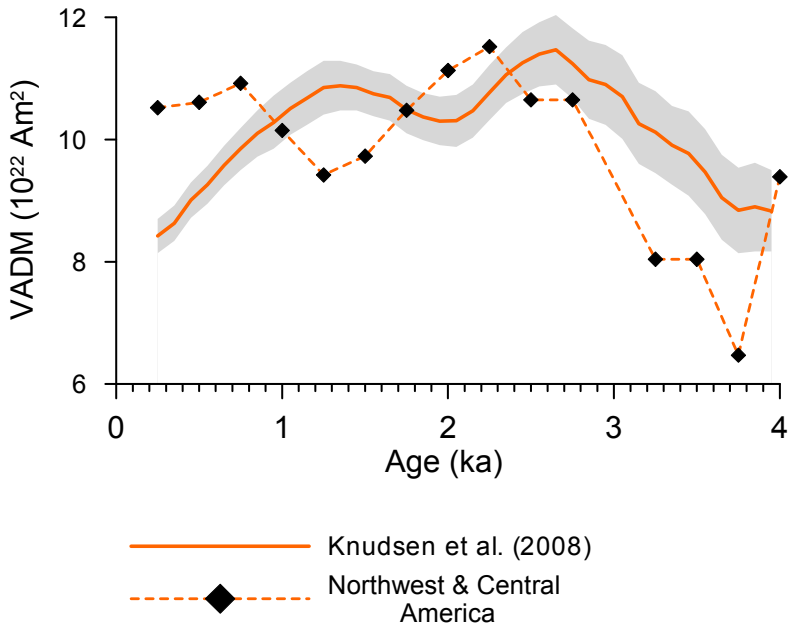

Figure 5.9. Virtual axial dipole moment reconstruction of Knudsen et al. (2008) compared to a regional dipole reconstruction based on palaeointensity data from a region around Mexico, including the U.S.A (black diamonds) (Lat. 0-50°N, Long. 210-300°W).

6 Potential factors causing PI overestimates

6.1 Cooling rate effects

The effects of differences in the cooling rates between the original remanence acquisition and the remanence acquired in the laboratory has been the subject of many previous theoretical and experimental studies (e.g. Pullaiah et al., 1975; Walton, 1980; Fox and Aitken, 1980; McClelland Brown, 1984; Selkin and Tauxe, 2000; Bowles et al., 2005; Leonhardt et al., 2006). Theoretical considerations predict that TRM intensity for SD grains is positively correlated with cooling time and overestimates the PI because the cooling time in the laboratory is significantly less (e.g. between 30 and 40 minutes in this study) than the natural cooling of a lava flow, which can take up to several months. This effect has been estimated to cause an increase in TRM of approximately 7% per order of magnitude increase in cooling time (Fox and Aitken, 1980). If this relationship is valid here, we might expect all the PIs (MS and Thellier) which are derived from lavas to be up to ~25% higher than PIs derived from fast-cooled archaeological materials. However, most subaerial lavas including those studied here, do not soley contain SD grains and this relationship may not be expected to hold for PSD grains or mixtures of SD and MD grains. Indeed, for MD grains, the relationship appears to be of the opposite sign (Perrin, 1998) so that longer cooling times produce lower TRM intensities leading to PI underestimates (Biggin et al., 2007). Furthermore, the SINT 2000 curve was calibrated using lava PI estimates and so, if such cooling rate effects were causing a significant bias, then this curve would also be influenced by it.

It could be argued that mini-samples are more prone to being biased by cooling rate effects on account of their higher ratio of surface area to volume. Aitken et al. (1991) obtained higher PIs on mini-samples with a volume of 1 cm^3, which is similar to the samples used in this study, than PIs obtained from standard

samples of 11 cm^3, and explained this discrepancy with a faster cooling of smaller samples. Similar observations were made by Donadini et al. (2008), who obtained higher PIs from baked clay samples of 0.5 to 2 cm^3 than on standard size samples. As stated above, we do not expect the PIs produced by the majority of subaerial lavas to be strongly affected by cooling rate effects, regardless of sample size. Moreover, there is some evidence from the comparison of PI results produced by microwave and conventional thermal experiments that sample size does not affect the measurement in the manner required here. The microwave approach uses samples with a higher surface area to volume ratio even than the mini-samples used in this study. The ferromagnetic particles within these very small samples do get hot but cool very quickly. If palaeointensity measurements were inversely proportional to sample size then we might expect microwave experiments to give higher results than thermal experiments performed on the same lava samples. In fact, the evidence from comparisons between microwave and Thellier PI results (e.g. Böhnel et al., 2003; Gratton et al., 2005; Biggin, 2008) strongly contradicts this. We therefore believe that cooling rate effects play, at most, a minor role for the observed bias of the MS estimates.

6.2 Sample heterogeneity, magnetomineralogical alteration and secondary overprints

In principle, all these three factors have the potential to bias the MS method but, as we will now show, it appears that none of them are likely candidates for causing the dominantly observed bias to high values. Sample heterogeneity (i.e. differences between the T_B spectra of samples from the same flow) will tend to produce more scatter in the palaeointensity plots (e.g. Fig. 5.6) and lower R^2 values of the linear regression. Figure 10a compares the R^2 values to VADMs from this study that have been normalised to the global VADM reconstructions. The comparison does not indicate any relationship between low R^2 values and biased PIs. Regarding undetected magnetomineralogical alteration as a biasing factor, samples used in the MS experiments were chosen according to their thermal stability (section 3), which was accounted for by thermomagnetic experiments and measurements of room-temperature susceptibility made after thermal demagnetisation experiments. In all samples, the temperature for the MS remagnetisation step was chosen well below any temperature at which alteration became evident. The five sites which displayed irreversible M_ST behaviour (indicated by stars in Figure 5.10) do not show a tendency to give higher PIs than the rest. In fact most of the biased PIs derive from lavas with reversible M_ST curves (shown as dots).

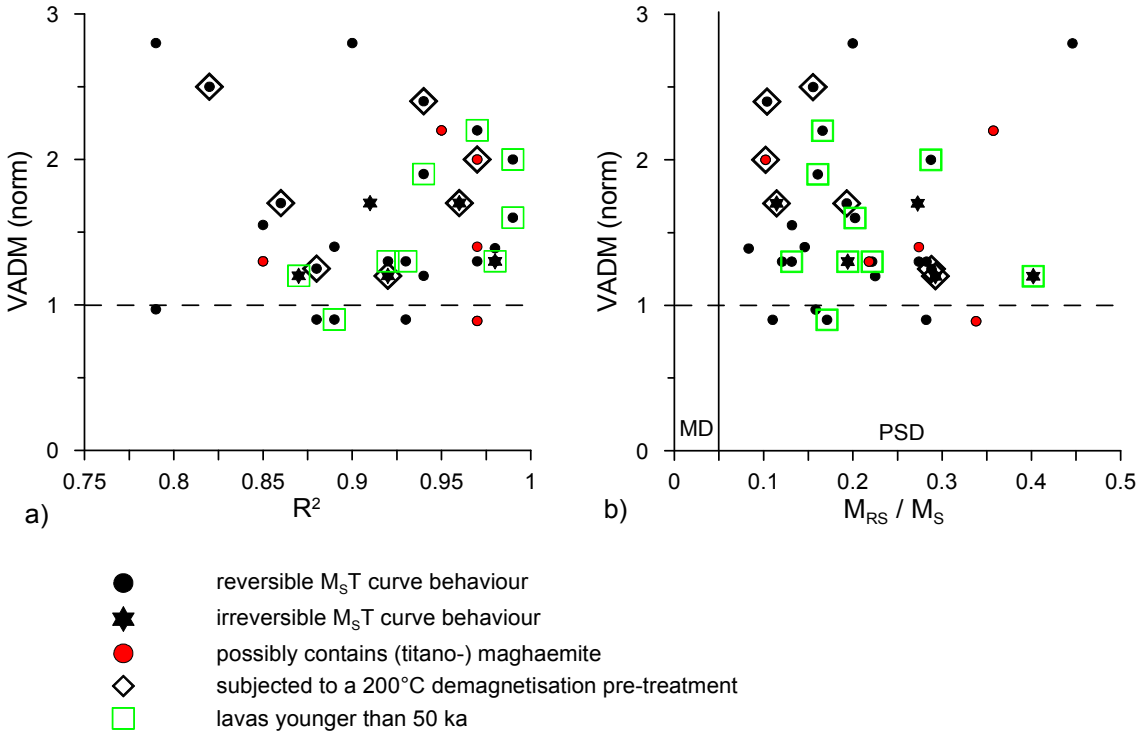

Figure 5.10. Virtual axial dipole moment values of lavas investigated in this study normalised to global values as deduced from dipole reconstructions versus a) the correlation coefficient (R^2) of the linear regression from the multispecimen experiments; b) the bulk magnetic domain state as approximated by the ration M_{RS} / M_S. The data is grouped according to: thermomagnetic behaviour (black dots and stars; reversible and non-reversible behaviour, respectively); samples which received a demagnetisation pre-treatment (diamonds); highly oxidised lavas, which probably contain additional (titano-) maghaemite (red dots) and data from lavas younger than 50 ka (green squares).

Magnetomineralogical alteration in nature due to low temperature oxidation (maghaemitisation) was only evident in five lavas (indicated by red dots) but these were not found to give results which were anomalous with respect to the rest. We also point out that undetected magnetomineralogical alteration in an MS experiment is at least as likely to cause underestimates as overestimates. Thermally-induced alteration frequently increases the capacity of a sample to acquire pTRM and this would ultimately result in a lower PI. However, from the data shown in figure 10, this is quite an unlikely scenario for the present data set. We therefore do not consider alteration as a likely candidate for causing overestimation of the PI. Although one criterion in the selection of samples for the MS experiments in this study was that the MAD value of the full component of the sister samples was < 5°, small unremoved secondary components may have been present in some samples (e.g. Fig. 5.6c). While we cannot rule out such overprints having a small effect on our measurements, it seems highly unlikely that they can cause a persistent overestimation of the PI that we have inferred from our results. The main reason for this conclusion is that unremoved overprints are likely to be VRMs which are not perfectly parallel to the primary TRM of the sample and which therefore reduce its net moment (unless they were acquired in a much stronger field). These would tend to underestimate, rather than overestimate, the PI measured in an MS experiment.

6 .3 Multidomain Grains

In a previous study, Michalk et al. (2008) observed an overestimate of the PI, which increased with grain size from SD to large PSD particles as estimated from hysteresis measurements. Figure 10b shows the PIs versus the bulk magnetic domain state as approximated by the M_{RS} / M_S ratio. Although a meaningful comparison can only be made for the 9 lavas younger than 50 ka (indicated by green squares), this study does not show any systematic relationship between the observed PIs and domain state.

The hysteresis analyses described in section 4.2 indicated that very few of the samples measured here contained pure MD assemblages. Nonetheless, there is plenty of evidence (e.g. Shcherbakova et al., 2000; Biggin and Thomas, 2003) showing that samples with relatively fine-grained hysteresis properties may display MD-like pTRM behaviour which can lead to overestimation of the PI. Could this behaviour be responsible for the inferred overestimation of both the Thellier and MS measurements based on Mexican lavas?

A large proportion of PI studies focusing on historic lava flows have observed overestimates that have been ascribed to the effect of MD grains in Thellier (Calvo et al., 2002; Carlut and Kent, 2002; Chauvin et al., 2005; Biggin et al., 2007) and MS (Michalk et al., 2008) experiments. The process through which MD grains may bias Thellier PI experiments is complex but has been studied in some depth (Levi, 1977; Fabian, 2001; Shcherbakov and Shcherbakova, 2001; Leonhardt et al., 2004; Yu et al., 2004; Biggin, 2006). The frequency of this form of biasing has largely been a matter of conjecture, but a very recent meta-study of microwave and thermal Thellier data concluded that it may be extremely common in studies of igneous rocks (Biggin, 2008). Furthermore, it can only be ruled out when either the *f* (fraction) parameter is close to its maximum value of unity or when pTRM tail checks are carefully employed and positive. The majority of the Mexican Thellier lava data (references given in Figure 5.7) do not meet

these criteria and indeed, the result from the Xitle 1670 BP lava (Böhnel et al., 1997) was explicitly judged to be biased to high PI values by MD grains (Böhnel et al., 2003). Consequently, we might expect that the Mexican Thellier PI data from lavas tend to be higher than expected at least partly because of bias from MD grains.

At least some of the bias observed for MS PI measurements may also be readily explained by MD (or PSD) grains. Although the MS method (using no pre-treatment) was originally claimed to produce reliable PI measurements independent of the domain state of the remanence carriers, this is only true as long as there is no significant asymmetry in the pTRM demagnetisation and remagnetisation process in those carriers, i.e. as long as the first-order symmetry laws outlined by Biggin & Poidras (2006) are valid. Violation of these laws is far from universal; both Biggin & Poidras (2006) and Dekkers & Böhnel (2006) found very little evidence for it in the samples they studied. However, McClelland et al. (1996) and Fabian & Leonhardt (2007) observed in their experiments that simply heating and cooling samples to temperatures below T_C while applying a magnetic field (the same process as is done in MS experiments) can cause partial demagnetisation. Interestingly, Fabian & Leonhardt (2007) observed that this process was even more severe in those samples they judged to contain PSD grains than in those with MD-like properties. If a sample demagnetises slightly during infield thermal cycling, then a field higher than that originally used to impart the full TRM is required to maintain the sample's magnetisation at its original level. This will produce an overestimate of the PI in an MS experiment.

This process may well explain why those samples which were not given any pre-treatment in this study apparently produced overestimates. However, it is likely only part of the explanation for the overestimates observed in the present study.

6.4 The effect of a demagnetisation pre-treatment

Most protocols of the Thellier method (e.g. Thellier and Thellier, 1959; Coe, 1967; Aitken et al., 1988) involve at least two heating treatments at each temperature step. When samples which do not contain uniquely non-interacting single domain grains are studied using such *double-heating* techniques then it appears inevitable that their results will be affected by at least some non-ideal behaviour (Fabian, 2001; Biggin, 2006). Other methods of palaeointensity measurements such as the MS and the perpendicular Thellier method may be termed *single-heating* methods on account of them only requiring the sample to be heated once at each of the one or more temperature steps employed. In this case, models of MD TRM predict that such nonideal behaviour is avoided, regardless of the domain state of the remanence carriers, providing that the first order symmetry laws outlined in Biggin & Poidras (2006) are not violated (see section 6.3).

Single-heating methods can only be carried out in their pure form when the studied samples contain only a single component of remanence. In cases where the remanence is partially overprinted, some form of baseline demagnetisation treatment must be applied to isolate the characteristic component. If the overprint is small, this can take the form of a small AF treatment (e.g. 5mT) which has been shown to have negligible effect (Biggin et al., 2007). However, if the overprint is larger then a thermal treatment may, as in this study, be required. The thermal demagnetisation treatment used in this study was to a peak temperature of 200°C and was applied immediately after the remagnetisation treatment as well as before it. Therefore, in this study the routine applied when a pre-treatment was used included at first a demagnetisation between 200°C and room temperature (T_R); secondly, a remagnetisation between $T >$ 200°C and T_R; and thirdly, a second demagnetisation between 200°C and T_R.

Employing demagnetisation treatments in conjunction with the MS method implies that it is no longer a strictly single-heating protocol and that nonideal MD effects have the potential to affect the results. We applied the numerical kinematic model of MD TRM used by Biggin (2006) to investigate this potential

problem. Figure 5.11 shows the results of this analysis and indicates that the addition of a baseline demagnetisation has the potential to affect the measured palaeointensity significantly. Specifically, if the temperature of the remagnetisation is only a small amount higher than the temperature of the demagnetisation (so that the slope of the line on the resulting plot is low) then the potential for significant overestimate appears to exist. It is interesting to note that this biasing effect does not in large part result from the overprint itself or the tail of this overprint that remains after the demagnetisation treatment. To demonstrate this, the results of identical sets of simulated experiments are shown in panels (a) and (c) of figure 5.11. In the first of these, the samples were assumed to be partially overprinted as shown in panel (b) and this was mostly removed by the baseline demagnetisation treatment. In the second, no overprint was simulated and the overestimate of the palaeointensity is actually made worse as a consequence. This is because the overestimation is caused, not by the overprint or its tail, but by the different magnetic states the samples adopt through the course of the three thermal treatments. The two identical thermal demagnetisation treatments are not identically effective on account of the different magnetic history the samples have experienced prior to each.

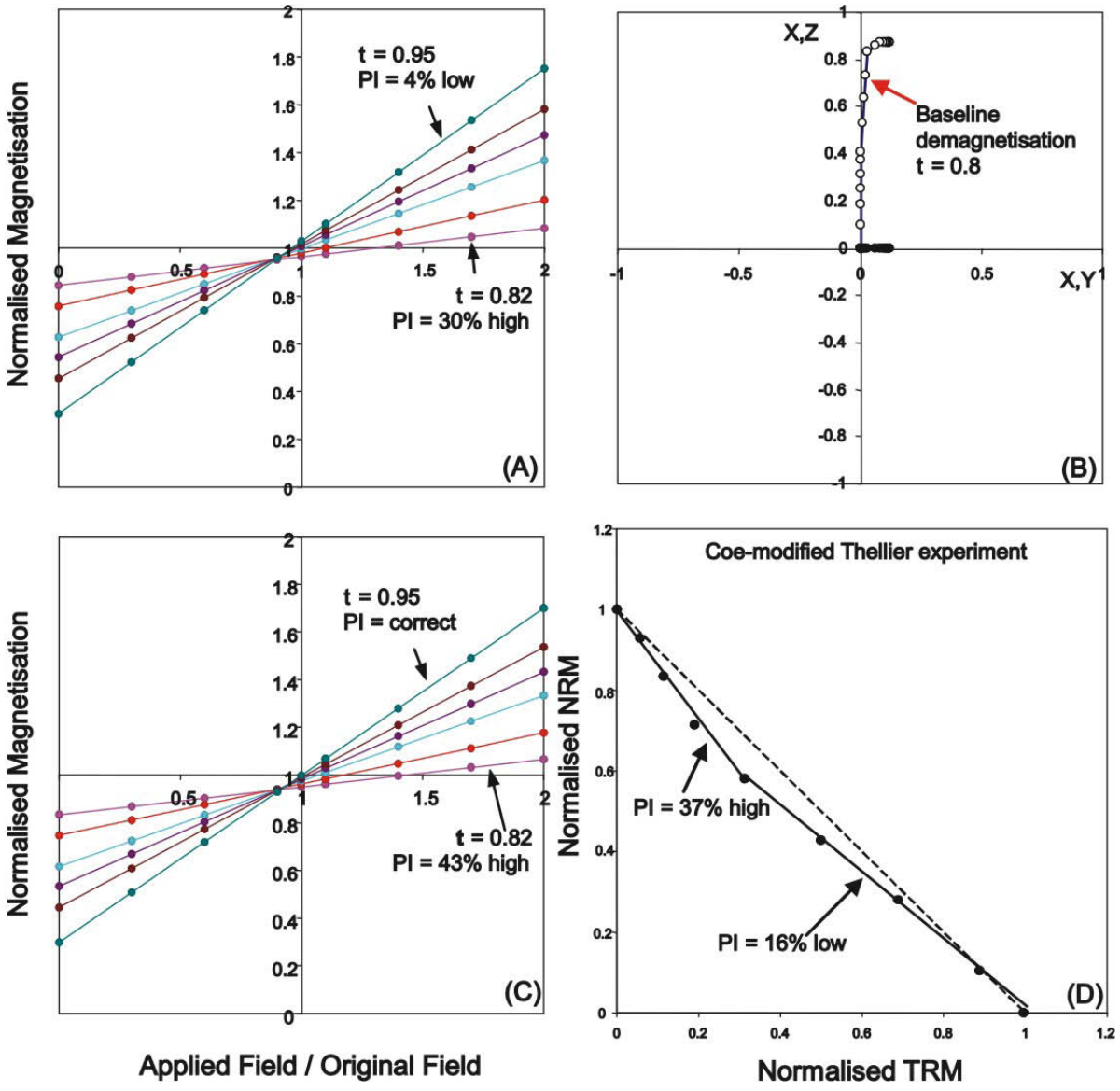

The prediction that the addition of baseline demagnetisation treatments to an MS experiment introduces non-ideal behaviour for samples containing 'multidomain' grains requires empirical verification. However, we point out that, insofar as it exists in theory, this behaviour is unlikely to be model-dependent: any similar kinematic (e.g. Shcherbakov et al., 1993) or statistical (e.g. Fabian, 2003) theory of TRM which incorporates a temperature dependent domain structure is likely to give the same qualitative result. That said, the illustrative simulated results shown in figure 11 should certainly not be quantitatively compared to any specific experimental results. The kinematic model predicts that the scale of any bias is highly sensitive to factors such as the unblocking temperature spectra of the samples, the size and direction of the overprint, and the extent to which the samples violate simple SD TRM behaviour.

There is some evidence suggesting that the addition of demagnetisation treatments may be biasing the results of the present study to high values: 5 of the 15 determinations (33%) using the MS method without pre-treatment yielded results within (or below) the VADM uncertainty envelope shown in Figure 8. By contrast, all 7 of the MS determinations using a pre-treatment were above this level. Unfortunately, the small size of these datasets prevents us from being certain if the demagnetisation treatments are indeed biasing the palaeointensity measurements in this study.

We attempted to use the kinematic model to provide approximations for the degree to which individual sites might be affected by this bias. Unfortunately, this was unsuccessful due to the very high sensitivity of the bias to the parameters mentioned earlier.

Figure 5.11. Predictions of a kinematic model of MD TRM (Biggin, 2006) with SD/MD = 2 for various palaeointensity experiments. (a) MS experiments performed with baseline demagnetisation (= 0.8). Coloured lines reflect experiments performed with different peak temperatures for the remagnetisation treatment (0.95 ≥ ≥ 0.82). (b) Zijderveld plot showing component structure of the samples simulated in the experiments shown in (a), prior to the palaeointensity experiments starting, a perpendicular partial overprint (= 0.75) was simulated for all samples. The red arrow indicates the temperature of the baseline demagnetisation. The component remaining after this demagnetisation was deflected less than 2° from the primary TRM direction and had a MAD value of 1°. (c) The same simulated experiments as shown in (a) but performed on samples with univectorial remanence structure to illustrate that it is not the tail of the overprint that is responsible for the overestimation of the palaeointensity. (d) For reference, the results of a Thellier experiment (lab-field = ancient field) simulated on the same samples as (a) and (c) with univectorial remanence.

7. Conclusions

Fifty-one lava flows were studied using the multispecimen parallel differential pTRM method from which thirty-two flows returned new palaeointensity estimates. The results were compared to reconstructions of the global dipole moment which revealed that, with a high degree of statistical significance, PI estimates tended to be significantly, by about 30% on average, higher than expected.

Published palaeointensity results produced by using the Thellier method on samples from Mexican lavas were also observed to be high with respect to the global records, although the paucity of such data older than 50 ka obscures the significance of this observation. This observation could be taken to indicate that persistent non-dipole geomagnetic features are responsible for the higher than expected results obtained here. However, while we cannot discount this possibility, we think that the balance of evidence rather points to an artificial biasing of all the measurements to high values.

The MS method, unlike the Thellier method, has been shown both theoretically and to some degree, experimentally to produce accurate results from samples with strongly MD-like properties. Nonetheless, it has also been shown in previous studies on historic lava flows and on synthetic samples that domain state effects can lead to PIs that are overestimated by up to 30%. The cause of this overestimate is related to an asymmetry in the pTRM demagnetisation and remagnetisation process, i.e. to effective demagnetisation during thermal cycling in an applied laboratory field. A previous study by Fabian and Leohardt (2007) has suggested that this asymmetry is more important for grains of pseudo-single domain size. Since hysteresis data from this study suggests PSD grains are present in most of the investigated rocks, their observation may explain some of the high PI values.

In addition, the PIs of seven lava flows subjected to a preceding demagnetisation step of 200°C may potentially be further biased towards high intensities. We have used theoretical arguments to show that, independent of the violation of pTRM symmetry constraints, samples with non-SD magnetic properties might be expected to produce an overestimate when such a pre-treatment is used.

Most geological material carries some secondary magnetic overprint, which must be removed for any PI method to be successful. The bias caused by demagnetisation pre-treatments therefore represents a major challenge that must be carefully evaluated in future studies if the MS method is to be successfully applied to older rocks in the future. We believe that the most promising means to overcome this problem in the future may be to omit any pre-treatment and instead to perform the measurements of the sample moment at a temperature which is higher than the blocking temperature of any overprint. This should overcome the bias associated with the pre-treatment, while simultaneously speeding up the experiment. However, it would obviously also require the use of rather specialist equipment (e.g. Le Goff and Gallet, 2004) that allows the moment of a sample to be measured as it is heated.

Acknowledgements

We would like to thank D. Berger, G. Arnold and M. Köhler (GFZ) for their help in the sample preparation, Michael Winklhofer (LMU) for providing the FORCobello computer program, J-P. Valet (IPGP) for providing the SINT2000 record, Angel Ramírez (UNAM) for TL data, and Monika Korte (GFZ) for providing magnetic field model data. Much appreciated assistance during fieldwork came from I. Barajas and G. Gonzalez (Centro de Geociencias, Queretaro). Peter Schaaf (UNAM) and Gerardo Carrasco Núñez (Centro de Geociencias, Queretaro) are thanked for providing us unpublished age data. This research was funded by DFG grants Ne154/45-1, No334/1-2 and No334/5-1 and Conacyt grant 46213.

References

Aguirre-Díaz, G.J. (1996), Volcanic stratigraphy of the Amealco caldera and vicinity, Central Mexican Volcanic Belt, Revista Mexicana de Ciencias Geológicas, 13, 10-51.

Aguirre-Díaz, G.J., L. Ferrari, S.A. Nelson, G. Carrasco-Núñez, M. López-Martínez, and J. Urrutia-Fucugauchi (1998), El Cinturón Volcánico Mexicano: Un Nuevo Proyecto Multidisciplinario, Unión Geofísica Mexicana, Geos, 18 (2), 131-138.

Aguirre-Díaz, G. J., M.C. Jaimes-Viera, and J. Nieto-Obregón (2006), The Valle de Bravo Volcanic Field. Geology and geomorphometric parameters of a Quaternary monogenic field at the front of the Mexican Volcanic Belt, in Neogene-Quaternary continental margin volcanism: A perspective from Mexico, edited by Siebe, C., J.L. Macías, and G.J. Aguirre- Díaz, Geological Society of America Special Paper No. 402, 125-140.

Aitken, M. J., A. L. Allsop, G. D. Bussel, and M. B. Winter (1988), Determination of the intensity of the Earth's magnetic field during archeological times: Reliability of the Thellier technique, Rev. Geophys., 26, 3-12.

Aitken, M.J., L.J. Pesonen, and M. Leino (1991), The Thellier palaeointensity technique: minisamples versus standard size, J. Geomag. Geoelectr., 43, 325-331.

Alva-Valdivia, L. M., A. Goguitchaichvili,, and J. Urrutia-Fuccugauchi, (2001), Further constraints for the Plio-Pleistocene geomagnetic field strength: New results from the Los Tuxtlas volcanic field (Mexico), Earth Planets Space, 53, 873-881.

Biggin, A.J., H.N. Böhnel, and F.R. Zúniga (2003), How many palaeointensity determinations are required from a single lava flow to constitute a reliable average?, Geophys. Res. Lett., 30 (11), doi:10.1029/2003GL017146.

Biggin, A.J., and D.N. Thomas (2003), The application of acceptance criteria to results of Thellier palaeointensity experiments performed on samples with pseudo-single-domain-like characteristics, Phys. Earth Planet. Inter., 138 (3-4), 279-287.

Biggin, A.J., and T. Poidras (2006), First-order symmetry of weak-field partial thermoremanence in multi-domain ferromagnetic grains. 1. Experimental evidence and physical implications. Earth Planet. Sci. Lett., 245(1-2), 438-453.

Biggin, A.J. (2006), First-order symmetry of weak-field partial thermoremanence in multi-domain (MD) ferromagnetic grains: 2. Implications for Thellier-type palaeointensity determination, Earth Planet. Sci. Lett., 245(1-2), 454-470.

Biggin, A.J., M. Perrin, and M. J. Dekkers (2007), A reliable absolute palaeointensity determination obtained from a non-ideal recorder, Earth Planet. Sci. Lett., 257(3-4), 545-563.

Biggin, A.J., and M. Perrin (2007), The behaviour and detection of partial thermoremanent magnetisation (PTRM) tails in Thellier palaeointensity experiments, Earth Planets Space, 59(7), 717-725.

Biggin, A.J., M. Perrin, and J. Shaw (2007), A comparison of a quasi-perpendicular method of absolute palaeointensity determination with other thermal and microwave techniques, Earth Planet. Sci. Lett., 257(3-4), 564-581.

Biggin, A.J. (2008), Why do microwave and thermal palaeointensity experiments give systematically different results? Phys. Earth Planet. Inter., (submitted).

Biswas, D.K., M. Hyodo, Y. Taniguchi, M. Kaneko, S. Katoh, H. Sato, Y. Kinugasa, and K. Mizuno (1999), Magnetostratigraphy of Plio-Pleistocene sediments in a 1700-m core from Osaka Bay, southwestern Japan and short geomagnetic events in the middle Matuyama and early Brunhes chrons, Palaeogeography, Palaeoclimatology, Palaeoecology, 148, 233-248.

Blatter, D.L., I.S.E. Carmichael, A.L. Deino, and P.R. Renne (2001), Neogene volcanism at the from of the central Mexican volcanic belt: Basaltic andesites to dacites, with contemporaneous shoshonites and high-TiO2 lava, GSA Bulletin, 113 (10), 1324-1342.

Bloemendal, J., J.W. King, F.R. Hall, and S.J. Doh (1992), Rock magnetism of late Neogene and Pleistocene deep-sea sediments: relationship to sediment source, diagenetic processes, and sediment lithology, J. Geophys. Res., 97, 4361-4375.

Bonhommet, N. and J. Babkine (1967), Sur la présence d'aimantations inversées dans la Chaîne des Puys, C. R. Acad. Sc. Paris, 264, 92-94.

Borradaile, G.J., B.S. Almqvist, and K. Lucas (2006), Specimen size and improved precision with the Molspin magnetometer, Earth Planet. Sci. Lett., 241, 381-386.

Bowles J., J.S. Gee, D.V. Kent, E. Bergmanis, and J. Sinton (2005), Cooling rate effects on paleointensity estimates in submarine basaltic glass and implications for dating young flows, Geochem. Geophys. Geosys., 6, Q07002, doi:10.1029/2004GC000900.

Böhnel, H., and J.F.W. Negendank (1981), Preliminary results of palaeomagnetic measurements of Tertiary and Quaternary igneous rocks from the eastern part of the Trans Mexican volcanic belt, Geofis. Int., 20, 235–248.

Böhnel, H., J. Morales, C, Caballero, L. Alva, G. McIntosh, S. González, and G. Sherwood (1997), Variation of rock magnetic parameters and paleointensities over a single Holocene lava flow, J. Geomagn. Geoelectr., 49(4), 523-542.

Böhnel, H. and E. Schnepp (1999), Precision of the paleomagnetic method: An example from the Quaternary Eifel volcanics (Germany), Earth Planets Space, 51, 403-412.

Böhnel, H., and R. Molina-Garza (2002), Secular variation in Mexico during the last 40,000 years, Phys. Earth Planet. Int., 133, 99-109.

Böhnel, H., A.J. Biggin, D. Walton, J. Shaw, and J.A. Share (2003), Microwave palaeointensities from a recent Mexican lava flow, baked sediments and reheated pottery, Earth Planet. Sci. Lett., 214(1-2), 221-236.

Böhnel, H.N., M.J. Dekkers, L.A. Delgado-Argote, and M.N. Gratton (2008), A comparison between the microwave and multispecimen parallel differential pTRM palaeointensity methods, Geophys J. Int. (accepted manuscript).

Brunhes, B. (1906), Recherches sur le direction d'aimantation des roches volcaniques, J. Phys., 5, 705-724.

Calvo, M., M. Prevot, M. Perrin and J. Riisager (2002), Investigating the reasons for the failure of palaeointensity experiments: A study on historical lava flows from Mt. Etna (Italy), Geophys. J. Int., 149, 44-63.

Cande, S.C., and D.V. Kent (1992), A new geomagnetic polarity time scale for the late Cretaceous and Cenozoic, J. Geophys. Res., 97, 13,917-951.

Cande, S.C., and D.V. Kent (1995), Revised calibration of the geomagnetic polarity timescale for the late Cretaceous and Cenozoic, J. Geophys. Res., 100, 6093-6095.

Cantagrel, J., and C. Robin, C. (1979), K-Ar dating on eastern Mexican vol canic rocks-Relations between the andesitic and the alkaline provinces, Journal of Volcanology and Geothermal Research, 5, 99-114, doi: 10.1016/0377-0273(79)90035-0.

Casas, L., J. Shaw, M. Gich, and J.A. Share (2005), High-quality microwave archaeointensity determinations from an early 18th century AD English brick kiln, Geophys. J. Int., 161 (3), 653-661.

Carcaillet, J.T., D.L. Bourles, and N. Touveny (2004), Geomagnetic dipole moment and ^{10}Be production rate intercalibration from autigenic ^{10}Be / ^{9}Be for the last 1.3 Ma. Geochem. Geophys. Geosyst., 5, Q05006, doi:10.1029/2003GC000641.

Carlut, J. and D.V. Kent (2002), Grain-size-dependent paleointensity results from very recent mid-oceanic ridge basalts, J. Geophys. Res., 107(B3): 10.1029/2001JB000439.

Carrasco-Núñez, G., M. Ort, and C. Romero (2007) Evolution and hydrological conditions of a maar volcano (Atexcac crater, Eastern Mexico), Journal of Volcanology and Geothermal Research, 159, 179-197.

Carrasco-Núñez, G., L. Siebert, R. Díaz, and L. Vázquez (2009),. Evolution and edifice stability conditions of a compound shield-line volcano: Cofre de Perote, Journal of Volcanology and Geothermal Research, submitted.

Carvallo, C., and A. Muxworthy (2006), Low-temperature first-order reversal curve (FORC) diagrams for synthetic and natural samples., Geochem. Geophys. Geosyst., 7, Q09003, doi:10.1029/2006GC001299.

Carvallo, C., A.P. Roberts, R. Leonhardt, C. Laj, C. Kissel, M. Perrin, and P. Camps (2006), Increasing the efficiency of paleointensity analyses by selection of samples using first-order reversal curve diagrams, J. Geophys. Res., 111, B12103, doi:10.1029/2005JB004126.

Ceja, M.R., A. Goguitchaichvili M. Calvo-Rathert, J. Morales-Contreras, L. Alva-Valdivia, J.R. Elguera, J. Urrutia-Fucugauchi, and H.D. Granados (2006), Paleomagnetism of the Pleistocene Tequila volcanic field (Western Mexico), Earth Planets Space, 58, 1349-1358.

Champion, D.E., M.A. Lanphere, and M.A. Kuntz (1988), Evidence for a new geomagnetic reversal from lava flows in Idaho: discussion of short polarity reversals in the Brunhes and late Matuyama Polarity Chrons, J. Geophys. Res., 93, 11,667-680.

Channell, J.E.T. (1999), Geomagnetic palaeointensity and directional secular variation at Ocean Drilling Program (ODP) Site 984 (Bjorn Drift) since 500 ka: Comparison with ODP Site 983 (Gardar Drift), J. Geophys. Res., 104, 22,937-951.

Channell, J.E.T., A. Mazaud, P. Sullivan, S. Turner, and M.E. Raymo (2002), Geomagnetic excursions and paleointensities in the Matuyama Chron at Ocean Drilling Program sites 983 and 984 (Iceland Basin), J. Geophys. Res., 107, No. B6, 10,1029/2001JB000491,2002.

Channell, J.E.T, J.H. Curtis, and B.P. Flower (2004), The Matuyama-Brunhes boundary interval (500-900 ka) in North Atlantic drift sediments, Geophys. J. Int., 158, 489-505.

Channell, J. E. T. (2006), Late Brunhes polarity excursions (Mono Lake, Laschamp, Iceland Basin and Pringle Falls) recorded at ODP Site 919 (Irminger Basin). Earth Planet. Sci. Lett., 244, 378-393.

Chauvin, A., P. Roperch, and R.A. Duncan (1990), Records of geomagnetic reversals from volcanic islands of French Polynesia, 2, Paleomagnetic study of a flow sequence (1.2 to 0.6 Ma) from the Island of Tahiti and discussion of reversal models, J. Geophys. Res., 95, 2727–2752.

Chauvin, A., P. Roperch, and S. Levi (2005), Reliability of geomagnetic paleointensity data: The effects of the NRM fraction and concave-up behavior on paleointensity determinations by the Thellier method. Phys. Earth Planet. Inter., 150(4), 265-286.

Christl, M., C. Strobl, and A. Mangini (2003), Beryllium-10 in deep-sea sediments: a tracer for the Earth's magnetic field intensity during the last 200,000 years, Quatern. Sci. Rev., 22 (5-7), 725-739.

Christl, M., A. Mangini, and P.W. Kubik (2007), Highly resolved Beryllium-10 record from ODP Site1089-A global signal? Earth Planet. Sci. Lett., 257, 245-258.

Clement, B.M., and D.V. Kent (1987), Short polarity intervals within the Matuyama: transitional field records from hydraulic piston cored sediments from the North Atlantic, Earth Planet. Sci. Lett., 81, 253-264.

Clement, B.M. (2004), Dependence of duration of geomagnetic polarity reversals on site latitude, Nature, 428, 637-640.

Coe, R.S. (1967), Paleointensities of the Earth's magnetic field determined from Tertiary and Quaternary rocks.,J. Geophys. Res., 72, 3,247-3,262.

Coe, R.S., S. Grommé, and E.A. Mankinen (1978), Geomagnetic paleointensities from radiocarbon-dated lava flows on Hawaii and the question of the Pacific nondipole low, J. Geophys. Res., 83, 1740-1756.

Coe, R. S., V. Hsu, and F. Theyer (1985), Matuyama-Brunhes record from Maui: Transitional directions, Eos Trans. AGU, 66, 872.

Coe, R. S., M.S. Pringle, and B.S. Singer (1995), Haleakala transition zone may be a concatenation. Eos Trans. AGU, 76(46), Fall Meet. Suppl., Abstract F176.

Coe, R.S., B.S. Singer, M.S. Pringle, and X. Zhao (2004), Matuyama-Brunhes reversal and Kamikatsura event on Maui: Palaeomagnetic directions, $^{40}Ar/^{39}Ar$ ages and implications. Earth Planet. Sci. Lett., 222, 667-684.

Collinson, D.W. (1983), Methods in Rock Magnetism and Palaeomagnetism, 503 pp, Chapman and Hall, London.

Constable, C.G., and C.L. Johnson (1999), Anisotropic paleosecular variation models: Implications for geomagnetic field observables, Phys. Earth Planet. Inter., 115, 35-51.

Conte, G., J. Urrutia-Fucugauchi, A. Goguitchaichvili, and J. Morales (2006), Low-latitude paleosecular variation and the time-averaged field during the late Pliocene and Quaternary-Paleomagnetic study of the Michoacan-Guanajuato volcanic field, Central Mexico, Earth Planets Space, 58, 1359-1371.

Cottrell, R.D., and J.A. Tarduno (1999), Geomagnetic paleointensity derived from single plagioclase crystals, Earth. Planet. Sci. Lett., 16 (1-2), 1-5.

Courtillot, V., Y. Gallet, J.-L. Le Mouel, F. Fluteau, and A. Genevey, (2007), Are there connections between the Earth's magnetic field and climate?, Earth Planet. Sci. Lett., 253, 328-339.

Cox, A. (1969), Confidence limits for the precision parameter κ, Geophys. J. R. astr. Soc., 18, 545-549.

Cox, A., J. Hillhouse, and M. Fuller (1975), Paleomagnetic records of polarity transitions, excursions, and secular variation, Rev. Geophys. Space Phys., 13, 185-190.

Creer, K.M., P.W. Readman, and A.M. Jacobs (1980), Palaeomagnetic and palaeontological dating of a section at Gioia Tauro, Italy: identification of the Blake event., Earth Planet. Sci. Lett., 50, 289-300.

Dankers, P (1978), Magnetic properties of dispersed natural iron-oxides of known grain size, Ph.D. thesis, State University of Utrecht.

Day, R., M. Fuller, and V.A. Schmidt (1977), Hysteresis properties of titanomagnetites: Grain-size and compositional dependence, Phys. Earth Planet. Inter., 13, 260-267.

Dekkers, M.J., and H.N. Böhnel, H.N (2006), Reliable absolute palaeointensities independent of magnetic domain state, Earth Planet. Sci. Lett., 248 (1-2), 507-516.

Demant, A., 1978, Características del Eje Neovolcánico Transmexicano y sus problemas de interpretación: Universidad Nacional Autónoma de México, Revista Mexicana de Ciencias Geológicas, 2, 172-182.

Doell, R.R. and A.V. Cox (1972), The Pacific geomagnetic secular variation anomaly and the question of lateral uniformity in the lower mantle, in The Nature of the Solid Earth, edited by E.C. Robertson, pp. 245-284, McGraw-Hill, New York.

Donadini, F., P., Riisager, K., Korhonen, K., Kahma, L. Pesonen, and I. Snowball (2007), Holocene geomagnetic paleointensities: A blind test of absolute paleointensity techniques and materials, Phys. Earth Planet. Inter., 161, 19-35.

Donadini, F., M. Kovacheva, M. Kostadinova, I.G. Hedley, and L.J. Pesonen (2008), Palaeointensity determination on an early medieval kiln from Switzerland and the effect of cooling rate, Phys. Earth Planet. Int., 33, 449-457.

Dunlop, D.J. (2002), Theory and application of the Day plot (Mrs/Ms versus Hcr/Hc) 1. Theoretical curves and tests using titanomagnetite data, J. Geophys. Res., 107, 4-1.

Elsasser, W.M. (1956), Hydrodynamic Dynamo Theory, Rev. Mod. Phys., 28 (2), 135-163.

Fabian, K. (2001), A theoretical treatment of paleointensity determination experiments on rocks containing pseudo-single or multi domain magnetic particles. Earth Planet. Sci. Lett. 188(1-2), 45-58.

Fabian, K. (2003), Some additional parameters to estimate domain state from isothermal magnetization measurements, Earth Planet. Sci. Lett., 213, 337-345.

Fabian, K., and R. Leonhardt (2007), Testing multiple specimen absolute paleointensity determination: Theory and experiments, IUGG, Perugia (Italy).

Ferrari, L., M. Lopez-Martinez, G. Aguirre-Díaz, and G. Carrasco-Núñez (1999), Space-time patterns of Cenozoic arc volcanism in central Mexico: From the Sierra Madre Occidental to the Mexican volcanic belt, Geology, 27, 303-306.

Ferrari, L., J. Rosas-Elguera, M. Orozco-Esquivel, G. Carrasco-Núñez, T. Norato-Cortez, and N. Gonzalez-Cervantes (2005), Digital geologic cartography of the Trans-Mexican Volcanic Belt (online), Digital Geosciences <http://satori.geociencias.unam.mx/digital_geosciences>, Universidad Nacional Autónoma de México.

Fisher, R.A. (1953), Dispersion on a sphere, Proc. R. Soc. London, 217, 295-305.

Fox, J.M.W., and M.J.Aitken (1980), Cooling rate dependence of the thermoremanent magnetization, Nature, 283, 462-463.

Frank, M., (2000), Comparison of cosmogenic radionuclide production and geomagnetic field intensity over the last 200,000 years, Phil. Trans. R. Soc. London, 358,1089-1107.

Frey, H.F., R.A. Lange, C.M. Hall, and H. Delgado-Granados (2004), Magma eruption rates constrained by 40Ar / 39Ar chronology and GIS for the Ceboruco-San Pedro volcanic field, western Mexico, GSA Bulletin, 116 (3/4), 259-276, doi: 10.1130/B25321.1.

Fuhrmann U., H.J. Lippolt and J.C. Hess (1987), Examination of some proposed K-Ar standards: 40Ar/39Ar analyses and conventional K-Ar data, Chemical Geology (isotope Geoscience Section), 66, 41-51.

Glatzmaier, G.A.., and P.H. Roberts (1995), A three-dimensional convective dynamo solution with rotating and finitely conducting inner core and mantle, Phys. Earth Planet. Inter. 91, 63-75.

Glatzmaier, G.A., R.S. Coe, L. Hongre, and P.H. Roberts (1999), The role of the Earth's mantle in controlling the frequency of geomagnetic reversals, Nature, 401, 805-810.

Gallet, Y., A. Genevey, and F. Fluteau (2005), Does Earth's magnetic field secular variation control centennial climate change? Earth Planet. Sci. Lett., 236, 339-347.

Goguitchaichvili, A., J. Urrutia-Fuccugauchi, L.M. Alva-Valdivia, J. Morales, J. Riisager, and P. Riisager (2004), Long term variation of the geomagnetic field strength: a cautionary note, Eos Trans. AGU, 85, 209-212.

Gonzalez, S., G. Sherwood, H. Böhnel, and E. Schnepp (1997), Palaeosecular variation in Central Mexico over the last 30,000 years: The record from lavas, Geophys. J. Int., 130, 201-219.

Gómez-Tuena, A., M.T. Orozco-Esquivel, and L. Ferrari (2007), Igneous petrogenesis of the Trans-Mexican Volcanic Belt, in: S.A., Alaniz-Álvarez, and Á.F. Nieto-Samaniego (Editors), Geology of México: Celebrating the Centenary of the Geological Society of México, Geological Society of America Special Paper, 422, 129-181, doi: 10.1130/2007.2422(05).

Gratton, M.N., J. Shaw, and E. Herrero-Bervera (2005), An absolute palaeointensity record from SOH1 lava core, Hawaii using the microwave technique, Phys. Earth Planet. Inter., 148 (2-4), 193-214.

Gubbins, D. (1999), The distinction between geomagnetic excursions and reversals, Geophys. J. Int., 137, F1-F3.

Guillou, H., B. S. Singer, C. Laj, C. Kissel, S. Scaillet, and B.R. Jicha (2004), On the age of the Laschamp geomagnetic excursion. Earth Planet. Sci. Lett. 227 (3-4), 331-343.

Guyodo, Y., and J.-P. Valet (1999), Global changes in intensity of the Earth's magnetic field during the last 800 kyr, Nature, 399, 249-252.
Guyodo, Y., C. Richter, and J.-P. Valet (1999), Paleointensity record from Pleistocene sediments (1.4-0 Ma) off the California Margin, J. Geophy. Res., 104, 22,953-964.

Haggerty, S.E. (1991), Oxide textures - a mini-atlas, oxide minerals: petrologic and magnetic significance, Rev. Miner., 25, 129–219.

Heller, F. (1980), Self-reversal of natural remanent magnetization in the Olby Laschamp lavas, Nature, 284, 334-335.

Herrero-Bervera, E., and S. Pal (1977), Paleomagnetic study of Sierra de Chichinautzin, Mexico, Geofis. Int., 17, 167–180.

Herrero-Bervera, E., J. Urrutia-Fucugauchi, A.L. Martin del Pozzo, H.N. Böhnel, and J. Guerrero (1986), Normal amplitude Brunhes paleosecular variation at low latitudes: A paleomagnetic record from the Trans-Mexican Volcanic Belt, Geophys. Res. Lett., 13, 1442–1445.

Hoffman, K.A.. (1981), Palaeomagnetic excursions, aborted reversals and transitional fields, Nature, 294, 67-68.

Hoffman, K.A. and B.S. Singer (2004), Regionally recurrent palaeomagnetic transitional fields and mantle processes, in Timescales of the Palaeomagnetic Field, Amer. Geophys. Union, Geophys. Monogr. Ser. 145, edited by J.E.T. Channell, D.V. Kent, W. Lowrie, and J.G. Meert, pp. 233-243, AGU, Washington D. C.

Hollerbach, R., and C.A. Jones (1993), Influence of the Earth's inner core on geomagnetic fluctuations and reversals, Nature 365, 541-542.

Hongre, L., G. Hulot, and A. Khokhlov, (1998), An analysis of the geomagnetic field over the past 2000 years. Phys. Earth Planet. Inter., 106, 311–335.

Jackson, A., A.R.T. Jonkers, and M.R. Walker (2000), Four centuries of geomagnetic secular variation from historical records, Phil. Trans. R. Soc. Lond., 358, 957-990.

Johnson, C.L., and C.G. Constable, (1998), Persistently anomalous Pacific geomagnetic fields, Geophys. Res. Lett., 25, 1011-1014.

Johnson, C.L., C.G. Constable, L. Tauxe, R. Barendregt, L.L. Brown, R.S. Coe, P. Layer, V. Mejia, N.D. Opdyke, B.S. Singer, H. Staudigel, and D.B. Stone (2008), Recent investigations of the 0-5 Ma geomagnetic field recorded by lava flows, Geochem. Geophys. Geosyst., 9(4), Q04032, doi:10.1029/2007GC001696.

Kirschvink, J.L. (1980), The least-squares line and plane and the analysis of palaeomagnetic data., Geophysical Journal Royal Astronomical Society, 62, 699-718.

Klitgord, K.D. and J. Mammerickx (1982), Northern East Pacific Rise-Magnetic anomaly and bathymetric framework, J. Geophys. Res., 87, 6725-6783.

Knudsen, M.F., N. Abrahamsen, and P. Riisager (2003), Palaeomagnetic evidence from Cape Verde Islands basalts for fully reversed excursions in the Brunhes Chron, Earth Plant. Sci. Lett., 206, 199-214.

Knudsen, M.F., G.M. Henderson, C.M. Mac Niocaill, and A.J. West (2007), Seven thousand year duration for a geomagnetic excursion constrained by $^{230}Th_{xs}$, Geophys. Res. Lett., 34, L22302, doi:10.1029/2007GL031090.

Knudsen, M.F., P., Riisager, F., Donadini, I. Snowball, R. Muscheler, K. Korhonen, and L.J. Pesonen (2008), Variations in the geomagnetic dipole moment during the Holocene and the past 50 kyr, Earth Planet. Sci. Lett., 272 (1-2), 319-329.

Kok, Y.S. and L. Tauxe, L. (1996), Saw-toothed pattern of relative paleointensity records and cumulative viscous remanence, Earth Planet. Sci. Lett., 137, 95-99.

Korhonen, K., F. Donadini, P. Riisager, and L.J. Pesonen (2008), GEOMAGIA50: An archeointensity database with PHP and MySQL. Geochem. Geophys. Geosyst., 9, Q04029, doi:10.1029/2007GC001893.

Korte, M., and C.G. Constable (2005), The geomagnetic dipole moment over the last 7000 years - New results from a global model, Earth Planet. Sci. Lett., 236, 348-358.

Korte, M., F. Donadini, and C.G. Constable (2008), The Geomagnetic Field for 0-3ka, Part II: A New Series of Time-Varying Global Models, J. Geophys. Res., (submitted).

Krása, D., C. Heunemann, R. Leonhardt, and N. Petersen (2003), Experimental procedure to detect multidomain remanence during Thellier-Thellier experiments, Phys. Chem. Earth, 28, 681-687.

Krása, D. and J. Matzka (2007), Inversion of titanomaghemite in oceanic basalt during heating, Phys. Earth planet. Inter., 160, 169–179.

Kristjansson, L., and A. Gudmundson (1980), Geomagnetic excursion in late-glacial basals outcrops in south-western Iceland, Geophys. Res. Lett., 7, 337-340.

Langereis, C.G., M.J. Dekkers, G.J. de Lange, M. Paterne, and P.J.M. Van Santvoort (1997), Magnetostratigraphy and astronomical calibration of the last 1.1 Myr from an eastern Mediterranean piston core and dating of short events in the Brunhes, Geophys. J. Int., 129, 75-94.

Lanphere, M. A., D.E. Champion, and W. Hildreth (1997), New evidence on the magentic reversal time scale from volcanic rocks in the Cascade Range, Washington, Oregon, and California, Eos Trans. AGU, 78(46), Fall Meet. Suppl., Abstract F196.

Laj, C., C. Kissel, and A.P. Roberts (2006), Geomagnetic field behaviour during the Icelandic basin and Lachamp geomagnetic excursions: A simple transitional field geometry?, Geochem. Geophys. Geosyst., 7, Q03004, doi:10.1029/2005GC001122.

Lawrence, K., C.G. Constable, and C.L. Johnson (2006), Palaeosecular Variation and the average geomagnetic field at ±20° latitude, Geochem. Geophys. Geosyst., 7, Q07007, doi:10.1029/2005GC001181.

LeGoff, M. and Y. Gallet (2004), A new three-axis vibrating sample magnetometer for continuous high-temperature magnetization measurements: Applications to paleo- and archeo-intensity determinations, Earth Planet. Sci. Lett., 229 (1-2), 31-43.

Leonhardt, R. (2004), Analyzing rock magnetic measurements: The RockMagAnalyzer 1.0 software, Computers and Geosciences, 32 (9), 1420-1431.

Leonhardt, R., D. Krása, and R.S. Coe (2004), Multidomain behavior during Thellier paleointensity experiments: a phenomenological model, Phys. Earth Planet. Inter., 147(2-3), 127-140.

Leonhardt, R., C. Heunemann, and D. Krása (2004), Analyzing absolute paleointensity determinations: Acceptance criteria and the software ThellierTool4.0, Geochem. Geophys. Geosyst., 5, Q12016, doi:10.1029/2004GC00807.

Leonhardt, R., J., Matzka, A.R.L. Nichols, and D.B. Dingwell (2006), Cooling rate correction of paleointensity determination for volcanic glasses by relaxation geospeedometry, Earth Planet. Sci. Lett., 243, 282-292.

Levi, S. (1977), The effect of magnetite particle size on palaeointensity determinations of the geomagnetic field, Phys. Earth Planet. Inter., 13, 245-259.

Levi, S., H., Audunsson, R.A. Duncan, L. Kristiansson, P.-Y. Gillot, and S.P. Jakobsson (1990), Late Pleistocene geomagnetic excursion in Icelandic lavs: confirmation of the Laschamp excursion. Earth Planet. Sci. Lett. 96, 443-457.

Le Goff, M., and Y. Gallet (2004), A new three-axis vibrating sample magnetometer for continuous high-temperature magnetization measurements: applications to paleo- and archeo-intensity determinations, Earth Planet. Sci. Lett., 229 (1-2), 31-43.

Lewis-Kenedi, C.B., R.A. Lange, C.M. Hall, and H. Delgado-Granados (2005), The eruptive history of the Tequila volcanic field, western Mexico: Ages, volumes, and relative proportions of lava types, Bulletin of Volcanology, 67, 391-414.

Love, J.J., (1999), A critique of frozen-flux inverse modelling of a nearly steady geodynamo, Geophys. J. Int., 138, 353-365.

Lund, S.P., G. Acton, B. Clement, M. Hastedt, M. Okada, and T. Williams (1998), Geomagnetic field excursions occurred often during the last million years, Eos Trans. AGU, 79 (14), 178-179.

Lund, S.P., G.D. Acton, B. Clement, M. Okada and T. Williams (2001a), Brunhes chron magnetic field excursions recovered from Leg 172 sediments, in: Keigwin, L.D., Rio, D., Acton, G.D., Arnold, E. (Eds.), Proc. ODP Sci. Results, 172, 1–18.

Lund, S.P., G.D. Acton, B. Clement, M. Okada and T. Williams (2001b), Paleomagnetic records of Stage 3 excursions, Leg 172, in Keigwin, L.D., Rio, D., Acton, G.D., Arnold, E. (Eds.). Proc. ODP Sci. Results, 172, 1-20.

Lund, S. P., M. Schwartz, L. Keigwin, and T. Johnson (2005), Deep-sea sediment records of the Laschamp geomagnetic field excursion (<41,000 calender years before present), J. Geophys. Res. 110, B04101, doi:10.1029/2003JB002943.

Lund, S., J.S. Stoner, J.E.T. Channell and G. Acton (2006), A summary of Brunhes paleomagnetic field variability recorded in Ocean Drilling Program cores, Phys. Earth planet. Inter., 156, 194-204.

Mankinen, E.A., M. Prevot,C.S. Gromme, and R.S. Coe (1985), The Steens Mountain (Oregon) geomagnetic polarity transition 1. Directional history, duration of episodes, and rock magnetism (USA), J. Geophys. Res., 90, 10,393-10,416.

McClelland-Brown, E. (1984), Experiments on TRM intensity dependence on cooling rate, Geophys. Res. Lett., 11, 205-208.

McClelland, E. (1996), Theory of CRM acquired by grain growth, and its implications for TRM acquisition and paleointensity, Geophys. J. Int., 126, 271–280.

McClelland, E., and V.P. Shcherbakov (1995), Metastability of domain state in MD magnetite: consequences for remanence acquisition, J. Geophys. Res., 100(B3), 3841–3857.

McClelland, E., and J.C. Briden (1996), An improved methodology for Thellier-type paleointensity determination in igneous rocks and its usefulness for verifying primary thermoremanence, J. Geophys. Res., 101, 21,995-22,013.

McClelland, E., A.R. Muxworthy, and R.M. Thomas (1996), Magnetic properties of the stable fraction of remanence in large multidomain (MD) magnetite grains: Single-domain or MD?, Geophys. Res. Lett., 23, 2831-2834.

McDougall, I., and H. Wensink (1966), Paleomagnetism and geochronology of the Pliocene-Pleistocene lavas in Iceland, Earth Planet. Sci. Lett., 1, 232-236.

Mejia, V., H. Böhnel, N.D. Opdyke, M.A. Ortega-Rivera, J.K.W. Lee, and J.J. Aranda-Gomez (2005), Paleosecular variation and time-averaged field recorded in late Pliocene–Holocene lava flows from Mexico, Geochem. Geophys. Geosyst., 6, Q07H19, doi:10.1029/2004GC000871.

Merrill, R.T., and P.L. McFadden (1994), Geomagnetic field stability: Reversal events and excursions, Earth Planet. Sci. Lett., 121, 57-59.

Merrill, R.T., McElhinny, M.E., and McFadden, P.L., 1996. The magneticfield of the Earth — palaeomagnetism, the core, and the deep mantle, Acad. Press Geophys. Ser., 63, 531 pp.

McElhinny, M.W., and P.L. McFadden (1997), Palaeosecular variation over the past 5 Myr based on a new generalized database, Geophys. J. Int., 131, 240-252.

McFadden, P.L. (1982), Two-tier analysis in palaeomagnetism, Geophys. J. astr. Soc., 71, 519-543.

McFadden, P.L., R.T. Merrill, and M.W. McElhinny (1988), Dipole/quadrupole family modeling of paleosecular variation, J. Geophys. Res., 93, 11,583-588.

McFadden, P.L., R.T. Merrill, M.W. McElhinny, and S. Lee (1991), Reversals of the Earth's magnetic field and temporal variations of the dynamo families, J. Geophys. Res., 96, 3923-3933.

Michalk, D.M.,A.R. Muxworthy, H.N. Böhnel, J. Maclennan, and N. Nowaczyk (2008a). Evaluation of the multispecimen parallel differential pTRM method: A test on historical lavas from Iceland and Mexico, Geophys. J. Int., 173 (2), 409-420.

Michalk, D.M., N.R. Nowacyzk, H.N. Böhnel, G.J. Aguirre-Diaz, S. Ownby, M. Lopez-Martinez and J.F.W. Negendank (2008b), Evidence for geomagnetic excursions recorded in Brunhes- and Matuyama-Chron lavas from the Trans-Mexican Volcanic Belt, J. Geophys. Res., (submitted).

Moskowitz, B.M. (1981), Methods for estimating Curie temperatures of titanomaghemites from experimental Js-T data, Earth Planet. Sci. Lett., 53, 84-88.

Mooser, F., (1972), The Mexican volcanic belt structure and tectonics, Geofís. Int., 12, 55-70.

Mooser, F., A.E.M. Nairn, and J.F.W. Negendank (1974), Palaeomagnetic investigations of the Tertiary and Quaternary igneous rocks: VIII, A palaeomagnetic and petrologic study of volcanics of the Valley of Mexico, Geol. Rundsch., 63, 451–483.

Morales, J., A. Goguitchaichvilli, and J. Urrutia-Fucugauchi (2001), A rock-magnetic and palaeointensity study of some Mexican volcanic lava flows during the Latest Pleistocene to the Holocene, Earth Planets Space, 53, 893-902.

Muscheler, R., J.B. Peter, W. Kubik, and H.A.. Synal (2005), Geomagnetic field intensity during the last 60,000 years based on 10Be and 36Cl from the Summit ice cores and 14C, Quatern. Sci. Rev., 24, 1849-1860.

Muxworthy, A., D. Heslop, and W. Williams (2004), Influence of magnetostatic interactions on first-order-reversal-curve (FORC) diagrams: A micromagnetic approach, Geophys. J. Int., 158 (3), 888-897.

Muxworthy, A.R., and W. Williams (2005), Magnetostatic interaction fields in first-order-reversal-curve (FORC) diagrams, J. Appl. Phys., 97: 063905.

Muxworthy, A.R., and A.P. Roberts (2007), First-order reversal curve (FORC) diagrams, in: E. Herrero-Bervera, and D. Gubbins (Editors), Encyclopedia of Geomagnetism and Paleomagnetism. Springer, Dordrecht, the Netherlands, 266–272.

Nagata, T., Y. Arai, and K. Momose (1963), Secular variation of the geomagnetic total force during the last 5000 years, J.Geophys. Res., 68, 5277-5281.

Néel, L. (1949), Théorie du traînage magnétique des ferromagnétiques en grains fins avec applications aux terres cuites, Ann. Géophys., 5, 99-136.

Néel, L. (1955), Some theoretical aspects of rock-magnetism, Advances in Physics, 14, 191-243.

Newell, A.J. (2005), A high-precision model of first-order reversal curve (FORC) functions for single-domain ferromagnets with uniaxial anisotropy, Geochem. Geophys. Geosyst., 6, Q05010, doi:10.1029/2004GC00877.

Nixon, G., A. Demant, R. Armstrong, and J. Harakal (1987), K-Ar and geologic data bearing on the age and evolution of the Trans-Mexican Volcanic Belt, Geofís. Int., 26,109-158.

Nowaczyk, N. R. and M. Antonow (1997), High-resolution magnetostratigraphy of four sediment cores from the Greenland Sea I - Identification of the Mono Lake excursion, Laschamp and Biwa I / Jamaica geomagnetic polarity event, Geophys. J. Int., 131, 310-324.

Nowaczyk, N.R., and J. Knies (2000), Magnetostratigraphic results from Eastern Arctic Ocean - AMS14C ages and relative palaeointensity data of the Mono Lake and Laschamp geomagnetic events, Geophys J. Int., 140, 185-197.

Nowaczyk, N.R., Antonow, M., Knies, J., Spielhagen, R.F. (2003), Further magnetochronostratigraphic results on reversal excursions during the last 50 ka as derived from northern high latitudes and discrepancies in their precise AMS 14C dating, Geophys. J. Int. 55 (3), 1065-1080.

Oda, H., K. Nakamura, T. Ikehara, and M. Nishimura (2002), Paleomagnetic record from Academician Ridge, Lake Baikal: a reversal excursion at the base of marine oxygen isotope stage 6, Earth Planet. Sci. Lett., 201, 117-128.

O'Reilly, W. (1984), Rock and Mineral Magnetism, 220 pp., Blackie, Glasgow and London; Chapman and Hall, New York.

Opdyke, N.D. (1972), Paleomagnetism of deep-sea cores, Rev. Geophys. Space Phys., 10, 213-249.

Opdyke, N.D, L.H. Burckle and A. Todd (1974), The extension of the magnetic time scale in sediments of the central Pacific Ocean, Earth Planet. Sci. Lett., 22, 300–306.

Ort, M.H., and G. Carrasco-Núñez, (2009), Lateral vent migration during phreatomagmatic and magmatic eruptions at Tecuitlapa Maar, east-central Mexico, J. Volcanol. Geotherm. Res., doi:10.1016/j.jvolgeores.2009.01.003.

Ownby, S., H. Delgado Granados, R.A. Lange, and C.M. Hall (2007), Volcán Tancítaro, Michoacán, Mexico, ^{40}Ar / ^{39}Ar constraints on its history of sector collapse, J. Volcan. Geoth. Res., 161, 1–14.

Ownby, S.E., R.A. Lange, C.M. Hall, and H. Delgado-Granados (2009), The Eruptive History of the Tancítaro Volcanic Field, Michoacán Mexico: Differentiation of Basalt to Andesite in the Deep Crust and Development of Compositionally Stratified Arc Crust, Geological Society of America Bulletin., (submitted)

Pardo, M., and G. Suárez, (1995), Shape of the subducted Rivera and Cocos plate in southern Mexico: Seismic and tectonic implications, J. Geophys. Res., 100, 12,357-12,373, doi: 10.1029/95JB00919.

Perrin, M. (1998), Paleointensity determination, magnetic domain structure, and selection criteria, J. Geophys. Res., 103(B12), 30,591-30,600.

Perrin, M., and V. Shcherbakov (1998), Paleointensity database updated, Eos Trans. AGU, 79(16), 198.

Perrin, M., and E. Schnepp, (2004), IAGA paleointensity database: Distribution and quality of the data set, Phys. Earth Planet. Inter., 147, 255-267.

Petronille, M., A. Goguitchaichvili, B. Henry, L.M. Alva-Valdivia, J. Rosas-Elguera, J. Urrutia-Fucugauchi, M. Rodriguez Ceja, and M. Calvo-Rathert (2005), Paleomagnetism of Ar-Ar dated lava flows from the Ceboruco-San Pedro volcanic field (western Mexico): Evidence for the Matuyama-Brunhes transition precursor and a fully reversed geomagnetic event in the Brunhes chron, J. Geophys. Res., 110, 1-11.

Pick, T., and L. Tauxe (1993), Geomagnetic palaeointensities during the Cretaceous normal superchron measured using submarine basaltic glass, Nature, 366, 238-242.

Prevot, M., E.A. Mankinen, R.S. Coe, and C.S. Gromme (1985), The Steens Mountain (Oregon) geomagnetic polarity transition 2. Field intensity variations and discussion of reversal models (USA), J. Geophys. Res., 90, 10,417-10,448.

Pullaiah, G., E. Irving, K.L. Buchan, and D.J. Dunlop (1975), Magnetization changes caused by burial and uplift, Earth Planet. Sci. Lett., 28, 133-143.

Riisager, P., and Riisager, J., 2001. Detecting multidomain magnetic grains in Thellier palaeointensity experiments. Phys. Earth Planet. Inter., 125: 111-117.

Roberts, A.P., C.R. Pike, and K.L. Verosub (2000), First-order reversal curve diagrams: A new tool for characterizing the magnetic properties of natural samples, J. Geophys. Res., 105, 28,461-28,475.

Roberts, A.P., and J.C. Lewin-Harris (2000), Marine magnetic anomalies: evidence that 'tiny wiggles' represent short-period geomagnetic polarity intervals, Earth Planet. Sci. Lett. 183, 375-388.

Roberts, A.P., and M. Winklhofer (2004), Why are geomagnetic excursions not always recorded in sediments? Constraints from post-depositional remanent magnetization lock-in modeling, Earth Planet. Sci. Lett., 227, 345-359.

Ruiz-Martinez, V. C., M.L. Osete, R. Vegas, J.I. Nunez-Aguilar, J. Urrutia-Fucugauchi, and D.H. Tarling (2000), Palaeomagnetism of late Miocene to Quaternary volcanics from the eastern segment of the Trans-Mexican volcanic belt, Tectonophysics, 318, 217–233.

Ryan, W.B. (1972), Stratigraphy of late Quaternary sediments in the eastern Mediteranean, in The Mediteranean Sea, edited by D.J. Stanley, pp. 149-169, Dowden, Hutchinson and Ross, Stroudsburg.

Schaaf, P., and A. Ramírez-Luna (2008), Advancement in Luminescence Dating of Volcanic Rocks: Examples from the Eastern Trans-Mexican Volcanic Belt, IAVCEI, General Assemby, Reykjavik, August 2008, abstracts.

Schnepp, E., (1994), Determination of palaeointensities from the Quaternary West Eifel volcanic field, Germany, Geophys. J. Int., 116, 688-714.

Schnepp, E. and H. Hradetzky (1994), Combined palaeointensity and ^{40} Ar / ^{39} Ar age spectrum data from volcanic rocks of the West Eifel field (Germany): Evidence for an early Brunhes geomagnetic excursion, J. Geophys. Res., 99, 9061-9076.

Selkin, P.A., and L. Tauxe (2000), Long-term variations in palaeointensity, Phil. Trans. R. Soc. London, 358, 1065-1088.

Siebert, L. and G.C., Carrasco-Nunez, (2002), Late-Pleistocene to precolumbian behind-the-arc mafic volcanism in the eastern Mexican Volcanic Belt; implications for future hazards, Journal of Volcanology and Geothermal Research, 115, 179-205.

Shaw, J. (1974), A new method of determining the magnitude of the paleomagnetic field: Application to five historic lavas and five archeological samples, Geophys. J. R. Astron. Soc., 39, 133-141.

Shcherbakova, V.V., V.P. Shcherbakov, and F. Heider (2000), Properties of partial thermoremanent magnetization in pseudosingle domain and multidomain magnetite grains, J. Geophys. Res., 105, 767-781.

Shcherbakov, V.P., E. McClelland, and V.V. Shcherbakova (1993), A model of multidomain thermoremanent magnetization incorporating temperature-variable domain structure, J. Geophys. Res., 98, 6,210-6,216.

Shcherbakov, V.P. and V.V. Shcherbakova (2001), On the suitability of the Thellier method of palaeointensity determinations on pseudo-single-domain and multidomain grains, Geophys. J. Int. 146 (1), 20-30.

Singer, B.S., M.K. Relle, K.A. Hoffmann, A. Battle, C. Laj, H. Guillou, and J.C. Carracedo (2002), Ar/Ar ages from transitionally magnetized lavas on La Palma, Carnary Islands, and the geomagnetic instability timescale, J. Geophys. Res., 107, B11,2307,doi:10.1029/2001JB001613.

Singer, B.S., K.A. Hoffman, R.S. Coe, L.L. Brown, B.R. Jicha, M.S. Pringle, and A. Chauvin (2005), Structural and temporal requirements for geomagnetic field reversal deduced from lava flows, Nature, 434, 633-636.

Singer, B.S. (2007), Polarity transitions: Radioscopic dating, in Encyclopedia of Geomagnetism and Palaeomagnetism edited by D. Gubbins, and E. Herrero-Bervera, pp. 834-839, Springer, Dordrecht, The Netherlands.

Singer, B.S., B.R. Jicha, B.T. Kirby, J.W. Geissman, and E. Herrero-Bervera (2008a), ^{40}Ar/^{39}Ar dating links Albuquerque Volcanoes to the Pringle Falls excursion and the Geomagnetic Instability Time Scale, Earth Planet. Sci. Lett., 267, 584-595.

Singer, B.S., K. Hoffmann, E. Schnepp, and H. Guillou (2008b), Multiple Brunhes Chron Excursions Recorded in West Eifel (Germany) Volcanics: Support for Long-Held Mantle Control Over the Non-Axial Dipole Field, accepted for publication in Phys. Planet. Int. 169 (1-4), 28-40.

Smirnov, A., J. Tarduno, and B. Pisakin (2003), Palaeointensity of the early geodynamo (2.45 Ga) as recorded in Korelia: a single crystal approach, Geology, 31 (5), 415-418.

Spell, T.L., and I. McDougall (1992), Revisions to the age of the Brunhes-Matuyama boundary and the Pleistocene geomagnetic polarity timescale, Geophys. Res. Lett., 19, 1181-1184.

Steele, W. K. (1985), Paleomagnetic constraints on the volcanic history of Iztaccihuatl, Geofis. Int., 24, 159–167.

Tanaka, H. and M. Kono (1994), Paleointensity database provides new resource, Eos Trans. AGU, 75 (42), 498-498.

Tauxe, L. (1993), Sedimentary records of relative paleointensity of the geomagnetic field: Theory and practice, Rev. Geophys., 31, 319-354.

Tauxe, L., T.A.T. Mullender, and T. Pick (1996), Potbellies, wasp-waists, and superparamagnetism in magnetic hysteresis, J. Geophys. Res., 101, 571-583.

Tauxe, L., H. Staudigel, and J.R. Wijbrans (2000), Palaeomagnetism and $^{40}Ar/^{39}Ar$ ages from La Palma in the Canary Islands, Geochem. Geophys. Geosyst., 1(9), doi:10.1029/2000GC000063.

Tauxe, L., C. Constable, C.L. Johnson, A.A.P. Koppers, W.R. Miller, and H. Staudigel (2003), Paleomagnetism of the southwestern U.S.A. recorded by 0-5 Ma igneous rocks, Geochem. Geophys. Geosyst., 4 (4), 8802, doi: 10,1029/2002/GC000343.

Tauxe, L., and D.V. Kent (2004), A simplified statistical model for the geomagnetic field and the detection of shallow bias in paleomagnetic inclinations: Was the ancient magnetic field dipolar?, in Timescales of the Paleomagnetic Field, Geophys. Monogr. Ser., vol. 145, edited by J.E.T. Channell, D.V. Kent, W. Lowrie, and J.G. Meert, pp. 101-115, AGU, Washington D. C.

Tauxe, L and H. Staudigel (2004), Strength of the geomagnetic field in the Cretaceous normal superchron: New data from submarine basaltic glass of the Troodos Ophiolite, Geochem. Geophys. Geosyst., 5, Q02H06 doi: 10.1029/2003GC00635.

Thellier, E., and O. Thellier (1959), Sur l'intensite? du champ magnetique terrestre dans le passe historique et geologique. Ann. Geophys., 15, 285-376.

Thouveny, N., D.L. Bourles, G. Saracco, J. Carcaillet, and F. Bassinot (2008), Palaeoclimatic context of geomagnetic dipole lows and excursions in the Brunhes, Clue for an orbital influence on the geodynamo? Earth Planet. Sci. Lett., (accepted manuscript).

Urrutia-Fucugauchi, J., C. Radakrishnamurty, and J.F.W. Negendank (1984), Magnetic properties of a columnar basalt from central Mexico. Geophys. Res. Lett., 9, 832-835.

Valet, J.-P. (2003), Time variations in geomagnetic intensity, Rev. Geophys., 41, 1004(doi:10.1029/2001RG000104).
Valet, J.-P., L. Meynadier, and Y, Guyodo (2005), Geomagnetic dipole strength and reversal rate over the past two million years, Nature, 435, 802-805.

Vlag, P., L. Alva-Valdivia, C.B. De Boer, S. Gonzalez, and J. Urrutia-Fucugauchi, (2000), A rock- and paleomagnetic study of a Holocene lava flow in Central Mexico, Phys. Earth Planet. Inter., 118, 259-272.

Vandamme, D. (1994), A new method to determine paleosecular variation, Phys. Earth Planet. Inter., 85, 131–142.

Walton D., (1980), Time-temperature relations in the magnetization of assemblies of single domain grains. Nature, 286: 245-247.

Watkins, N.D., I. McDougall, and L. Kristjansson (1975), A detailed paleomagnetic survey of the type location for the Gilsa geomagnetic polarity event, Earth Planet. Sci. Lett., 27, 436-444.
Watson, G.S. (1956), A test for randomness of directions, Mon. Not. R. Astron. Soc. Geophys. Suppl., 7, 160-161.

Wicht, J. (2005), Palaeomagnetic interpretation of dynamo simulations. Geophys. J. Int., 162, 371-380.

Wilson, R.L., N.D. Watkins, T. Einarsson, T. Sigurgeirsson, S.E. Haggerty, P.J. Smith, P. Dagley, and A.G. McCormack (1972), Paleomagnetism of ten lava sequences from SW Iceland, Geophys. J. R. Astron. Soc., 29, 459-471.

Xu, S. and D.J. Dunlop (2004), Thellier palaeointensity theory and experiments for multidomain grains, J. Geophys. Res., 109, B07103, doi: 10.1029/2004JB003024.

Yamamoto, Y., H. Tsunakawa, and H. Shibuya (2003), Palaeointensity study of the Hawaiian 1960 lava: Implications for possible causes of erroneously high intensities, Geophys. J. Int., 153, 263-276.

Yu, Y. and D.J. Dunlop, D.J. (2003), On partial thermoremanent magnetization tail checks in Thellier paleointensity determination, J. Geophys. Res., 108, B11 2523, doi:10.1029/2003JB002420.

Yu, Y., L. Tauxe and A. Genevey (2004), Toward an optimal geomagnetic field intensity determination technique, Geochem. Geophys. Geosyst. 5, Q02H07, doi: 10.1029/2003GC000630.